universität wien

DISSERTATION

Titel der Dissertation

Regulation of substrate recognition by the
Anaphase Promoting Complex / Cyclosome

angestrebter akademischer Grad

Doktor/in der Naturwissenschaften (Dr. rer.nat.)

Verfasserin / Verfasser:	Ivana Primorac
Matrikel-Nummer:	0649677
Dissertationsgebiet (lt. Studienblatt):	Molekulare Biologie
Betreuerin / Betreuer:	Dr. Jan-Michael Peters

Wien, am 8. September 2009

TABLE OF CONTENTS

Zusammenfassung

Der Zellzyklus stellt einen praezise kontrollierten Ablauf von Ereignissen dar, welche in der Erzeugung von zwei identischen Tochterzellen gipfeln. Um eine ordnungsgemaeße Abfolge der notwendigen Ereignisse zu ermoeglichen produziert die Zelle regulatorische Protein, welche an bestimmten Kontrollpunkten das Fortschreiten des Zellzyklus verhinden. Sind alle Voraussetzungen fuer das Fortsetzen des Zellzyklus erfuellt, werden Polyubiquitinketten an die inhibitorischen Zellzyklusproteine geheftet, wodurch diese fuer die proteasomabhaengige Degradation freigeben werden. Der Anaphase-einleitende Komplex (APC/C) ist ein 1,5 MDa grosser Proteinkomplex bestehend aus ueber 12 unterscheidlichen Proteinuntereinheiten. Am Ende der Metaphase katalysiert der APC/C die Anheftung von Ubiquitinmolekuelketten an die zwei Zellzyklusregulatoren Secruin und CyclinB. Deren Degradation fuehrt zum Uebergang in die Anaphase, in der die zwei Schwesterchromatide auf die zukuenftigen Tochterzellen aufgeteilt werden. Um eine einwandfreie Aufteilung zu ermoeglichen, muss zuerst eine bidirektionale Anheftung beider Schwesterchromatide an den Spindelapparat sichergestellt sein, bevor der APC/C akitviert werden kann. Solange diese bidirektionale Orientierung nicht gewaehrleistet ist, wird der APC/C durch den Spindelassemblierungs-Kontrollpunkt (SAC) in seiner Funktion gehemmt.

Manche Zellzyklusregulatoren enthalten bestimmte Sequenzmotife, sogenannte Degradationsmotife, welche diese Proteine als Substrate fuer die APC/C-abhaengige Ployubiquitinierungsreaktion kennzeichnen. Die gelaeufigsten Degradationsmotife sind die D-Box und die KEN-Box. Die Rekrutierung dieser Substrate an den APC/C sowie dessen katalytische Aktivierung wird durch sogenannte Koaktivatorproteine, Cdc20 oder Cdh1, sichergestellt. Diese Koaktivatoren besitzen eine WD40 Domaene, welche auch als Protein-Protein-Interaktionsdomaene bekannt ist. Ausserdem sind die C-Box im N-terminus sowie das C-terminale IR-Ende eine wichtige Voraussetzung fuer eine funktionelle Interaktion der Koaktivatoren mit dem APC/C.

Mittels Koexpressionsstudien in Hefe- und Insektenzellen konnte gezeigt werden, dass APC/C-Modellsubstrate spezifisch an die WD40 Domaene von Cdh1 binden. Durch zahlreiche in vitro Experimente konnte weiterhin gezeitg werden, dass die C-Box eine wichtige Voraussetzung fuer eine effiziente Rekrutierung dieser Cdh1-Substrat-Komplexe an den APC/C darstellt. Cdh1 C-Box Mutanten haben ausserdem negative Auswirkung auf in vitro Ubiquitinierungsreaktionen im Vergleich zu wildtyp Cdh1. Ergebnisse aus elektronenmikroskopischen Aufnhamen unterschiedlicher APC/C-Komplexe und anschließender 3D Modellierung weisen darauf hin, dass sich die Bindestelle des mitotisches

Kontrollkomplexes (MCC) am APC/C teilweise mit der der Koaktivatoren ueberschneidet. MCC-gebundener APC/C ist stark inhibiert in seiner Faehigkeit, Substrate in vitro zu binden. Diese Ergebnisse legen den Schluss nahe, dass der mitotische Kontrollomplex die Substratbindestelle am APC/C physikalisch blockiert.

Abstract

The cell cycle is a highly ordered and coordinated sequence of events which results in two daughter cells emerging from one mother cell. To properly carry out the cell cycle program the cell produces regulatory proteins that inhibit the progression to the next stage if they are not destroyed. The degradation of mitotic regulators depends on the ubiquitin-proteasome system.

The Anaphase Promoting Complex/ Cyclosome (APC/C) is a 1.5 MDa ubiquitin ligase complex composed of at least a dozen subunits. The APC/C ubiquitylates its specific substrates with the help of the activator proteins, Cdc20 and Cdh1, and thereby targets substrates for proteasomal destruction. Strict regulation of APC/C activity is essential for faithful chromosome segregation and timely mitotic exit. The most prominent mechanism of APC/C control at the metaphase-to-anaphase transition is the spindle assembly checkpoint (SAC). The SAC inhibits APC/C until every single chromatid pair has been attached to the mitotic spindle and bi-oriented.

The aim of this project was to understand how substrates are recruited to APC/C and if substrate recruitment is controlled by the spindle assembly checkpoint (SAC).

All APC/C substrates contain one or more degradation motifs, the most common are the D-box and the KEN box, which specifically target them to the APC/C and its activator proteins. Substrate recruitment to the APC/C, as well as activation of the APC/C in the ubiquitylation reaction, depends on activators, Cdc20 and Cdh1. APC/C activators contain several conserved motifs, the most prominent one is the WD40 propeller domain, present in a variety of proteins and implicated in protein-protein interactions. By co-expression experiments in yeast and insect cells I could show that a WD40 domain of Cdh1 is sufficient to bind an APC/C substrate in a D box and KEN box dependent manner.

Anchoring of activators to the APC/C is mediated by their carboxy-terminal IR tail. Efficient binding of activators to APC/C also depends on another conserved activator sequence, called the C-box. Through a set of in vitro protein binding experiments I could show that the C-box is, in addition, also necessary to recruit substrates efficiently to APC/C-activator complexes. I could further show that restoring APC/C binding to wild type levels did not restore the activator function of C-box mutant Cdh1 in an *in vitro* ubiquitylation reaction.

ABSTRACT

To understand how the SAC inhibits the APC/C we used single-particle electron microscopy to obtain three dimensional models of human APC/C in various functional states: bound to a Mitotic Checkpoint Complex (MCC), to Cdc20, or to neither (apo-APC/C). These experiments revealed that the MCC binding site on APC/C partially overlaps with Cdc20 binding site, which suggested that the MCC might physically prevent substrate binding to the APC/C. To test this prediction I performed *in vitro* substrate binding assays which showed that substrate binding to APC/C^{MCC} is strongly reduced.

1. Introduction

In biology “life” is a characteristic of all functioning organisms on Earth with heritable genetic information which are able to exhibit continued, self-sustaining processes, such as the capacity to extract energy from the environment to drive their various functions, to respond to changes in the environment, with the ability to grow, and without exception, to reproduce. Cells are the basic units of life and cell division is the basic reproductive process of life.

1.1 The cell cycle

Once a eukaryotic cell receives a mitogenic stimulus, complex signaling pathways inhibit factors that maintain it in quiescent state and the cell enters the cell cycle. The cell cycle is a highly ordered and coordinated sequence of events that involves accumulation of cell’s components and, importantly, precise duplication of the cell’s genome in S or “synthetic” phase of the cell cycle. The duplicated material of the mother cell is then accurately segregated into two daughter cells by a spectacular event called mitosis, or M phase. These two phases of the cell cycle are separated by two, so called, gap phases, G1 and G2.

Most of mother cell’s components, the organelles, membranes, proteins and RNAs, are gradually doubling throughout the cell cycle, finally resulting in sufficient amounts of all of these components for both daughter cells to start their life. The genetic information, however, is present as a single copy distributed in a distinct number of chromosome pairs, and it is essential for the cell to duplicate it only once per cell cycle. A complex chromosome segregation mechanism later ensures that the duplicated genome is precisely distributed into the two daughter cells. The right order of events in the cell cycle is essential for the fidelity of cell division. Often causally interconnected these cell cycle events are governed by an elaborate regulatory system based on feedback control (reviewed by Guardavacarro and Pagano, 2006). Three major regulatory checkpoints control three crucial steps in the cell cycle: G1 checkpoint (“start” in yeast, and “restriction point” in animal cells) controls entry into the cell cycle in late G1; G2/M controls the entry into mitosis; and the metaphase-to-anaphase transition controls the final events in mitosis (Morgan, 2007).

At the heart of the cell cycle control system is an oscillator based on the activity of cyclin-dependent kinases (Cdks). As the cell progresses through the cell cycle the enzymatic activities of these kinases change which leads to changes in phosphorylation state, and thus state of activation, of proteins that control the cell cycle processes (Morgan, 2007). The levels of Cdks do not change during the cell cycle, it is their regulatory subunits, the cyclins, that drive the oscillations in their activity. Thus, three parts of the cell cycle can be distinguished: the engine, which produces fluctuations in the levels of cyclins and thereby the activity of their associated Cdks; the downstream events that the engine drives, such as DNA replication and mitosis; and signaling pathways that regulate the engine in response to environment inside and outside of the cell (Murray, 2004). Cell cycle stage-specific cyclin synthesis leads to its accumulation which results in formation of cyclin-Cdk complexes that drive cell cycle stage specific events. For example, in animal cells the A-type cyclins appear at the onset of S phase and contribute to DNA synthesis, initiation of chromosome condensation and nuclear envelope breakdown. B-type cyclins associate with Cdk1 at the end of G2, to complete chromosome condensation and promote spindle assembly (Morgan, 2007). The activity of cyclin-Cdk is fine-tuned by another layer of control through phosphorylation and inhibitor binding. It is becoming increasingly apparent, however, that the cyclins and Cdks have redundant roles, and that it is their specific localization and expression levels that determine their specificity (reviewed in Guardavacarro and Pagano, 2006; Hochegger et al, 2008). Abolishing Cdk activity is necessary for exit from mitosis and for loading of pre-replicative complexes (pre-RCs) at the origins of replication in G1, and this is conserved throughout the eukaryotic world. Only when E- and A-type cyclins accumulate and activate Cdk again at the end of G1, the origins start firing in S phase (reviewed by Diffley, 2004). High Cdk activity prevents pre-RC assembly until the end of metaphase, when the Cdk activity drops again, thereby ensuring that the DNA is replicated only once per cell cycle. Irreversible and unidirectional transitions from one cell cycle stage to the next are achieved by destruction of cyclins which inactivates their associated Cdks.

1.2 Protein destruction machinery behind the cell cycle engine

All known cyclins, as well as many other cell cycle regulators, are degraded by the ubiquitin-proteasome degradation system. Multiple copies of a 7 kDa protein ubiquitin are assembled on the protein to be degraded. A polyubiquitin chain of at least 4 ubiquitins serves as a signal that targets the modified protein for degradation by the 26S proteasome (Thrower et al, 2000). The ubiquitylation reaction is performed by a three-enzyme cascade (Figure 1). First, ubiquitin is activated by ubiquitin-activating enzyme, E1, which adenylates ubiquitin using ATP before it forms a thioester bond between the carboxy terminus of ubiquitin and the sulfhydril group of a cysteine in its active site. The activatiated ubiquitin is then transferred to the active-site cysteine of the ubiquitin conjugating enzyme (E2) in a trans-esterification reaction. The third, tightly regulated, step is the transfer of ubiquitin on the target protein by isopeptide bond formation between the carboxy terminus of ubiquitin and the ε-amino group of a lysine in the substrate protein. Ubiquitin ligase enzymes (E3s) catalyze substrate ubiquitylation, and it is the E3s that provide substrate specificity in the ubiquitylation reaction. (reviewed in Pickart, 2001; Wickliffe et al, 2009). Depending on whether they themselves form a thioester bond with ubiquitin before transferring it to the substrate E3s are divided in two groups. HECT (Homologous to E6AP C terminus) type E3s harbor an active-site cysteine which accepts ubiquitin before transferring it to a substrate. RING (Really Interesting New Gene) type E3s, on the other hand, do not form a thioester bond with ubiquitin. Instead, they bind the E2s charged with ubiquitin and the target substrate thereby bringing them into reactive proximity. The ubiquitylation of proteins can be reversed by the activity of deubiquitinating enzymes (Reviewed by Amerik and Hochstrasser, 2004), therefore whether a protein is degraded or not depends on the balance between its ubiquitylation and deubiquitylation.

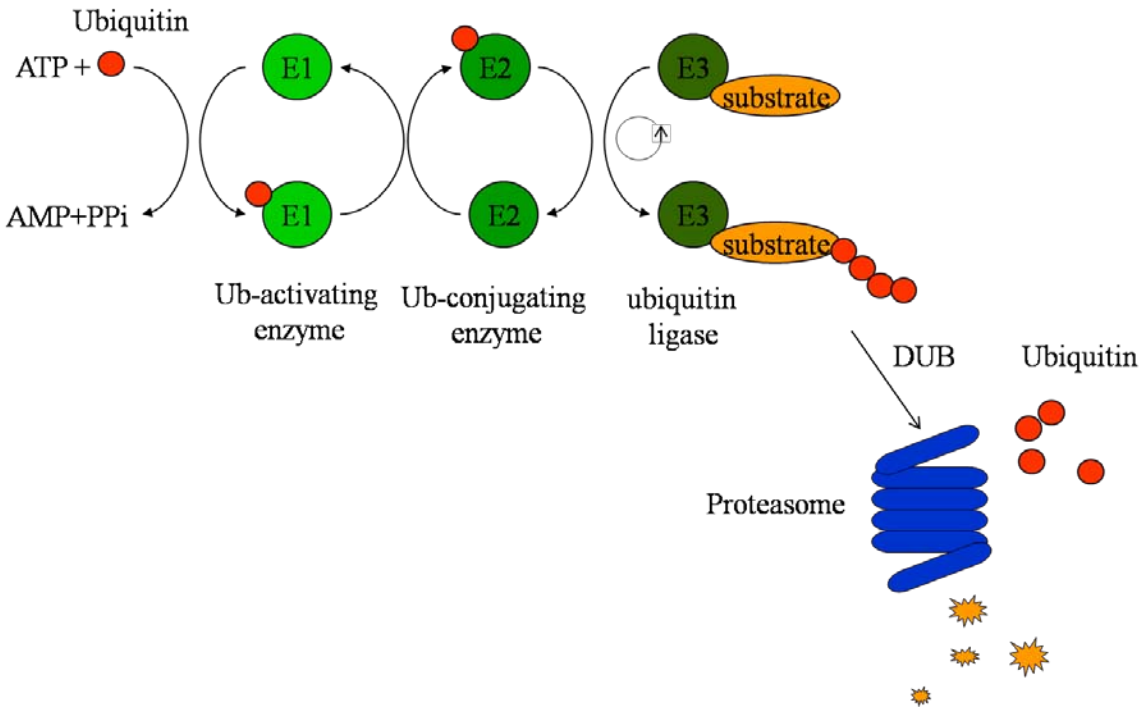

Figure 1. The ubiquitin-proteasome pathway. A ubiquitin- activating enzyme (E1) forms a thiol ester with the carboxyl group of ubiquitin, thereby activating the C terminus of ubiquitin for nucleophilic attack. Ubiquitin-conjugating enzyme (E2) transiently carries the activated ubiquitin molecule as a thiol ester. Ubiquitin ligase (E3) transfers the activated ubiquitin from the E2 to the substrate (or ubiquitin) lysine residue. Substrates tagged with a polyubiquitin chain are selectively targeted to a multisubunit ATP-dependent protease known as the 26S proteasome. Deubiquitinating enzymes (DUBs) associated with the proteasome remove ubiquitin before substrate degradation initiates (Reviewed by Pickart, 2001).

The cell cycle engine is controlled by the activity of two RING type ubiquitin ligases. The APC/C (Anaphase Promoting Complex/Cyclosome) controls progression through mitosis and G1, while the SCF (Skp1-Cul1-F-box) operates at all stages of the cell cycle (reviewed by Peters, 1998; Nakayama and Nakayama, 2006). APC/C and SCF share their core subunit architecture. The RING-finger subunit (Rbx1/Rbx1/Hrt1 in SCF and Apc11 in APC/C) is the catalytic subunit that associates with the ubiquitin-charged E2. The RING-finger subunit is anchored to the scaffold cullin protein (Cul1 in SCF and Apc2 in APC/C). Unlike SCF, the APC/C has a very complex subunit composition. At least 12 subunits have been identified in this 1.5 MDa large complex and for many of them we still do not know what their function is.
Specific substrates are recruited to the SCF by a plethora of so-called F-box proteins that that bind substrates via their WD40 or LRR domains (reviewed in Petroski and Deshaies, 2005).

Substrate adaptors of the APC/C, Cdc20 and Cdh1, are also WD40 domain containing proteins (reviewed in Vodermaier, 2001). A crucial difference between SCF and APC/C is how their substrate recognition is regulated. The SCF is constitutively active and it is the phosphorylation of substrate proteins that triggers their recognition by the F-box adaptor proteins and their recruitment to the SCF (Petroski and Deshaies, 2005). In case of APC/C it is the enzyme itself that is being regulated by phosphorylation, regulated activator-protein association and association of inhibitors (reviewed in Peters, 2006, and described in more detail below).

1.3 The architecture of the APC/C

The APC/C is the most structurally complex ubiquitin ligase of the Cullin-RING family. This 1.5 MDa large macromolecule contains one or more copies of at least 12 core subunits, termed collectively the apo-APC. In a mitotic cell cycle apo-APC/C associates sequentially with 2 different activator proteins, Cdc20 and Cdh1, that function as substrate-adaptors (reviewed by Peters, 2006; Thornton and Toczyski, 2006). So far it has been impossible to reconstitute the APC/C, from purified subunits, therefore a crystal structure of the complex or of its subcomplexes is still lacking. Todays knowledge about the overall structure of this elaborate enzyme mainly comes from genetic studies in yeast (Thornton and Toczyski, 2006) and cryo-EM analyses (Gieffers et al.,2001; Dube et al., 2005; Passmore et al.,2005; Ohi et al., 2007; Herzog et al.,2009).

Cryo-EM models of APC/C purified from human cells, Xenopus egg extracts (Gieffers et al.,2001; Dube et al.,2005; Herzog et al.,2009), budding yeast (Passmore et al.,2005) and fission yeast (Ohi et al.,2007) revealed that the APC/C is an asymmetric, triangular, molecule, 180 by 200 Å in size, and that it consists of an outer wall that, more or less, encloses a cavity. In the structure of the vertebrate APC/C two large domains can be distinguished, a relatively flat platform which closes the central cavity together with an “arc lamp”- like structural element. Within the enclosed cavity a prominent inner mass can be distinguished (Dube et al., 2005). The platform and the arc lamp show a certain degree of flexibility relative to each other, which is reduced upon binding of activator Cdh1 (Dube et al.,2005). This raises a possibility that an activator-induced conformational change has a role in the catalysis.

The APC/C can be rendered nonessential in budding yeast by genetic manipulation (Schwab et al.,1997; Thornton and Tocyszki, 2003), which allowed a systematic single subunit-deletion analysis and dissection of the APC/C into subcomplexes (Thornton and Tocyszki, 2006). The largest subunit Apc1 seems to be a scaffold that associates with two subcomplexes: a subcomplex composed of TPR subunits, Apc3 (Cdc27), Apc6 (Cdc16) and Apc8 (Cdc23); and the catalytic subcomplex, composed of Apc2, Apc11 and Doc1. The feasibility to isolate the catalytic core of APC/C was in agreement with studies of APC/C from human cells, where the catalytic core, Apc2 and Apc11, could be separated from the rest of APC/C (Vodermaier et al.,2003). Under high salt conditions the Apc2 /11 can be separated from the rest of the APC/C in a stable complex with Apc1, 4 and 5 (Vodermaier et al., 2003).

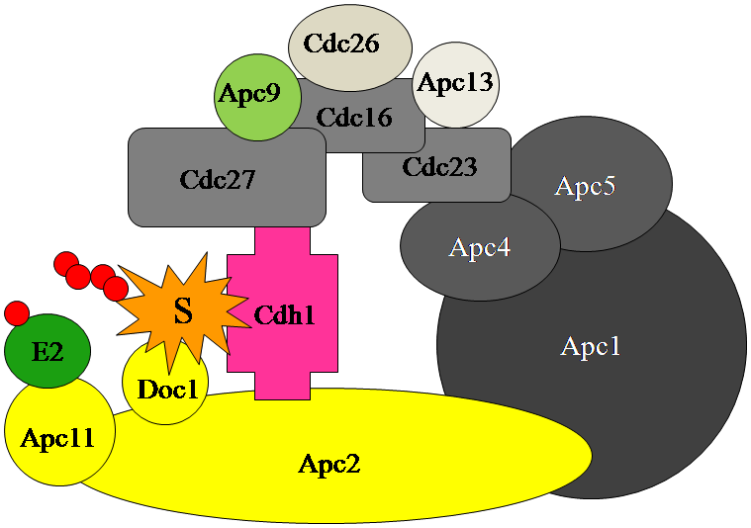

Figure 2. A model of APC/C in a ubiquitylation reaction based on subunit interactions. A more detailed description of subunit interactions is in the main text. The catalytic sub-complex is shown in yellow. The E2 enzyme is recruited by the RING finger Apc11. The cullin subunit, Apc2, might, in analogy to SCF complexes, serve as a scaffold that positions substrate receptor(s) and Apc11-bound E2. The TPR subunits are shown in light gray. Apc7 is a TPR subunit found only in vertebrate APC/C, and is not shown in this model. Cdc26 is a chaperone of Cdc16. Apc9 is found only in budding yeast. Cdc26, Apc13 (Swm1) and Apc9, seem to have a role in stabilizing the Cdc27 and Cdc16 association with the rest of the APC/C Substrates (S) are recruited to the APC/C by the activator, Cdh1 in this model, and possibly by a core APC/C subunit, Doc1. Activator proteins bind to Cdc27 via their IR tail, and it is suspected that they also interact with Apc2, which might place the the substrate bound activator close to the ubiquitin-charged E2 which is recruited by the Apc11. Modified after (Peters, 2006; Thornton et al., 2006).

APC/C collaborates with two E2 enzymes from the Ubc4/5 and E2-C family, in humans those are UbcH5 and UbcH10, respectively. UbcH5 can also function with other E3s while UbcH10 is APC/C-specific (Peters, 2006). RING–finger subunits underlie ubiquitin ligase activity by directly binding E2 enzymes (reviewed by Deshaies and Joazeiro, 2009). RING-finger subunit Apc11 interacts with the E2 enzyme Ubc4 (Gmachl et al.,2000; Leverson et al., 2000, Tang et al.,2001), RING-finger subunits of the SCF also interact with E2s (Zheng et al.,2000; Zheng et al.,2002). Recombinant Apc11 alone can form unanchored multiubiquitin in the presence of E1 and Ubc4. It can also ubiquitylate substrates, but with reduced specificity (Gmachl et al., 2000; Leverson et al., 2000). When UbcH10 was in the reaction a heterodimeric complex of Apc2 and Apc11 was the minimal catalytic module (Tang et al., 2001). All these results suggest that Apc11 alone, or together with Apc2, is the catalytic core of the APC/C, and that other subunits of the APC/C have a function in regulation and conferring substrate specificity. An interesting finding is that the binding of the substrate adaptor, Cdh1, is affected upon Apc2 deletion, indicating that Cdh1 interacts closely with the catalytic core (Thornton and Tocyszki, 2006). A small subunit Doc1 has been found to associate with the Apc2/11 catalytic core by binding to Apc2 (Thornton and Tocyszki, 2006). Doc1 deletion in yeast renders them temperature sensitive (Hwang and Murray, 1997), whereas in fission yeast and *Drosophila* it is an essential subunit (Kominami et al., 1998; Pal et al., 2007). The crystal structure of Doc1 (Wendt et al., 2001; Au et al., 2002) revealed that it almost entirely consists of a conserved DOC domain that has been found in other Doc1 orthologs (Grossberger et al., 1999). The DOC domain is present in multidomain proteins that have a role in ubiquitylation reactions and that also contain Cullin homology regions and HECT domains, which suggests that the DOC domain may be linked to ubiquitylation reactions (Grossberger et al., 1999, Kominami et al.,1998). It is interesting that the DOC domain folds into a “jelly-roll” structure that is found in both eukaryotic and prokaryotic proteins, that has a function in binding various ligands, such as sugars, nucleotides and polypeptides. Budding yeast Doc1 has been proposed to be the substrate receptor within the apo-APC/C (Passmore et al., 2003). Moreover, kinetic analysis of APC/C lacking Doc1 revealed that its processivity in the ubiquitylation reaction is reduced (Carrol and Morgan, 2002, Carrol et al., 2005). A reaction is processive if upon one APC/C binding event multiple ubiquitin molecules are assembled on the substrate. If the retention of the substrate on the APC/C during multiple rounds of ubiquitylation reactions depends on its direct binding to Doc1 is still not clear. Human Doc1 can bind to Cdc27,

one of tetratrico peptide repeat (TPR)-containing subunits that were found in vertebrate APC/C (Wendt et al., 2001). The TPR motifs are thought to mediate protein-protein interactions. A single TPR is composed of a 34 amino acid residue stretch, folded into two anti-parallel α-helices. Multiple repeats are packed together to form a protein-interacting groove (reviewed in Blatch et al., 1999; D'Andrea and Regan, 2003). In APC/C subunit deletion studies in yeast TPR-containing subunits, Cdc16, Cdc23 and Cdc27, were found to cluster together in a subcomplex (Thornton and Tocyszki, 2006). Apc7 is a TPR subunit that has been found in vertebrates that is closely related to Cdc27 (Yu et al., 1998; Peters, 2006). Antibody labeling followed by cryo-EM analysis revealed the locations of TPR subunits in human and fission yeast APC/C (Herzog et al., 2009; Ohi et al., 2007). Cdc27 antibodies bound to the head-like protrusion at the end of the arc lamp domain. Cdc16 and Apc7 were located in the arc lamp domain, and are thought to be present in several copies (Herzog et al., 2009). Association of the TPR subdomain with the largest subunit Apc1 was dependent on Apc4 and Apc5 (Thornton and Tocyszki, 2006). Nothing is known about the function of Apc4 and Apc5. Apc4 is bioinformatically predicted to contain a WD40 propeller domain (Peters, 2002). Cryo-EM analysis of antibody labeled human APC/C has shown that Apc4 and Apc5 are located at the front bottom part of the platform domain (Herzog et al., 2009). The activator proteins Cdc20 and Cdh1 were shown to associate with Cdc27 and Cdc23 via their IR tail (Vodermaier et al., 2003; Kraft et al.,2005, Matyskiela and Morgan, 2009), a C terminal Ile-Arg motif conserved among activator proteins, that they share with Doc1, which was also shown to associate with Cdc27 (Wendt et al.,2001). Three yeast nonessential subunits, Cdc26, Apc13 (Swm1) and Apc9, seem to have a role in stabilizing the Cdc27 and Cdc16 association with the rest of the APC/C (Zachariae et al., 1996; Zachariae et al., 1998; Schwickart et al.,2004; Thornton and Tocyszki, 2006, Wang et al.,2009).

Although the subunit composition of APC/C is so complex, it is completely inactive without the assistance of activator proteins, Cdc20 and Cdh1 (reviewed in Vodermaier, 2001). Cdc20 and Cdh1 are essential for the activity of the APC/C and are conserved from yeast to humans. In budding yeast a third, meiosis-specific, variant of activator protein, Ama1, was identified (Cooper et al., 2000). It is thought that the activator proteins function as substrate adaptors for the APC/C (Burton and Solomon, 2005; Kraft et al., 2005), in analogy with the F-box proteins of SCF. However, it seems that activators have additional functions apart from

substrate recruitment (Kimata et al., 2008). Mitotic phosphorylation of APC/C promotes its association with Cdc20 in metaphase. Cdc20 recruits substrates to the APC/C until late anaphase when it is itself targeted for degradation and replaced by Cdh1 which functions as the substrate adaptor until the end of G1 (Figure 3). The current knowledge about the structure and function of activator proteins will be summarized in more detail in section 1.6.2.

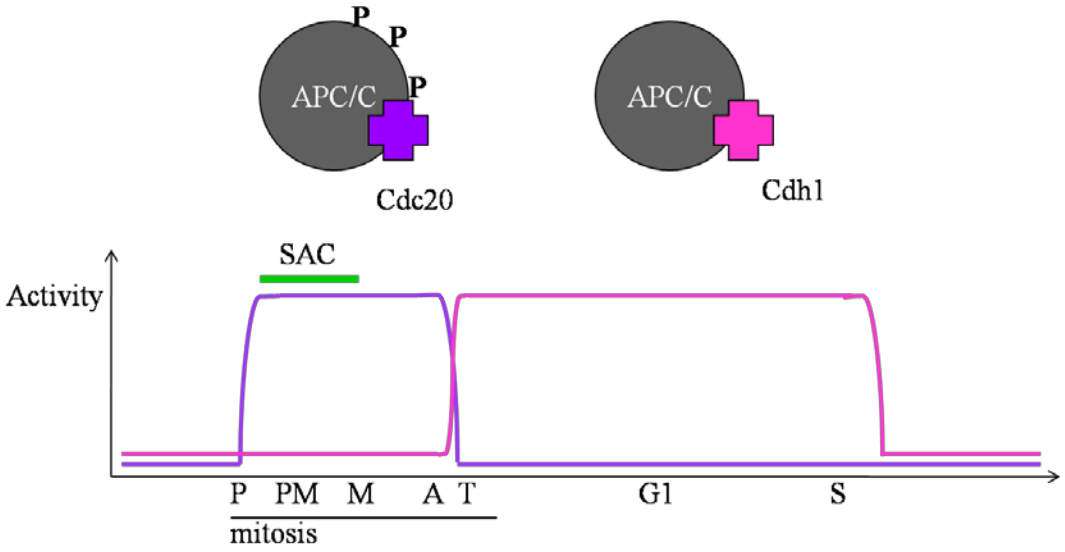

Figure 3. APC/C activation by activator proteins during the cell cycle. APC/C is activated in prometaphase (PM) by its association of Cdc20. Cdc20 binding to the APC/C is facilitated by mitosis-specific phosphorylation. APC/C-Cdc20 initiates degradation of cyclin A in prometaphase. Cyclin B and securin are also APC/C-Cdc20 substrates, however, their degradation is delayed until metaphase (M) by the spindle assembly checkpoint (SAC). In anaphase (A) and telophase (T) Cdh1 takes over the activating role of the APC/C and keeps it active until the end of G1. Modified from (Peters, 2006).

1.4 The roles of APC/C in mitosis

Tim Hunt's legendary discovery of cyclins "whose synthesis is strongly activated after fertilization" of sea urchin eggs and that "appear to be destroyed more or less completely every time the embryos divide" (Evans et al, 1983) was the first time when the result of the APC/C's activity was spotted. Cyclin, the activating component of the maturation-promoting factor (MPF) drives the cells into mitosis, and its ubiquitin-mediated destruction is required to allow the cell to

exit mitosis (Murray et al., 1989; Murray and Kirschner, 1989; Glotzer et al., 1991). About twelve years after the cyclin discovery the APC/C was identified as the E3 activity in clam and *Xenopus* egg extracts that is responsible for its destruction (Hershko et al., 1994, Sudakin et al., 1995; King, Peters et al., 1995). Cdc16 and Cdc23, two APC/C subunits, were identified in a genetic screen in budding yeast as genes required for sister chromatid separation at the metaphase-to-anaphase transition as well as for cyclin destruction in anaphase and G1 (Irniger, et al.,1995).

Cyclin B is a conserved inhibitor of mitotic exit, from yeast to humans. Its destruction is initiated at the metaphase-to-anaphase transition and is required for Cdk1 inactivation (Clute and Pines, 1999). Protein phosphatases subsequently dephosphorylate Cdk1 substrates which is a prerequisite for mitotic spindle disassembly, chromosome decondensation, cytokinetic furrow formation and nuclear envelope reassembly (reviewed in Sullivan and Morgan, 2007). The notion that cyclin B degradation is a prerequisite for cells to exit mitosis came from experiments in CSF arrested *Xenopus* egg extracts (Murray et al., 1989). Before fertilization vertebrate eggs are arrested in metaphase of meiosis II by an activity known as cytostatic factor (CSF) (Masui and Markert, 1971, reviewed in Tunquist and Maller, 2003). Fertilization-induced calcium burst in the egg relieves it from the arrest and the cell exits metaphase II. Calcium-mediated CSF release caused cyclin B degradation in *Xenopus* egg extracts. If, however, cyclin B was made indestructible by deleting 90 amino acids at its N terminus, the extract remained arrested in metaphase after addition of calcium (Murray et al., 1989). Cyclin B was the first substrate in which a “destruction box” (D-box) was identified, (Glotzer et al., 1991), a nine amino acid long motif located at the amino-terminus of cyclin B, that the APC/C generally recognizes in its substrates. Recognition motifs in APC/C substrates will be described in section 1.5.

The role of APC/C in regulating sister chromatid separation is one of its two essential functions in yeast (Thornton and Toczyski, 2003). At the beginning of mitosis the replicated sister chromatids are held together by a ring-like protein complex called cohesin (reviewed by Nasmyth, 2001). By metaphase all the chromosomes are condensed and aligned at the cells equator, captured by microtubules emanating from the opposing spindle poles. Only when every single chromatid pair is bioriented and properly attached, a protease called separase is allowed to cleave the cohesin subunit Scc1, which releases the sister chromatids to be pulled apart by the spindle apparatus. The importance of the APC/C here comes in spotlight. Separase that cleaves

cohesin cannot perform its function while it is bound to its chaperone and inhibitor, securin. Only when all the requirements for faithful sister chromatid segregation have been met the APC/C gets activated, targets securin for destruction and thereby releases separase to initiate anaphase (reviewed by Nasmyth, 2005). Another layer of control of the APC/C over anaphase has been found in *Xenopus* egg extracts (Stemmann et al., 2001). Phosphorylation of separase by cyclinB-Cdk1 and its direct binding inhibits the activity of separase and it seems that both securin and cyclin B have to be destroyed to allow its activation.

If you are a metazoan, the APC/C has a third essential role in your cells. High APC/C activity at the end of mitosis is maintained in the subsequent G1 phase by replacement of the mitosis-specific activator Cdc20 with G1-specific Cdh1. Low Cdk1 activity at the end of mitosis allows phosphatases to dephosphorylate Cdh1, thereby promoting its association with the APC/C. High APC/C-Cdh1 activity throughout G1 phase keeps the cyclin levels low, and thereby creates a window in the cell cycle with low Cdk activity which is a prerequisite for pre-replication complex (pre-RC) assembly at the origins or replication. Pre-RCs assembly is inhibited by Cdk- mediated phosphorylation of its components (reviewed in Diffley, 2004), and, in metazoans, also by a protein called geminin. Geminin is present in the nucleus in S, G2 and M phase of the cell cycle and prevents the incorporation of Mcm2-7 subunits into the pre-RC during these phases of the cell cycle. Geminin is degraded at the metaphase-to-anaphase transition and throughout G1 as a result of APC/C-Cdh1 mediated ubiquitylation (McGarry and Kirschner, 1998).

1.5. Degradation motifs in APC/C substrates and substrate ordering

The targets of the APC/C contain amino acid sequence motifs, so called degrons, usually located in low complexity regions of the protein, that are required for their ubiquitylation. The most widespread motif is the “destruction-box” (D-box), a somewhat degenerate motif, a variation of the sequence RxxLxxxxN (R is arginine, L is leucine, N is asparagine, x is any amino acid). Mutation of any of these three residues stabilizes the substrate (Glotzer et al., 1991; King et al., 1996). Another short motif that is often present in APC/C substrates is the KEN box, with the basic sequence KENxxxN (K is lysine, E is glutamate) (Pfleger and Kirschner, 2000).

All APC/C substrates contain one or more copies of each degradation motif, often in combination. Other degrons have also been described in certain APC/C substrates, such as GxEN in XKid (Castro et al., 2003), or the A-box in Aurora A (Littlepage and Ruderman, 2002). Mutation of these recognition motifs tends to inhibit degradation of the substrates in vivo, but these sequences alone are generally not sufficient to target a protein for ubiquitylation. One of the reasons for this is the fact that the degron itself lacks a conserved lysine residue capable of accepting ubiquitin (King et al., 1996). It also seems likely that the context in which the degron is placed is important. If the D-box of cyclin B is replaced with a KEN box, Cdh1, but not Cdc20, can promote its degradation. This was possible only if the KEN box is placed in the location where the D box was and not if it was placed anywhere else in within the N terminus of cyclin B (Zur and Brandeis, 2002). A peptide encompassing the D box of fission yeast cyclin B, Cdc13, alone has to be 35 times more concentrated than a 70 amino acid long fragment of Cdc13 that contains the same D box to compete for full length Cdc13 degradation in *Xenopus* egg extract (Yamano et al., 1998). It is sufficient to fuse a D-box-baring fragment of *Xenopus* cyclin B (amino acids 13-66) to Protein A to render it degradable in a cell cycle dependent manner, whereas a fragment of 13-53 amino acids is not (Glotzer, 1991). Unlike D box-containing fragments of cyclin B, D-box-containing fragment of *Xenopus* cyclin A1 (amino acids 3-91) was unable to render Protein A unstable (King et al., 1996). Studies of chimeric proteins have shown that fusing the D-box-containing amino-terminus of *Xenopus* cyclin A1 to the carboxy-terminus of cyclin B1 rendered the fusion protein stable, and it was not the case the other way around (Klotzbuecher et al., 1994). One of the best characterized model substrates of APC/C, the budding yeast Hsl1, can be reduced to a fragment of 200 amino acids ($Hsl1^{667-872}$) and still be degraded with the same kinetics as the full length protein. Further truncation at the N terminus of the fragment renders it indestructible, although both D and the KEN box are still present within the remaining Hsl1 fragment (Burton and Solomon, 2001).

Substrate ordering, or the correct sequence of APC/C-mediated ubiquitylation reactions, ensures orderly progression of events in mitosis and G1. This is firstly ensured by sequential association of APC/C substrate adaptors, Cdc20 and Cdh1, with the APC/C. Cdc20 recognizes a set of substrates from metaphase until end of anaphase, and is then replaced by Cdh1 which recognizes specific substrates until the end of mitosis and throughout G1. A nice example of substrate ordering through sequential recruitment to the APC/C by specific activators is budding

yeast Pds1, Clb2 and Ase1 (Amon et al., 1994; Schwab et al., 1997; Visintin et al., 1997; Juang et al., 1997). Pds1, but not Clb2 and Ase1, is specifically recognized by Cdc20 in metaphase, which leads to Pds1 destruction and sister chromatid separation. At this time Ase1, involved in microtubule bundling in cytokinesis, should stay intact, as well as Clb2 whose destruction causes disassembly of the spindle and decondensation of chromosomes. Pds1 destruction, along with sister chromatid separation, triggers Cdc14 phosphatase activation, which leads to decline of Clb2-mediated phosphorylation. Dephosphorylation of Cdh1 promotes its association with and substrate recruitment to the APC/C. Ase1 and Clb2 are Cdh1-specific targets which ensures that cytokinesis and mitotic exit occurs only after the sister chromatids have been separated.

An additional mechanism of substrate ordering is substrate-intrinsic and based on the processivity by which the substates are ubiquitylated by the APC/C (Rape et al., 2006). According to this model, more processive substrates are degraded before the less processive ones, because they accumulate longer ubiquitin chains upon single binding to the APC/C. This allows them to reach the chain length threshold faster, and also makes them less sensitive to the action of deubiquitinating enzymes (Rape et al., 2006; Stegmeier et al., 2007). It could be that the sequential degradation of Cyclin A, cyclin B and cyclin B3 observed in *Drosophila* embryos is also governed by this mechanism. These three substrates are ubiquitylated by APC/C-Cdc20, however, cyclin A is degraded before cyclin B, which is in turn degraded before cyclin B3. This order of degradation has been proposed to be important for proper mitosis progression, since it was found that stable cyclin A arrests cells transiently in metaphase, stable cyclin B arrest cells in early anaphase, and stable cyclin B3 later in anaphase (Sigrist et al., 1995).

Two peculiar substrates that are degraded already in prometaphase, Nek2A and cyclinA, are recognized by the APC/C somewhat differently than a typical substrate. Nek2A has been shown to be recruited to the APC/C in a Cdc20-independent manner via its C terminal MR tail, which resembles the TPR-binding motif found in APC/C activators and Doc1, the IR tail (Hayes, et al., 2006). The ubiquitylation of Nek2A by the APC/C, however, still requires the assistance of Cdc20 (Hames et al., 2001; Kimata et al., 2008). Degradation of cyclin A depends on its binding to Cdk, as a mutation in cyclin A that abolishes Cdk binding stabilizes it (Stewart et al., 1994, Geley et al., 2001; Sorensen et al., 2001; Wolthuis et al., 2008). Cdk binding is not sufficient for cyclin A ubiquitylation because deletion of a D-box containing segment of cyclin A, with Cdk1 binding domain intact, stabilizes the protein (Kobayashi et al., 1992; Geley et al., 2001). Type A

cyclins have a D box sequence that is instead of 9 amino acids (RxxLxxxxN), 10 or 11 amino acids long (RxxLxxxxxxN), and this feature is conserved among cyclin A1 and A2 molecules across species, respectively (Geley et al., 2001). Deletion of this motif alone does not stabilize human cyclin A2, but if additional 30 amino acids downstream of this sequence are deleted cyclin A2 is stabilized. Deleting these 30 amino-acid without the D box sequence does not stabilize the protein, indicating that this D box does function as a degradation signal. From this result it was concluded that A type cyclins are targeted for ubiquitylation by an "extended D box" (Geley et al., 2001). There is still much to be learned about the features of the APC/C target proteins that promotes their timely recognition by the APC/C.

1.6. Regulation of the APC/C activity

It is crucial for the cell to segregate its replicated chromosomes only when every single sister chromatid pair is properly attached and bioriented on the mitotic spindle; to disassemble the mitotic spindle, decondense chromosomes and split the cytoplasm in two only when the two chromosome sets have been well separated; and to replicate its genome once, and only once, in the cell cycle. All these events are governed by regulated proteolysis of its key regulators, initiated by the APC/C-mediated ubiquitylation. It is, therefore, essential for the cell to tightly regulate the activity of the APC/C. The APC/C activity is controlled by reversible phosphorylation; by sequential and regulated association of its activators; and by association of inhibitors, one of which is the effector of the spindle assembly checkpoint (SAC), the mitotic checkpoint complex (MCC).

1.6.1. Regulation of APC/C by phosphorylation

Several subunits of the APC/C are phosphorylated in mitosis (King et al., 1995; Peters et al.,1996; Yamada et al.,1997). These modifications were implicated in mitotic APC/C activation, because dephosphorylation of APC/C reduced its activity (Lahav-Baratz, et al.,1995; Peters et al.,1996; Fang et al., 1998; Shteinberg et al.,1999). This inactivation was reversible, as *in vitro*

phosphorylation of the dephosphorylated APC/C with Cdk1 could restore its activity (Lahav-Baratz et al., 1995). The activity of interphase APC/C can be stimulated by Cdk1-mediated phosphorylation (Sudakin et al., 1995). Analysis of APC/C purified from mitotic and S phase HeLa cells by mass spectrometry revealed that 9 out of 11 subunits were phosphorylated during these two phases of the cell cycle, and the great majority of phosphosites were mitosis-specific (Kraft et al., 2003). 30 out of 34 mitosis-specific phosphosites were found in the subunits Apc1, Cdc27, Cdc16 and Cdc23. The phosphorylation of these subunits in mitosis causes a retardation in their gel-mobility (Peters et al., 1996; Kraft et al.,2003). One of the effects of mitosis-specific phosphorylation of APC/C subunits seems to be stimulation of the activator protein Cdc20 association, as *in vitro* phophorylation of APC/C increases (Kraft et al.,2003) and dephosphorylation reduces (Shteinberg et al.,1999; Kramer et al.,2000) the amount of recombinant Cdc20 that can be loaded onto APC/C. Mutation of all potential phosphosites to alanines in TPR subunits, five in Cdc27, or six in Cdc16, reduces the amount of Cdc20 that co-purifies with APC/C (Rudner and Murray, 2000). Whether phosphorylation has additional functions in stimulating APC/C in mitosis is still not clear. The activator subunit Cdc20 was also found to be phosphorylated in mitosis, but this phosphorylation seems not to affect its ability to bind or activate APC/C (Kramer et al., 2000). It was proposed that the phosphorylation of Cd20 has a role in the spindle assembly checkpoint function (Tang et al., 2004; Chung and Chen, 2003). In vertebrates the two main kinases are known to stimulate APC/C activity in mitosis are Cdk1 and Plk1 (Patra and Dunphy, 1998; Descombes and Nigg, 1998), but Cdk1 seems to have a major role. *In vitro* phosphorylation experiments have shown that many, but not all *in vivo* APC/C phosphosites are created by Cdk1/cyclinB/p9 complex, a few are created by Plk1, and that the efficiency of direct APC/C phosphorylation is increased if both kinases act combined (Kraft et al.,2003; Golan et al., 2002). There are indications that Plk1 maintains the APC/C in an active state when cyclin B is degraded by antagonizing the activity of a microcystin-sensitive phosphatase (Brassac et al., 2000). It was proposed that in fission and budding yeast, as well as in human cells protein kinase A (PKA) phosphorylates APC/C and thereby inhibits APC/C mediated proteolysis (Yamashita et al., 1996), but its mechanism and physiological relevance still remains to be clarified. Cdk1 also phosphorylates the APC/C activator Cdh1 in mitosis, and thereby prevents its association with the APC/C (Kramer et al., 2000). The kinase which causes the inactivation of APC/C-Cdh1 at the end of G1 seems to differ across species. In *Drosophila*

overexpression of cyclin E stabilizes APC/C substrates. This could be due to cyclin E-mediated Cdh1 phosphorylation (Knoblich et al., 1994). In budding yeast Cdh1 homolog, Hct1, is inactivated by Cln1, Cln2 and Clb5 which are refractory to the activity of Hct1 (Schwab et al., 1997; Zachariae et al., 1998). Once established the Cdk1 activity can be maintained by cyclins susceptible to Hct1 activity, such as Clb2 and Clb3, during mitosis. Dephosphorylation of APC/C and Cdh1 upon exit from mitosis is mediated by Cdc14 phosphatase in budding yeast (Visintin et al., 1998, Jaspersen et al., 1999; reviewed by Stegmaier and Amon, 2004). Phosphatases in vertebrate cells with analogous activity have not yet been described. Dephosphorylation and activation of Cdk1 inhibitor Sic1 in yeast also contributes to dephosphorylation of Cdh1, which allows Cdh1 association with APC/C and maintenance of its activity until the end of G1 phase. In budding yeast dephosphorylation of Cdh1 causes its export from the nucleus to the cytoplasm (Jaquenoud et al., 2002), whereas in HeLa cells this seems not to be the case (Miller et al., 2006).

1.6.2. APC/C activators Cdc20 and Cdh1

The activity of the APC/C is controlled by the regulated binding of one of several activator proteins. In mitosis, the activator Cdc20 (Fizzy in *Drosophila*, Slp1 in *Schizocaccharomyces pombe*) is required for APC/C activity in anaphase when the Cdk activity is high, whereas Cdh1 (Fizzy-related in *Drosophila melanogaster*, Srw1/Ste9 in *Schizocaccharomyces pombe* , Fzr1 in *Homo sapiens*) maintains its activity during late mitosis and G1 when the Cdk activity is low (reviewed by Yu, 2007). In meiotic cycle-specific activators have been described, Ama1 in budding yeast and Cort in *Drosophila* (Cooper et al., 2000; Swan et al., 2007). Cdc20 was one of 32 temperature-sensitive cell division cycle (*cdc*) genes found in a genetic screen in *Saccharomyces cerevisiae* (Hartwell et al., 1973), which was later characterized as a gene whose mutation causes chromosome losses in mitosis (Hartwell and Smith, 1985). Mutations in the *Drosophila* Fizzy gene caused cells in mitosis to arrest in metaphase (Dawson et al., 1993). In a screen for *cdc* genes required for APC-dependent proteolysis, Cdc20 was identified as a *cdc* gene required for APC- dependent degradation of Pds1, whereas Cdh1 (Cdc20 homolog 1), in budding yeast also known as Hct1 (Homolog of Cdc

twenty 1) was a factor required for APC-dependent degradation of Clb2 and Ase1 (Schwab et al., 1997; Visintin, et al., 1997). It was later shown that Cdc20 and Cdh1 directly bind to APC/C and activate its ubiquitin ligase activity toward cyclin B *in vitro* (Fang et al., 1998). Cdc20 and most genes that encode apo-APC/C subunits are essential for viability in yeast (Zachariae et al., 1998). Cdh1 is not essential for viability in yeast (Schwab et al., 1997; Visintin et al., 1997). In mammalian cells the APC/C is also essential for the completion of the cell-division cycle (Wirth et al., 2004), depletion of Cdh1 by RNA interference (RNAi) in human cells, however, does not significantly perturb the cell cycle (Qi and Yu, 2007) and Cdh1-deficient mice are viable (Garcia-Higuera et al., 2008).

Cdc20 and Cdh1 are highly conserved in all eukaryotes, and are characterized by the seven WD40 repeat domain in their C terminal region (Visintin et al., 1997). WD40 repeats fold into a rigid propeller-like structure, a secondary structure found in many proteins with different functions. No catalytic function has been attributed to the WD40-repeat propeller domain, instead it has been proposed to be ideal for protein-protein interaction function (reviewed in Smith et al., 1999). The folding of the WD40 propeller of Cdc20 and Cdh1, and thereby the activation of APC/C by these activators, is dependent on the CCT chaperonin complex, which was shown to associate with the activators throughout the cell cycle (Camasses, et al., 2003). Apart from the conserved WD40 motif several other short amino acid stretches in activators were found to be conserved. The carboxy terminal IR tail was shown to be required for activator binding to the Cdc27 TPR subunit of human and budding yeast APC/C (Vodermaier et al., 2003; Thornton et al., 2006; Matyskiela and Morgan, 2009), although the IR tail of Cdc20 seems to be dispensable for viability of yeast (Thornton et al., 2006). In the N terminal region of Cdc20 and Cdh1 a seven amino acid motif, the C-box, was shown to be essential for the activity of APC/C activators. The C-box promotes activator binding to the APC/C, but also to stimulate the activity APC/C in a ubiquitylation reaction. (Schwab et al., 2001; Vodermaier et al., 2003; Thornton et al., 2006, Kimata et al., 2008). A Cdh1 specific motif (CSM) motif was found MtCcs52A, the *Arabidopsis thaliana* homolog of Cdh1, which is conserved across species from yeast to humans, and was implicated in APC/C binding and activation (Tarayre et al., 2004).

There is increasing evidence that Cdc20 and Cdh1 function as substrate-specific adaptors for APC/C, analogous to the function of WD40-propeller containing F-box substrate adaptors of SCF, most likely by binding to the substrate via their WD40 domain (Hilioti et al, 2001; Schwab

et al, 2001; Burton and Solomon, 2001; Pfleger et al, 2001; Burton and Solomon, 2005; Kraft et al., 2005). However, substrate recognition has been attributed to the apo-APC/C as well. Tandem copies of the D box containing cyclinB fragment is able to pull down the apo-APC/C that is largely free of Cdc20 or Cdh1 from Xenopus egg extracts (Yamano et al., 2004). Yeast Doc1 is required for D box-dependent substrate processivity of APC/C in an *in vitro* ubiquitination reaction, suggesting that Doc1 could be the substrate receptor on apo-APC/C (Carrol and Morgan, 2002; Carrol et al., 2005). All these findings suggest that both the activators and the APC/C itself cooperatively bind substrates (Eytan et al., 2006; Matyskiela and Morgan, 2008, reviewed by Yu, 2007).

1.6.3. Mechanisms of APC/C inactivation and APC/C inhibitors

Inactivation of APC/C-Cdc20 at the mitotic exit occurs through APC/C-Cdc20 mediated degradation of cyclins and thereby inactivation of Cdk1. As a consequence of Cdk1 inactivation APC/C is dephosphorylated which allows Cdh1 association. APC/C-Cdh1-mediated ubiquitylation and degradation of Cdc20 inactivates the mitotic version of APC/C (Prinz et al., 1998; Shirayama et al., 1998; Huang et al., 2001). G1/S cyclin expression at the end of G1 phase causes phosphorylation of Cdh1 and supposedly its dissociation from the APC/C which thereby remains inactive until the next wave of Cdk activation at the mitotic entry. However, several reports suggest that Cdh1 remains associated with the APC/C during the interphase and that there are other mechanisms involved in the regulation of APC/C-Cdh1 activity. Several pseudosubstrates have been found that also inhibit APC/C-mediated ubiquitylation of substrates. Acm1 was found to associate with Cdh1 in budding yeast at the cell cycle stages when APC/C-Cdh1 activity is absent (Martinez et al., 2006). Acm1 interacts with its several D and KEN boxes with the substrate binding interface on Cdh1 and thereby prevents ubiquitylation of other substrates. Acm1 itself is a substrate of APC/C-Cdc20, and can be ubiquitylated by APC/C-Cdh1 but with very low efficiency. It is probably a very high affinity substrate which, by having a low off rate prevents other substrates binding (Enquist-Newman et al., 2008). This regulatory mechanism is reminiscent of the fission yeast meiotic APC/C inhibitor Mes1, which also competes with ubiquitylation of other substrates by being ubiquitylated itself (Izawa et al., 2005,

Kimata et al., 2008). In vertebrates cyclin A, but not cyclin E, mediates Cdh1 phosphorylation and dissociation from the APC/C (Lukas et al., 1999), which poses a question how cyclin A can inhibit APC/C-Cdh1 if it is itself a substrate of the same complex. In vertebraes Emi1 (early mitotic inhibitor 1), was found to be an E2F-inducible gene product which inhibits APC/C-Cdh1 at the G1/S transition and thereby allow accumulation of cyclin A (Hsu et al., 2002). In HeLa cells Emi1 was shown to associate with the majority of Cdh1 and APC/C in interphase by direct interaction with both Cdh1 and APC/C core which is dependent on a D-box sequence and ZBR (zinc-binding region) within Emi1, which was shown to compete with substrates for APC/C-Cdh1 binding and ubiquitylation *in vitro*. The ZBR function seems to, possibly by steric hinderance, inhibit the APC/C activity. If the ZBR is mutated Emi1 becomes an efficient D-box dependent APC/C-Cdh1 substrate (Miller et al., 2006). Emi1 in Xenopus egg extracts is able to inhibit both APC/C-Cdc20 and APC/C-Cdh1 by preventing substrate binding (Reimann et al., 2001a; Reimann et al., 2001b). Emi1 phosphorylation by Plk1 targets it for SCF-βTrCP1 ubiquitylation and degradation in prophase (Hansen et al., 2004). Emi1 homolog in *Drosophila* is a protein called “regulator of cyclinA 1“(Rca1) which specifically inhibits APC/C –Cdh1 and allows cyclin A accumulation in G2 (Grosskortenhaus et al., 2002).

In early mitosis a messenger RNA export factor Rae1 and nucleoporin Nup98 are reported to form a complex with APC/C-Cdh1 and thereby specifically inhibit APC/C-Cdh1-mediated ubiquitylation of securin (Jeganathan et al., 2005). The release of Rae1-Nup98 complex from the APC/C-Cdh1 coincides with the release of spindle assembly checkpoint proteins from APC/C-Cdc20 (spindle assembly checkpoint, SAC, will be described in the next section), but the mechanism of this release, and its coordination with the SAC is not clear. Another mechanism proposed to inhibit APC/C-Cdh1 at the end of G1 phase is the autoregulation of the E2 enzyme UbcH10. At the end of G1 the UbcH10 starts its autoubiquitylation and degradation, which allows cyclin A accumulation subsequent phosphorylation and inhibition of APC/C-Cdh1 (Rape and Kirschner, 2004).

1.6.3.1. The spindle assembly checkpoint

Duplicated sister chromatids are alingned at the metaphase plate prior to their segregation. This is achieved by capture of kinetochores by the microtubules of the mitotic spindle. Kinetochores are large protein structures embedded in centromeric regions of chromosomes (reviewed by Westermann et al., 2007; Musacchio and Salmon, 2007, Cheeseman and Desai, 2008, Santaguida and Musacchio, 2009). Far from being a simple microtubule-chromosome interface, the kinetochore is an elaborate molecular machine that controls and powers chromosome segregation by harnessing microtubule dynamics. Importantly, the kinetochore also functions as a signaling module that monitors its own assembly and microtubule attachment status, and in case the attachment does not satisfy certain criteria, produces a diffusible "wait anaphase" signal which inhibits the process of chromosome segregation. This surveillance mechanism that is active in prometaphase which prevents precocious sister chromatid separation is called the Spindle Assembly Checkpoint (SAC) (Figure 4). The effector of the SAC is the mitotic checkpoint complex (MCC), consisting of Mad2, BubR1, Bub3 and APC/C activator Cdc20, which acts by inhibiting the APC/C. SAC comprises many other components, kinases, motor proteins and structural components (reviewed by Musacchio and Salmon, 2007). The SAC proteins were shown to concentrate at unattached kinetochores in mitosis and are removed from kinetochores as the attachment process advances. The SAC monitors two aspects of microtubule-kinetochore interaction, the attachment and the tension exerted across the centromere (reviewed by Pinski and Biggins, 2005; Musacchio and Salmon, 2007).

Kinetochore capture by the mitotic spindle is a stochastic process, and will give rise to intermediate states of attachment. Non-bipolar attachments will the sensed by lack of stretching within the kinetochore and this intra-kinetochore stretching is essential for determining the state of checkpoint signaling (Maresca and Salmon, 2009; Uchida et al., 2009). Tensionless attachments are actively destabilized by the action of Aurora B kinase, which recruits SAC proteins (Ditchfield et al., 2003), and unattached kinetochores enter a new cycle of microtubule attachment until bipolar attachment is achieved (Tanaka et al., 2002; Lampson et al., 2004). Destabilization of microtubule-kinetochore interaction is thought to be achieved by Aurora B

mediated phosphorylation of Ndc80/Hec1 and Dam1 complexes, microtubule capture factors, (Cheeseman et al., 2002), which reduces their affinity for the microtubules (Cheeseman et al., 2006, DeLuca et al., 2006). The phosphorylation of kinetochore substrates was shown to depend their distance from the inner kinetochore where Aurora B resides, and these substrates become separated from the kinase as the attachment becomes bipolar (Liu et al., 2009). In cells in culture the SAC can be elicited by treatment with "spindle poisons". These drugs can cause destabilization (e.g. Nocodazol), or stabilization (e.g. Taxol) of microtubules. If the SAC is elicited by stabilizing the microtubules with Taxol, it can be overridden my inhibition of Aurora B (Ditchfield et al., 2003; Hauf et al., 2003).

Mad2 is recruited to unattached kinetochores by its binding partner Mad1 (Chen et al., 1996; Sironi et al., 2001; Shah et al., 2004). The fact that Mad2 is prominently localized to unattached kinetochores, and that kinetochores fully saturated with microtubules exhibit no detectable Mad2 suggested that Mad2 senses the microtubule attachment to kinetochores (Waters et al., 1998). There is increasing evidence that the MCC forms in a two-step process in which Mad2 binding to Cdc20 is required to make Cdc20 sensitive to its inhibition by BubR1 (Fang et al., 2001; Fraschini et al., 2001; Davenport et al., 2006; Burton and Solomon, 2007; Kulukian et al., 2009). Mad2-Cdc20 interaction involves a large conformational change in Mad2 which may be the limiting step for the MCC formation (Luo et al., 2002; Sironi et al., 2002). According to the "template" model the binding of Mad2 to Cdc20 is facilitated by initial Mad1-Mad2 binding at the unattached kinetochore. This interaction causes a large conformational change in Mad2, which is converted from the open form (O-Mad2) to a closed form (C-Mad2). The Mad1-C-Mad2 complex at the kinetochore serves as a template for soluble O-Mad2 to convert to C-Mad2 and thereby capture Cdc20 (DeAntoni et al., 2005; Luo et al., 2004; reviewed by Musacchio and Salmon, 2007). C-Mad2-Cdc20 complex can also serve as a template for the soluble O-Mad2, which results in "wait anaphase" signal amplification. Mad2-Cdc20 complexes have been detected in yeast and human cell lysates (Tang et al., 2001; Fang et al., 2002; Poddar et al., 2005), but Mad2 has also been isolated from yeast and human cell extracts as part of a mitotic checkpoint complex (MCC), which also contains Mad3/BubR1, Bub3 and Cdc20 (Fraschini et al., 2001; Sudakin et al., 2001).

A

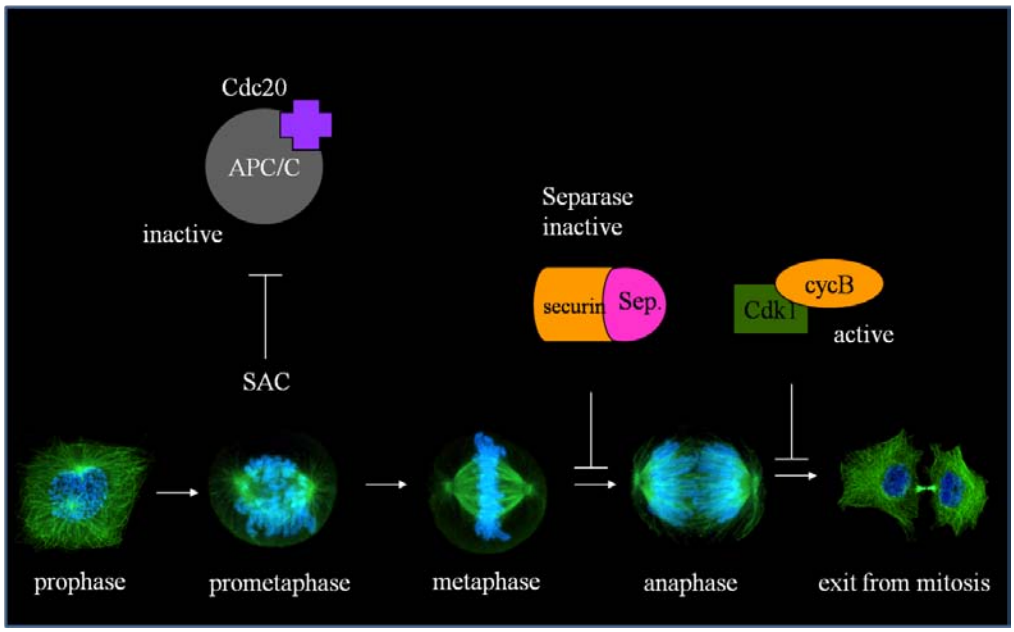

B

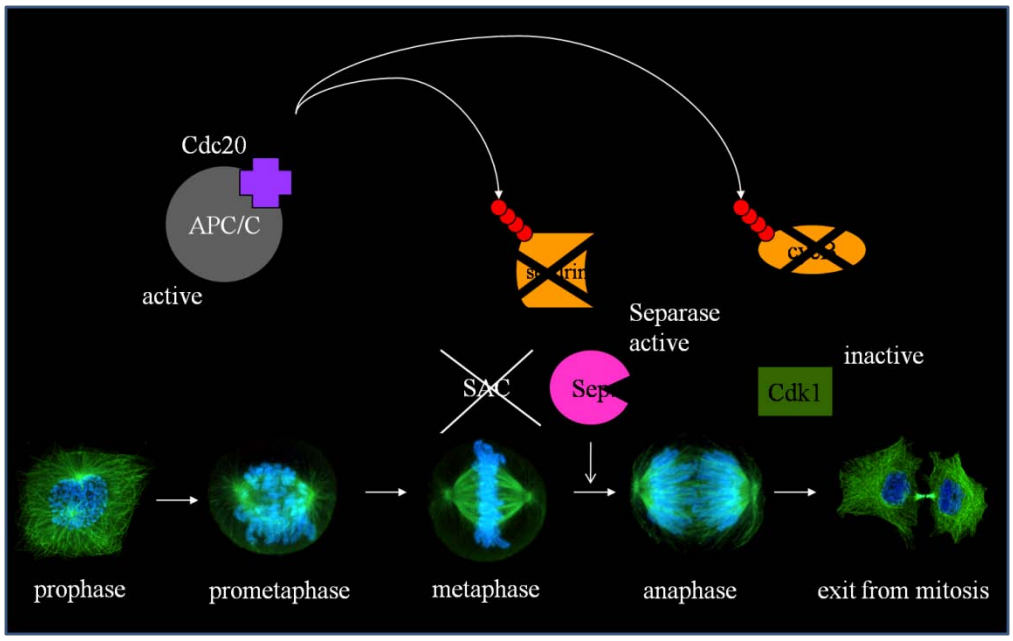

Figure 4. APC/C-Cdc20 is inhibited by the spindle assembly checkpoint (SAC). A. In prometaphase duplicated chromosomes are progressively attached to the mitotic spindle and bioriented. Until every single kinetochore of all the chromatid pairs is properly attached to the spindle APC/C-Cdc20 is kept inactive by the spindle assembly checkpoint (SAC). This prevents the degradation of two key mitotic APC/C substrates, cyclin B, the activator of Cdk1, and securin, the inhibitor of separase. B. Once all the sister chromatids are attached and bioriented, the SAC is inactivated, APC/C-Cdc20 gets activated and targets securin and cyclin B for destruction. This allows the protease separase to resolve cohesion between chromatid sisters and start anaphase. Inactivation of Cdk1 allows mitotic exit.

BubR1 is a kinase which, like Mad2, localizes to unattached kinetochores, but also microbutubule-occupied kinetochores that are not under tension (Skoufias et al., 2001). It contains a kinase domain at the carboxy terminus which is not required for interaction with other MCC components (Hardwick et al., 2000; Davenport et al., 2006), and seems not to be essential for the MCC assembly. The kinase activity of BubR1 is activated at the kinetochore by CENP-E (Mao et al., 2003, 2005), and kinetochore kinase activity of BubR1 is essential for cell viability (Kops et al., 2004). A "GLEBS-like" motif mediates the interaction of BubR1 with the WD40 propeller-containing protein Bub3, and this is necessary for BubR1 accumulation at kinetochores in early mitosis (Wang et al., 2001). Kinetochore localization of BubR1, as well as of Mad2 and CENP-E, is dependent on Aurora B kinase activity (Ditchfield et al., 2003).

Recombinant Mad2 and BubR1 can each inhibit APC/C-mediated ubiquitination reactions in vitro (Li et al., 1997, Fang et al., 1998; Fang, 2002; Tang et al., 2001a) but MCC isolated from HeLa cells is much more potent in this assay (Sudakin et al., 2001). The mechanisms of MCC inhibition of the APC/C proposed in the literature vary. *In vitro*, binding of recombinant Mad2 or BubR1 to Cdc20 prevents the association of Cdc20 with APC/C (Reimann et al., 2001; Tang et al., 2001a), however, these proteins could also be detected in complex with APC/C bound to Cdc20 (Kallio et al., 1998; Morrow et al., 2005; Braunstein et al., 2007). High-salt treatment or Cdc20 ubiquitination causes dissociation of Mad2 and BubR1 from the APC/C, and increases APC/C activity, indicating that Mad2 and BubR1 can inhibit APC/C by physical interaction (Braunstein et al., 2007; Reddy et al., 2007). For Mad2 it has also been proposed that it inhibits APC/C by reducing substrate release from Cdc20 (Pfleger et al., 2001), and for Mad3 it has been shown that it binds to Cdc20 as a pseudosubstrate and prevents the association of substrates with Cdc20 (Burton and Solomon, 2007; Malureanu et al., 2009).

Once all the chromosomes are properly attached and bioriented, the SAC is inactivated which leaves APC/C free to ubiquitylate its substrates. Several mechanisms contribute to SAC inactivation. The key mechanism is the removal of SAC proteins from the kinetochore, that depends on dynein motility along microtubules (Howel et al., 2001; reviewed by Musacchio and Salmon, 2007). The Mad2 positive feedback loop predicted by the "template" model, is dampened by $p31^{comet}$ which competes with O-Mad2 for binding to C-Mad2 that is bound to either Mad1 or Cdc20 (Xia et al., 2004; Vink et al., 2006). Once the SAC signaling from the

kinetochore is shut off, the MCC assembled on the APC/C should also disassemble to allow activity of the APC/C. There are indications that this is facilitated by UbcH10- and APC/C-mediated ubiquitylation of Cdc20 (Reddy et al., 2007)

The spindle assembly checkpoint (SAC) delays degradation of cyclin B and securin until all the chromosomes are properly attached, however this does not seem to affect cyclin A and Nek2A degradation which starts already in prometaphase (Geley et al., 2001; den Elzen and Pines, 2001; Hames et al.,2001). Nek2A has been shown to be recruited to the APC/C in a Cdc20-independent manner via its C terminal MR tail, which resembles the TPR-binding motif found in APC/C activators and Doc1, the IR tail (Hayes, et al., 2006). For cyclin A it has been proposed that its degradation requires Cdk binding, as a mutation that abolishes Cdk binding stabilizes cyclinA (Stewart et al., 1994, Geley et al., 2001; Wolthuis et al., 2008). It is not clear what the biological relevance of early, SAC-independent, degradation of cyclin A and Nek2A is. There are several possible scenarios how the early prometaphase substrates circumvent the SAC-mediated inhibition of the APC/C (see Discussion). It will be important to address these questions in the future.

1.7. The aim of this study

The aim of this project was to understand how substrates are recruited to APC/C and if this process is controlled by the spindle assembly checkpoint (SAC).

Not much is known about the interactions of APC/C with its activators and substrates in mechanistic terms. Starting from the finding that the WD40 propeller region of activators is implicated in substrate recognition, I first asked whether the WD40 domain is sufficient for substrate binding, and whether there is specificity in this binding conferred by the degradation motifs within the substrates. I also aimed to purify the WD40 domain in complex with a substrate for structure determination by X-ray crystallography, which would provide an insight into which amino acid residues within the activator and the substrate are involved in their interaction and offer an explanation for what determines the specificity of this interaction.

I have also addressed the question if the stimulation of APC/C in a ubiquitylation reaction by activator proteins stems from solely recruiting substrates to the APC/C or they have additional

activating functions. It has been observed that the flexibility of the APC/C is reduced upon Cdh1 binding (Dube et al., 2005), which suggests a possibility that Cdh1 binding has a role in the catalytic activity of the APC/C. Activator proteins interact with the APC/C via two conserved motifs, the C-box and the IR tail. If the IR tail is deleted, the activator binding is abolished, suggesting that the IR tail is the major APC/C-binding motif. Mutation of the C box also influences APC/C binding, but has less effect than the IR tail deletion. Mutation in the C-box, however, completely abolishes the activity of the APC/C in a ubiquitylation reaction. One of the questions addressed in my project was whether the Cdh1 binding deficiency upon C-box mutation was the only cause of its inability to activate the APC/C in a ubiquitylation reaction, and if this mutation affects substrate recognition by the APC/C-Cdh1.

Ubiquitylation of substrates in prometaphase by the APC/C is inhibited by the SAC and this inhibition is mediated by MCC that binds to the APC/C. How the MCC inhibits the APC/C was not known. The fact that one of the components of the MCC, BubR1, binds Cdc20 as a pseudosubstrate suggests that the MCC prevents substrate binding to the APC/C. I tested this possibility in an *in vitro* substrate binding assay in which I compared APC/C molecules isolated from cells in different SAC conditions in their ability to bind a variety of different substrates.

2. Results

2.1 Does the substrate bind the APC/C activator-independently?

APC/C activation requires the association of one of two related activator proteins, Cdc20 and Cdh1. Based on several studies (Hilioti et al, 2001; Schwab et al, 2001; Burton and Solomon, 2001; Pfleger et al, 2001, Burton et al, 2005; Kraft et al, 2005) it is thought that the activators have a role in recruiting the substrates to the APC/C, analogously to the substrate adaptors of the SCF complexes. However, several studies suggest that substrates are not recognized by activators alone. For example, a mutation in the D box of Clb2 or Cdc5 in budding yeast does not abolish their binding to Cdh1 but does reduce substrate proteolysis in vivo (Schwab et al, 2001). It is important to mention that an APC/C that lacks the Doc1 subunit in budding yeast cannot bind substrates in a native gel APC/C binding assay, although the binding of Cdh1 is intact (Passmore et al, 2003). Removal of Doc1 increases the rate of substrate dissociation from the active site, resulting in a decrease in reaction processivity (Carrol et al., 2005, Carol and Morgan, 2002; Matyskiela and Morgan, 2009). It was found that the presence of substrates stimulates activator binding to the APC/C (Burton et al., 2005; Matyskiela and Morgan, 2009) suggesting that a substrate binding surface on APC/C must exist. Finally, there are two reports about the interaction between substrate and the APC/C in the absence of activator (Yamano et al., 2004; Eytan et al., 2006). What is important to point out is that Eytan et al. reported that in the preparations they used the APC/C contained traces of Cdc20, therefore, strictly speaking, they did not examine the apo-APC/C binding to the substrates. Experiments with APC/C from Xenopus egg extracts clearly showed that a substrate is able to bind the APC/C directly and that this binding was Fizzy independent (Yamano et al., 2004), which is contradicting the result from an experiment with budding yeast APC/C where no substrate binding at all was detected unless Cdh1 was present (Burton et al., 2005).

All the above listed data supports a model of multivalent substrate recognition by the APC/C and its activators, whereby both the APC/C and the activators contribute to the substrate binding (reviewed by Yu, 2007). I have tried to answer the question whether

apo-APC/C and Cdh1 can bind substrates independently of each other by using purified components. First I wanted to see if activators can stimulate substrate binding to human APC/C.

2.1.1 Activators stimulate substrate binding to the interphase and mitotic APC/C

I tested if the activators can stimulate the activity of APC/C isolated from mitotic HeLa cells. Mitotic HeLa cells were obtained by prometaphase arrest induced by stabilizing microtubules with Taxol. Taxol treatment activates the spindle assembly checkpoint, which prevents mitotic progression by inhibiting the APC/C. To obtain an active mitotic APC/C, which is not inhibited by the SAC, the Taxol arrest was overridden by treating the Taxol-arrested cells with Hesperadin, a small molecule inhibitor of Aurora B kinase (see Materials and methods). The mitotic progression of cells released from the SAC arrest was prevented by the addition of the proteasome inhibitor, MG132 which prevented degradation of securin and cyclin B and thereby inhibited the onset of anaphase (This mitotic arrest protocol is schematically represented in Figure 23).

The APC/C was immunopurified from mitotic HeLa cell extracts with α-Cdc27 (Apc3) antibodies coupled to sepharose beads. Next the beead-bound APC/C was incubated with recombinant activators, Cdc20 or Cdh1, purified from Sf9 cells. The unbound activators were washed away with IP buffer (as described in Materials and methods) and the APC/C-activator complex was then incubated in 60nM solution of N70-2x-GST. N70-2x-GST is a tandem repeat of 70 N terminal amino acids of Cdc13, fission yeast cyclin B, C terminally fused to a GST tag (Figure 5A). A substrate specific recognition motif, the D box, is located within the N terminal 70 amino acids of Cdc13 (this somewhat artificial substrate was used in experiments by Yamano et al., 2004, as well as Eytan et al., 2006). N70-2x-GST with both D boxes mutated (dm) was used as a control for unspecific binding. The unbound N70-2x-GST was washed away and the bound complex was eluted off the beads with a solution containing 0.1M glycine, pH2. The eluates were analyzed by SDS-PAGE add Western blotting (Figure 5B). Mitotic APC/C is already bound to substantial amounts of endogenous Cdc20 (faster migrating band, “endo”). When no activators are loaded on the APC/C, binding of wild type (wt) but not of D box mutant

(dm) N70-2x-GST could be detected (compare lanes 1 and 2). Loading the APC/C with additional recombinant Cdc20 or Cdh1 stimulated the binding of APC/C to the wild type, but not to the D box mutant, N70-2x-GST (compare lane 7 with 8 and lane 9 with 10).

A

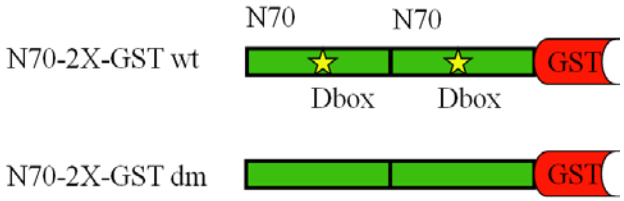

B

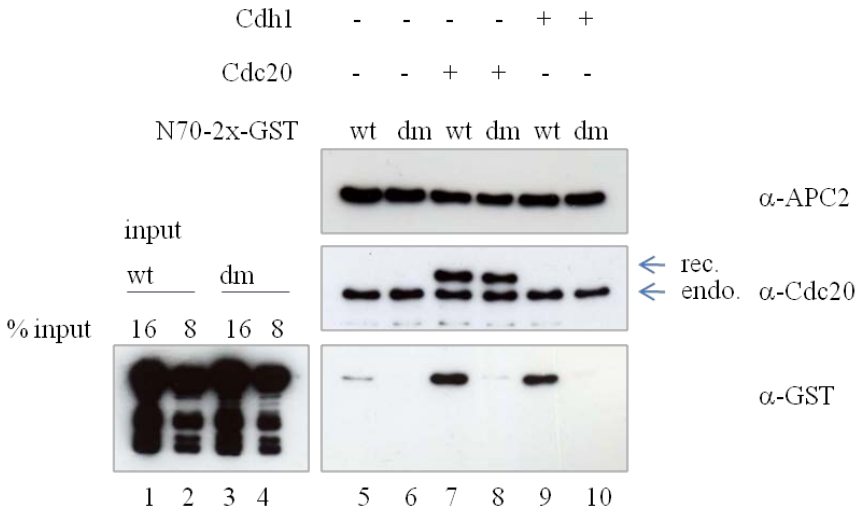

Figure 5. Activators stimulate substrate binding to the mitotic APC/C. A. Schematic representation of N70-2x-GST constructs. B. APC/C was immunopurified from mitotic HeLa cells in which the spindle assembly checkpoint has been inactivated (SAC off) with α-Cdc27 antibodies coupled to sepharose beads. Bead-bound APC/C was loaded with a 3μM solution of recombinant 6xHis tagged activators, either with Cdc20 or Cdh1, purified from baculovirus infected Sf9 cells. The unbound activators were washed away and the APC/C-activator complex was then incubated in 60nM solution of wild type (wt) or D box mutant (dm) N70-2x-GST. The unbound substrates were washed away and the APC/C-activator-substrate complex was eluted off the beads with 0.1M glycine pH2. The eluates were analyzed by SDS PAGE followed by Western blotting. It was blotted only for Cdc20, but not for Cdh1 in this experiment. rec= recombinant, endo= endogenous.

Next I tested if Cdh1 can stimulate the interphase APC/C in substrate binding. APC/C was immunopurified from exponentially proliferating HeLa cells with α-Cdc27 antibodies coupled to sepharose beads. Recombinant Cdh1 purified from Sf9 cells was loaded on the APC/C, the unbound activator was washed off with IP buffer (Materials and methods) and the bead-bound APC/C-Cdh1 complex was then incubated in 60nM or 15nM solution of GST-Hsl1$^{667-872}$. Hsl1$^{667-872}$ is a fragment (amino acids 667-872) of budding yeast Hsl1 kinase, a well described APC/C substrate that contains a KEN and a D box (Burton and Solomon, 2001). I have decided to use this substrate because it is more "natural" compared to the N70-2x-GST substrate, namely the distance between two degrons is not imposed by cloning. The fact that Hsl1$^{667-872}$ contains two different type of degrons, the D and the KEN box, will allow addressing questions regarding their individual importance in substrate recognition by the APC/C and its activators. The unbound substrate was washed away and the bound complex was eluted with the antigenic Cdc27 peptide. The eluates were analyzed by SDS-PAGE followed by Western blotting (Figure 6). The faster migrating band on the Cdh1 blot present in lanes 5-12 is the endogenous Cdh1 bound to the APC/C purified from the asynchronous population of HeLa cells. I assume that the presence of the endogenous Cdh1 allowed wild type (wt) GST-Hsl1$^{667-872}$ binding to the APC/C (lanes 7 and 11). GST- Hsl1$^{667-872}$ in which the D box and the KEN box have been mutated (dk) bound to a much lower extent (lanes 8 and 12). Adding recombinant Cdh1 to the APC/C increased the amount of wild type (wt, lanes 5 and 9), but not of the D box KEN box mutant (dk, lanes 6 and 10) substrate that it could capture. From this experiment I could conclude that Cdh1 can stimulate substrate binding to the interphase APC/C in a D box and KEN box specific manner.

A

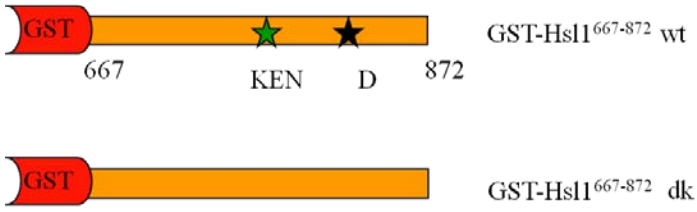

B

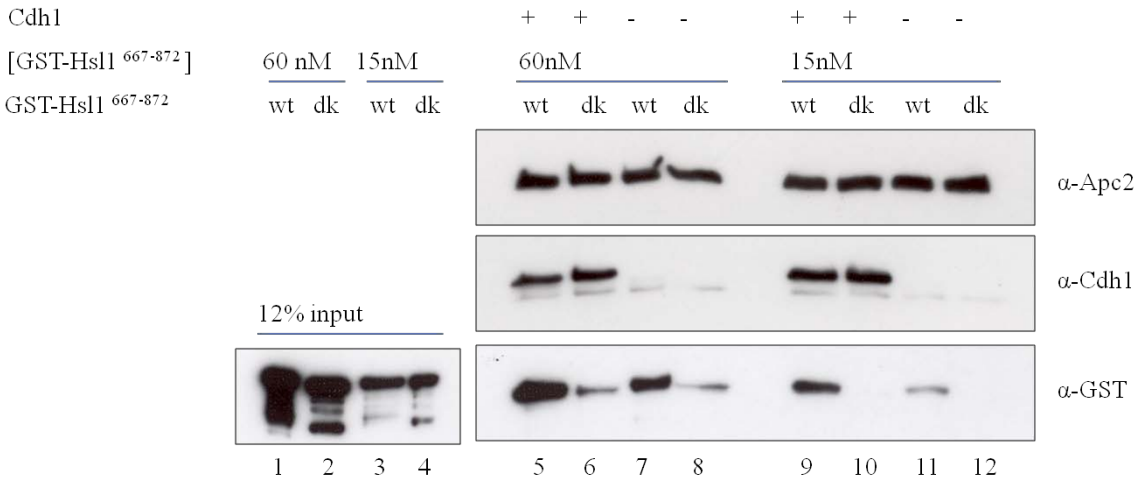

Figure 6. Cdh1 stimulates substrate binding to the interphase APC/C. A. Schematic representation of GST-Hsl1$^{667-872}$ constructs. B. The APC/C was immunopurified from logarithmically proliferating HeLa cells with α-Cdc27 antibodies coupled to sepharose beads. Bead-bound APC/C was loaded with a 0.23μM recombinant His6 tagged Cdh1 purified from baculovirus infected Sf9 cells. The unbound Cdh1 was stringently washed away and the APC/C-activator complex was then incubated in 60nM or 15nM solution of wild type (wt) or D box KEN box double mutant (dk) GST-Hsl1$^{667-872}$. The unbound substrates were washed away and the APC/C-Cdh1-substrate complex was eluted off the beads with 1mg/ml solution of Cdc27 antigenic peptide. The eluates were analyzed by SDS PAGE followed by Western blotting.

Having confirmed that the activators participate in substrate binding by the APC/C I wanted to see if apo-APC/C is able to bind substrates in the absence of activators. I assumed that the most straightforward method to obtain apo-APC/C would be to immunodeplete HeLa cell extracts of the Cdh1 or Cdc20 prior to APC/C IP. However, two antibodies against Cdh1 (one raised against the antigenic peptide 452 (RINENEKSPSQNRKAKDATSDNGKDC) and the other raised against a recombinant protein, antibody Sat106) failed to immunoprecipitate any significant fraction of Cdh1 from the log phase HeLa extracts (data not shown). A Cdc20 antibody raised against the antigenic peptide 450 (RWQRKAKEATGPAPSPMRAANRC), that could immunoprecipitate the free Cdc20 pool from mitotic HeLa extracts, failed to remove the Cdc20 fraction that was bound to the APC/C, even after three consecutive immunodepletion steps (data not shown).

Another approach I have used to purify apo-APC/C is the one used to separate APC/C^{MCC} from apo-APC/C particles analysed by cryo-EM (Herzog et al, 2009), starting with the hypothesis that during spindle assembly checkpoint arrest all the Cdc20 molecules are sequestered to the APC/C^{MCC} and that the remaining APC/C is devoid of any activator. A mixed population of APC/C molecules was first purified from HeLa cells under spindle assembly checkpoint arrest (SAC-on cells) by Cdc27 immunoprecipitation, followed by elution with a Cdc27 antigenic peptide. The eluate was then subjected to APC/C^{MCC} depletion with α-BubR1 antibodies and the remaining APC/C was then purified with an antibody against another APC/C subunit, Apc4. This fraction of APC/C, however, always contained traces of Cdc20, which could be observed after long exposure (Figure 7B, lanes 5, 6 and data not shown).

A

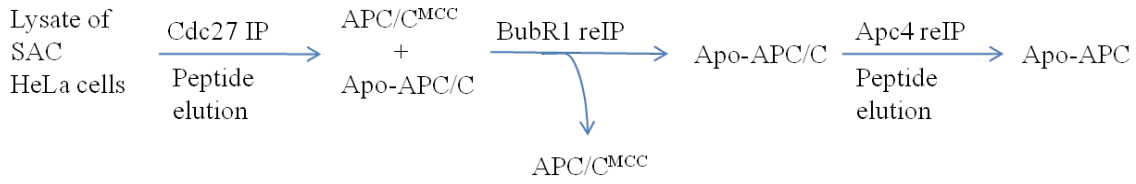

B

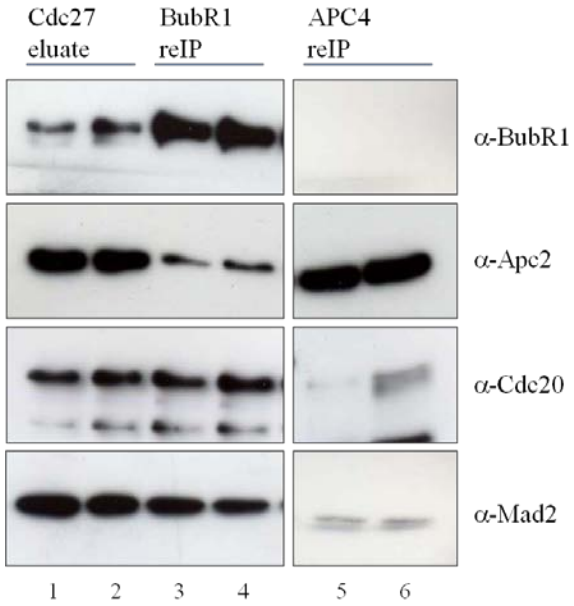

Figure 7. A small fraction of APC/C isolated from SAC on HeLa cells is bound to Cdc20

A. Schematic representation of APC/C^{MCC} and apo-APC/C purification from mitotic HeLa cells with an active checkpoint (SAC = spindle assembly checkpoint; IP = immunoprecipitation; reIP = re-immunoprecipitation). A mixed population of apo-APC/C and APC/C-MCC is purified from SAC-on cells by Cdc27 IP. APC/C-MCC is removed from the mixture by BubR1 IP, and the apo-APC/C that remained in the supernatant was immunopurified with α-Apc4 antibodies coupled to sepharose beads. B. Western blot analysis of Cdc27 peptide eluate, BubR1 reIP and Apc4 reIP glycine pH2.2 eluate.

To purify the apo-APC/C would probably be possible by inserting another Cdc20 depletion step into the purification procedure shown in Figure 7A, prior to Apc4 re-immunoprecipitation. This would, however, further dilute the APC/C solution that should be loaded onto substrates. Typically the concentration of APC/C would be reduced to about 90% of the initial concentration by every immunodepletion step (data not shown). High concentration of APC/C is essential in the substrate binding experiments, most probably because these interactions are weak. An ideal APC/C purification procedure for substrate binding assays therefore should involve a single step of immunoprecipitation. Although the described purification procedure could have perhaps been improved, I have decided to try other, more straightforward ways to purify the APC/C devoid of activators.

The activity of APC/C is regulated by reversible phosphorylation (Lahav-Baratz et al., 1995, Peters et al., 1996, Kotani et al., 1998) Although the precise role of mitotic APC/C phosphorylation is poorly understood, there are indications that it affects Cdc20 binding (Kramer et al, 2000, Rudner and Murray, 2000). Cdc20 binds preferentially to mitotically phosphorylated APC/C (Kallio et al., 1998, Kramer et al., 1998, 2000). APC/C phosphorylation by Cdk1, or Cdk1 and Plk1 combined, increased its ability to bind Cdc20 *in vitro* and correlated with 4-fold and 6-fold increase in APC/C activity, respectively. The increase in activity was due to Cdc20 binding (Kraft et al., 2003). It was found that the most heavily phosphorylated subunits of the APC/C are the TPR subunits, and it may be that this phosphorylation directly regulates the association of the IR tail of Cdc20 and APC/C's TPR subunits (Vodermaier et al., 2003, Kraft et al., 2003). From all these studies it seems likely that the mitotic phosphorylation of APC/C stimulates Cdc20 binding, however if dephosphorylation of APC/C causes Cdc20 dissociation was never tested. If that were the case, dephosphorylation of mitotic APC/C and washing away Cdc20 could be a way to obtain apo-APC/C.

2.1.2 Dephosphorylation of APC/C does not cause dissociation of Cdc20

To test if dephosphorylation of APC/C causes Cdc20 dissociation, the APC/C was immunoprecipitated from mitotic HeLa cells and the bead-bound APC/C was dephosphorylated with λ-protein phosphatase. After extensive washing (see Materials and methods) the complex was eluted with 0.1M glycine pH2 (Figure 8A). In parallel I have purified the APC/C from G2 HeLa cells and subjected it to the same treatment as mitotic APC/C/. The G2 APC/C should contain very little, if any, activators bound. I wanted to see if those trace amounts of activators could be removed by APC/C dephosphorylation. The efficiency of dephosphorylation of APC/C was verified by increased Cdc27 (Apc3) mobility of the mitotic APC/C caused by removal of phosphates (lanes 4, 5, and 6). Cdc20 as well as Cdh1, however, remained bound to the APC/C at the same levels as in the sample where APC/C was incubated in phosphatase buffer without λ-protein phosphatase (lanes 1, 2 and 3). The trace amounts of activators bound to G2 APC/C also remained the same after phosphatase treatment.

It is known that the TPR subunit Cdc27 is a docking site for Cdh1 and Cdc20 IR tails (Vodermaier et al.,2003; Thornton et al.,2006). In the experiment described above the APC/C was bound to beads coupled to antibodies against an epitope on Cdc27. To exclude the possibility that the activators could not be removed from the APC/C because the antibody somehow blocked their “exit route”, I immunoprecipitated the APC/C with antibodies against another APC/C subunit, Apc4 (Figure 8B). The APC/C was purified from mitotic HeLa cells, dephosphorylated with λ-protein phosphatase and washed extensively. The complex was eluted off the beads with the antigenic peptide solution. Again, the levels of Cdc20 bound to APC/C remained the same after APC/C dephosphorylation, regardless of whether the APC/C was anchored to the beads via Cdc27 or Apc4 subunit.

A

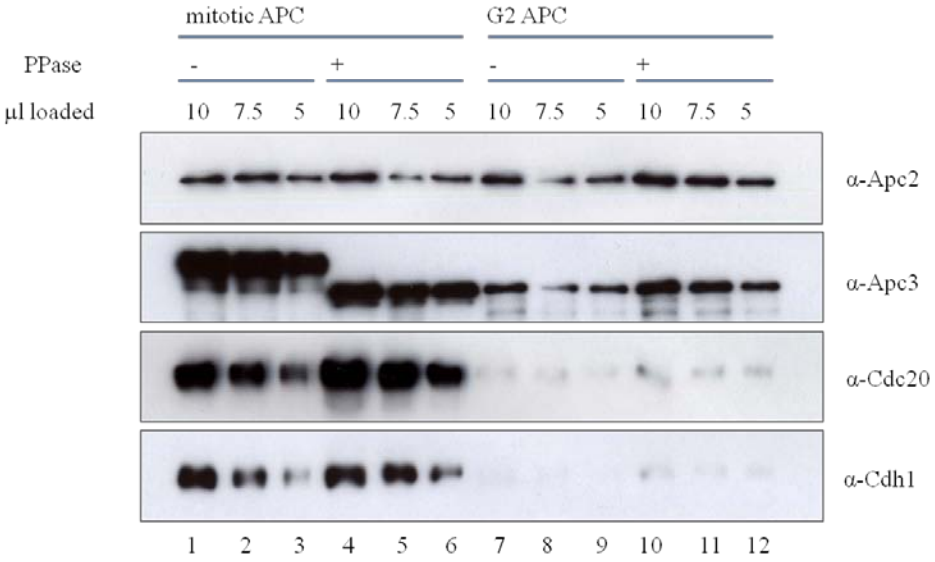

B

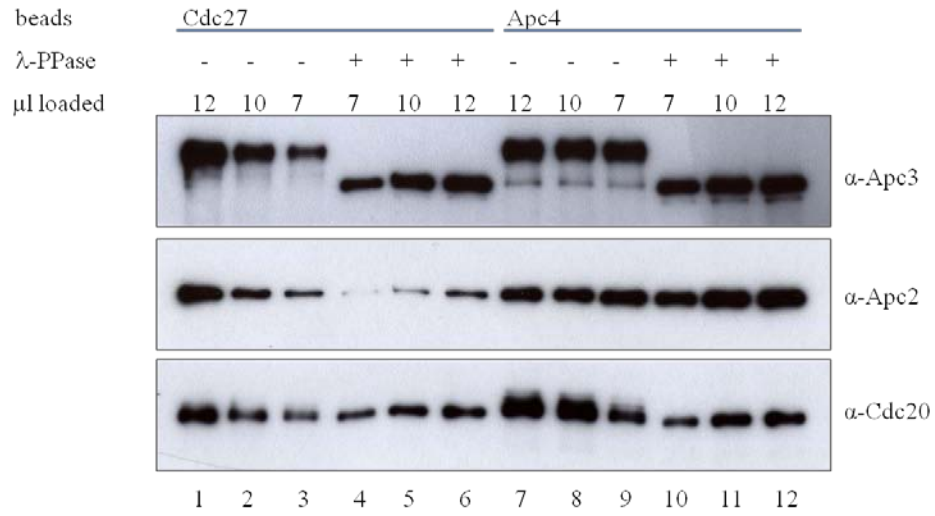

Figure 8. Dephosphorylation of APC/C does not cause Cdc20 dissociation. A. APC/C was immunopurified from mitotic (SAC OFF) or G2 HeLa cells with sepharose beads coupled to α-Cdc27 antibodies. Bead-bound APC/C was incubated in phosphatase buffer (see Materials and Methods) with (+) or without (-) λ-protein phosphatase (λ-PPase) for 30 minutes at 30°C. After extensive washing the complex was eluted off the beads with 0.1M glycine pH2. Three volumes of the eluates, 10, 7.5 and 5µl, were analyzed on SDS PAGE followed by western blotting. The phosphoshift of Cdc27 (Apc3) can be observed in the samples treated with λ-protein phosphatase (lanes 4, 5 and 6). B. APC/C was immunopurified from mitotic (SAC OFF) HeLa cells with sepharose beads coupled to α-Cdc27 or α-Apc4 antibodies. Dephosphorylation and washing was carried out as in (A), followed by elution of APC/C with a 1mg/ml solution of Cdc27 and Apc4 antigenic peptide, respectively.

Another reason for Cdc20 remaining bound to dephosphorylated APC/C could be that some unknown factors present in the cell remove it after APC/C dephosphorylation. It could be that the Cdc20 was not released from the dephosphorylated APC/C because these hypothetical factors were missing in the reaction. To test this I dephosphorylated the mitotic APC/C in the HeLa cell extract and only after this step the APC/C was immunopurified. After extensive washing the immunopurified APC/C was eluted with an antigenic peptide. Figure 9 shows that Cdc20 does not dissociate from the APC/C if the dephosphorylation occurred in the cell extract. Also Cdc20 remained bound to dephosphorylated APC/C in mitotic extracts regardless of whether the extracts were from HeLa cells in which the spindle assembly checkpoint was active (SAC on) or inactive (SAC off). A detailed description of the method to obtain the mitotic extracts with an active or inactive spindle assembly checkpoint is in the Results section 2.4.

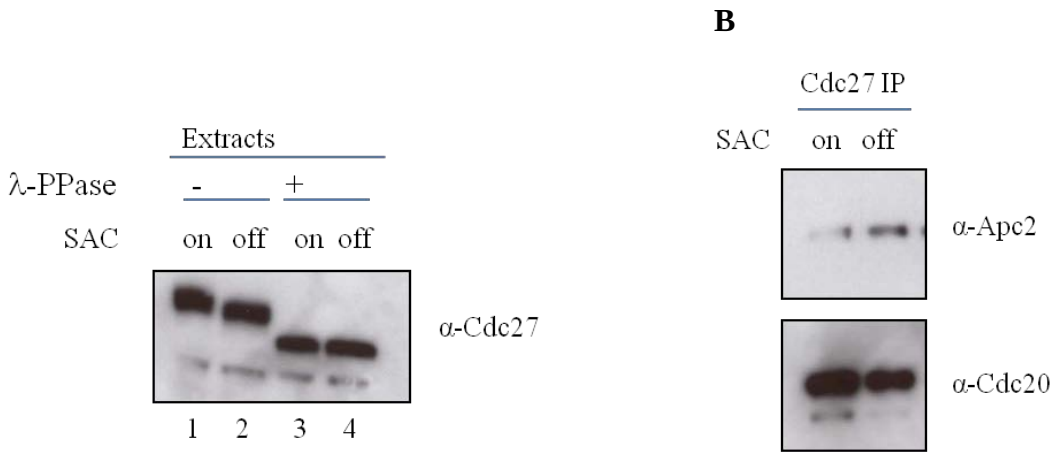

Figure 9. Dissociation of Cdc20 from the APC/C does not occur if the APC/C is dephosphorylated in the HeLa extract prior to IP. Extracts of mitotic HeLa cells with an active (SAC on) or inactive (SAC off) spindle assembly checkpoint were incubated with λ-protein phosphatase (λ-PPase) for 30 minutes at 30°C. APC/C was immupoprecipitated with sephasose beads coupled to α-Cdc27 antibodies. After extensive washing the complex was eluted off the beads with the antigenic peptide. A. Extracts were analyzed by SDS PAGE followed by western blotting for Cdc27 subunit of APC/C to confirm that the dephosphorylation was efficient. B. Cdc27 peptide eluates were separated by SDS PAGE and blotted for APC/C and Cdc20.

2.2 Which part of the activator is required and sufficient to bind the substrate?

The literature so far has been rather controversial about the substrate recognition by the APC/C activators. Different domains of activators were assigned to substrate binding and conclusions about the importance of degrons in substrates for the interaction with activators varied in studies from different labs (Schwab et al, 2001; Hilioti et al, 2001; Pfleger et al, 2001; Burton and Solomon, 2001; Sorensen et al, 2001, Eytan et al, 2006). The sequence of Cdc20 and Cdh1 predicts folding of the C terminal part of the protein into a WD40 propeller structure. SCF adaptor proteins Cdc4 and β-TrCP1 share this feature with APC/C activators. Structural studies of Cdc4 and β-TrCP1 have clearly shown that WD40 domains bind SCF substrates (Orlicky et al, 2003; Wu et al, 2003).

Conclusions about the involvement of WD40 domain of Cdh1 in substrate binding came from two independent studies. Both describe mutations in this domain that abolish substrate binding.

Burton et al (2005) performed a genetic screen and found 9 point mutants within the WD40 propeller region of Cdh1 that were all unable to degrade Hsl1 $^{667\text{-}872}$ substrate. These mutants were unable to bind the HA-Hsl1 $^{667\text{-}872}$ substrate. All of these mutants were also unable to bind the APC/C leaving the possibility that these mutations influenced the folding of the protein thereby rendering it nonfunctional. This was never tested or excluded.

Kraft et al (2005) adopted a more sophisticated approach. Assuming that the interactions between the activator and the substrate are evolutionarily conserved, given their importance for APC/C function, only conserved amino acid residues were mutated and mutant activators were tested for substrate binding and APC/C activation. A cluster of conserved amino acids was bioinformatically predicted to reside on the surface of the WD40 domain. To avoid disruption of the propeller structure only amino acids residing in the loop regions between the β-sheets of the propeller were mutated. Mutating four amino acids was sufficient to abolish ubiquitylation of an established APC/C substrate, cyclinB (1-87) *in vitro*. These mutations also reduced photo-crosslinking of a substrate

peptide to Cdh1 to background levels. This was also an evidence that substrate binding to the activator is required for substrate ubiquitylation.

What remained unclear was if the WD40 domain of APC/C activators is sufficient for substrate binding, and if so, if is there any specificity of this interaction determined by the destruction motifs in substrates. An ideal approach to understand this interaction would be to analyze it by X-ray crystallography.

2.2.1 The WD40 propeller domain of Cdh1 is sufficient to bind the Hsl1$^{667-872}$ substrate

To test the involvement of the WD40 propeller domain of Cdh1 in substrate binding, I compared the full length human Cdh1 with the WD40 propeller domain of human Cdh1 (amino acids 150-496) in their ability to bind to Hsl1$^{667-872}$ when co-expressed in Sf9 cells. The boundaries of the WD40 propeller region were estimated bio-informatically from the multiple sequence alignment of Cdh1 proteins from different species (The Clustal X protein sequence alignment is in the Appendix). Sf9 cells were co-infected with equal volumes of baculoviruses encoding N terminally Myc3-His6 or HA3-His6 tagged human Cdh1 and the untagged Hsl1$^{667-872}$. Hsl1$^{667-872}$ with mutated D box and KEN box (dk) served as a negative control. The complexes were purified from cell lysates by pulling on Cdh1 with Ni-NTA resin, and eluted with imidazole. The eluates were analyzed by SDS-PAGE and Coomassie staining, shown in Figure 10. The WD40 propeller domain could bind Hsl1$^{667-872}$ with comparable efficiency as the full length Cdh1. The binding was dependent on the D box and the KEN box on the substrate, as no binding could be observed when these two motifs were mutated (dk). When the cells were infected with Hsl1$^{667-872}$ baculoviruses only, no Hsl1$^{667-872}$ could be eluted off the Ni-NTA beads. From this experiment we could learn that the WD40 propeller domain of Cdh1 is sufficient to bind substrates, and that this binding is dependent on the D and KEN box.

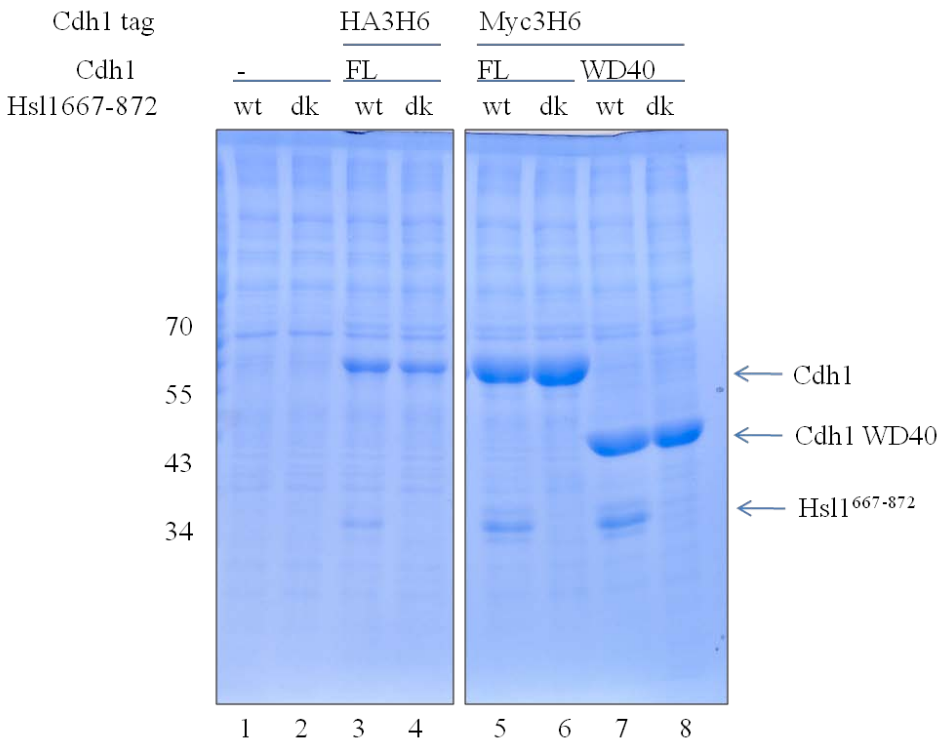

Figure 10. The WD40 domain of Cdh1 is sufficient to bind Hsl1$^{667-872}$ in a D box KEN box dependent manner. Sf9 cells were co-infected with baculoviruses encoding Cdh1encoding N terminally Myc3-His6 or HA3-His6 tagged full length or a N terminally Myc3-His6 tagged WD40 domain of human Cdh1 and the untagged Hsl1$^{667-872}$. Hsl1$^{667-872}$ with mutated D box and KEN box (dk) served as a negative control for unspecific binding to Cdh1. Cell lysates from insect cells infected with Hsl1$^{667-872}$ baculovirus only was used to control unspecific Hsl1$^{667-872}$ binding to the Ni-NTA beads. The complexes were purified from cell lysates by pulling on Cdh1 with Ni-NTA resin and eluted with imidazole. The eluates were analyzed by SDS PAGE and Coomassie staining. FL = full length.

To confirm that baculoviruses encoding the wild type (wt) and D box KEN box mutant (dk) Hsl1$^{667-872}$ were expressing proteins at comparable levels the soluble fraction of the cell extracts as well as the eluates were blotted for Hsl1 with an α-Hsl1 antibody, shown in Figure 11.

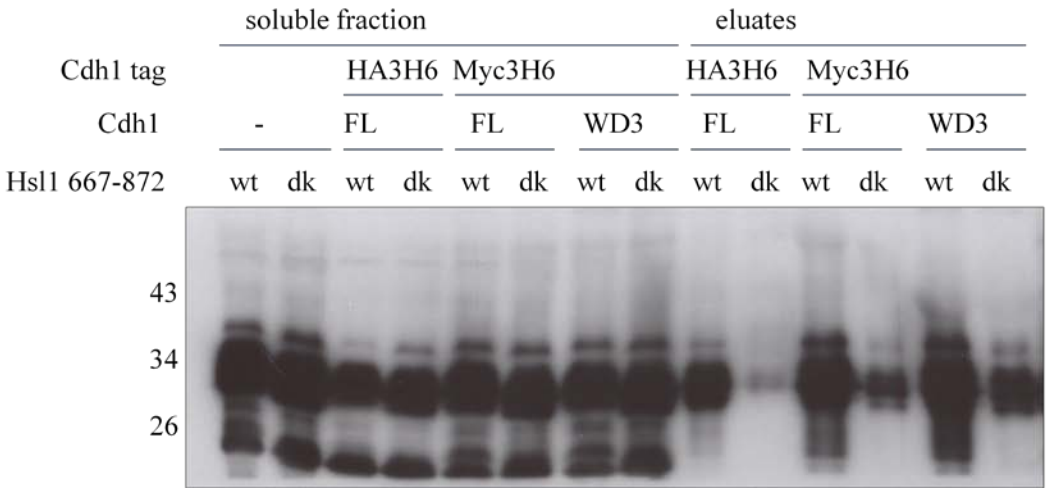

Figure 11. Comparable amounts of protein is expressed by baculoviruses encoding Hsl1$^{667-872}$ wild type (wt) and D box KEN box mutant (dk). Equal volumes of soluble fraction of the Sf9 cell extracts as well as the Cdh1-pull down imidazole eluates were analyzed by SDS PAGE and blotted for Hsl1$^{667-872}$ with an α-Hsl1 antibody.

From the Coomassie stained gel in Figure 10 one could conclude that the stoichiometry of the complex might not be 1:1, since it appears that the Cdh1 band stains more strongly than the Hsl1$^{667-872}$ band. To test if the Cdh1 molecules could bind more Hsl1$^{667-872}$ molecules I titrated the amount of Hsl1$^{667-872}$ baculovirus used for co-infection with a constant amount of baculovirus encoding the WD40 propeller domain of Cdh1 (Myc3H6-Cdh1 WD40). The complexes were purified the same way as in the experiment in Figure 10 and analyzed by SDS PAGE followed by Coomassie staining. The apparent stoichiometry could not be improved by increasing the amount of Hsl1$^{667-872}$ baculovirus used in co-infection with the Cdh1 baculovirus (Figure 12). From this I concluded that the Cdh1 molecules are saturated with the Hsl1$^{667-872}$ fragment.

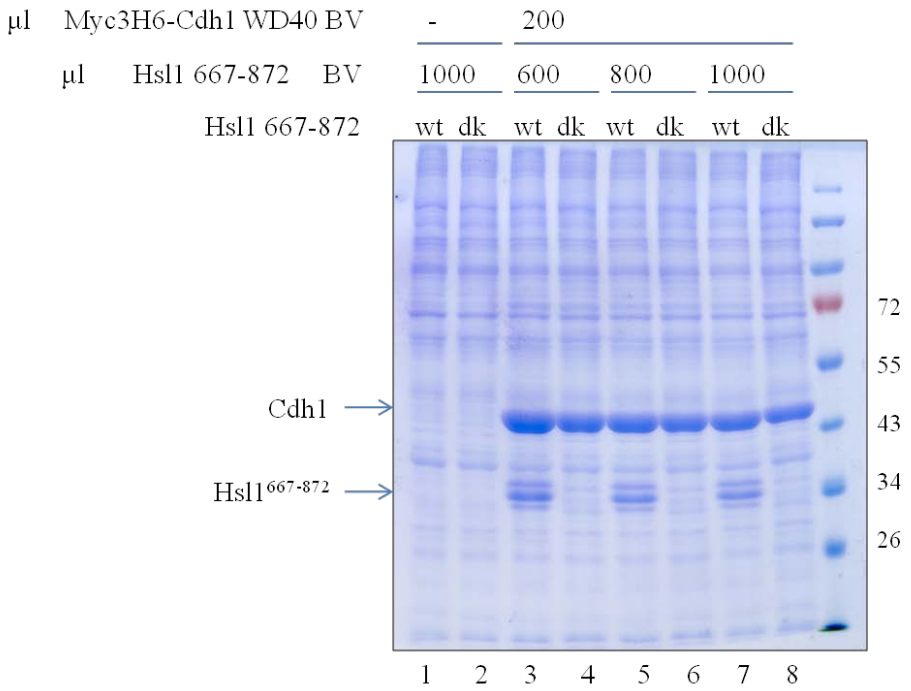

Figure 12. Increasing the volume of baculovirus encoding Hsl1$^{667-872}$ relative to the Cdh1 baculovirus used to infect Sf9 cells does not improve the stoichiometry of the eluted complex. 50% confluent adherent Sf9 cell T175 flask culture was infected with 200µl of baculovirus encoding Myc3-H6-Cdh1 WD40 in combination with 600, 800 and 1000 µl of baculovirus encoding Hsl1$^{667-872}$. 42h after infection cells were harvested. The complexes were purified from soluble fractions of cell lysates on NiNTA resin and eluted with imidazole. The eluates were analyzed by SDS PAGE and coomassie staining.

2.2.2 Co-expression and purification of Cdh1 with Hsl1$^{667-872}$ in *S. cerevisiae*

To gain insight into Cdh1 WD40 domain binding to its substrates, I made an attempt to purify a stoichiometric complex of Hsl1$^{667-872}$ and the WD40 domain of Cdh1 for X-ray crystallography studies. Cdh1 and Cdc20 are expressed at very low levels in insect cells, and for crystallography purposes these protein amounts would not be sufficient. The drawback of low expression levels could be overcome by growing large cultures of expressing cells. We chose budding yeast *Saccharomyces cerevisiae* as an expression system because these cells can be grown at large scale. Expression in bacteria, the usual and optimal expression system used in crystallography, was not an option because it has been impossible so far to express soluble Cdh1 in bacteria. This could be

due to the fact that Cdc20 and Cdh1 require TRiC/CCT chaperonin for folding (Camasses et al, 2003). The TRiC/CCT chaperonin is only present in eukaryotic cells (reviewed in Dunn et al, 2001). Another advantage of budding yeast as an expression system is that there is a variety of over-expression promoters which would allow control over relative expression levels of the two co-expressed proteins.

I placed full length budding yeast Cdh1 and three truncation constructs of Cdh1, called WD1 (amino acids 164-567), WD2 (amino acids 195-567) and WD3 (amino acids 227-567) as well as Hsl1$^{667-872}$ under GAL1-10 promoter. Cdh1 constructs were N terminally tagged with a Flag tag. Protein A was fused the N terminus of Hsl1$^{667-872}$ and was separated from it with a Tobacco Etch Virus (TEV) protease recognition sequence (Figure 13).

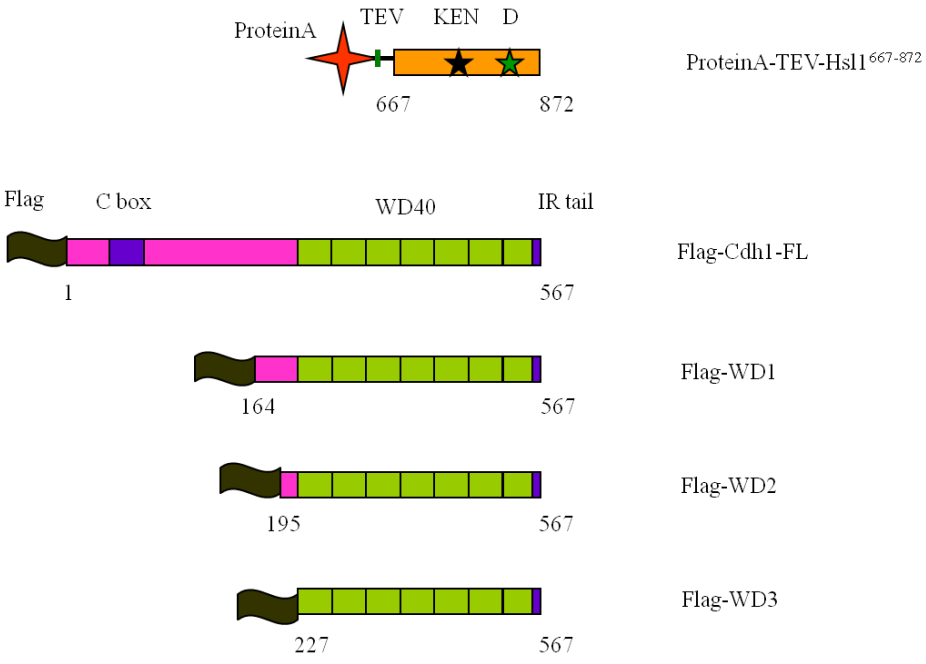

Figure 13. Hsl1 and Cdh1 constructs used in co-expression studies. Protein A was fused with a fragment of budding yeast protein Hsl1 (amino acids 667-872) at its C terminus and was separated from Hsl1$^{667-872}$ with a Tobacco Etch Virus (TEV) recognition sequence. Full length and three truncated forms of Cdh1, WD1 (amino acids 164-567), WD2 (amino acids 195-567) and WD3 (amino acids 227-567) were N-terminally tagged with a Flag tag.

A

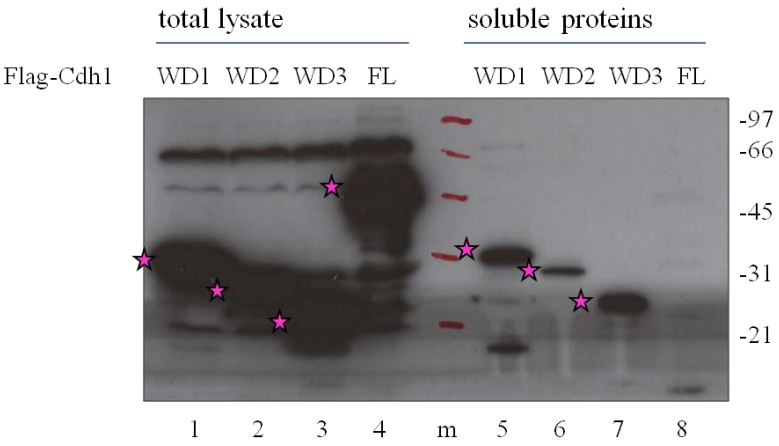

B

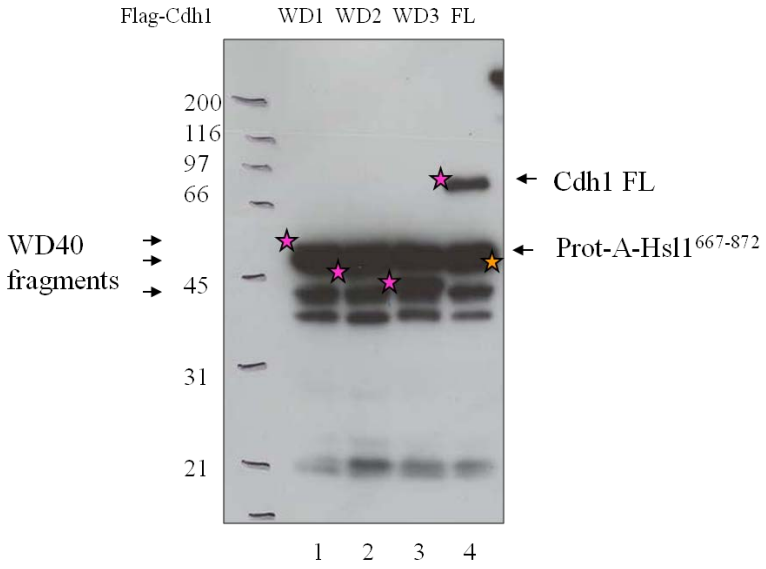

Figure 14 . When over-expressed in yeast full length Flag-Cdh1 is insoluble. Co-expression with Protein-A-Hsl1$^{667-872}$ renders it soluble. A. Flag-Cdh1 full length and truncated forms, WD1 (amino acids 164-567), WD2 (amino acids 195-567) and WD3 (amino acids 227-567) were over-expressed under GAL1-10 promoter in *S.cerevisiae*. The cells were harvested and lysed, and the soluble fraction of the lysate was separated from the insoluble fraction by centrifugation. Total cell lysate and the soluble fraction were analysed by SDS PAGE and Western blotting. Cdh1 constructs were detected with an antibody against the Flag tag. B. The four Flag-Cdh1 constructs were co-expressed with Protein A-TEV- Hsl1$^{667-872}$, and the complex was purified from the cell extracts with IgG sepharose beads. The glycine eluates were analyzed by SDS PAGE and Western blotting. Cdh1 was detected with α-Flag antibodies, and the Protein A-TEV- Hsl1$^{667-872}$ was detected with the secondary antibody. Cdh1 bands are marked with a pink star, Protein A-TEV- Hsl1$^{667-872}$ is marked with an orange star. m=marker.

All four Cdh1 constructs could be detected in the total cell lysate when over-expressed in budding yeast (Figure 14A, lanes 1, 2, 3 and 4), however, only the truncated forms of Flag-Cdh1, WD1, WD2 and WD3 were soluble (Figure 14A, lanes 5, 6 and 7), whereas the full length Flag-Cdh1 was not (Figure 14A, lane 8). Protein A-TEV- Hsl1$^{667-872}$ was also soluble when over-expressed (not shown). Co-expression of full length Flag-Cdh1 with Protein-TEV- Hsl1$^{667-872}$ rendered Cdh1 soluble (Figure 14B). The Flag-Cdh1-WD3 construct was expressed at the highest level, therefore I continued to further optimize expression and purification conditions with this construct only.

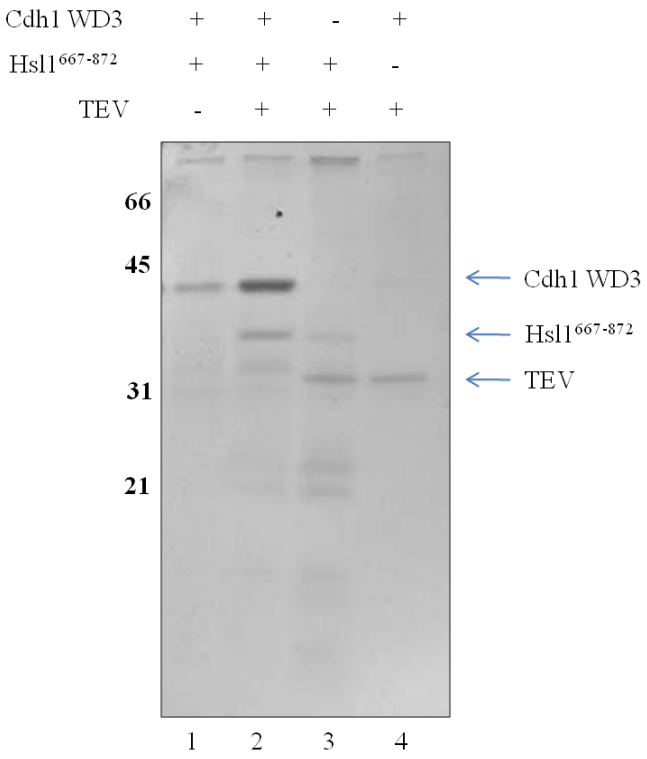

Figure 15. Cdh1 WD3 and Hsl1$^{667-872}$ can be co-purified from *Saccharomyces cerevisiae.* Lysates of budding yeast cells that overexpressed ProteinA-TEV-Hsl1$^{667-872}$ together with Flag-Cdh1 WD3 (lanes 1 and 2), ProteinA-TEV-Hsl1$^{667-872}$ alone (lane3) or Flag-Cdh1 WD3 alone (lane 4) were incubated with IgG-coupled sepharose beads, the unbound material was washed away and the beads were incubated in TEV cleavage buffer with (lanes 2, 3, 4) or without TEV protease (lane 1). The eluates were analyzed by SDS PAGE and coomassie staining. The expression of all the overexpressed proteins was driven by gal1-10 promoter

The co-expressed Cdh1-WD3 and Hsl1$^{667-872}$ could be isolated in a complex by pulling on the Protein A tag on Hsl1$^{667-872}$ and cutting the complex off the tag with TEV protease (Figure 15, lane 2). When expressed without Cdh1 lower amounts of Hsl1$^{667-872}$ could be eluted (Figure 15, lane 3), compared to levels when the protein was co-expressed with Cdh1 , indicating that co-expression stabilizes Hsl1$^{667-872}$. Besides eluting in a complex with Hsl1$^{667-872}$, Cdh1-WD3 also seems to bind to IgG sepharose beads unspecifically since some of it eluted off the beads also when no TEV cleavage was performed (Figure 15, lane 1). This also indicates that the there may also be free Cdh1-WD3 in the cell, unbound to Protein A-TEV- Hsl1$^{667-872}$.

To increase the proportion of Cdh-WD3 in the cell bound to ProteinA-TEV-Hsl1$^{667-872}$ I placed Protein A-TEV- Hsl1$^{667-872}$ under a promoter that is stronger than GAL1-10, the GAL10-PGK promoter. Figure 16 shows the comparison of TEV eluates of Cdh1-WD3 in complex with Hsl1$^{667-872}$ whose expression was driven by GAL1-10 promoter (lane 1) and by GAL10-PGK promoter (lane 2). When expressed from GAL10-PGK promoter the amount of Hsl1$^{667-872}$ that can be pulled down with Protein A beads and eluted with TEV protease is higher than when it is expressed from GAL1-10 promoter (compare lane 1 with 2 and lane.3 with 4, Figure 16). The stoichiometry of Cdh1-WD3 that can be pulled down together with Hsl1$^{667-872}$ is also changed. When the Hsl1$^{667-872}$ and Cdh1-WD3 bands are compared on the Coomassie gel (Figure 16, lanes 2 and 4), it seems that the Hsl1$^{667-872}$ band is stained more than Cdh1-WD3, suggesting that not all Hsl1$^{667-872}$ molecules elute in a complex with Cdh1-WD3, some elute as monomers. Mass spectrometry analysis of the co-eluting 70kDa band identified a heat shock protein SSA1 as its major component. The samples were concentrated (Figure 16, lanes 4 and 5) and further purified by size exclusion chromatography on Sephadex200_HR_10/30 column. The eluates that corresponded to the peak fractions in the chromatogram were analyzed by SDS PAGE and Coomassie staining, as shown in Figure 17.

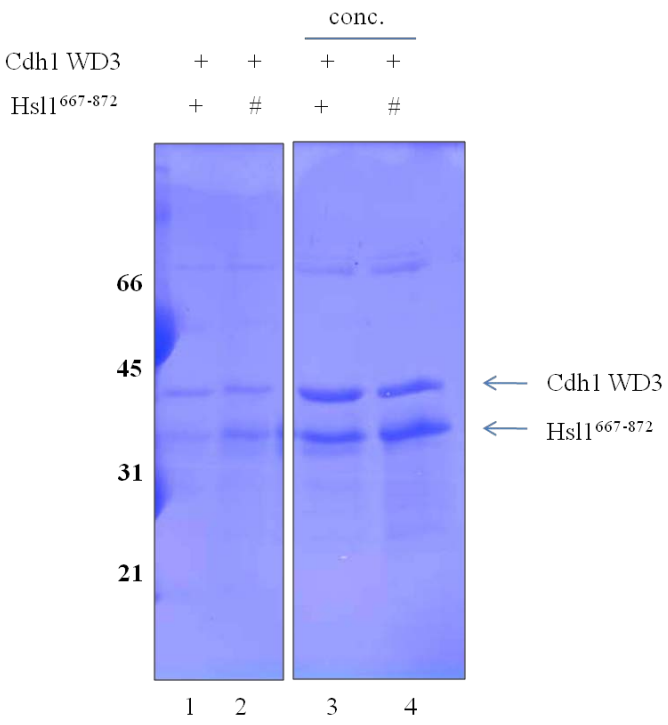

Figure 16. Protein expression level of Hsl1$^{667-872}$ is higher when its driven by gal10-PGK promoter compared to gal1-10 promoter. Cdh1WD3 under gal1-10 promoter (+) was co-expressed with Hsl1$^{667-872}$ under either gal1-10 (+) or gal10-PGK (#) promoter. The complexes were purified as described and concentrated by precipitation in 85% ammonium sulphate followed by re-suspension of the complex in 1/10 of the starting volume. Equal volumes of the eluates (lanes 1 and 2) and of the concentrated samples (lanes 3 and 4) were analyzed by SDS PAGE and Coomassie staining. Conc= concentrated eluates.

Analysis of the eluate by size exclusion chromatography confirmed that when expressed from the GAL10-PGK promoter the TEV elution contained the complex of Hsl1$^{667-872}$ and Cdh1 WD3, which elutes at the molecular weight of about 65 kDa, but it also contains Hsl1$^{667-872}$ monomers, which elute in lower molecular weight fractions. The Hsl1$^{667-872}$ monomers could not be separated from the complex on this gel filtration column. The Hsl1$^{667-872}$ seems to be degraded if it is not bound to the WD40 domain of Cdh1, this can be seen as a smear below the Hsl1$^{667-872}$ band in the lower molecular weight fractions, where increasing amounts of monomer elute.

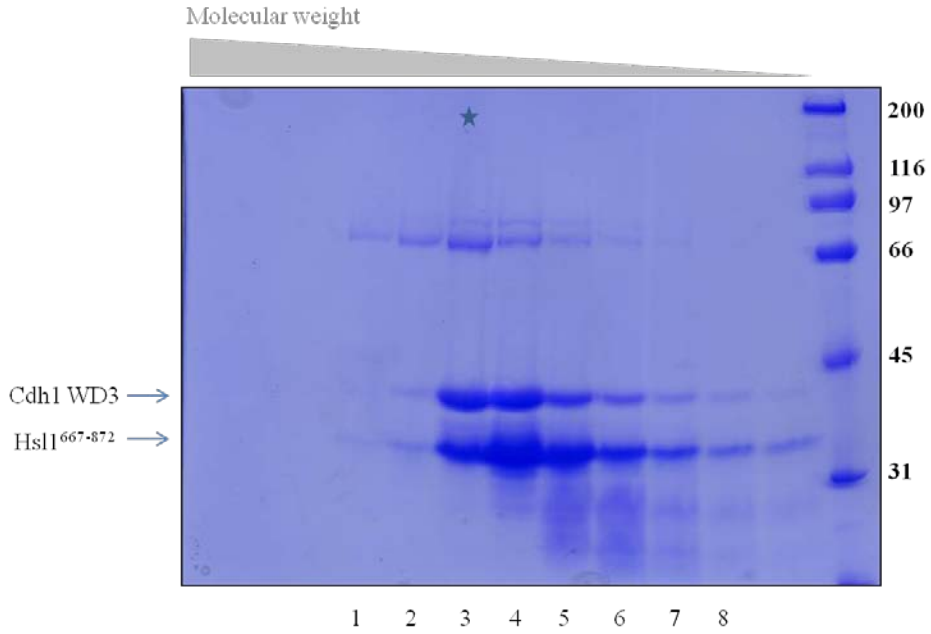

Figure 17. Cdh1WD3 and Hsl1$^{667-872}$ form a stable complex. The concentrated solution of the Cdh1WD3 and Hsl1$^{667-872}$ complex (Figure 16, lane 4) was purified by size exclusion chromatography using Sephadex200_HR_10/30 column (Amersham). The eluates corresponding to the peak fractions in the chromatogram were analyzed by SDS PAGE and Coomassie staining. The BSA-standard peak fraction corresponds to the fraction marked with a star, lane 3.

The chaperones co-elute with the complex. Both the complex and the chaperones elute at about 65 kD, which suggests that they dissociate from the complex. Below the chaperones there is a contaminating band that I suspect to be the BSA, used for calibration that stayed in the column. Only the fraction 3 contains a stoichiometric complex of Hsl1$^{667-872}$ and Cdh1-WD3, and the amount of this complex is rather low. The eluate loaded on this column was obtained from 2 liters yeast culture.

Because of very low yield of the stoichiometric complex, irreproducibility of the concentration step by ammonium sulphate precipitation, and inability to remove chaperones by ATP treatment I did not pursue this project further.

2.3 The role of the C-box

Within the largely non-conserved N terminal part of Cdh1 and Cdc20 a short conserved sequence motif was identified whose removal destroyed the ability of budding yeast Cdh1 to degrade Clb2 (Schwab et al.,2001). This motif has been shown to be essential for the function of budding yeast Cdh1 and to be required for its association with the APC/C (Schwab et al., 2001). In another study of the C box in yeast Cdh1 only a mild defect in APC/C stimulation by the mutant Cdh1 was reported (Thornton et al., 2006). Binding of human recombinant Cdh1 was significantly, but not completely, reduced if the C box was mutated. However, this mutant of Cdh1 was completely unable to activate APC/C (Vodermaier et al., 2003). It remained therefore unclear if the only function of the C box was to bind the activator to the APC/C or if it has other functions. Recently it has been found that the N terminal part of Cdh1 bearing the C box was sufficient to activate the *Xenopus laevis* APC/C in a ubiquitylation reaction if the substrate is recruited to it in an activator independent manner (Kimata et al., 2008). All the mentioned reports are of qualitative nature and we decided to study the effect of the C box mutation in Cdh1 in a more quantitative manner, using purified components, which might allow a clearer view at the role of the C box in mechanistic terms.

2.3.1 APC/C binding of Cdh1 with a mutated C box is reduced 10-fold

The IR tail and the C box both contribute to activator binding to the APC/C. The first question we asked was what the effect of the C box mutation in Cdh1 was on APC/C binding. To answer this question I purified human Cdh1 with a wild type C box (DRFIP) and Cdh1 with the C box amino acids mutated to alanines (AAAAA) from Sf9 cells that were infected with Baculoviruses encoding these his-tagged Cdh1 constructs (constructs published in Vodermaier et al, 2003). The APC/C was purified from exponentially proliferating HeLa cells with α-Cdc27 antibody coupled to sepharose beads. A certain amount of endogenous Cdh1 bound to the APC/C could always be detected because the majority of exponentially proliferating HeLa cells is in the G1 phase. APC/C bound to

the α-Cdc27-sepharose beads was then incubated in increasing concentrations of recombinant Cdh1, wild type (wt) or C box mutant (Cm). After the unbound activators were washed away with IP buffer (see Materials and methods) the APC/C-Cdh1 complexes were eluted off the beads with a Cdc27 antigenic peptide. The eluates were analyzed by SDS PAGE and Western blotting against the APC/C subunit Apc2 and Cdh1 (Figure 18).

A

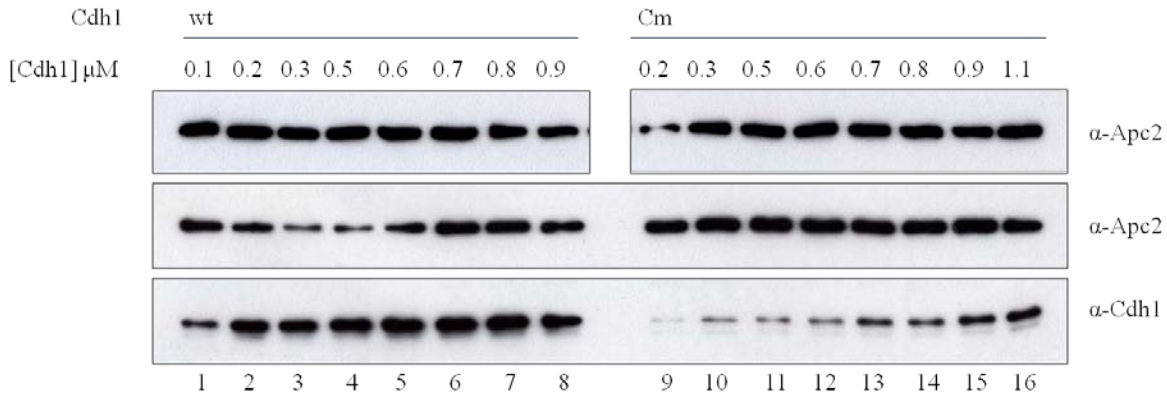

B

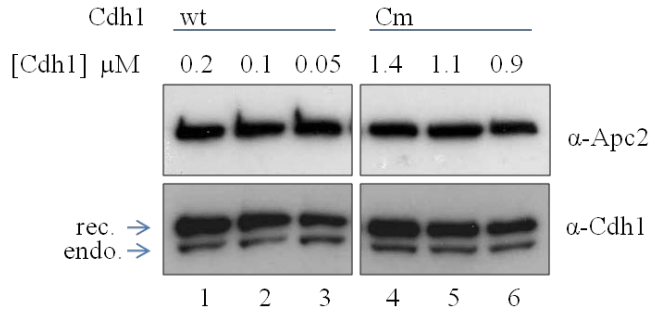

Figure 18 . APC/C binding of Cdh1 with a mutated C box is reduced 10-fold. A. The APC/C was isolated from logarithmically proliferating HeLa cells with with α-Cdc27 antibodies coupled to sepharose beads. Bead-bound APC/C was loaded with increasing concentrations of wild type (wt) or C box mutant (Cm) recombinant His-tagged Cdh1 purified from baculovirus infected Sf9 cells. The unbound Cdh1 was washed away with IP buffer (see Materials and Methods) and the APC/C-activator complex was eluted with a 1mg/ml Cdc27 antigenic peptide solution. The same samples were analyzed and blotted for Apc2 twice, due to apparent unequal loading in lanes 2-5. B. The experiment was carried out as in (A). The eluted samples were analyzed by SDS PAGE and Western blotting. Rec.=recombinant, endo = endogenous.

The concentration of recombinant C-box-mutant Cdh1 solution that has to be incubated with the APC/C is about 10 times higher than the concentration of the recombinant wild type Cdh1 to achieve equal binding of these two forms of Cdh1 to the APC/C (compare lanes 2 and 5, Figure 18B).

From this experiment we learned that it is possible to compensate for the C-box mutant APC/C binding defect by increasing the concentration of Cdh1 that is loaded onto the APC/C. Having the binding restored to wild type levels it was possible to ask the next question. If the role of the activators is solely to recruit the substrates to the APC/C and if the C-box functions solely as an APC/C-interaction motif, restoring wild type binding of the Cdh1 Cm to the APC/C the way described above should also restore the wild type activator function in a ubiquitylation reaction. I tested this hypothesis by comparing the activity of APC/C bound to equal levels of either wild type or C-box mutant Cdh1 in an *in vitro* substrate ubiquitylation assay.

2.3.2 Substrate ubiquitylation by the APC/C loaded with C-box mutant Cdh1 is impaired

To compare the ability of C-box mutant Cdh1 to activate the APC/C in an ubiquitylation reaction with the wild type Cdh1, I purified APC/C from logarithmically proliferating HeLa cells with α-Cdc27 antibodies coupled to sepharose beads and loaded it with comparable amounts of either wild type (wt) or C-box mutant (Cm) recombinant human Cdh1 purified from Sf9 cells, as described above. The APC/C-Cdh1 complex was eluted off the beads with a Cdc27 antigenic peptide solution. A fraction of the eluate was analyzed by SDS PAGE and Western blotting, to confirm that the levels of recombinant wt and Cm Cdh1 that were bound to the APC/C were comparable (Figure 19A). The remainder of the eluates was used in an *in vitro* ubiquitylation assay. The APC/C-Cdh1 substrate used in the reaction was I^{125}-labeled human cyclin B1 fragment (amino acids 1-87). The I^{125}-labeled substrate was incubated with APC/C-Cdh1 complex eluates mixed with E1, E2, ubiquitin, ATP and ATP-regenerating system and incubated at 37°C for 1, 2,

5, or 9 minutes. The whole reaction volume was analyzed by SDS PAGE and phosphoimaging (Figure 19B and C).

Comparable levels of C-box mutant and wild type Cdh1 bound to APC/C if they were incubated with the APC/C as a 1.1μM solution (Figure 19A, lanes 3, 4, 5) and 0.2 μM solution (Figure 19A lanes 12, 13, 14), respectively. The corresponding samples in the ubiquitylation reaction are underlined in Figure 19B. From this experiment we learned that restoring the wild type binding of the C box mutant Cdh1 to the APC/C does not restore its activity to wild type levels in an *in vitro* ubiquitylation reaction. The C box mutated Cdh1 has no stimulatory effect in the ubiquitlylation reaction despite its binding to the APC/C. Note that the stimulation of APC/C activity that can be observed upon wild type Cdh1 pre-binding to the APC/C is not as pronounced as it can be usually seen when recombinant activators are added directly to the ubiquitylation reaction. This could be due to the fact that the amount of recombinant activator that is retained on the APC/C upon pre-binding is relatively low compared to the usual amounts of activator added directly to the *in vitro* ubiquitylation reaction.

The defect in APC/C activation could arise from defective substrate recruitment to the APC/C or from defective catalytic activation of APC/C towards a properly recruited substrate. To start dissecting this problem I first tested if the substrate recruitment to the APC/C by Cdh1 was impaired upon C-box mutation.

A

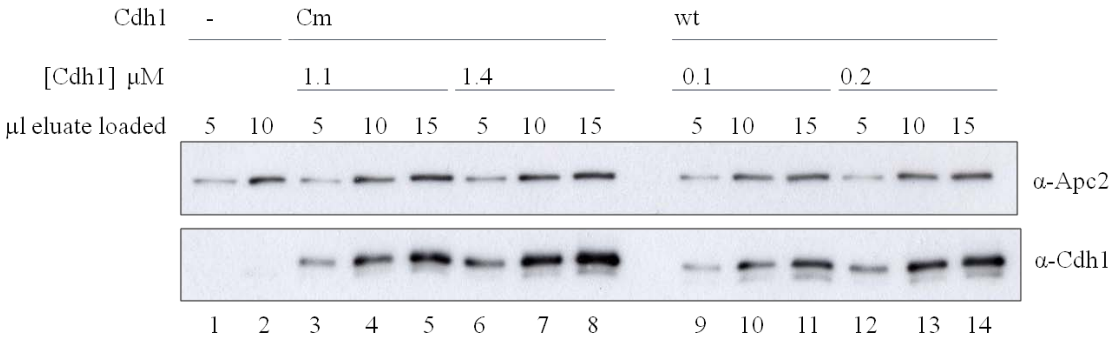
Cdh1 - Cm wt
[Cdh1] µM 1.1 1.4 0.1 0.2
µl eluate loaded 5 10 5 10 15 5 10 15 5 10 15 5 10 15
α-Apc2
α-Cdh1
1 2 3 4 5 6 7 8 9 10 11 12 13 14

B

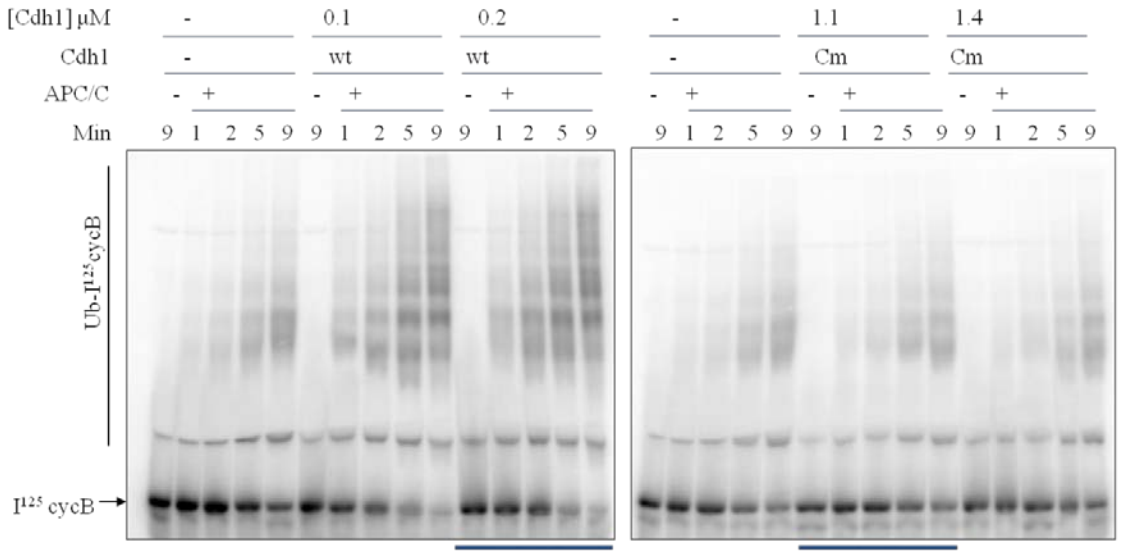
[Cdh1] µM - 0.1 0.2 - 1.1 1.4
Cdh1 - wt wt - Cm Cm
APC/C - + - + - + - + - + - +
Min 9 1 2 5 9 9 1 2 5 9 9 1 2 5 9 9 1 2 5 9 9 1 2 5 9 9 1 2 5 9
Ub-I125cycB
I125 cycB

C

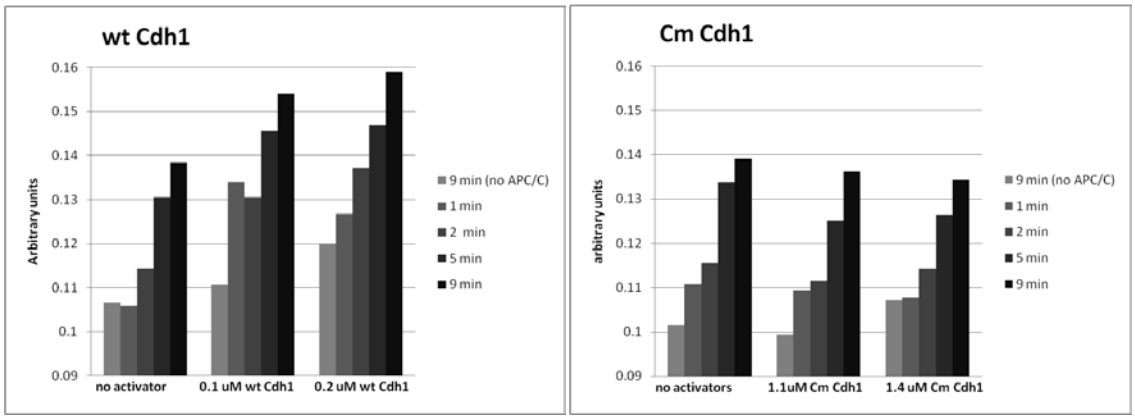
wt Cdh1
Arbitrary units
0.16
0.15
0.14
0.13
0.12
0.11
0.1
0.09
no activator
0.1 uM wt Cdh1
0.2 uM wt Cdh1
9 min (no APC/C)
1 min
2 min
5 min
9 min
Cm Cdh1
arbitrary units
no activators
1.1uM Cm Cdh1
1.4 uM Cm Cdh1

Figure 19 . C box mutation in Cdh1 abolishes its ability to activate the APC/C. A. APC/C purified from log phase HeLa cells with an α-Cdc27 antibody coupled to sepharose beads was loaded with comparable amounts of wild type (wt) and C box mutant (Cm) Cdh1 (compare lanes 3, 4, 5 for Cm with 12, 13, 14 for wt Cdh1) . The APC/C-Cdh1 complexes were eluted off the beads with a 1mg/ml Cdc27 antigenic peptide solution. A sample of each eluate was analyzed by SDS PAGE and Western blotting against the APC/C subunit and Cdh1. B. The remaining eluates from A were mixed with ubiquitylation reaction mix and radioactive I125-labeled human cyclin B fragment (amino acids 1-87) as an APC/C-Cdh1 substrate. The ubiquitylation reaction was carried out for 1, 2, 5 and 9 minutes at 37°C. The reaction was stopped by adding 4x sample buffer. APC/C without recombinant Cdh1 was a control for endogenous Cdh1-mediated APC/C activation. The whole reaction volume was analyzed on an SDS PAGE gel and analyzed by phosphoimaging. Ubiquitlylation reaction timepoints where comparable amounts of recombinant Cdh1 were loaded onto APC/C are underlined. C. The phosphoimage ubiquitylation profile shown in B was quantified by Image J.

2.3.3 Substrate binding by the APC/C loaded with C-box mutant Cdh1 is impaired

The APC/C was isolated from logarithmically proliferating HeLa cells and loaded with comparable levels of recombinant wild type or C-box mutant Cdh1, as described above. Excess of activator was removed by washing with IP buffer. The bead-bound APC/C-Cdh1 complex was then incubated in 150nM solution of recombinant human securin. His6-tagged human securin was expressed and purified from E.coli. To prevent unspecific binding of the substrate the solution also contained 4mg/ml BSA. The unbound substrate was then washed away and the bound complexes were eluted off the beads with Cdc27 antigenic peptide solution. The eluates were analyzed by SDS PAGE and Western blotting (Figure 20). Some securin binding to the APC/C could be detected if no recombinant Cdh1 was additionally bound to it. This binding is due to the endogenous Cdh1 (lane 8). The endogenous Cdh1 was present in all samples, and it can be seen as a faster migrating thin band on the Cdh1 blot. Loading APC/C with recombinant wild type Cdh1 increased the amount of securin it could retain compared to the APC/C that was bound to endogenous Cdh1 only (compare lanes 1, 2, 3 with lane 8). The increase in securin binding was Cdh1 dose-dependent (lanes 1, 2, 3). However, loading comparable amounts of recombinant C-box mutant Cdh1 onto the APC/C had no

stimulatory effect in securin binding (lanes 4, 5, 6). From this we could conclude that the C-box mutant Cdh1 is impaired in substrate recruitment to the APC/C.

A

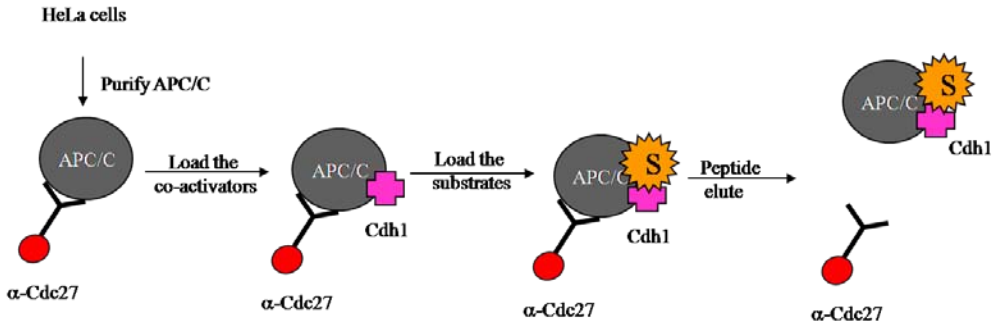

B

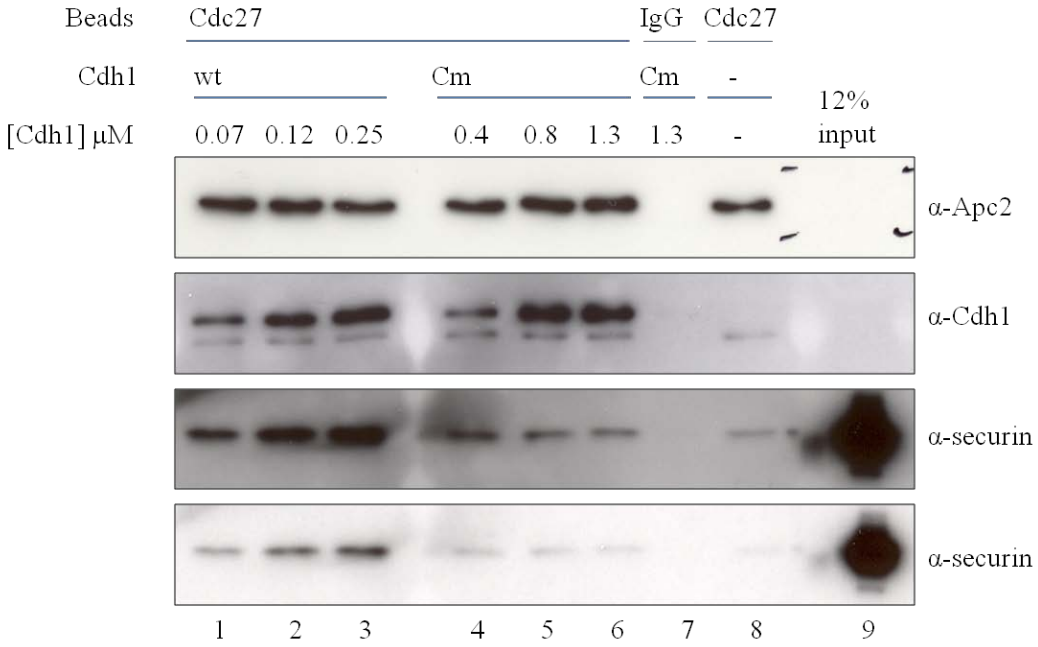

Figure 20. APC/C loaded with C-box mutant Cdh1 is impaired in securin binding. A. Schematic representation of the experimental outline. S = substrate. B. APC/C isolated from log phase HeLa cells and loaded with a range of equal levels of wild type (wt) or C-box mutant (Cm) Cdh1, as described in Figure 18. The bead bound APC/C-Cdh1 complex was then incubated in 150nM solution of recombinant human His6-tagged securin that was expressed and purified from E.coli. The unbound securin was washed away and the bound complex was eluted off the beads with a 1mg/ml Cdc27 antigenic peptide solution. The eluates were analyzed by SDS PAGE and Western blotting. Endogenous Cdh1 is a faster migrating band, the recombinant Cdh1 runs slower. Two different exposures of the securin blot are shown.

To confirm this finding I performed the same experiment with GST-Hsl1$^{667-872}$ substrate (Figure 21). In addition to the wild type (wt) GST-Hsl1$^{667-872}$ I also looked at D-box mutant (dm), KEN box mutant (km) and D box KEN box double mutant (dkm) GST-Hsl1$^{667-872}$ binding. As observed with securin, wt GST-Hsl1$^{667-872}$ binding was increased when the APC/C was loaded with recombinant wild type Cdh1 (lanes 2 and 3), compared to binding of wt GST-Hsl1$^{667-872}$ when only endogenous Cdh1 was bound to the APC/C (lane 1). Wt GST-Hsl1$^{667-872}$ binding could also be stimulated by C-box mutant Cdh1 (lanes 4 and 5) above basal levels (lane 1), but this stimulation was not as high as the one seen with recombinant wt Cdh1 (lanes 2 and 3). The difference between wt Cdh1 and C-box mutant Cdh1 in GST-Hsl1$^{667-872}$ binding stimulation was more pronounced if the KEN box of GST-Hsl1$^{667-872}$ was mutated (compare lanes 10 and 11 with lanes 3 and 4). D box mutant (dm) and D box KEN box double mutant (dkm) GST-Hsl1$^{667-872}$ did not bind above background levels regardless of whether wt or C-box mutant Cdh1 was loaded onto the APC/C (lanes 7, 8, and 13, 14, 15, 16).

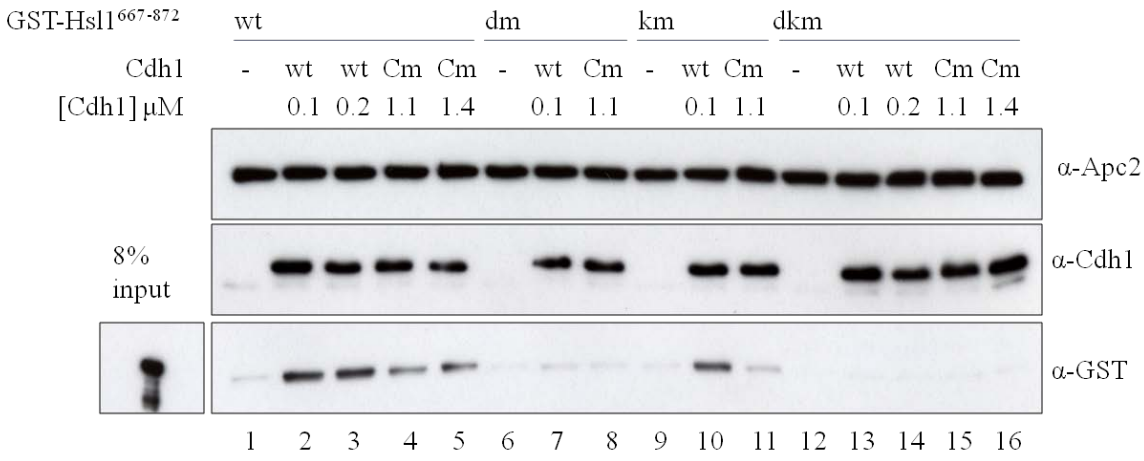

Figure 21 . APC/C loaded with C-box mutant Cdh1 is mildly impaired in GST-Hsl1$^{667-872}$ binding. APC/C isolated from log phase HeLa cells and loaded with a range of concentrations of wild type (wt) or C-box mutant (Cm) Cdh1, as described in Figure 18. The bead bound APC/C-Cdh1 complex was then incubated in 60nM solution of wild type (wt) D box mutant (dm), KEN box mutant (km) or D box KEN box double mutant (dkm) GST-Hsl1$^{667-872}$ that were expressed and purified from E.coli. The unbound substrates were washed away and the bound complex was eluted off the beads with 1mg/ml of Cdc27 antigenic peptide solution. The eluates were analyzed by SDS PAGE and Western blotting.

It might be important to point out here that the D box mutation has a stronger effect in abolishing Hsl1$^{667-872}$ binding to APC/C-Cdh1 than the KEN box has, which is contradicting previous proposal (Pfleger and Kirschner, 2000 and Burton and Solomon, 2001, Passmore et al, 2003) that the KEN box is preferentially recognized by Cdh1 and the the D box by Cdc20. In the experiment shown in Figure 21 it is clear that a mutation in the D box abolishes GST-Hsl1$^{667-872}$ biding to APC/C-Cdh1 more strongly than the mutation in KEN box does (compare lanes 2, 7 and 10). Therefore, the D-box is more important for Cdh1 recognition of Hsl1$^{667-872}$ than the KEN box is.

2.3.4 C-box mutation in Cdh1 seems not to affect Hsl1$^{667-872}$ binding to Cdh1

The reduction in substrate binding by APC/C-Cdh1 when the C-box in Cdh1 is mutated could be for two reasons. Either the C-box is directly involved in substrate recognition by Cdh1 or the C-box binding to a certain site on APC/C positions the substrate-bound Cdh1 in such a way to expose the substrate to a substrate-binding surface on the APC/C itself. The latter possibility would fit to a model where the APC/C and the activators bind the substrate in a cooperative way, as well as to the observed phenomenon of reduced APC/C flexibility upon Cdh1 binding (Dube et al., 2005)

To exclude the possibility that the C-box is directly involved in substrate binding I co-infected Sf9 cells with baculoviruses encoding the untagged substrate Hsl1$^{667-872}$ together with either wt or C-box mutant (Cm) human HA3H6-tagged Cdh1. After 42 hours of co-expression the substrate-activator complexes were purified from Sf9 cells via Ni-NTA agarose resin (Figure 22). The amounts of Hsl1$^{667-872}$ that could co-purify with wild type and C-box mutant HA3H6-Cdh1 were very similar (compare lanes 3 and 5). The observed binding was specific since mutating the D box and the KEN box in Hsl1$^{667-872}$ abolished its binding to both wt and Cm Cdh1 (lanes 4 and 6) and no Hsl1$^{667-872}$ binding to the Ni-NTA agarose beads could be observed if HA3H6-Cdh1 was not co-infected with it (lanes 1 and 2).

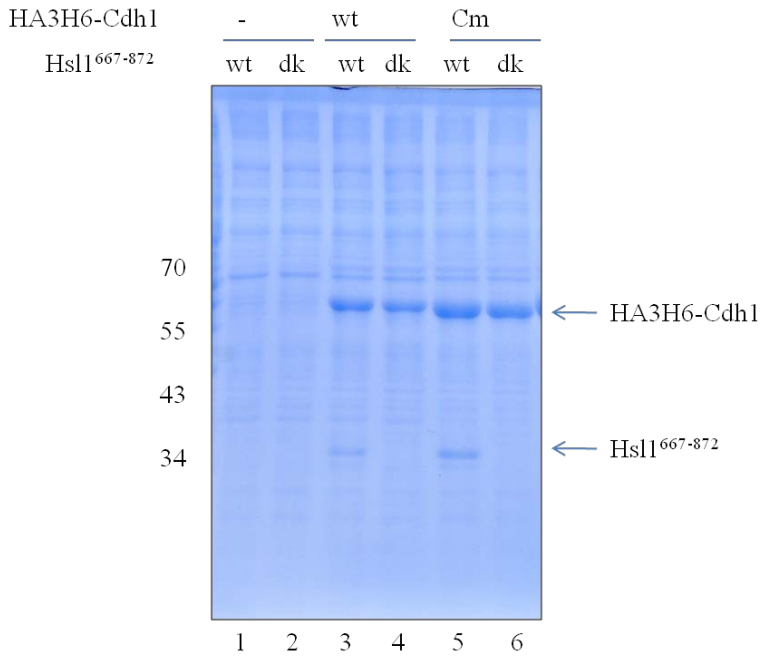

Figure 22 . Outside of the context of APC/C the C-box mutant Cdh1 can bind Hsl1$^{667-872}$ as well as the wild type Cdh1. Sf9 cells were infected with baculoviruses encoding Cdh1encoding N terminally HA3-His6 tagged full length human wild type (wt) or C-box mutant (Cm) Cdh1 together with the baculovirus encoding an untagged Hsl1$^{667-872}$. Hsl1$^{667-872}$ with mutated D box and KEN box (dk) served as a negative control for Cdh1 binding. Cell lysates from cells infected with Hsl1$^{667-872}$ baculovirus only was used to control unspecific Hsl1$^{667-872}$ binding to the Ni-NTA beads. The complexes were purified from cell lysates by pulling on Cdh1 with Ni-NTA resin, and eluted off the beads with imidazole. The eluates were analyzed by SDS PAGE and Coomassie staining.

From this experiment we could conclude that the substrate binding to the activator is not impaired by a C-box mutation in Cdh1. However one should be careful with basing such a conclusion on an experiment with Hsl1$^{667-872}$. Equal binding of Hsl1$^{667-872}$ to wt and Cm Cdh1, as well as the fact that the C-box mutation in Cdh1 has a much smaller effect on APC/C-Cdh1 recognition of Hsl1$^{667-872}$ compared to a strong defect in securin binding, could also be explained by the latest finding in the Morgan lab (Matyskiela and Morgan, 2009) that the Hsl1$^{667-872}$ is a substrate with an extraordinary high affinity for the APC/C-Cdh1. For this reason additional co-infection experiments with substrates such as securin

or Aurora kinases should be done to confirm that the C-box has no direct role in substrate recognition by Cdh1.

2.3.5 A C-box binding site on APC/C

If the C-box is an APC/C interaction motif, knowing which subunit of the APC/C it binds to might help explaining the behaviour of the C-box mutant Cdh1 we could observe in the experiments described above. I can think of at least two ways how to find out which APC/C subunit it might be. The best candidate for C box binding is Apc2. It has been shown that upon Apc2 deletion in budding yeast the amount of Cdh1 bound to the APC/C is reduced. This could be relatively easily tested by comparing wild type APC/C with APC/C that lacks subunits Apc2 and Apc11 (Δ2/11-APC/C Vodermaier et al., 2003) in their ability to bind a C-box containing Cdh1 N- terminal fragment. Another, more elaborate and time consuming way would be to map the C-box binding site by cryo-EM analysis of APC/C loaded with a C-box baring Cdh1 fragment fused to a bulky tag or by cross-linking the C-box containing fragment to the APC/C (B. Buschhorn and G. Petzold, personal communication). Alternatively, crosslinking of a C-box containing fragment of Cdh1 to the APC/C could capture the C-box interacting subunit.

For all the proposed approaches I needed first to see if it is possible to bind a Cdh1 fragment that contains the C-box to the APC/C. To test this I fused N-terminal 116 amino acids of Cdh1 to the C-terminus of glutathione-S-transferase (GST). The C-box in human Cdh1 starts at the amino acid 46 and the WD40 domain starts at amino acid 150. I expressed and purified the GST-N116 Cdh1 constructs, both wild type and C-box mutant, in *E. coli*. Five different concentrations of GST-N116 Cdh1 ranging from 1μM to 70nM were bound to glutathione sepharose beads and loaded with APC/C in solution that was purified from logarithmically proliferating HeLa cells. I could detect no APC/C binding to GST-N116 Cdh1 at any concentration (data not shown). This was somewhat surprising given that a fragment of N-terminal 159 amino acids of Fizzy (GST-N159 Fizzy) could pull out APC/C from *Xenopus* egg extracts (Kimata et al., 2008). Longer Cdh1 C-box baring fragments should be tested in APC/C binding for the purpose of the C-box-binding

site determination on the APC/C. Another reason for this discrepancy might lie in the fact that I have used interphase HeLa cell extracts, whereas Kimata et al. used CSF arrested *Xenopus* egg extracts. This will have to be resolved in the future.

2.4 APC/C inhibition by the SAC

The association of Mad2 and Mad3/BubR1 with Cdc20 has been studied in some detail, but how these interactions lead to inactivation of the APC/C is poorly understood. Mad2 is recruited to unattached kinetochores by its binding partner Mad1 (Chen et al., 1996; Sironi et al., 2001; Shah et al., 2004), where the Mad2-Mad1 heterodimer has been proposed to function as a template that catalyzes the assembly of Mad2-Cdc20 complexes (DeAntoni et al., 2005; reviewed by Nasmyth, 2005; Mapelli and Musacchio, 2007). Mad2-Cdc20 complexes have been detected in yeast and human cell lysates (Tang et al., 2001a; Fang, 2002; Poddar et al., 2005), but Mad2 has also been isolated from yeast and human cell extracts as part of a mitotic checkpoint complex (MCC), which also contains Mad3/BubR1, Bub3 and Cdc20 (Fraschini et al., 2001; Sudakin et al., 2001). Recombinant Mad2 and BubR1 can each inhibit APC/C-mediated ubiquitination reactions in vitro (Li et al., 1997, Fang et al., 1998; Fang, 2002; Tang et al., 2001a) but MCC isolated from HeLa cells is much more potent in this assay (Sudakin et al., 2001). *In vitro*, binding of recombinant Mad2 or BubR1 to Cdc20 prevents the association of Cdc20 with APC/C (Reimann et al., 2001; Tang et al., 2001a), however, these proteins could also be detected in complex with APC/C bound to Cdc20 (Wassmann and Benezra, 1998; Morrow et al., 2005; Braunstein et al., 2007). High-salt treatment or Cdc20 ubiquitylation causes dissociation of Mad2 and BubR1 from the APC/C, and increases APC/C activity, indicating that Mad2 and BubR1 can inhibit APC/C by physical interaction (Braunstein et al., 2007; Reddy et al., 2007). For Mad2 it has also been proposed that it inhibits APC/C by reducing substrate release from Cdc20 (Pfleger et al., 2001), and for Mad3 it has been shown that it binds to Cdc20 as a pseudosubstrate and prevents the association of substrates with Cdc20 (Burton and Solomon, 2007; Maleureanu et al., 2009).

The state of the APC/C itself was never analyzed in detail in cells with an active checkpoint. To gain insight into the mechanism of APC/C inhibition by the MCC, the APC/C was isolated from mitotic HeLa cells in which the spindle assembly checkpoint was active (SAC-on) or switched off (SAC-off), and compared structurally and

biochemically (Herzog et al., 2009). These data indicate that the activation of the spindle assembly checkpoint leads to association of BubR1, Bub3 and Mad2 with APC/C-Cdc20. Three dimensional models of human APC/C obtained by single-particle electron microscopy in various functional states: bound to a Mitotic Checkpoint Complex (MCC), to Cdc20, or to neither (apo-APC/C) revealed that the MCC binding site partially overlaps with the Cdc20 binding site on APC/C and suggested that the MCC might inhibit the APC/C by repositioning Cdc20 (Figure 2 in Herzog et al., 2009). Association of checkpoint proteins with APC/C coincides with inhibition of APC/C ubiquitylation activity towards securin and cyclin B, but also towards cyclin A and Nek2A, the early prometaphase substrates. My contribution to this study was to show that this inhibition is, at least in part, caused by the prevention of substrate binding. For this purpose I performed *in vitro* substrate binding assays which I will describe in this chapter in more detail. The publication itself (Herzog F, Primorac I, Dube P, Lenart P, Sander B, Mechtler K, Stark H, Peters JM. (2009) Structure of the anaphase-promoting complex/cyclosome interacting with a mitotic checkpoint complex. Science. 5920:1477-81) is in the Appendix of this thesis.

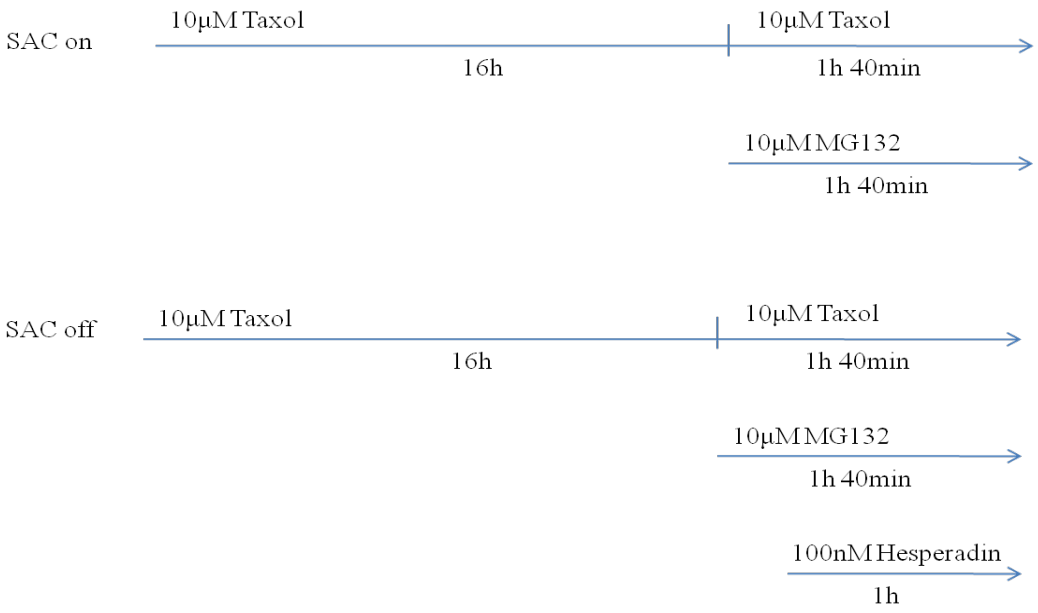

Figure 23. Protocols to arrest HeLa cells in a SAC on or SAC off state. To obtain HeLa cells with an active checkpoint (SAC-on) the cells were arrested in prometaphase by incubation in DMEM medium containing Taxol for 17h 40 min. The SAC arrest was overcome (SAC-off) by addition of Hesperadin 1h before harvest. To make sure that he cells do not exit mitosis, the proteasome was inhibited with MG132 40 minutes prior to Hesperadin addition. To reduce the number of variables that differ between SAC-on and SAC-off cells, for the last 1h 40 min before harvesting SAC-on cells proteasome inhibitor MG132 was also added.

To obtain mitotic extracts in a SAC-on state HeLa cells were arrested in prometaphase by stabilizing microtubules with Taxol. The SAC-off state was generated by overriding the Taxol arrest in SAC-on HeLa cells with Hesperadin, a small molecule inhibitor of Aurora B kinase. The mitotic progression of cells released from the SAC arrest was prevented by the addition of the proteasome inhibitor, MG132, which prevented degradation of securin and cyclin B and thereby inhibited the onset of anaphase. To reduce the number of variables that differ between SAC-on and SAC-off cells MG132 was added also to the cells in SAC-on condition (Figure 23).

2.4.1 Binding of substrates to APC/C isolated from SAC-on cells is reduced

First I compared N70-2x-GST substrate binding to APC/C isolated from HeLa cells with an active (SAC-on) or inactive (SAC-off). Substrates were first bound to glutathione sepharose beads by incubation in 70nM and 20nM solution of N70-2x-GST wild type (wt) or D-box mutant (dm) in buffer A that contained 4 mg/ml of BSA (see Materials and methods) at room temperature for 1 hour on an end-over-end rotator. To reduce unspecific binding the beads were pre-incubated in Buffer A that contained 2 mg/ml BSA prior to substrate binding for 30 minutes at room temperature on an end-over-end rotator. To remove unbound substrates the beads were washed with buffer A. APC/C was immunopurified from mitotic extracts of HeLa cells in which the spindle assembly checkpoint was active or inactivated, with α-Cdc27 antibodies coupled to Protein A beads. The immunoprecipitated APC/C was eluted off the beads with the

Cdc27 antigenic peptide. Glutathione beads bound to N70-2x-GST, wt or dm, were then incubated in the 4 bead volumes of APC/C peptide elution for another 1h at room temperature with end-over-end rotation. Unbound APC/C was washed off glutathione beads with Buffer B (see Materials and methods), and the bound proteins were eluted off the beads by boiling in 1.5 bead volumes of 2xSDS PAGE sample buffer that contained 5mg/ml of BSA. The eluted samples were analyzed by SDS PAGE and Western blotting (Figure 24). APC/C-Cdc20, isolated from HeLa cells with SAC-off could bind wild type N70-2x-GST, but not the D-box mutant (compare lane5 with 6 and lane 9 with 10), confirming that the binding observed is specific. No Mad2 or BubR1 was associated with the APC/C from SAC-off cells that was retained on wt N70-2x-GST. APC/C-MCC, however, could bind very low levels of wild type N70-2x-GST (lanes 3 and 7).

A

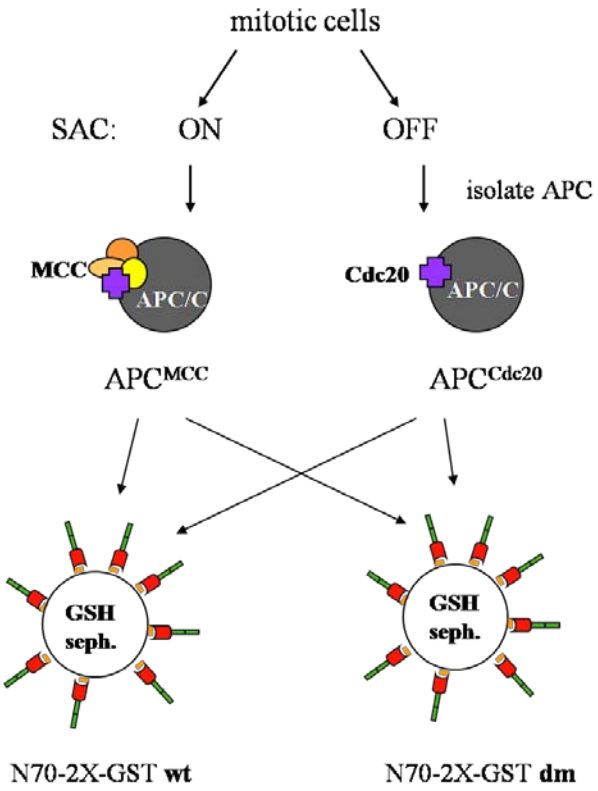

B

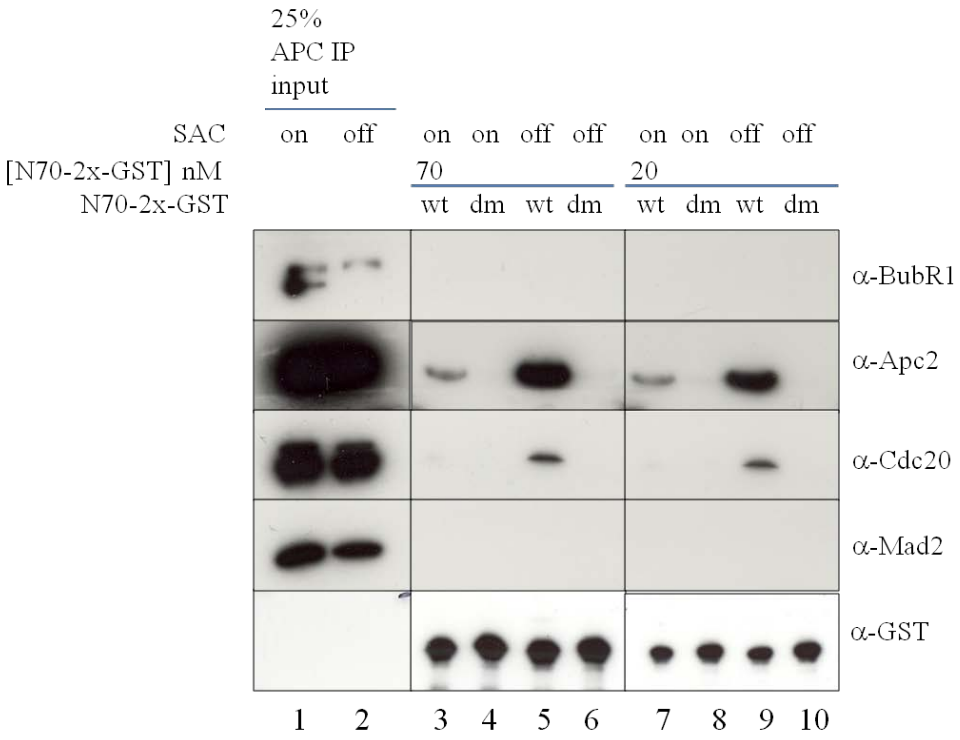

Figure 24. APC/C binding to the N70-2x-GST is impaired when it is isolated from HeLa cells with an active spindle assembly checkpoint. A. Schematic representation of the experimental outline. GSH-seph = glutathione sepharose beads. B. Glutathion beads bound to the WT or DM N70-2x-GST substrate were incubated in a solution of APC/C-MCC or APC/C-Cdc20 purified from mitotic cells extracts obtained from HeLa cells in which the SAC was turned on or off, respectively. Unbound APC/C was washed off and the beads were boiled in sample buffer, analyzed by separation on an SDS-PAGE gel followed by Western blotting. APC/C was detected with antibodies against Apc2 and MCC was detected with antibodies against Mad2 and BubR1. The substrate was detected with antibodies against the GST tag.

The reduction in the amount of MCC subunits, Mad2 and BubR1, that co-immunoprecipitate with APC/C upon checkpoint release is not so dramatic (compare the input lanes 1 and 2), yet the difference in binding to the substrates between the APC/C molecules isolated from two checkpoint states is quite large (compare lane 3 with 5 and lane 7 with 9). The reason for this remains unclear.

Next I wanted to see if the observed difference in substrate binding between APC/C molecules that were isolated from SAC-on and SAC-off cells, when the APC/C in solution was loaded on bead-bound substrates, would be the same if the APC/C was anchored to the beads. The procedure outline of this type of experiment is shown in Figure 25.

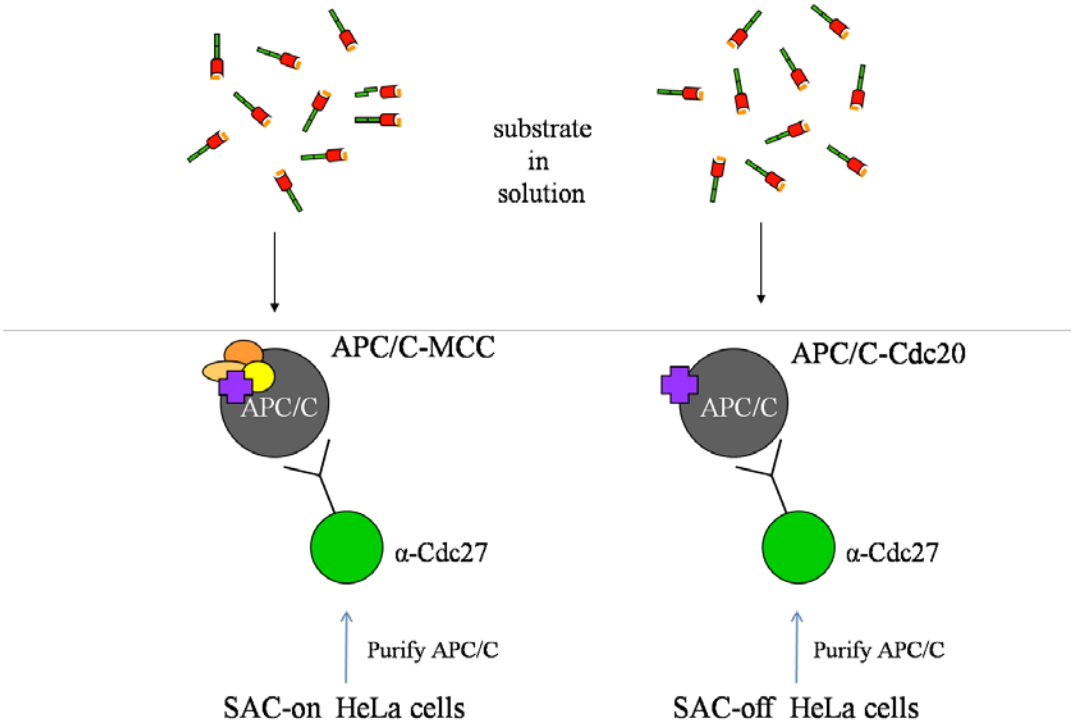

Figure 25. Schematic representation of an *in vitro* substrate binding experiment in which the APC/C bound to beads is exposed to substrates in solution. APC/C was purified from mitotic HeLa extracts with α-Cdc27 antibody coupled to Protein A sepharose beads. Bead-bound APC/C was then incubated in a solution of substrates, as described in the text.

APC/C was immunopurified from mitotic HeLa cells with an active or inactive SAC with α-Cdc27 antibodies coupled to Protein A beads. The beads were washed with TBS-T and subsequently incubated in 3 bead volumes of Buffer A (Materials and methods) that contained different concentrations of recombinant substrates for 1 hour at room

temperature with end-over-end rotation. To prevent unspecific binding the substrate dilutions in Buffer A also contained 4mg/ml of BSA. The unbound substrates were then washed away with Buffer B, and the bound proteins were eluted off the beads in 1.7 bead volumes of 0.1M glycine solution pH2.2. I have tested three different recombinant substrates in this assay, the fission yeast cyclinB construct N70-2x-GST (Figure 26); budding yeast H6-Hsl1$^{667-872}$ (Figure 27) and human H6-securin (Figure 28). All three substrates were expressed and purified from *E. coli*, as described in Materials and methods. When the SAC was inactivated (SAC-off) the amounts of MCC components, Mad2 and BubR1, that co-immunoprecipitated with the APC/C were reduced (compare Mad2 and BubR1 blots in lanes 3 and 4 in Figure 26; compare lane 3 with lane 4 and lane 5 with lane 6 in Figure 28). Both in the case of N70-2x-GST and H6-securin binding I could observe that the presence of MCC proteins on APC/C is inversely correlated with its ability to bind the substrate. In the experiment with N70-2x-GST I have compared the ability of APC/C from SAC-n and SAC-off cells to bind to substrates diluted in Buffer A to 180nM, 70nM, 20nM and 7nM concentration (Figure 26 A, B, C, D, respectively). With as little as 7nM substrate concentration I could detect specific binding of the wild type N70-2x-GST, but not of the D-box mutant to APC/C from SAC-off cells (Figure 26, lane 4 and 6). APC/C from SAC-on cells could bind neither wild type nor D-box mutant N70-2xGST at this concentration. At higher concentrations some unspecific binding could be detected, but this was much lower than the specific, wild type, N70-2x-GST binding to APC/C from SAC-off cells at any of the four concentrations.

A

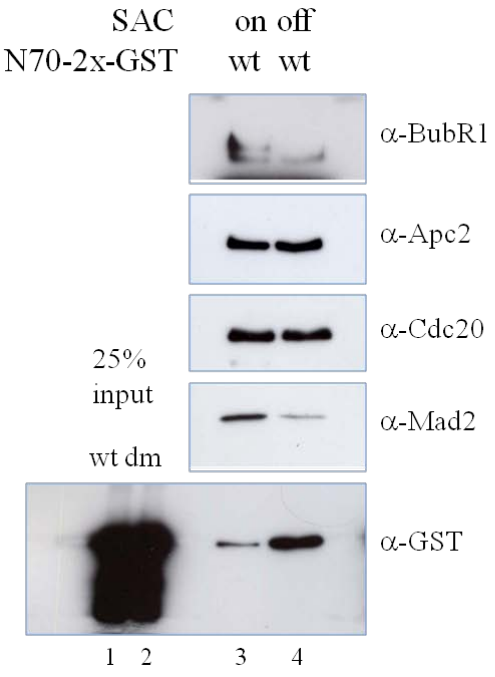
SAC
N70-2x-GST
on off
wt wt
α-BubR1
α-Apc2
α-Cdc20
25%
input
wt dm
α-Mad2
α-GST
1 2 3 4

B

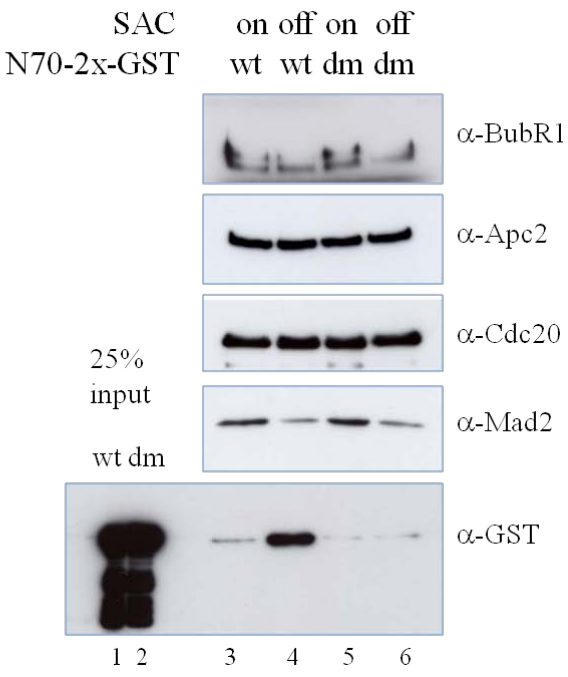
SAC
N70-2x-GST
on off on off
wt wt dm dm
α-BubR1
α-Apc2
α-Cdc20
25%
input
wt dm
α-Mad2
α-GST
1 2 3 4 5 6

C

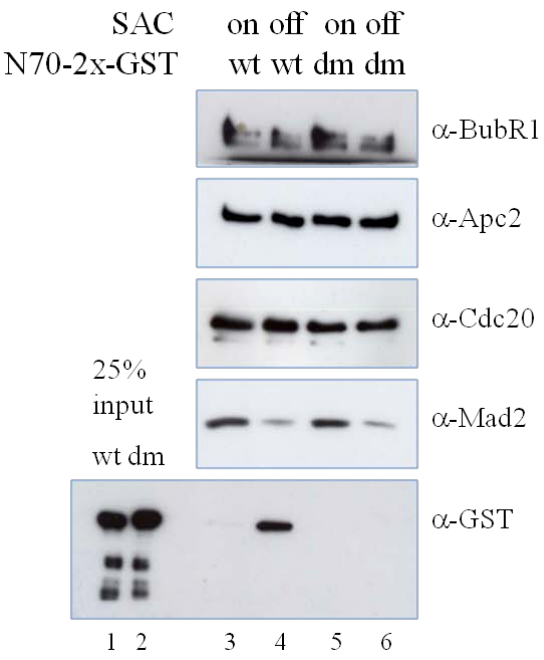
SAC
N70-2x-GST
on off on off
wt wt dm dm
α-BubR1
α-Apc2
α-Cdc20
25%
input
wt dm
α-Mad2
α-GST
1 2 3 4 5 6

D

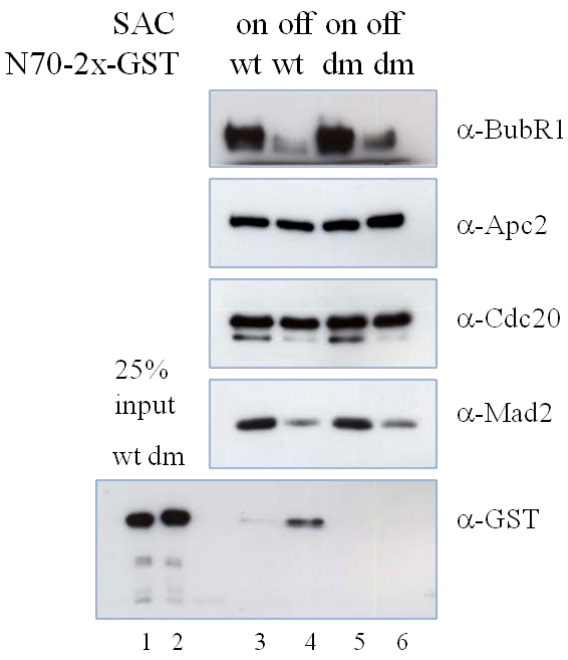
SAC
N70-2x-GST
on off on off
wt wt dm dm
α-BubR1
α-Apc2
α-Cdc20
25%
input
wt dm
α-Mad2
α-GST
1 2 3 4 5 6

Figure 26. Comparison of N70-2x-GST binding to APC/C from SAC-on and SAC-off HeLa cells. APC/C was immunopurified from mitotic cell extracts obtained from HeLa cells in which the SAC was turned on or off, with α-Cdc27 antibodies coupled to Protein A beads . The APC/C- bound beads were then washed in TBS-T and subsequently incubated in a Buffer A solution that contained 180nM wild type (wt) N70-2x-GST (A), 70nM N70-2x-GST wild type (wt) or D-box mutant (dm) N70-2x-GST (B), 20nM N70-2x-GST wild type (wt) or D-box mutant (dm) N70-2x-GST (C) and 7nM N70-2x-GST wild type (wt) or D-box mutant (dm) N70-2x-GST (D). The unbound substrates were washed off the beads with Buffer B and subsequently eluted in 1.7 bead volume of 0.1M glycine solution pH2.2. The eluates were analyzed by SDS PAGE and Western blotting. APC/C was detected with antibodies against Apc2, MCC was detected with antibodies against Mad2 and BubR1, and the N70-2x-GST was detected with antibodies against the GST tag.

It was interesting to find that the binding of H6-Hsl1$^{667-872}$, a substrate that has a very high affinity for the APC/C, is also reduced if the APC/C is isolated from cells with an active checkpoint (Figure 27). Even at concentrations as high as 700nM the difference in binding of H6-Hsl1$^{667-872}$ to APC/C from SAC-on and SAC-off cells was about eight-fold (compare lanes 2 and 3 in Figure 27).

Finally I performed the same experiment with human securin. To test securin in this assay was important because it is, besides cyclin B, one of the two key mitotic APC/C substrates whose degradation is inhibited by the SAC. I used human securin in this experiment because it is an “isogenic” substrate of the APC/C used in this assay. The results of this experiment are shown in Figure 28.

A

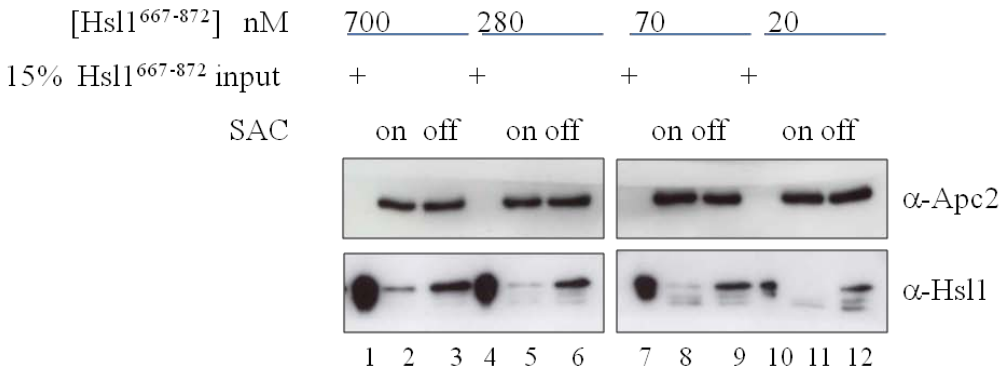

B

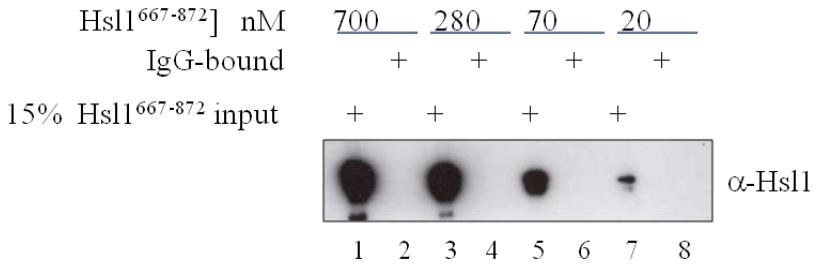

Figure 27. Comparison of H6-Hsl1$^{667-872}$ binding to APC/C isolated from SAC-on and SAC-off HeLa cells. APC/C was immunopurified from mitotic cell extracts obtained from HeLa cells in which the SAC was turned on or off , with α-Cdc27 antibodies coupled to Protein A beads. The APC/C- bound beads were then washed in TBS-T and subsequently incubated in a Buffer A solution that contained H6-Hsl1$^{667-872}$ at a concentration of 700, 280, 70 or 20nM. The unbound substrates were washed off the beads with Buffer B and subsequently eluted in 1.7 bead volume of 0.1M glycine solution pH2.2. The eluates were analyzed by SDS PAGE and Western blotting. APC/C was detected with antibodies against Apc2, and the APC/C-bound H6-Hsl1$^{667-872}$ with an α-Hsl1 antibody (A). Unspecific binding of H6-Hsl1$^{667-872}$ to Protein A beads was controlled by performing the same assay with IgG-coupled Protein A beads instead of α-Cdc27-coupled Protein A beads (B).

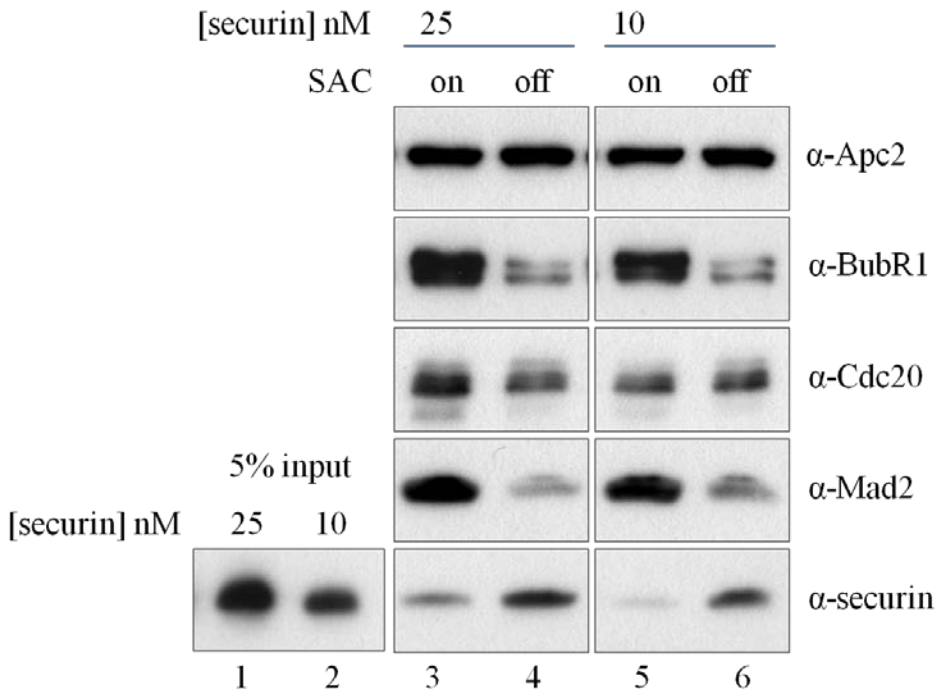

Figure 28. Comparison of human H6-securin binding to APC/C from SAC-on and SAC-off HeLa cells. APC/C was immunopurified from mitotic cell extracts obtained from HeLa cells in which the SAC was turned on or off, with α-Cdc27 antibodies coupled to Protein A beads. The APC/C- bound beads were then washed in TBS-T and subsequently incubated in a Buffer A solution that contained recombinant N-terminally 6x Histidine (H6) tagged human securin at concentrations 25nM or 10nM. To prevent unspecific binding, the substrate solution also contained 4mg/ml of BSA. The unbound substrate was washed off the beads with Buffer B and the bound proteins were eluted with a 0.1M solution of glycine pH 2.2. The eluates were analyzed by SDS PAGE and Western blotting. APC/C was detected with antibodies against Apc2, the MCC was detected with antibodies against Mad2 and BubR1, and the bound H6-securin was detected with α-securin antibodies.

From all the experiments described in this section we could conclude that the MCC association with the APC/C prevents its binding to substrates.

3. Discussion

3.1 Involvement of apo-APC/C and activators in substrate recognition

3.1.1 Interaction of the WD40 domain of Cdh1 with Hsl1$^{667-872}$

APC/C activation requires the association of one of two related activator proteins, Cdc20 and Cdh1. Based on several studies (Hilioti et al, 2001; Schwab et al, 2001; Burton and Solomon, 2001; Pfleger et al, 2001) it is thought that the activators have a role in recruiting the substrates to the APC/C, analogously to the substrate adaptors of the SCF complexes. Mutational analysis by Burton et al, (2005) and cross-linking experiments by Kraft et al, (2005), suggest that the WD40 domain of activator proteins is involved in substrate recognition. I could show that the WD40 domain of Cdh1 is sufficient to bind a D box and KEN box containing fragment of Hsl1 protein (amino acids 667-872) when co-expressed in insect cells and in budding yeast, and that this binding is dependent on the D and the KEN box in Hsl1$^{667-872}$. I have aimed to co-express and purify a stoichiometric complex of the WD40 propeller region of Cdh1 and a fragment of Hsl1 encompassing the degrons D and KEN box, in budding yeast *Saccharomyces cerevisiae*, for the analysis of their interaction by X-ray crystallography. I did not pursue this project further for several reasons. The yield of the stoichiometric complex was very low. It is known that the folding of APC/C activator proteins depends on the CCT chaperonin complex (Camasses et al., 2003), therefore it is possible that the cell cannot process all the over-expressed Cdh1 proteins with its chaperone arsenal. Another problem was that the stoichiometry upon co-expression of Cdh1WD40 and Hsl1$^{667-872}$was unpredictable. This was probably due to the fact that the proteins were expressed from two separate plasmids. Cloning the two constructs in one expression plasmid would make more sense, or, were the protein levels higher, a second step of re-immunopurification of the complex could be introduced in the purification procedure. The Hsl1 fragment I have been using was prone to degradation which introduced heterogeneity to the purified sample. Deleting regions surrounding the D and KEN box resulted in reduced binding to the WD40 propeller. Deletions with a single amino-acid residue resolution might be necessary to find the right length of the Hsl1 fragment that still binds to the WD40 propeller of Cdh1 with high affinity, but that is not degraded. It might be worth trying to obtain this same complex, or a

WD40 region of Cdh1 in complex with other substrates, in Sf9 cells. I have used an Hsl1 fragment as a substrate for this purpose because it binds to activator proteins with unusually high affinity, but conditions could be optimized for co-purification of the WD40 region of Cdh1 with substrates with lower affinity. A serendipitous discovery opened a new window of opportunity for Cdh1 over-expression in Sf9 cells, namely, tagging this protein with a 3xmyc tag yielded about ten-fold more protein that can be purified (Georg Petzold, personal communication). I have compared this myc-tagged Cdh1 with an old preparation of 6xHis-tagged Cdh1 in an in vitro ubiquitylation assay, and could find that the activity these two versions of Cdh1 can provide to the APC/C was comparable. This excluded the possibility that the tag folded back onto the substrate-binding interface of Cdh1 and thereby stabilized it. Another problem with expressing and purifying APC/C activators is the fact that they are prone to aggregation, therefore the purification procedure should be kept as short as possible. I have been succesfully avoiding the aggregation of Cdh1 when, instead of dialyzing the protein after the imidazole elution, I exchanged the buffer by using a desalting column (NAP-5 column, GE Healthcare)

3.1.2 Attempts to purify apo-APC/C

Several findings suggest that, in addition to Cdc20 and Cdh1, the apo-APC/C also contributes to substrate binding. A peptide containing tandem copies of the D box is able to pull down apo-APC/C that is largely free of Cdc20 or Cdh1 from *Xenopus* egg extracts (Yamano et al., 2004). Yeast Doc1 is required for D box-dependent substrate processivity of APC/C in an in vitro ubiquitination assay suggesting that Doc1 plays a rather direct role in the recognition of the D box (Carroll et al., 2005). Native-gel binding assays and ‘‘isotope trapping’’ have demonstrated that the complex between APC/C and Cdc20 binds to substrates with higher affinity than either APC/C largely free of activators or Cdc20 alone (Passmore and Barford, 2005; Eytan et al., 2006). The presence of substrates stimulates co-activator binding to the APC/C (Burton et al., 2005; Matyskiela and Morgan, 2009). I have made an attempt to purify apo-APC/C using several methods, but the APC/C I could purify always contained detectable amounts of activator proteins. Depletion of mitotic extracts of Cdc20 with an antibody raised against a peptide could remove almost all Cdc20 from the extract, as detected by Western blot,

however the APC/C purified from these Cdc20-depleted extracts, even after 3 rounds of extract depletions before APC/C immunoprecipitation, was still bound to detectable amounts of Cdc20. The α-Cdc20 antibody I have used in these depletion experiments was raised against a peptide (RWQRKAKEAAGPAPSPMRAANR, kpep 450), located in the amino terminal, low complexity region of Cdc20. It is interesting that this peptide encompasses a serine residue, S41, which has been shown to be one of six residues in Cdc20 that are phosphorylated by Bub1 in human cells and whose phosphorylation is required for the spindle assembly checkpoint function (Tang et al., 2004). It could be that the phosphorylation of this residue masked the epitope which α-Cdc20 recognizes and thereby prevented depletion of this pool of Cdc20. This serine was however not found to be phosphorylated in the study by Kraft et al., 2003. In this study the phosphorylation state of Cdc20 which is bound to the APC/C in mitosis was analyzed. Analysis of Cdc20 phosphorylation under spindle assembly checkpoint conditions in *Xenopus* egg extracts showed that phosphorylation of Cdc20 in its amino-terminus is facilitates Mad2 and BubR1 binding (Chung and Chen, 2003). If one of residues found in this study corresponds to Ser41 in human Cdc20 is not clear.

3.2 Dephosphorylation of APC/C is not sufficient to cause dissociation of Cdc20

The activity of APC/C is regulated by reversible phosphorylation (Lahav-Baratz et al., 1995, Peters et al., 1996, Kotani et al., 1998) Although the precise role of mitotic APC/C phosphorylation is poorly understood, there are indications that it affects Cdc20 binding (Kramer et al, 2000, Rudner and Murray, 2000). Cdc20 binds preferentially to mitotically phosphorylated APC/C (Kramer et al., 1998; Kramer et al., 2000). APC/C phosphorylation by Cdk1, or Cdk1 and Plk1 combined, increased its ability to bind Cdc20 in vitro and correlated with 4-fold and 6-fold increase in APC/C activity, respectively. The increase in activity was due to Cdc20 binding (Kraft et al., 2003). It was found that the most heavily phosphorylated subunits of the APC/C are the TPR subunits, and it may be that this phosphorylation directly regulates the association of the IR tail of Cdc20 and APC/C's TPR subunits (Vodermaier et al., 2003, Kraft et al., 2003). From all these studies it seems likely that the mitotic phosphorylation of APC/C stimulates Cdc20 binding, however if dephosphorylation of APC/C causes Cdc20 dissociation was never tested. I

tested this by dephosphorylating immunopurified APC/C, as well as by dephosphorylating APC/C in mitotic HeLa extracts, with lambda phosphatase. The efficiency of dephosphorylation was confirmed by increased mobility of Cdc27 subunit, however, no reduction in the levels of Cdc20 bound to the APC/C could be observed. Therefore it seems that dephosphorylation of APC/C is not sufficient to cause dissociation of Cdc20. Studies of APC/C isolated from *Xenopus* egg extracts revealed that the a interphase APC/C contained 2.5-fold less Cdc20 compared to mitotic APC/C, however substantial amounts of Cdc20 were bound to the interphase APC/C, although it was dephosphorylated, as confirmed by shift in gel mobility of Apc1, 3, 6 and 8, but also of Cdc20 mobility shift (Yamano et al., 2004). This interphase APC/C could not bind to cyclin B, and it could not stimulate cyclin B destruction in extracts, therefore it seems that it is sufficient to dephosphorylate APC/C-Cdc20 in interphase, at least in *Xenopus* egg extracts, to inactivate it, and that dissociation of Cdc20 is not necessary. Cdc20 is an APC/C-Cdh1 substrate, and *Xenopus* egg extracts contain no Cdh1. It could be that the removal of Cdc20 from APC/C requires its ubiquitylation, and possibly also degradation, mediated by APC/C-Cdh1. It would be interesting to follow up this question. There are several reports that show that it is possible to activate *Xenopus* interphase APC/C with purified recombinant Cdc20 in vitro (Fang et al., 2002; Tang et al., 2004), and that it is possible to bind purified recombinant Cdc20 to human interphase APC/C (Georg Petzold, personal communication). Whether the bound Cdc20 in the latter case is also able to activate APC/C in an *in vitro* ubiquitylation assay should be tested.

3.3 The role of the C box

The C box was shown to be essential for the function of budding yeast Cdh1 and to be required for its association with the APC/C (Schwab et al., 2001). In another study of the C box in yeast Cdh1 only a mild defect in APC/C stimulation by the mutant Cdh1 was reported (Thornton et al., 2006). Binding of human recombinant Cdh1 was significantly, but not completely, reduced if the C box was mutated. However, this mutant of Cdh1 was completely unable to activate APC/C (Vodermaier et al., 2003). It remained therefore unclear if the only function of the C box was to bind the activator to the APC/C or if it has other functions. Recently it has been found that the N terminal part of Cdh1 bearing the C box was sufficient to activate

the *Xenopus* APC/C in an ubiquitylation reaction if the substrate is recruited to it in an activator independent manner (Kimata et al., 2008). Insight into the role of the C-box of APC/C activators was provided by studies of Nek2A, an extraordinary APC/C substrate. Nek2A does not require the substrate-recruiting function of Cdc20, it is recruited independently by its own MR tail. However, Cdc20 is still required for Nek2A ubiquitylation. (Hames et al., 2001). Kimata et al, (2008) took advantage of this property of Nek2A and have shown that a fragment of 159 amino terminal residues of *Xenopus* Cdc20 (GST-N159 Fizzy) as well as 186 amino terminal residues of Cdh1 (GST-N186 Fzr1) could stimulate Nek2A degradation in *Xenopus* egg extracts, and that this stimulation was C-box dependent. Fusing Mes1, a fission yeast APC/C pseudosubstrate that contains a D and a KEN box, to the amino terminal 159 amino acids of Fizzy could stimulate Mes1 ubiquitylation. This was however, not dependent on the degron motifs in Mes1. How the C-box-containing fragment of activator proteins stimulates the ubiquitylation by the APC/C remains unclear.

All the mentioned reports are of qualitative nature and we decided to study the effect of the C-box mutation in Cdh1 in a more quantitative manner, using purified components, which might allow a clearer view at the role of the C-box in mechanistic terms. I could show that the binding of Cdh1 with a mutated C-box was reduced 10-fold compared to the wild type Cdh1. Wild type levels of the C-box mutant (Cm) Cdh1 could be restored by increasing the concentration of C-box mutant Cdh1 that was incubated with the APC/C to 10-fold of the concentration of the wild type Cdh1. Restoring wild type levels of Cdh1 Cm, however did not restore the wild type activation of the APC/C in an *in vitro* ubiquitylation assay. The defect in APC/C activation could arise from defective substrate recruitment to the APC/C or from defective catalytic activation of APC/C towards a properly recruited substrate. I could show that the substrate binding to APC/C loaded with C-box mutant Cdh1 was impaired. This defect in substrate binding I could not compensate for by increasing the substrate concentration. However, co-expression experiments of Cdh1 wt or Cm with $Hsl1^{667-872}$ showed that the C-box mutation has no effect on $Hsl1^{667-872}$ binding.

My explanation of the listed results is based on a hypothesis that Cdh1 interaction with the APC/C via two motifs, the IR tail and C-box, closes or distorts the conformation of APC/C in a way that exposes its substrate-binding surface, that can either “take over” the Cdh1-recruited substrate or hold it together with Cdh1 in the proximity of ubiquitin-charged E2. The following

findings support this hypothesis: The flexibility of apo-APC/C is reduced upon Cdh1 binding (Dube et al., 2005); the IR tail was shown to bind to Cdc27 on APC/C (Vodermaier et al., 2003, Passmore and Barford, 2003; Thornton et al., 2006, Matyskiela and Morgan, 2009); and the binding of the substrate adaptor, Cdh1, is affected upon Apc2 deletion, indicating that Cdh1 interacts closely with the catalytic core (Thornton et al., 2006). The latter proposal could not be supported by crosslinking experiments with human Cdh1 and APC/C. Bi-functional crosslinkers always crosslinked Cdh1 to Cdc27 and no other APC/C subunit. Site-specific crosslinking experiments also showed that if the crosslinker amino-acid is located near the C-box in Cdh1, the captured APC/C subunit is Cdc27 (Kraft et al., 2005). It might be worthwhile repeating these crosslinking experiments using a C-box containing fragment of Cdh1, or testing this finding by a different approach. For example, since positions of the two candidate subunits, Apc2 and Cdc27, in a 3D model of APC/C are mapped (Herzog et al., 2009) and since the location of a subunit can also be mapped by tagging it with a bulky tag (Bettina Buschhorn, unpublished data), a C-box fragment fused to a bulky tag could be loaded onto the APC/C and analyzed by cryo-EM. If the resolution of the resulting model would be high enough it might be possible to determine which APC/C subunit the tag points to. In an attempt to pull down APC/C with a 116 amino-acid long C-box containing fragment of Cdh1 I have failed to detect any APC/C binding to this fragment. Although the C-box starts at amino-acid 46, it could be that the fragment has to be longer to efficiently pull down APC/C. It might be worth repeating this experiment with a longer C-box containing Cdh1 fragment, using, interphase and mitotic, Xenopus egg and HeLa cell extracts. It would also be interesting to see if the flexibility of APC/C is reduced upon Cdh1 binding when its C-box is mutated, as it could be observed with the wild type Cdh1 (Dube et al., 2005).

3.4 How does the SAC affect substrate recognition by the APC/C?

An important contribution to understanding how the MCC inhibits the APC/C was the structural and biochemical comparison of APC/C species isolated from mitotic HeLa cells in which the spindle assembly checkpoint was active (SAC-on) or switched off (SAC-off) (Herzog et al., 2009). These data indicate that the activation of the spindle assembly checkpoint leads to association of BubR1, Bub3 and Mad2 with APC/C-Cdc20. Three dimensional models of human

APC/C obtained by single-particle electron microscopy in various functional states: bound to a Mitotic Checkpoint Complex (MCC), to Cdc20, or to neither (apo-APC/C) revealed that the MCC binding site partially overlaps with the Cdc20 binding site on APC/C and suggested that the MCC might inhibit the APC/C by repositioning Cdc20 (Figure 2 in Herzog et al., 2009). When we compared the ability of APC/C isolated from SAC-on and SAC-off cells to bind substrates we found that the binding of a variety of substrates to the APC/C upon SAC activation is also reduced. Association of checkpoint proteins with APC/C coincides with inhibition of APC/C ubiquitylation activity towards securin and cyclin B, but also towards cyclin A and Nek2A, the early prometaphase substrates, *in vitro*.

In vivo the spindle assembly checkpoint (SAC) delays degradation of cyclin B and securin until all the chromosomes are properly attached, however this does not seem to affect cyclin A and Nek2A degradation which starts already in prometaphase (Geley et al., 2001; den Elzen and Pines, 2001; Hames et al.,2001). Nek2A has been shown to be recruited to the APC/C in a Cdc20-independent manner via its C terminal MR tail, which resembles the TPR-binding motif found in APC/C activators and Doc1, the IR tail (Hayes, et al., 2006). This activator-independent recruitment of Nek2A to the APC/C might overcome the SAC-mediated inhibition of APC/C-Cdc20. There are several scenarios that describe how this might be possible, and I will come back to this below. What has been puzzling many of those studying the APC/C and its regulation by the SAC, is how is it that cyclin A, but not cyclin B, avoids the inhibition of APC/C by the MCC and gets degraded in spindle assembly checkpoint arrested cells. It is not known if the degenerate D-box in cyclin A has any role in this, therefore it would be interesting to see if cyclin B in which the D-box is replaced by the "extended D-box" characteristic of cyclin A could be degraded under SAC-n conditions in the cell. It has been proposed that degradation of cyclin A requires Cdk binding, as a mutation that abolishes Cdk binding stabilizes cyclinA (Stewart et al., 1994, Geley et al., 2001). Purified recombinant I^{125}-labeled cyclin A alone cannot be ubiquitylated in vitro (my observation, not presented in the thesis) contributes to the evidence for this mechanism. I have, however, never tested if placing cyclin A into a cyclinA/Cdk/Cks1 complex would facilitate ubiquitylation of cyclin A *in vitro*. It has been proposed that Cks1-mediated recruitment of cyclin A to the APC/C in prometaphase is the mechanism by which cyclin A avoids D-box-mediated binding to the APC/C, and thereby circumvents the SAC

(Wolthuis et al., 2008). The proposed mechanism, however, immediately imposes the next question. How is it then that cyclin B, although potentially recruited to the APC/C by the same mechanism, is not ubiquitylated as cyclin A is? Since both cyclin A and cyclin B share the Cks1/p9 subunit as a binding partner, they should both be recruited to the APC/C Cks1-dependent manner, however, it is not clear what makes the difference between these two cyclins that renders one prone to APC/C mediated ubiquitylation and the other not. Both cyclin A and cyclin B associate with Cdk and Cks1 to be able to perform their kinase function, and the observed binding to the APC/C could simply be because APC/C is a Cdk1 substrate (Patra and Dunphy, 1998; Rudner and Murray, 2000). It has been elegantly shown that the Xenopus Cks1 homolog, p9, is not required for cyclin B degradation once the APC/C is phosphorylated and thereby activated (Patra and Dunphy, 1998). Following cyclin A degradation in the same experimental setting might answer the question if p9 is required for its degradation.

The above mentioned model of cyclin A recruitment and ubiquitylation by the APC/C also further implies that the MCC binding to the APC/C does not influence the catalytic activity of the enzyme. This contrasts our observation that APC/C-MCC shows reduced overall ubiquitylation activity, not only towards cyclin B and securin, but also cyclin A and Nek2A (Herzog et al., 2009, Figure S2). Prometaphase substrates might be ubiquitylated by the APC/C before the SAC becomes fully active. Although recruited to the APC/C Cdc20- independently, both Nek2A and cyclin A still need Cdc20 for their ubiquitylation (Hames et al., 2001; Geley et al., 2001). Based on this one could imagine that the prometaphase substrates are recruited to the APC/C before the SAC becomes fully active and before the MCC is assembled on the APC/C; and that substrates that are already recruited to the APC/C are refractory to inhibitory factors and will proceed with the ubiquitylation process. In line with this hypothesis is the observation that neither Mad2 nor BubR1 inhibit the ubiquitin ligase activity of pre-formed Cdc20-APC/C, and that Mad2 and BubR1 have an inhibitory effect on Cdc20-APC/C only if Cdc20 is pre-incubated with these proteins, and then bound to the APC/C (Fang, 2002, figure 2D). Could it be that all the cyclin A molecules are already bound to the APC/C-Cdc20 as a substrate when the fully active MCC starts to be assembled? One could further speculate that cyclin A in these pre-assembled complexes with APC/C-Cdc20 “reserves” Cdc20 for its ubiquitylation, and once the ubiquitylation is over, and this trimeric complex disassembles, cyclin A is sent for degradation to

the proteasome and free Cdc20 can be captured by the SAC signalling into the MCC. In line with this idea is the fact that BubR1, the pseudosubstrate that blocks the substrate-binding surface on APC/C-Cdc20 (Burton and Solomon, 2007) stays cytoplasmic until the nuclear envelope breakdown (Björn Hegemann, personal communication), and also with the fact that cyclin A is predominantly nuclear from S phase onwards (Pines and Hunter, 1991), which gives cyclin A time to bind APC/C-Cdc20. If this is early enough to allow cyclin A binding of Cdc20 before Mad2 captures Cdc20 remains an open question. The observation that cyclin A associates with Cdc20 in G2 and early M phase and that this complex is devoid of Mad2 feeds this speculation (Wolthuis et al, 2009, Figure 3).

There are several ways one could test if cyclin A prometaphase, SAC-independent, degradation depends on its pre-binding to APC/C-Cdc20. Cells could be arrested in mitosis and, before cyclin A degradation starts, proteasomal degradation could be inhibited for a short period of time by MG132, thereby creating a window during which cyclin A could be ubiquitylated (and deubiquitylated once it is released from APC/C), the MCC could fully assemble, and only then release the proteasome from inhibition, but leave it in SAC-on condition, and look if cyclin A degradation is inhibited as that of cyclin B. This experiment is based on an assumption that, if there is a pre-assembled cyclin A APC/C-Cdc20 complex, it disassembles during the proteasome inhibition period, with a ubiquitin chain, which is subsequently removed by deubiquitinating enzymes without being degraded by the proteasome. Another, possibly more straightforward and based on less assumptions, way would be to arrest cells in mitosis, allow the APC/C-MCC to fully assemble, and only then add exogenous cyclin A and cyclin B and compare the kinetics of their degradation. To avoid the difficulty of injection of proteins or mRNAs into rounded up, mitotic cells, an inducible plasmid-based system to express these proteins in the cell could be used.

In our *in vitro* experiments where we compared the APC/C from SAC-on and SAC-off HeLa cells in ubiquitylation assays or substrate binding assays, the APC/C isolated from these cells was already fully bound to the MCC. This “final” form of APC/C-MCC did not discriminate between IVT generated substrates in a *in vitro* ubiquitylation assay, the APC/C isolated from cells with an active SAC did show reduced ubiquitylation activity towards cyclin A and Nek2A, as it did towards cyclin B and securin, compared to the APC/C isolated from cells with an inactive SAC (Herzog et al., 2009). This implies that the MCC binding has a negative

impact on overall activity of the APC/C. It has been observed that upon MCC binding the flexibility of APC/C is reduced (Herzog et al., 2009), this rigid state could also contribute to inactivity of APC/C-MCC. We could also show that the ability of APC/C to bind a variety of substrates is reduced in SAC-on conditions. This can be at least partially explained by BubR1-mediated blocking of Cdc20 substrate-recognition surface (Burton and Solomon, 2007; Malureanu et al., 2009). The substrates we tested were substrates whose destruction is prevented by the SAC. The next obvious question is if the binding of Nek2A and cyclin A to APC/C isolated from SAC-on cells is reduced compared to their binding to APC/C from SAC-off cells. To answer this question I am going to use recombinant Nek2A expressed and purified from *E. coli.* Answering the same question with cyclin A will be somewhat complicated by the fact that a Cdk/Cks1/cyclin A complex might be necessary to be used as a substrate.

4. Material and methods

4.1 Material

4.1.1 cDNA constructs

Site directed mutagenesis was performed using QuikChange® Site-Directed Mutagenesis Kit.

cDNA	species	tag	vector
Hsl1 (aa667-882)	S.cerevisiae	N‘ Protein A	pRS-424-GAL1-10 (trp)
Hsl1 (aa667-882)	S.cerevisiae	N‘ Protein A	pM346-GAL-PGK (leu)
Cdh1	S.c	N‘ flag	pRS-426-GAL1-10 (ura)
Cdh1 (aa164-567)	S.c	N‘ flag	pRS-426-GAL1-10 (ura)
Cdh1 (aa195-567)	S.c	N‘ flag	pRS-426-GAL1-10 (ura)
Cdh1 (aa227-567)	S.c	N‘ flag	pRS-426-GAL1-10 (ura)
Nek2A	Homo sapiens	N‘ his6	pME33
N70-2x wt-wt	S. pombe	C‘ GST	pET16
N70-2x wt-dm	S. pombe	C‘ GST	pET16
N70-2x dm-wt	S. pombe	C‘ GST	pET16
N70-2x dm-dm	S. pombe	C‘ GST	pET16
N70-1x wt	S. pombe	C‘ GST	pET16
N70-1x dm	S. pombe	C‘ GST	pET16
Hsl1 (aa667-882) wt	S.cerevisiae	N‘ GST	pGEX-TEV
Hsl1 (aa667-882) dm	S.cerevisiae	N‘ GST	pGEX-TEV
Hsl1 (aa667-882) km	S.cerevisiae	N‘ GST	pGEX-TEV
Hsl1 (aa667-882) dm km	S.cerevisiae	N‘ GST	pGEX-TEV
Nek2A KD	H. sapiens	N‘ his6	pET16
Nek2A KD	H. sapiens	N’ GST	pGEX-TEV
Securin (aa1-172)	H. sapiens	C‘ his	pET16
Securin (aa1-172)	H. sapiens	C‘ GST	pET16

H.s. cyclin B1, 1-87, -myc-his6 in pTrcHis2A was generated by Michael Gmachl.

N70-2x-GST wt-wt and dm-dm were a gift from Hiroyuki Yamano.

4.1.2 Baculoviruses

Baculoviruses are generated using the BAC-to-BAC expression system (Invitrogen, Carlsbad California, USA).

cDNA	species	tag	vector
Cdh1 wt	H.sapiens	N‘ HA3-his6	pFastBAC1
Cdh1 wt	H.sapiens	N‘ myc3-his6	pFastBAC1
Cdh1 C box mutant	H.sapiens	N‘ HA3-his6	pFastBAC1
Cdh1 C box mutant	H.sapiens	N‘ myc3-his6	pFastBAC1
Hsl1 (aa667-882) wt	S.cerevisiae	No tag	pFastBAC1
Hsl1 (aa667-882) dm	S.cerevisiae	No tag	pFastBAC1
Hsl1 (aa667-882) km	S.cerevisiae	No tag	pFastBAC1
Hsl1 (aa667-882) dm km	S.cerevisiae	No tag	pFastBAC1

H.s. his6-HA- Cdh1 wt and Cm were generated by Hartmut Vodermaier.
H.s. his6-HA-Cdc20 was generated by Edgar Kramer.

4.1.3 Antibodies

Antibodies raised against Apc2, Cdc27, Apc4, Cdh1 and Cdc20 have been described (Kramer et al., 1998; Gieffers et al., 1999; Kramer et al., 2000; Gieffers et al., 2001; Vodermaier et al., 2003).
Antibodies against BubR1, Mad2 and Bub3 were generated by Gregor Kohlmaier and Franz Herzog.

protein	„name“	species	Produced in	working dilution
BubR1	1676	H.s.	rabbit	1µg/ml
Mad2	283/2	H.s.	rabbit	1µg/ml
Bub3	0525	H.s.	rabbit	1:500 (serum)
Cdh1	452	H.s	rabbit	1µg/ml
Cdh1	Sat106	H.s.	rabbit	1µg/ml
Cdc20	450/2	H.s.	rabbit	1µg/ml
Apc2	APC2-30	H.s.	Mouse (monoclonal)	1:100 (supernatant)
Cdc27	03338	H.s.	rabbit	1µg/ml
Apc4	761	H.s.	rabbit	1µg/ml
Hsl1	1113	S.c.	rabbit	1µg/ml
Hsl1	1114	S.c.	rabbit	1µg/ml

Commercial antibodies:

antigen	supplier	species	Working dilution
GST	Amersham Biosciences	goat	1:500
Flag	Sigma-Aldrich	mouse	1:1000

4.2 Methods

4.2.1 HeLa cell culture

4.2.1.1 Cultivation of HeLa cells

Adherent HeLa cells were typically grown in 245x245cm tissue culture dishes and 37°C in the presence of 5% CO2 in Dulbecco's Modified Eagle Medium (DMEM) supplemented with 10% (v/v) fetal bovine serum (PAA Laboratories GmbH, Pasching Austria), 0.3µg/ml L-glutamine (Sigma-Aldrich), 100 units/ml penicillin (Sigma-Aldrich) and 100µg/ml streptomycin (Sigma-Aldrich).

4.2.1.2 Mitotic arrest of HeLa cells

To arrest cells in mitosis by activating the spindle assembly checkpoint (SAC-on), we treated logarithmically proliferating cells at 70% confluency with 10µM taxol (Paclitaxel, Sigma-Aldrich, St.Louis, MO) for 16h. Taxol stabilized microtubules and thereby prevented tension establishment between kinetochore sisters which activated the SAC and arrested cells in prometaphase-like state.

To synchronize cells in a mitotic state in which the SAC is inactivated (SAC-off), the Taxol arrested cells were treated with 100nM Hesperadin for 60 minutes (Boeringer Ingelheim, Vienna, Austria) to override the checkpoint. Hesperadin is a small molecule inhibitor of Aurora B kinase which corrects improper microtubule-kinetochore attachments and is therefore essential for SAC

signaling. To prevent cells exiting mitosis, 40 minutes prior to Hesperadin treatment the cells were treated with 10µM of proteasome inhibitor MG132 (Sigma-Aldrich). By inhibiting the proteasome MG132 prevents securin and cyclin B1 degradation and thereby prevents the anaphase onset and renders cells arrested in metaphase. To compare the two mitotic populations (SAC-on and SAC-off) that differed in only one variable the SAC-ON cells were also treated with 10µM MG132 100 minutes before harvesting.

4.2.1.3 Synchronization of HeLa ells by double thymidine arrest-release

HeLa Kyoto cells that were 90% confluent were split 1:10 into DMEM medium (10% FBS, 0.3µg/ml L-glutamine, 100 units/ml penicillin) containing 0.2mM Thymidine (Sigma T1895). Cells were incubated in thymidine under standard conditions for 24 hours when they were washed twice with prewarmed (37°C) PBS and relased into fresh DMEM medium (10% FBS, 0.3µg/ml L-glutamine, 100 units/ml penicillin) for 8 hours. The second thymidine arrest in 2mM thymidine was 16 hours long after which the cells were again released into fresh DMEM (10% FBS, 0.3µg/ml L-glutamine, 100 units/ml penicillin) after two washes in PBS. G2 cells were harvested 4 hours after the second thymidine release.

4.2.2. Recombinant protein expression

4.2.2.1 Yeast transformation

0.5ml of overnight culture of wt (700) yeast strain was diluted into 50 ml YEP-glucose medium, to obtain an OD600=0.2 and was subsequently incubated in a shaker at 30°C until the colony reaches OD600=0.8 (maximum 1). The cells are spun at 3500 rpm in for 5 minutes at room temperature.

The cells were the washed in 1 ml 1M LiAc and re-suspended in 350µl of 1M LiAc. 30 µl of this cell suspension was then mixed with 1µl of miniprep DNA (100 ng/ µl), 10 µl (10 mg/ml) of pre-

heated salmon sperm DNA and 112.5 µl 50% PEG 3350 and subsequently incubated in a thermomixer (Eppendorf, Hamburg, Germany) at 1200rpm for 30 minutes at room temperature. After this 15 µl of 60% glycerol was added and continued shaking for another 30 minutes shaking at room temperature. After this second incubation the cells were heat-shocked for 10 minutes in a waterbath at 42°C. As the transformed plasmids (pRS-424 (-trp) and pRS-426 (-ura), a gift from Prakash Arumugam, Nasmyth lab) contained auxotrophy markers, 300 µl of H20 were added to cells after the heatshock, of which 125µl were plated onto selective plates using glass beads. The cells were grown on selective plates at 30°C.

4.2.2.2 Recombinant protein expression in *S. cerevisiae*

50 ml of appropriate selective minimal medium (-ura, -trp and –leu media were prepared by the IMP media kitchen) containing 2% raffinose was inoculated from a single colony from the selective plate. The culture was grown over night at 30°C shaking.
the over-night culture was diluted the next day to OD_{600} = 0.2 in the same medium and the culture was grown at 30°C until OD_{600} = 0.6 when protein expression was induced by adding galactose to the culture to final concentration of 2%. The cells were further grown in the shaking incubator 30°C for 4-5 hours, and harvested by centrifugation at 1500g for 5 minutes at 4°C. The cell pellet was washed in 3 pellet volumes of ice cold water twice and frozen in liquid nitrogen.

4.2.2.3 Recombinant protein expression in *E.coli*

N702x-GST, N701x-GST, GST-Hsl1 (aa667-872), H6-securin, Cyclin B- myc-his(1-87aa)
N702x-GST is a tandem repeat of 70 N-terminal amino acid residues of fission yeast cyclin B, Cdc13, fused with a C-terminal GST (glutathione-S-transferase) tag. N70-1x-GST is a single repeat of the 70 N-terminal amino acid residues of fission yeast Cdc13 fused with a C-terminal GST (glutathione-S-transferase) tag. GST-Hsl1 (aa667-872) is a fragment of budding yeast protein Hsl1 described previously (Burton and Solomon, 2001), fused N-terminally with a GST

(glutathione-S-transferase) tag. Cyclin B- myc-his(1-87aa) is the N-terminal 87 residues of human cyclinB1. The constructs were expressed and purified from E.coli BL21(DE3) strain. An overnight starter culture was diluted into two liters of LB medium to OD600=0.1. The culture was grown at 37°C until OD600=0.6 when the expression of recombinant proteins was induced with 1mM IPTG (isopropyl-1-thio-β-D-galactopyranoside). Proteins were expressed at 37°C for 2h.

H6-Nek2A KD, GST-Nek2A KD, securin(1-172)

H6-Nek2A KD is a kinase-deficient mutant of human Nek2A generated by mutating a single amino acid residue in the kinase domain, D141A, by site directed mutagenesis system (Invitrogen). The construct was expressed and purified from BL21 E.coli strain. An overnight starter culture was diluted into two liters of LB medium to OD600=0.1. The culture was grown at 37°C until OD600=0.6 and then transferred to 18°C .The expression of recombinant proteins was induced with 1mM IPTG. Proteins were expressed at 18°C for 4h.

4.2.2.4 Recombinant protein expression in Sf9 cells

Sf9 cells were grown in Grace's medium supplemented with 10% (v/v) of Fetal Bovine Serum (FBS Gold, PAA Laboratories) 0.3µg/ml L-glutamine, 100 units/ml penicillin at 27°C. A confluent culture was split 1:5 into T175 flask (Nunc). The next day the 50% confluent culture was infected with 1ml of p4 baculovirus stock. This method was later modified, and different volumes (200-800µl) of BV p3 stock were used for infection instead. Proteins were expressed for 42-48h by growing the cultures at 27°C. The cells were harvested by tapping the flasks and washing off remaining cells with PBS. The cells were spun down at 500g in 50ml Falcon tubes and pellets were never frozen before purification.

4.2.3. Protein purification

4.2.3.1 Coupling antibodies to beads

The antibodies were bound and crosslinked to Affiprep protein A beads (BioRad). One volume protein A beads is washed twice with 10 volumes of TBS-T (20 mM Tris-HCl pH 7.5, 150 mM NaCl, 0.05% Tween-20). Beads are resuspended in 10 volumes TBS-T, and affinity purified Cdc27 antibodies are added in a ratio of 1.5 mg antibody per 1 ml of beads Beads are then incubated on an over-end rotator for 1 hour at room temperature. After three washes with TBS-T and two washes with 0.2 M sodiumborate solution (titrated to pH 9 with HCl), the beads are resuspended in 20 volumes of 0.2 M sodiumborate solution (pH 9) and, while mixing, solid dimethylpimelimidate (Sigma-Aldrich) is added to a final concentration of 20 mM. The mixture is rotated at room temperature for 30 minutes. The cross-linking reaction is stopped by washing the beads twice with 20 volumes of a buffer containing 150 mM NaCl and 200 mM Tris-HCl, pH 7.5, by incubating the beads each time for 10 minutes on a end-over-end rotator. The antibody-coupled beads are then washed twice with TBS-T and stored in TBS-T containing 0.05% NaN3 at 4 °C.

4.2.3.2 Purification of human APC/C form HeLa cells

HeLa cells pellets were thawn on ice and resuspended in 0.3 pellet volume lysis buffer (20mM Tris pH7.5, 150mM NaCl, 5 % glycerol, 2 mM EDTA, 0.05 % Tween 20) containing protease inhibitors (0.1 M PMSF, 20 µg/ml each aprotinin, pepstatin, and leupeptin) and phosphatase inhibitors (4µg/ml okadaic acid (Alexis), NaF 20 mM, 20 mM beta-glyerophoshate, 10 mM Na-pyrophosphate, 1 mM Na-Vanadate). The cell suspension was passed several times through syringe needles (1-2 x 0.8 mm and 4-5 x 0.4 mm in diameter) and the extract was cleared by centrifugation (13000 rpm, 30 minutes, 4°C). APC was isolated with antibodies against Cdc27 or Apc4. Antibodies were coupled to protein A beads (BioRad) and crosslinked using DMP as described. Typically the concentration of HeLa cell extract obtained using this method was 20-22

mg/ml. The lysate was incubated on an end-over-end rotator at 4°C for 60-90 min with 1/10 volume of antibody coupled beads. The APC/C-bound beads were washed 3x with TBS-T, of which 2x was with incubation for 5 minutes on an end-over-end rotator at 4°C. The APC/C was eluted off the beads by incubation in the 1mg/ml antigenic peptide buffered solution (20 mM Tris pH 7.5, 5% glycerol, 0.1% Tween-20 (Sigma-Aldrich), 1mM DTT).

4.2.3.3 Purification of H6-tagged activators from Sf9 cells

Cell pellet of one T175 flask was resuspended in 300µl lysis buffer (50mM Tris-HCl pH 7.5, 150mM KCl, 0.1% Tween20, 10% glycerol, 0.2mM PMSF, 10µg/ml of aprotinin, pepstatin and leupeptin each). Cells were lysed by passing them through a needle 4-5 times with 2-3 minutes breaks. The soluble protein fraction was obtained by centrifugation of the homogenized cell extract at 13000rpm, 20minutes at 4°C in an Eppendorf table top centrifuge. The supernatant was incubated with 20µl of Ni2+-NTA agarose beads (Qiagen) per harvested flask for 1 hour at 4°C on an end-over-end rotator. Samples were washed 3 times with wash buffer (50mM Tris pH7.5, 300mM KCl, 10% glycerol, 0.1% Tween20), of which 2 times were with 5 minute incubation with rotation at 4°C. The proteins were eluted by incubating the protein-bound Ni2+-NTA agarose beads in two volumes of elution buffer (50mM Tris pH7.5, 300mM KCl, 10% glycerol, 250mM imidazole) for 15 minutes at 4°C. Imidazole was removed from the eluates by running them on a desalting column (NAP-5 column, GE Healthcare) in storage buffer (50mM Tris-HCl pH7.5, 150mM KCl, 10% glycerol, 1mM DTT). Fractions containing the highest co-activator concentrations were pooled and aliquoted. Aliquots were frozen in liquid nitrogen.

4.2.3.4 Purification of activators co-expressed with Hsl1$^{667-872}$ in Sf9 cells

Cell pellet of one T175 flask was resuspended in 300µl CytoBuster (Novagen) that contained 0.2mM PMSF, 10µg/ml of aprotinin, pepstatin and leupeptin each. After 30 minutes of incubation at 4°C with end-over-end rotation the soluble protein fraction was obtained by

centrifugation of the homogenized cell extract at 13000rpm, 20minutes at 4°C in a Heraeus Biofuge table top centrifuge. The supernatant was incubated with 20µl of Ni2+-NTA agarose beads (Qiagen) per harvested flask for 1 hour at 4°C on an end-over-end rotator. Samples were washed 3 times with wash buffer (50mM Tris pH7.5, 300mM KCl, 10% glycerol, 0.1% Tween20), of which 2 times were with 5 minute incubation with rotation at 4°C. The proteins were eluted by incubating the protein-bound Ni2+-NTA agarose beads in two volumes of elution buffer (50mM Tris pH7.5, 300mM KCl, 10% glycerol, 250mM imidazole) for 15 minutes at 4°C.

4.2.3.5 Purification of GST-tagged substrate proteins from *E.coli*

N702x-GST, N701x-GST, GST-Hsl1 (aa667-872), GST-securin, GST-Nek2A KD

E.coli pellets were resuspended in 2V of lysis buffer (50mM Tris-HCl pH7.5, 150mM KCl, 0.01%Tween20, 10% glycerol, 1mM β-mercaptoethanol, 1 tab of Complete EDTA-free (Roche) per 20ml of cell suspension) and sonicated. The sonicated cell suspension was centrifuged (16000rpm, 30 minutes, SS34 rotor). The soluble fraction, whose concentration was typically 10mg/ml, was then incubated with GSH-Sepharose beads (Amersham), with lysate/ bead volume = 1/0.05, for 1h at 4°C on an end-over-end rotator. The beads were washed once with wash150 buffer (50mM Tris-HCl pH7.5, 150mM KCl, 0.01% Tween20), two times with wash300 buffer (50mM Tris-HCl pH7.5, 300mM KCl, 0.01% Tween20) and then once again with wash150 buffer. Each washing step was a 5 minute incubation in the wash buffer on an end-over-end rotator at 4°C. The bound protein was eluted three times with 2.5 bead volumes of elution buffer (50mM Tris HCl pH7.5, 150mM KCl, 0.01% Tween20, 0.5mM β-mercaptoethanol, 50mM reduced glutathione), each time rotating for 15 minutes at 4°C. the eluates were dialysed in dialysis buffer (20mM Tris-HCl pH7.5, 150mM KCl, 10% glycerol, 0.5mM β-mercaptoethanol) for 3 hours and over night. Eluates were stored in aliquotes at -80°C.

4.2.3.6. Purification of H6-tagged substrate proteins from *E.coli*

Frozen cell pellets were resuspended in 1 pellet volume of Lysis buffer (50mM Tris-HCl pH8, 150mM KCl, 2 mM β-mercapto-ethanol, 1% Triton, 1 tab of Complete EDTA-free (Roche) per 20ml of cell suspension). The cell suspension was incubated on ice for 30 minutes, and then sonicated (in the "rosetta" or in a 50ml Falcon tube) 6 x 10s with 10s pauses (settings of the sonicator: duty cycle: 50%, output control: microtip limit). The lysed cells were then spun at 13000rpm for 30 at 4°C in a SS34 rotor, Sorwall centrifuge. NiNTA agarose beads (Qiagen) equilibrated with Lysis buffer were incubated in the cleared cell lysate for 1 hour at 4°C with end-over-end rotation, spun at 500g. The beads were then washed twice with Wash buffer 1 (50 mM Tris-HCl pH 8, 500 mM KCl, 0.5% TritonX-100, 2 mM β-mercapto-ethanol, 20mM imidazole), with 5 minutes incubation with rotation at 4°C; then washed twice with Wash Buffer 2 (50 mM Tris-HCl, pH8, 150mM KCl, 0.5% TritonX-100, 2 mM β-mercapto-ethanol) with 5 minutes incubation with rotation at 4°C, then once with Wash buffer 2 without TritonX-100 with 5 minutes incubation with rortation at 4°C.The proteins were eluted by two subsequent incubations in 2 bead volumes of Elution buffer (50mM Tris-HCl pH8, 150mM KCl, 250mM Imidazole, 2 mM β-mercapto-ethanol) for 20-30 minutes at 4°C on an end-over-end rotator.
Imidazole was removed by dializing the eluates in Dialysis buffer (50mM Tris-HCl pH8, 150mM KCl, 10% glycerol , 0.5mM DTT) at 4°C. First dialysis was carried out for 2 hours, and the second over night. The eluates were aliquoted and frozen in liquid nitrogen.

4.2.3.7 Purification of proteins expressed in *S.cerevisiae*

Frozen cell pellets were thawn on ice and resuspended in 2 pellet volumes of TLB buffer (20 mM Tris-HCl, pH 7.9, 10 mM MgCl2, 5 mM CaCl2, 5% glycerol, 1 mM DTT , 100 mM ammonium sulfate, 150 mM NaCl). Complete© (Roche) protease inhibitor tab per 50ml of cell suspension just before use. The cells were lysed in French Press 2x at 2.1 kbar , incubated on ice during the procedure. The lysate was cleared by centrifugation in SS34 rotor, 19,000 rpm 40

minutes at 4°C. the lysate was subsequently incubated with 1/10 volume of IgG sepharose ™ 6 Fast Flow (Amersham) beads in a 0.8x4 cm Poly-Prep column (BIORAD).
Prior to incubation with the lysatem the beads were activated by washing them first in TBS pH 7.5 and then with 0.5 M HAc/NH4Ac pH 3.4. this is repeate once more, and at the end the beads were washed with TBS until the pH was 7.5 again.
The beads were incubated in the lysate for 3 hours at 4°C and subsequently washed in the Poly-Prep column with at least 100 bead volumes of TLB. The beads were then transfered to 1.5ml Eppendorf tube, spun down at 2000rpm for 5 min, in a Sowrall tabletop centrifuge. The buffer was remover and the beads were resuspended in 3.5 bead volumes of AcTEV lysis buffer (Invitrogen). DTT was added to 1mM final concentration and 3µl of TEV protease (Invitrogen).
The reaction was incubated with end-over-end rotation over night at 4°C.

4.2.4 Oxidative Iodination of proteins

An N-terminal fragment of human cyclin B1 (amino acids 1-87, -myc-his6) was iodinated using the chloramin T procedure according to Parker (Parker, 1990). 2–10 µg of the protein to be labelled was incubated in a 30 µl reaction containing 24µl 250 mM Tris-HCl, pH 8.0, 3µl chloramin T (10mg/ml) and 3 µl Na125I (DuPont NEN, NEZ-033A, pH 8-10, 100µCi/µl) for 3 minutes at room temperature. To stop the reaction, 10 µl of 1M DTT was added, and the mixture was dialyzed for four hours in a Slide-A-Lyzer Mini Dialysis unit with a molecular weight cut off of 3.5 kDa (Pierce, Rockford, IL) against 2x250 ml of XB buffer for 2 hours each. (10 mM Hepes-KOH pH 7.7, 100 mM KCl, 2 mM MgCl2, 0.1 mM CaCl2 and 1 mM DTT). The iodinated protein was then mixed 1:1 with 87 % glycerol and stored at -20 °C.

4.2.5 *In vitro* ubiquitylation of iodinated APC/C substrates

To measure the activity of the immunopurified APC/C, the complex was incubated with ubiquitin, E1 and E2 enzyme and analyzed for it’s ability to form polyubiquitin chains on a

substrate protein. For ubiquitylation assays, 1-3 µl APC/C bound antibody beads were used in XB buffer containing purified E1 (0.26 µM), UbcH10 (6.2 µM), ubiquitin (0.3 mM), ATP regenerating system (7.5 mM creatine phosphate, 1 mM ATP, 1 mM MgCl2, 0.1 mM EGTA, 30 U/ml rabbit creatine phosphokinase type I (Sigma-Aldrich)) in a total volume of 7-10 µl. As a substrate, we used an iodinated proteins. Ubiquitylation reactions catalyzed by human APC/C were incubated at 37°C and 1400 rpm in a thermomixer (Eppendorf, Hamburg, Germany). The reaction was stopped by the addition of 4x sample buffer (125 mM Tris-HCl pH 6.8, 4% SDS, 20% Glycerol, 200mM DTT, 0,02% Bromphenolblue). Radiolabeled substrates could be detected by autoradiography which allowed quantification of the reactions.

4.2.6. *In vitro* protein binding assays

4.2.6.1 *In vitro* binding of activators to the APC/C

The APC/C was purified from HeLa cells as described in 4.4.2 with protein-A sepharose beads (BioRad) coupled to α-Cdc27 antibodies. Bead bound APC/C was incubated for 30 minutes at 4°C on a end-over-end rotator in 2 bead volumes of a recombinant activator solution in IP buffer (20 mM Tris pH 7.5, 150mM KCl, 10% glycerol, 0.1% Tween 20 (Sigma). 0.5 mM DTT) that contained 4mg/ml of BSA. The unbound activators were washed by washing the beads 4x in 20 bead volumes of IP buffer, of which 2x was with 5 minute incubation at 4°C on a end-over-end rotator.

4.2.6.2 *In vitro* substrate binding assay: APC/C on beads

The APC/C was purified from HeLa cells as described in 4.4.2 with protein-A sepharose beads (BioRad) coupled to α-Cdc27 antibodies. Bead bound APC/C was incubated for 60 minutes at room temperature on a end-over-end rotator in 3 bead volumes of a substrate protein solution in buffer A (50mM Tris-HCl pH 7.5, 10% glycerol, 1mM DTT) that contained 4mg/ml BSA. The

unbound substrate was washed off by washing the beads 3 times in 40 bead volumes of buffer B (50mM Tris-HCl pH 8, 150 mM NaCl, 0.5% Tween 20, 5 mM EDTA). The bound proteins were eluted off the beads wither by a solution of 0.1M Glycine pH2.2 (adjuste with HCl) or by incubating the beads in a buffered solution that contained 1mg/ml of antigenic peptide (20mM Tris-HCl pH 7.5, 5% glycerol, 0.1% Tween 20, 0.5mM DTT)

4.2.6.3 *In vitro* substrate binding assay: substrate on beads, APC/C in solution

To prevent unspecific binding 20 µl of glutathione sepharose beads (Glutathione High Performance, GE Healthcare) for 30 minutes at room temperature on an end-over-end rotator in 50µl Buffer A (50mM Tris-HCl pH 7.5, 10% glycerol, 1mM DTT) that contained 2 mg/ml BSA prior to substrate binding. The beads were subsequently incubated in 30µl of substrate solution in Buffer A that contained 4mg/ml BSA at room temperature for 1 hour on an end-over-end rotator. To remove unbound substrates the beads were washed 3 times with 560µl of buffer A, of which the second time the beads were incubated for 5 minutes on an end-over-end rotator at room temperature. The APC/C, was immunopurified from extracts of HeLa cells as described in 4.4.2, with Cdc27 antibodies coupled to protein A beads and eluted by incubating the beads in a buffered solution that contained 1mg/ml of antigenic peptide (20mM Tris-HCl pH 7.5, 5% glycerol, 0.1% Tween 20, 0.5mM DTT). Substrate–bound glutathione were then incubated in the 80µl (4 bead volumes) of APC/C peptide elution for another 1h at room temperature with end-over-end rotation. Unbound APC/C was washed off glutathione beads with Buffer B (50mM Tris-HCl pH 8, 150 mM NaCl, 0.5% Tween 20, 5 mM EDTA), and the bound proteins were eluted off the beads by boiling in 30µl (1.5 bead volumes) of 2xSDS PAGE sample buffer that contained 5mg/ml of BSA.

4.2.7 *In vitro* dephosphorylation of APC/C

Dephosphorylation of APC/C bound t beads: 25µl beads were incubated in 50µl of reaction buffer (New England Biolabs. 5µl of 10x buffer, 5µl of 10x MnCl2, 40 µl MonoQ) with 4µl of lambda phosphatase (New England Biolabs) for 45minutes at 30°C at 400rpm shaking in the termomixer (Eppendorf) Since the beads settle down at this low rpm, they were pipetted up and down every 5-10 mins. The beads were subsequently washed three times with TBS-T of that the last two times were with 5 minute incubation on a end-over-end rotator. The APC/C was then eluted with 2 bead volumes of 0.1M glycine solution pH2.2. Dephosphorylation of APC/C in HeLa extracts: to 110µl of mitotic HeLa extract (SAC-on and SAC-off) 13µl of 10x phosphatase buffer (New England Biolabs), 13µl 10x MnCl2 and 9µl Lambda phosphatase (New England Biolabs). 30 minuites at 30°C, 700rpm shaking.

4.2.8 Ammonium sulphate precipitation

(NH4)2SO4 crystals were chrushed to make it a powder. To obtain 85% saturation 0.57g was added to 1ml of protein solution. The (NH4)2SO4 power was added into the protein solution stepwise in small portions during 30 minutes while the protein solution was being stirred with a magnetic stirrer, on ice. when all the (NH4)2SO4 poeder was added to the solution, it was stirred for additionaly 30 minutes on ice, after which it was centrifuged at 4400 rpm in an Heraeus Biofuge tabletop centrifuge at 4°C for 15 minutes. The pellets were resuspend in TLB buffer (see Methods section 4.2.3.7) for storage on ice.

5. Appendix

5.1 Clustal X multiple protein sequence alignment of Cdh1 homologs

A selected set of ortholog sequences was identified using NCBI BLAST (Altschul, PMID: 92546942231712). A multiple amino-acid sequence alignment was performed using the Multiple Alignment using Fast Fourier Transform

(MAFFT) algorithm (Katoh, PMID: 12136088), and graphically processed using Clustal X software (Larkin, PMID: 17846036). The sequences are the following:

Cdh1_Hs: gi|6463679|dbj|BAA86954.1| [Homo sapiens],

Cdh1_Mm: gi|9789959|ref|NP_062731.1| [Mus musculus],

Cdh1_Xl: gi|2326943|emb|CAA74576.1| [Xenopus laevis],

Cdh1_Am: gi|66562652|ref|XP_623291.1|[Apis mellifera],

Cdh1_Dm: gi|2326419|emb|CAA74575.1| [Drosophila melanogaster],

Cdh1_Ce: gi|17538129|ref|NP_496075.1| [Caenorhabditis elegans],

Cdh1_Cn: gi|50257089|gb|EAL19804.1| [Cryptococcus neoformans var. neoformans B-3501A],

Cdh1_Um: gi|71019667|ref|XP_760064.1| [Ustilago maydis 521],

Cdh1_Sp: gi|6138904|emb|CAB59693.1| [Schizosaccharomyces pombe],

Cdh1_At: gi|20259635|gb|AAM14174.1| [Arabidopsis thaliana],

Cdh1A1_A: gi|79482624|ref|NP_194022.3| [Arabidopsis thaliana],

Cdh1_An: gi|67525015|ref|XP_660569.1| [Aspergillus nidulans FGSC A4],

Cdh1_Sc: gi|6321435|ref|NP_011512.1| [Saccharomyces cerevisiae].

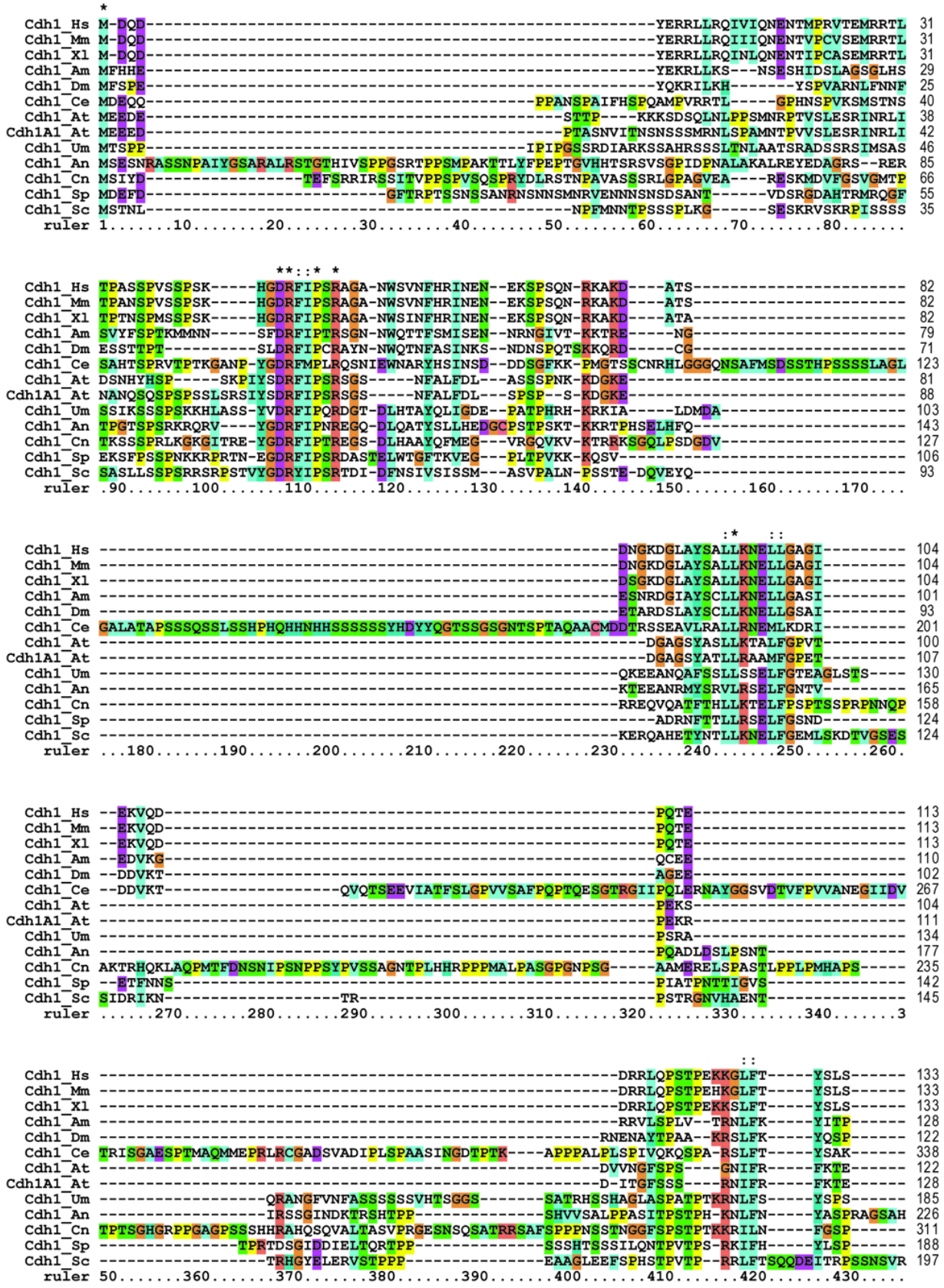
Cdh1_Hs
Cdh1_Mm
Cdh1_Xl
Cdh1_Am
Cdh1_Dm
Cdh1_Ce
Cdh1_At
Cdh1A1_At
Cdh1_Um
Cdh1_An
Cdh1_Cn
Cdh1_Sp
Cdh1_Sc
ruler

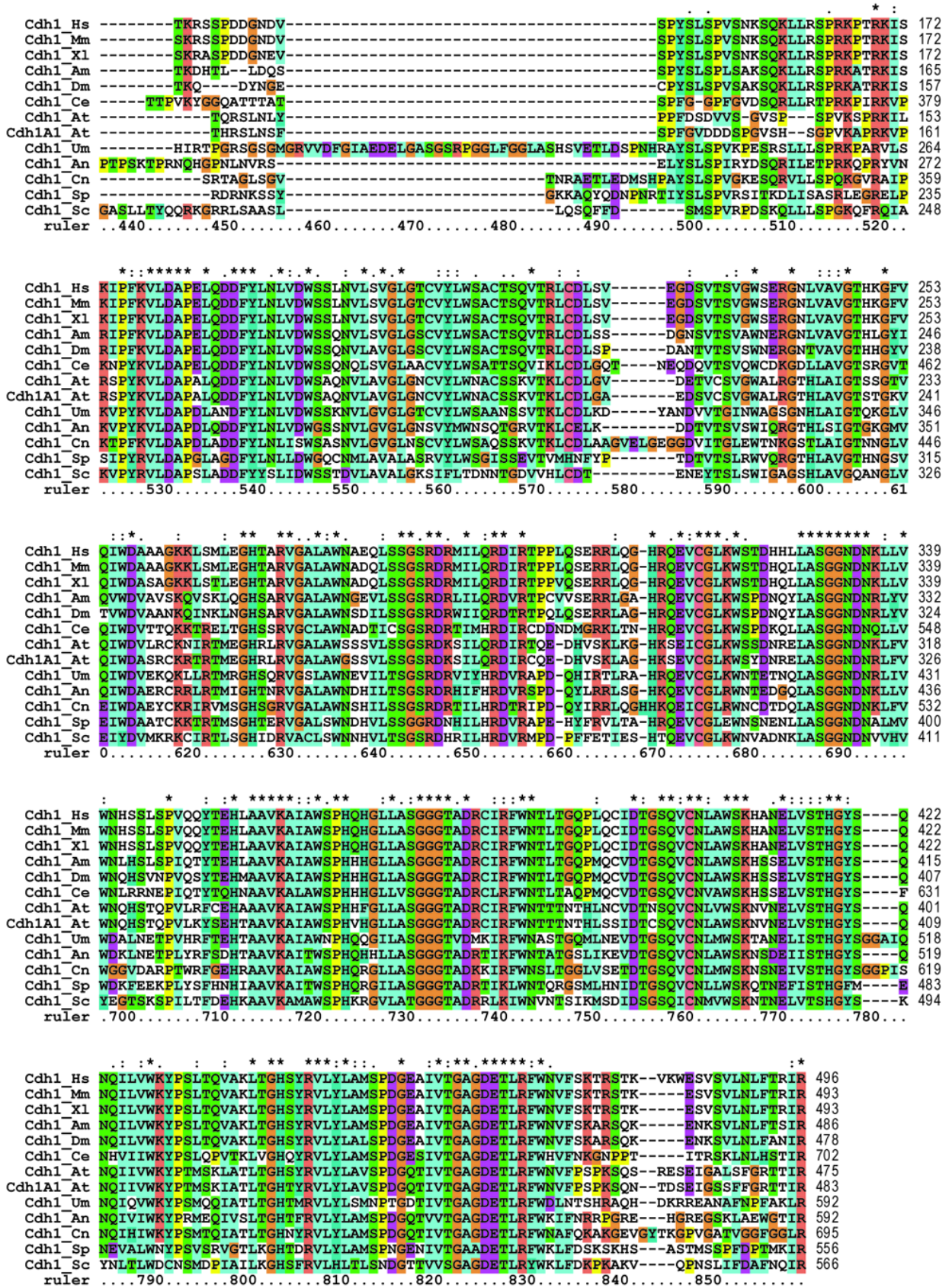
Cdh1_Hs
Cdh1_Mm
Cdh1_Xl
Cdh1_Am
Cdh1_Dm
Cdh1_Ce
Cdh1_At
Cdh1A1_At
Cdh1_Um
Cdh1_An
Cdh1_Cn
Cdh1_Sp
Cdh1_Sc
ruler

Science
AAAS

Structure of the Anaphase-Promoting Complex/Cyclosome Interacting with a Mitotic Checkpoint Complex

Franz Herzog, *et al.*

Science **323**, 1477 (2009);
DOI: 10.1126/science.1163300

9. R. C. Petersen *et al.*, *Arch. Neurol.* **58**, 1985 (2001).
10. M. Cecchini, R. Curcio, M. Pappalardo, R. Melki, A. Caflisch, *J. Mol. Biol.* **357**, 1306 (2006).
11. T. Tomiyama *et al.*, *Ann. Neurol.* **63**, 377 (2008).
12. A. D. Williams *et al.*, *J. Mol. Biol.* **335**, 833 (2004).
13. K. H. Lim, *ChemBioChem* **7**, 1662 (2006).
14. Y. Hori *et al.*, *J. Biol. Chem.* **282**, 4916 (2007).
15. F. Bard *et al.*, *Proc. Natl. Acad. Sci. U.S.A.* **100**, 2023 (2003).
16. M. L. Peacock, J. T. Warren, A. D. Roses, J. K. Fink, *Neurology* **43**, 1254 (1993).
17. J. Meinhardt *et al.*, *Protein Sci.* **16**, 1214 (2007).
18. C. Soto *et al.*, *Nat. Med.* **4**, 822 (1998).
19. C. Adessi *et al.*, *J. Biol. Chem.* **278**, 13905 (2003).
20. This work was supported by grants from the Italian Ministry of Health (533F/Q/1 to F.T. and M.S., and 71.6/2006 and RFPS 2007/02 to F.T.), CARIPLO Foundation (Guard) to F.T. and M.S., ERA-Net Neuron (nEUROsyn) to F.T., Negri-Weizmann Foundation to M.S., the National Institute of Neurological Disorders and Stroke (NS42029) to E.L., and the American Heart Association (0040102N) to E.L. A patent application related to this work has been filed by Fondazione IRCCS Istituto Nazionale Neurologico "Carlo Besta."

Supporting Online Material

www.sciencemag.org/cgi/content/full/323/5920/1473/DC1
Materials and Methods
SOM Text
Figs. S1 to S5
Tables S1 and S2

25 November 2008; accepted 12 January 2009
10.1126/science.1168979

Structure of the Anaphase-Promoting Complex/Cyclosome Interacting with a Mitotic Checkpoint Complex

Franz Herzog,[1]* Ivana Primorac,[1] Prakash Dube,[2] Peter Lenart,[3] Björn Sander,[2] Karl Mechtler,[1] Holger Stark,[2]† Jan-Michael Peters[1]†

Once all chromosomes are connected to the mitotic spindle (bioriented), anaphase is initiated by the protein ubiquitylation activity of the anaphase-promoting complex/cyclosome (APC/C) and its coactivator Cdc20 (APC/C^{Cdc20}). Before chromosome biorientation, anaphase is delayed by a mitotic checkpoint complex (MCC) that inhibits APC/C^{Cdc20}. We used single-particle electron microscopy to obtain three-dimensional models of human APC/C in various functional states: bound to MCC, to Cdc20, or to neither (apo-APC/C). These experiments revealed that MCC associates with the Cdc20 binding site on APC/C, locks the otherwise flexible APC/C in a "closed" state, and prevents binding and ubiquitylation of a wide range of different APC/C substrates. These observations clarify the structural basis for the inhibition of APC/C by spindle checkpoint proteins.

Chromosome segregation is delayed by the spindle checkpoint until all chromosomes are connected to both poles (bioriented) of the mitotic or meiotic spindle. Defects in this checkpoint can lead to aneuploidy, which is associated with tumorigenesis, congenital trisomies, and aging (*1*). The spindle checkpoint is activated in prometaphase by the presence of kinetochores that are not properly attached to microtubules or not under tension by spindle-pulling forces (*2*, *3*). The checkpoint inhibits Cdc20, which activates the ubiquitin-protein ligase APC/C in mitosis and helps to recruit substrates to APC/C. APC/C initiates chromosome segregation by ubiquitylating cyclin B, an activating subunit of cyclin-dependent kinase 1 (Cdk1), and securin, an inhibitor of the protease separase. After ubiquitin-mediated degradation of these proteins, separase becomes active and dissolves the cohesion between sister chromatids (*4*).

Inhibition of Cdc20 by the spindle checkpoint depends on mitotic arrest–deficient 2 (Mad2) (*5*). This protein associates with Cdc20 at unattached kinetochores (*6*–*9*). In animal cells, Cdc20 is also inhibited by association with budding uninhibited by benzimidazoles–related 1 (BubR1) and its binding partner budding uninhibited by benzimidazoles 3 (Bub3). Mad2 and BubR1-Bub3 can bind to Cdc20 either separately (*10*, *11*) or simultaneously, forming a MCC (*12*), and these proteins can associate with APC/C (*13*–*16*). Similar complexes exist in yeast, in which a BubR1-related Mad3 protein might inhibit Cdc20 as a pseudosubstrate (*17*, *18*).

Structural information will be essential to understand how checkpoint proteins inhibit APC/C^{Cdc20}, but it is known only how Mad2 interacts with a short Cdc20 peptide (*19*, *20*). We therefore analyzed with single-particle electron microscopy (EM) the structure of APC/C that is bound to checkpoint proteins. We first established conditions under which checkpoint-inhibited APC/C could be purified and characterized these complexes biochemically. We isolated APC/C from human HeLa cells that had been arrested in prometaphase by the microtubule-stabilizing agent Taxol, which keeps the checkpoint active. For comparison, we purified APC/C from Taxol-arrested cells in which the checkpoint had been inactivated by hesperadin, an inhibitor of Aurora B kinase (*15*, *21*). Quantitative fluorescence microscopy of chromosome morphology, cyclin B levels, and kinetochore association of Mad2, BubR1, and Bub1 confirmed that cells had been arrested in prometaphase with either an active or inhibited spindle checkpoint (fig. S1). Mass spectrometry (table S1) and SDS–polyacrylamide gel electrophoresis (SDS-PAGE) followed by silver staining (Fig. 1A) or semi-quantitative immunoblotting (Fig. 1B) revealed that four times more BubR1, Bub3, and Mad2 were associated with APC/C in cells in which the checkpoint was active than in hesperadin-treated cells. The amount of Cdc20 bound to APC/C was twofold greater when the checkpoint was active, perhaps because checkpoint proteins stabilize APC/C–Cdc20 interactions. Immunoprecipitation of BubR1 confirmed that more BubR1, Bub3, Mad2, and Cdc20 were bound to APC/C when the checkpoint was active (Fig. 1A and table S1). In a reconstituted system, ubiquitylation of cyclin B and securin was reduced to 17% when APC/C was isolated from cells with an active checkpoint as compared with reactions mediated by APC/C from cells with an inactive checkpoint. This difference was even greater when samples were normalized to the amounts of APC/C–associated Cdc20, which is rate-limiting for APC/C activity (Fig. 1, C and D). Surprisingly, APC/C from cells with an active checkpoint was similarly less active toward cyclin A and never-in-mitosis A (NIMA)–related kinase 2A (Nek2A), which are normally degraded in prometaphase when the checkpoint is active (Fig. 1E and fig. S2). The checkpoint appears not to inhibit APC/C^{Cdc20} in a substrate-specific manner, as was proposed to explain Nek2A degradation in prometaphase (*22*), but by recruiting substrates before checkpoint activation, as shown for cyclin A (*23*).

Similar results were obtained when APC/C was isolated from cells with active or inactive checkpoints that were obtained with a different protocol in which cells had not been treated with hesperadin (fig. S3), indicating that hesperadin caused changes in APC/C's subunit composition and activity by checkpoint inhibition and not by an unrelated mechanism. Our results therefore indicated that checkpoint activation leads to association of BubR1, Bub3, and Mad2 with APC/C and to the general inhibition of APC/C's ubiquitylation activity. However, our SDS-PAGE–silver staining analysis of APC/C from cells in which the checkpoint is active suggested that BubR1, Bub3, and Mad2 were present in substoichiometric amounts relative to APC/C (Fig. 1A). We therefore separated APC/C purified from cells with an active checkpoint into different subpopulations (Fig. 1F). We first captured a subpopulation of APC/C with BubR1, Cdc20, or Mad2 antibodies and then isolated the remaining

[1]Research Institute of Molecular Pathology, Dr. Bohr-Gasse 7, 1030 Vienna, Austria. [2]Max-Planck-Institute for Biophysical Chemistry, Am Fassberg 11, 37077 Goettingen, Germany. [3]European Molecular Biology Laboratory, Meyerhofstraße 1, 69117 Heidelberg, Germany.

*Present address: Institute of Molecular Systems Biology, Eidgenössische Technische Hochschule Zurich, 8093 Zurich, Switzerland.

†To whom correspondence should be addressed. E-mail: hstark1@gwdg.de (H.S.); peters@imp.univie.ac.at (J.-M.P.)

particles with antibodies to the APC/C subunit Apc4 (Fig. 1, G and H, and fig. S4). These experiments revealed that cells with an active checkpoint contained two forms of APC/C. One contained BubR1, Bub3, Cdc20, and Mad2, whereas the other one lacked all of these proteins. We refer to these forms as APC/C^{MCC} and apo-APC/C, respectively. In cyclin B–ubiquitylation assays, the specific activities of APC/C^{MCC} and apo-APC/C were similarly low (Fig. 1I). Purified Cdc20 and the related coactivator Cdc20 homolog 1 (Cdh1) activated apo-APC/C in a dose-dependent manner, suggesting that this form of APC/C is inactive because it is lacking a co-activator. In contrast, APC/C^{MCC} could be stimulated by coactivators only to a small degree, indicating that this form of APC/C represents a truly inhibited state (Fig. 1I).

To understand how checkpoint proteins inhibit APC/C, we determined the structures of APC/C^{MCC}, apo-APC/C, and APC/C^{Cdc20}. We isolated APC/C^{MCC} by means of sequential immunoprecipitation with antibodies to Cdc27 and BubR1. We isolated apo-APC/C with antibodies to Apc4 from the supernatant of the BubR1 immunoprecipitation. After a peptide elution, both samples were further purified by use of glycerol density-gradient centrifugation (*24*) and analyzed by use of both negative staining at low temperatures and unstained cryo-EM in a vitrified buffer (Fig. 2, figs. S5 and S6, and table S2). We used a technique based on three-dimensional (3D) alignment of random conical tilt (RCT) reconstructions and subsequent 3D multivariate statistical analysis for initial structure determination and simultaneous unsupervised analysis of the heterogeneity in the data set. For apo-APC/C, we identified three conformers that differ mainly in the relative orientation of their two major domains: the platform and

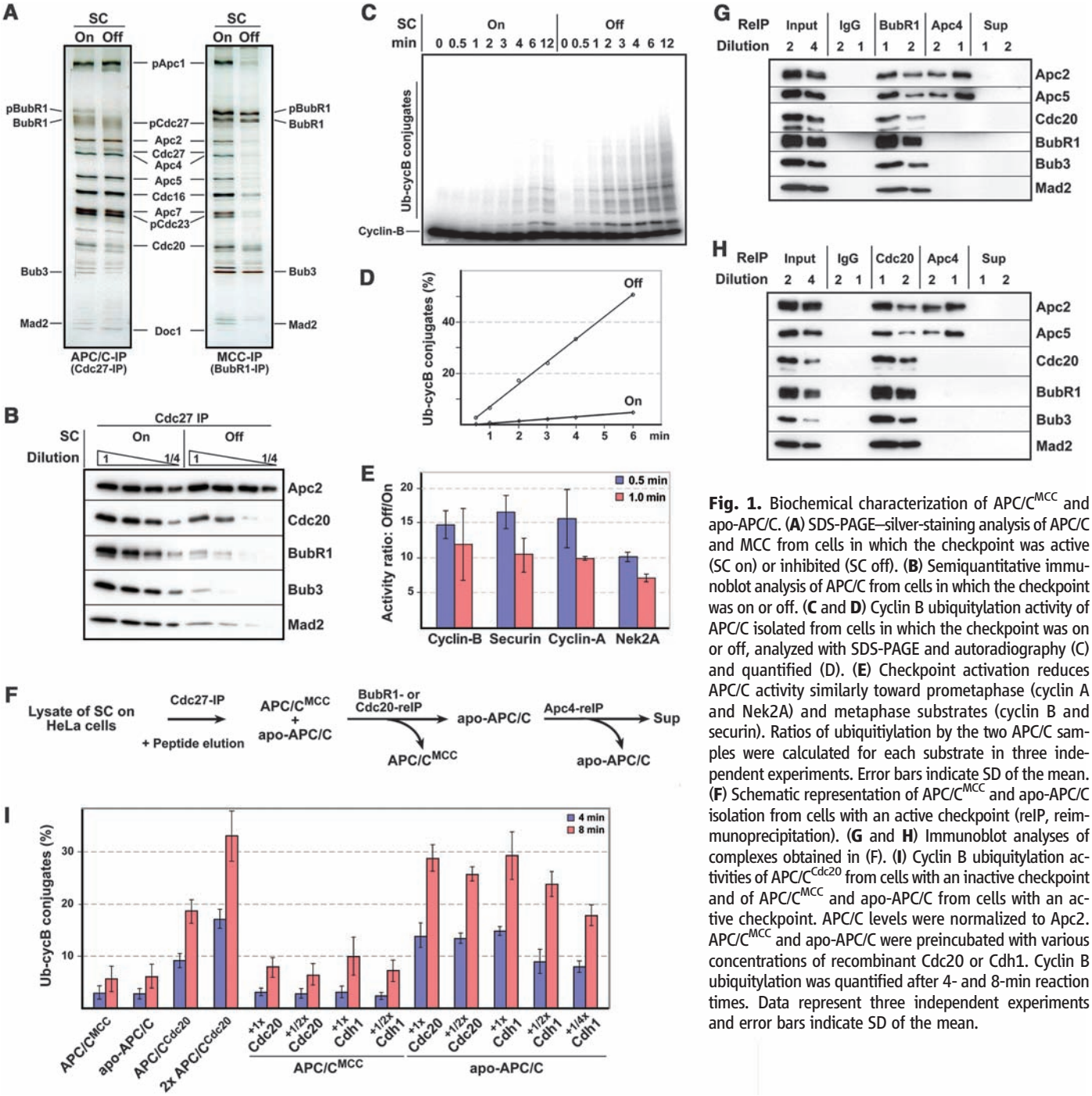

Fig. 1. Biochemical characterization of APC/C^{MCC} and apo-APC/C. (**A**) SDS-PAGE–silver-staining analysis of APC/C and MCC from cells in which the checkpoint was active (SC on) or inhibited (SC off). (**B**) Semiquantitative immunoblot analysis of APC/C from cells in which the checkpoint was on or off. (**C** and **D**) Cyclin B ubiquitylation activity of APC/C isolated from cells in which the checkpoint was on or off, analyzed with SDS-PAGE and autoradiography (C) and quantified (D). (**E**) Checkpoint activation reduces APC/C activity similarly toward prometaphase (cyclin A and Nek2A) and metaphase substrates (cyclin B and securin). Ratios of ubiquitiylation by the two APC/C samples were calculated for each substrate in three independent experiments. Error bars indicate SD of the mean. (**F**) Schematic representation of APC/C^{MCC} and apo-APC/C isolation from cells with an active checkpoint (reIP, reimmunoprecipitation). (**G** and **H**) Immunoblot analyses of complexes obtained in (F). (**I**) Cyclin B ubiquitylation activities of APC/C^{Cdc20} from cells with an inactive checkpoint and of APC/C^{MCC} and apo-APC/C from cells with an active checkpoint. APC/C levels were normalized to Apc2. APC/C^{MCC} and apo-APC/C were preincubated with various concentrations of recombinant Cdc20 or Cdh1. Cyclin B ubiquitylation was quantified after 4- and 8-min reaction times. Data represent three independent experiments and error bars indicate SD of the mean.

the arc lamp domains (Fig. 2A and 3D-PDF S1) (*25*). The initial RCT 3D structures were used to determine the handedness (fig. S7) and as templates for further refinement of the existing subpopulations of apo-APC/C (Fig. 2A). We suspect that these conformers represent the structural variability of apo-APC/C in solution and represent a continuum of flexible states (for an animation of the corresponding movements, see movie S1).

In the APC/C^{MCC} sample, a large additional density was found inserted into the "front" side of the platform domain (Fig. 2C, red, and 3D-PDF S2). The 3D volume of this density element corresponds to a mass of 180 to 200 kD, slightly less than MCC's theoretical mass of 236 kD (if every subunit is present once). We confirmed that this mass represents MCC by identifying the location of BubR1 by means of antibody labeling (fig. S8). To obtain a 3D model of APC/C^{Cdc20}, we bound recombinant Cdc20 to purified apo-APC/C and determined the structures as above. In 30% of APC/C molecules, we found an additional globular 50-kD mass on the front side of APC/C in a location that overlaps with the site to which MCC is bound in APC/C^{MCC} (Fig. 2B and fig. S9). The Cdc20 density does not fully overlap with the MCC density and is ~20 Å away from a perfect fit. The precise position of Cdc20 may thus change upon MCC binding to APC/C (Fig. 2D). APC/C^{Cdc20} showed similar conformational flexibility as apo-APC/C.

Comparison of the apo-APC/C and APC/C^{MCC} structures revealed a number of differences in addition to the presence of an extra mass in APC/C^{MCC}. To interpret these changes, we mapped the 3D location of APC/C core subunits with antibody labeling (fig. S8). Antibodies to Apc1, Apc4, and Apc5 bound to distinct sites in the platform domain with Apc5 at the bottom, Apc4 at the front, and Apc1 at the right-hand side (Fig. 3, A and B). The volumes of the labeled domains are consistent with the predicted masses of Apc1, Apc4, and Apc5 (Fig. 3B). The modeling of these subunits into the APC/C 3D structure suggests that Apc5 is close to the interface of the platform and arc lamp domains, and the mass accommodated by Apc1 spans from the front to the inner mass (Fig. 3B). Part of the subunit that we identified as Apc4 has a ring-shaped structure (Fig. 3B, right), which is consistent with bioinformatic analyses that Apc4 contains an N-terminal propeller-shaped WD40 domain (*4*). Cdc27 antibodies bound to the headlike protrusion that is located at the top end of the arc lamp domain (Fig. 3A). We confirmed that Apc2 is located at the inner mass on the front side of APC/C (*25*), residing in close vicinity to Apc1 and Cdc27 (Fig. 3, A and B). Antibodies to Cdc16 and Apc7 were bound at multiple locations on the arc lamp domain (fig. S8), presumably because these subunits are present in more than one copy per APC/C molecule (*25*). The arc lamp domain is bent and has an unusual repetitive regularity (Fig. 3B), features that are characteristic of tetratricopeptide repeat (TPR) domains present in Cdc16 and Apc7 and also in Cdc27 and Cdc23. These observations indicate that a major part of the arc lamp domain consists of TPR subunits. With the exception of Apc2 and Apc4 topology, our 3D model of subunit topology is consistent with the 2D positions of subunits determined in fission yeast APC/C (*26*).

This subunit map indicates that MCC binds in the vicinity of Apc2, Apc4, and Apc5, which are located toward the right-hand side of MCC (Fig. 3, B, D, and E, and 3D-PDFs S1 and S2). On the left-hand side, MCC contacts the arc lamp domain, which suggests that MCC also interacts with TPR subunits. Little if any conformational flexibility was observed among populations of APC/C^{MCC}. Instead, APC/C^{MCC} adopts a closed conformation (Fig. 3D). In addition, Apc4 is bent upward by 35° in APC/C^{MCC} as compared with its position in apo-APC/C, and the position of a more centrally located subunit, possibly Apc2, is also changed (Fig. 3E). This rearrangement might be required for MCC binding and, together with a higher curvature of the arc lamp, results in a more compact appearance of APC/C^{MCC} as compared with that of apo-APC/C.

To understand the functional consequences of these structural changes, we compared the interactions of different forms of APC/C with the ubiquitin-conjugating enzyme UbcH10 and substrate proteins. Binding of UbcH10 to APC/C was reduced to 50% when the checkpoint was active (fig. S10). It is unlikely that this small change can explain the almost complete inhibition of APC/C by checkpoint proteins. In contrast, we saw a substantial reduction in substrate binding to checkpoint-inhibited APC/C. When APC/C was isolated from cells with an active checkpoint, much less binding of an N-terminal fragment of fission yeast cyclin B or of full-length human securin was detected as compared with the binding that was observed with APC/C from cells in which the checkpoint was inhibited (Fig. 4, A to C). As reported (*27*), binding of cyclin B to APC/C required the presence of a destruction box (D box) in the substrate (Fig. 4, A and B). Similar results were obtained when a D box–containing fragment of budding yeast Hsl1 was used as a substrate (fig. S11). Even a 35-fold increase in substrate concentration resulted

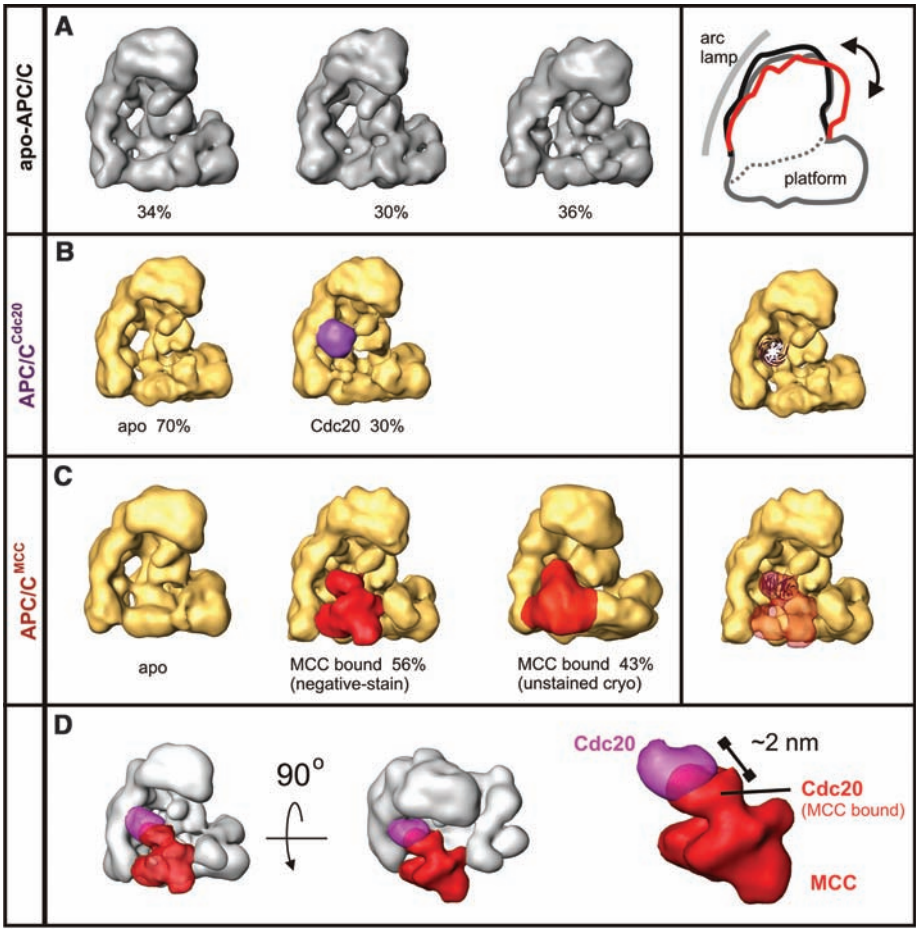

Fig. 2. Localization of Cdc20 and MCC bound to APC/C, analyzed by negative-staining EM. (**A**) Distinct conformers of apo-APC/C isolated from cells with an active checkpoint. (**B**) Localization of recombinant Cdc20 (purple) bound to apo-APC/C. A model of Cdc20's WD40 propeller is projected onto APC/C. (**C**) 3D structure of APC/C^{MCC}. MCC is labeled in red. (**D**) Superposition of the MCC (red) and Cdc20 (purple) densities shown from orthogonal directions.

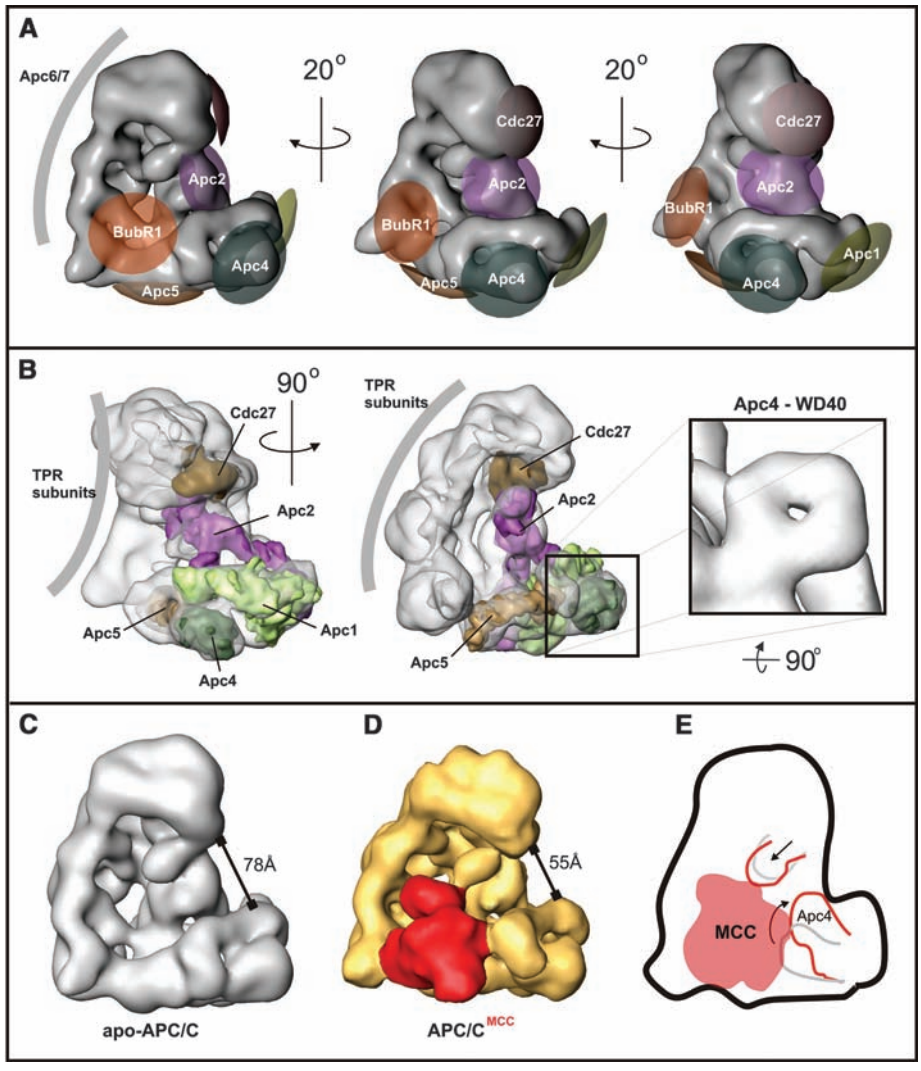

Fig. 3. APC/C subunit topology and structural changes upon MCC binding. (**A**) APC/C subunits were localized with antibody labeling. Antibody epitopes are marked on the surface of the APC/C 3D model, and the labeling accuracy is indicated by the size of the differently colored areas. (**B**) Models of Apc1, Apc2, Apc4, Apc5, and Cdc27 were docked into the 3D density of the APC/C reconstruction. (**C**) The apo-APC/C structure in its most open conformation. (**D**) The APC/C^{MCC} structure with a closed conformation. (**E**) Conformational changes induced by MCC binding to APC/C.

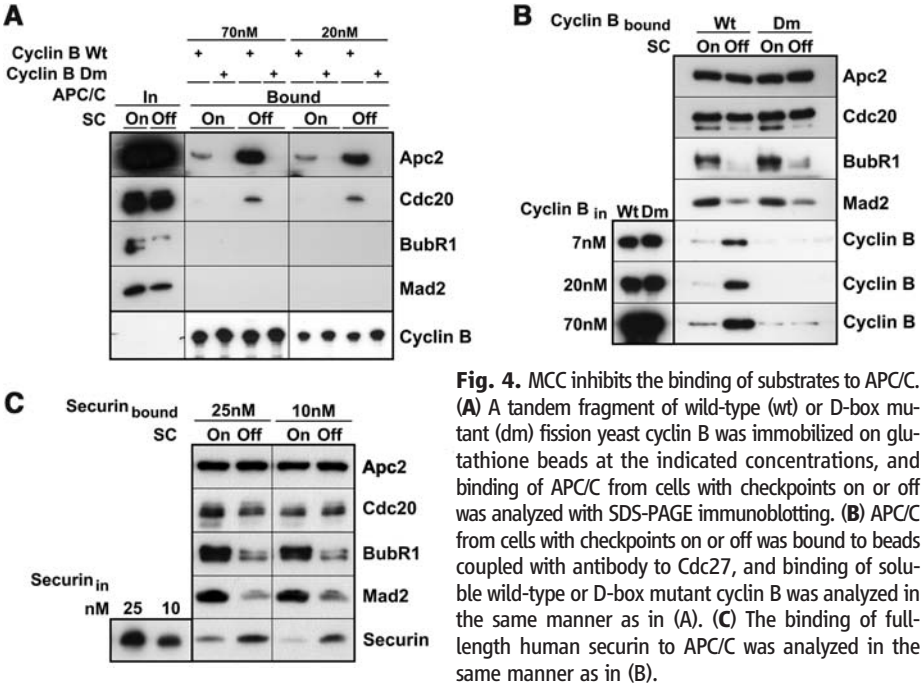

Fig. 4. MCC inhibits the binding of substrates to APC/C. (**A**) A tandem fragment of wild-type (wt) or D-box mutant (dm) fission yeast cyclin B was immobilized on glutathione beads at the indicated concentrations, and binding of APC/C from cells with checkpoints on or off was analyzed with SDS-PAGE immunoblotting. (**B**) APC/C from cells with checkpoints on or off was bound to beads coupled with antibody to Cdc27, and binding of soluble wild-type or D-box mutant cyclin B was analyzed in the same manner as in (A). (**C**) The binding of full-length human securin to APC/C was analyzed in the same manner as in (B).

in less Hsl1 binding to APC/C from cells with an active checkpoint, as compared with Hsl1 binding to APC/C from cells in which the checkpoint was inactive.

Our data indicate that activation of the spindle checkpoint leads to association of BubR1, Bub3, and Mad2 with APC/C^{Cdc20}, in which the checkpoint proteins occupy a site that partially overlaps with the Cdc20 binding site. The association of checkpoint proteins with APC/C coincides with inhibition of APC/C toward a broad range of prometaphase and metaphase substrates, indicating that checkpoint activation inhibits APC/C generally and not in a substrate-specific manner. This inhibition is at least in part caused by the prevention of substrate binding, which agrees well with the proposed role of Cdc20 as a substrate adaptor (*28*, *29*) and of yeast Mad3 as a pseudosubstrate inhibitor (*17*). Partial overlap of positions of Cdc20 binding to APC/C^{Cdc20} and APC/C^{MCC} raises the possibility that APC/C inhibition may be mediated by MCC-induced repositioning of Cdc20. MCC binding also induces conformational changes in APC/C itself and appears to lock it in a closed conformational state.

References and Notes

1. D. J. Baker, J. Chen, J. M. van Deursen, *Curr. Opin. Cell Biol.* **17**, 583 (2005).
2. C. L. Rieder, R. W. Cole, A. Khodjakov, G. Sluder, *J. Cell Biol.* **130**, 941 (1995).
3. B. M. Stern, A. W. Murray, *Curr. Biol.* **11**, 1462 (2001).
4. J. M. Peters, *Mol. Cell* **9**, 931 (2002).
5. R. Li, A. W. Murray, *Cell* **66**, 519 (1991).
6. G. Fang, H. Yu, M. W. Kirschner, *Genes Dev.* **12**, 1871 (1998).
7. L. H. Hwang *et al.*, *Science* **279**, 1041 (1998).
8. S. H. Kim, D. P. Lin, S. Matsumoto, A. Kitazono, T. Matsumoto, *Science* **279**, 1045 (1998).
9. A. DeAntoni, V. Sala, A. Musacchio, *Philos. Trans. R. Soc. London Ser. B* **360**, 637 (2005).
10. Z. Tang, R. Bharadwaj, B. Li, H. Yu, *Dev. Cell* **1**, 227 (2001).
11. G. Fang, *Mol. Biol. Cell* **13**, 755 (2002).
12. V. Sudakin, G. K. Chan, T. J. Yen, *J. Cell Biol.* **154**, 925 (2001).
13. M. Kallio, J. Weinstein, J. R. Daum, D. J. Burke, G. J. Gorbsky, *J. Cell Biol.* **141**, 1393 (1998).
14. K. Wassmann, R. Benezra, *Proc. Natl. Acad. Sci. U.S.A.* **95**, 11193 (1998).
15. C. J. Morrow *et al.*, *J. Cell Sci.* **118**, 3639 (2005).
16. I. Braunstein, S. Miniowitz, Y. Moshe, A. Hershko, *Proc. Natl. Acad. Sci. U.S.A.* **104**, 4870 (2007).
17. J. L. Burton, M. J. Solomon, *Genes Dev.* **21**, 655 (2007).
18. M. Sczaniecka *et al.*, *J. Biol. Chem.* **283**, 23039 (2008).
19. X. Luo, Z. Tang, J. Rizo, H. Yu, *Mol. Cell* **9**, 59 (2002).
20. L. Sironi *et al.*, *EMBO J.* **21**, 2496 (2002).
21. S. Hauf *et al.*, *J. Cell Biol.* **161**, 281 (2003).
22. M. J. Hayes *et al.*, *Nat. Cell Biol.* **8**, 607 (2006).
23. R. Wolthuis *et al.*, *Mol. Cell* **30**, 290 (2008).
24. Materials and methods are available as supporting material on *Science* Online.
25. P. Dube *et al.*, *Mol. Cell* **20**, 867 (2005).
26. M. D. Ohi *et al.*, *Mol. Cell* **28**, 871 (2007).
27. H. Yamano, J. Gannon, H. Mahbubani, T. Hunt, *Mol. Cell* **13**, 137 (2004).
28. J. L. Burton, V. Tsakraklides, M. J. Solomon, *Mol. Cell* **18**, 533 (2005).
29. C. Kraft, H. C. Vodermaier, S. Maurer-Stroh, F. Eisenhaber, J. M. Peters, *Mol. Cell* **18**, 543 (2005).
30. We are grateful to M. Madalinski, M. Gmachl, and G. Kohlmaier for reagents; J. Deckert and R. Lührmann for support; and S. Westermann for comments on the manuscript. Research in the laboratory of H.S. was supported by grants from the Federal Ministry of Education and Research, Germany, and the Sixth Framework Programme of the European Union via the Integrated Project 3DRepertoire. Research in the laboratories of J.-M.P. and K.M. were supported by Boehringer Ingelheim, the Vienna Spots of Excellence Programme, and the Austrian Science Fund. The structural coordinates have been deposited in the Electron Microscopy Data Bank Database at the European Molecular Biology Laboratory–European Bioinformatics Institute. The structures of APC/C^{MCC} and apo-APC/C can be accessed under the codes EMD-1591 and EMD-1592, respectively.

Supporting Online Material

www.sciencemag.org/cgi/content/full/323/5920/1477/DC1
Materials and Methods
Figs. S1 to S11
Tables S1 and S2
References
3D PDFs S1 and S2
Movie S1

15 July 2008; accepted 29 January 2009
10.1126/science.1163300

A Functional Genomics Approach Reveals CHE as a Component of the *Arabidopsis* Circadian Clock

Jose L. Pruneda-Paz, Ghislain Breton, Alessia Para, Steve A. Kay*

Transcriptional feedback loops constitute the molecular circuitry of the plant circadian clock. In *Arabidopsis*, a core loop is established between CCA1 and TOC1. Although CCA1 directly represses *TOC1*, the TOC1 protein has no DNA binding domains, which suggests that it cannot directly regulate *CCA1*. We established a functional genomic strategy that led to the identification of CHE, a TCP transcription factor that binds specifically to the *CCA1* promoter. CHE is a clock component partially redundant with LHY in the repression of *CCA1*. The expression of *CHE* is regulated by CCA1, thus adding a CCA1/CHE feedback loop to the *Arabidopsis* circadian network. Because CHE and TOC1 interact, and CHE binds to the *CCA1* promoter, a molecular linkage between TOC1 and *CCA1* gene regulation is established.

The circadian system provides an adaptive advantage by allowing the anticipation of daily changes in the environment (*1*, *2*). For example, in plants, the resonance between the internal timekeeper and environmental cues enhances their fitness and survival (*3*, *4*).

Circadian networks are composed of multiple positive and negative factors organized in interlocked autoregulatory loops (*1*, *2*). In *Arabidopsis thaliana*, the molecular wiring of these regulatory circuits is mainly based on transcriptional feedback loops (*5*, *6*). The core clock stems from the reciprocal regulation between the evening-phased pseudoresponse regulator TIMING OF CAB EXPRESSION 1 (TOC1) and the two morning-expressed MYB transcription factors CIRCADIAN CLOCK ASSOCIATED 1 (CCA1) and LATE ELONGATED HYPOCOTYL (LHY) (*7*). CCA1 and LHY are DNA binding proteins that repress *TOC1* expression through direct binding to its promoter region (*7*, *8*). In contrast, no functional domains have been recognized in the TOC1 protein (*9*), and direct regulators of *CCA1* or *LHY* expression have never been identified (*5*, *6*, *10*).

Functional redundancies among gene families provide barriers to identifying clock-related transcription factors by classic forward genetic screens. Thus, to uncover direct regulators of *CCA1/LHY*, we implemented an alternative genomics approach in which the yeast one-hybrid system was used to screen a collection of transcription factors for their binding to the *CCA1/LHY* regulatory regions (fig. S1). The high-throughput design of this strategy allowed us to test several tiled fragments for each promoter, thus minimizing the negative effect that the distance from the cis elements to the TATA box has over transcriptional activation in yeast (*11*). We termed this approach "promoter hiking." Because most clock components identified to date exhibit a circadian pattern of mRNA expression, we created a comprehensive library of circadian-regulated transcription factors (table S1) (*12*). We identified a transcription factor that belongs to the class I TCP (TB1, CYC, PCFs) family (*13*) (*Arabidopsis* Genome Initiative locus identifier At5g08330), hereafter referred to as CCA1 HIKING EXPEDITION (CHE). CHE specifically binds to the *CCA1* promoter fragment encompassing nucleotides (nt) –363 to –192 (Fig. 1A) but not to any of the *LHY* promoter fragments tested (Fig. 1B and fig. S2). Consistent with this result, a motif present in the promoter fragment bound matches the consensus class I TCP-binding site (TBS) (GGNCCCAC) (*14*). The binding of CHE to the TBS in the *CCA1* promoter (GGTCCCAC) was confirmed by electrophoretic mobility shift assays (EMSAs) (Fig. 1C) and was further corroborated by the yeast one-hybrid system with a synthetic TBS trimer (fig. S2).

To address whether CHE regulates *CCA1* in vivo, we performed assays in *Arabidopsis* protoplasts in which the *CCA1* promoter activity was monitored with a CCA1::LUC+ reporter construct. The overexpression of CHE when a 35*S*::CHE effector construct was used caused a reduction of the luciferase activity, suggesting that CHE functions as a repressor of *CCA1* (fig. S3). This possibility is consistent with the observation that *CHE* mRNA levels oscillate 9 hours out of phase with the *CCA1* transcript (Fig. 1D). Moreover, we demonstrated that CHE protein accumulates in the nuclei (Fig. 1, E and F) and that both CHE and CCA1 exhibit a similarly broad tissue expression pattern (Fig. 1, G and H). If CHE act as a repressor through binding to the TBS, mutations in this motif should result in increased *CCA1* promoter activity. This hypothesis was confirmed by using promoter::LUC+ fusions (Fig. 1I and fig. S4), indicating that the TBS mediates a repressor function. Altogether, these results support the notion that CHE directly represses *CCA1* promoter activity in a TBS-

Section of Cell and Developmental Biology, Division of Biological Sciences, University of California San Diego, La Jolla, CA 92093, USA.

*To whom correspondence should be addressed. E-mail: skay@ucsd.edu

www.sciencemag.org/cgi/content/full/323/5920/1477/DC1

Supporting Online Material for

Structure of the Anaphase-Promoting Complex/Cyclosome Interacting with a Mitotic Checkpoint Complex

Franz Herzog, Ivana Primorac, Prakash Dube, Peter Lenart, Björn Sander, Karl Mechtler, Holger Stark,* Jan-Michael Peters*

*To whom correspondence should be addressed. E-mail: hstark1@gwdg.de (H.S.); peters@imp.univie.ac.at (J.-M.P.)

Published 13 March 2009, *Science* **323**, 1477 (2008)
DOI: 10.1126/science.1163300

This PDF file includes:

Other Supporting Online Material for this manuscript includes the following:
(available at www.sciencemag.org/cgi/content/full/323/5920/1477/DC1)

Supporting Online Material for

Structure of the anaphase-promoting complex/cyclosome interacting with a mitotic checkpoint complex

Franz Herzog, Ivana Primorac, Prakash Dube, Peter Lenart, Björn Sander,
Karl Mechtler, Holger Stark,* and Jan-Michael Peters*

* Corresponding authors
Holger Stark
(Telephone +49-551-201 1305; E-mail hstark1@gwdg.de)
Jan-Michael Peters
(Telephone +43 179730 886; E-mail peters@imp.univie.ac.at)

This supplement includes:

Materials and methods
Supplementary figures S1 to S7
Tables S1 and S2
Movie S1
3D-pdf S1 and S2
Supplementary references

Materials and methods

Cell culture

HeLa cells were grown in DMEM supplemented with 10% FCS, 0.2 mM L-glutamine, 100 units/ml penicillin and 100 µg/ml streptomycin (all Sigma) and were plated on 12-well plates containing an 18 mm diameter coverslip for immunofluorescence microscopy (IFM), or on 145-mm tissue culture dishes (Greiner bio-one) for subsequent protein purification. For synchronization prior to IFM studies, cells were treated with 2 mM thymidine for 24 hr, released for 6 hr, and then treated with 10 µM Taxol (Paclitacxel, Sigma) for 4 hr. For the last 100 min the proteasome inhibitor MG132 (Sigma) was added at 10 µM final concentration. To obtain mitotic cells which were arrested in the presence of an active (on) or inhibited (off) spindle checkpoint, cells were incubated without or with 100 nM of the Aurora B inhibitor Hesperadin (Boehringer-Ingelheim, Vienna) for the last 60 min, respectively. Alternatively, following the 6 hr release cells were incubated for 4 hr with 50 ng/ml Nocodazole (Sigma). Nocodazole was washed out and cells were incubated for 2 hr with MG132 alone or MG132 plus 100 ng/ml Nocodazole. For synchronization prior to protein purification, cells were initially arrested by incubating them either with 10 µM Taxol or with 50 ng/ml Nocodazole for 14 hr. Subsequently, cells were treated as described in the synchronization protocol for IFM analysis. For the cytospin-IFM experiments cells were synchronized as for protein purification.

Immunofluorescence microscopy

Cells were fixed with 4% formaldehyde in PBS at room temperature on coverslips or after spinning them onto slides by Cytospin (Shandon Brand). After fixation samples were permeabilized with 0.5% Trition-X100 in PBS for 15 min and thereafter blocked with 10% FCS in PBS containing 0.01% Triton-X100. Samples were incubated for 1 hr each at room temperature with primary and secondary antibodies and mounted with ProLong Gold (Molecular Probes). Images were taken on a Zeiss Axioplan 2 microscope using a 100x Plan-Apochromat objective lenses (Carl Zeiss, Jena) equipped with a CoolSnapHQ CCD camera (Photometrics).

Antibodies were used at the following dilutions: human Crest (Cortex Biochem) 1:1000; mouse anti-cyclin-B (GNS1, Santa Cruz Biotechnology) 1:500, rabbit anti-Mad2 (Covance) 1:500; mouse anti-Bub1 (MBL International) 1:500; rabbit anti-BubR1 (see below) 1:1000.

Alexa 488, Alexa 568 and Alexa 633 labeled secondary antibodies as well as DAPI were from Molecular Probes (Invitrogen).

Image processing and quantification

Images were acquired as raw 12-bit images taken at identical exposure times within each experiment. Images were processed in ImageJ (http://rsb.info.nih.gov/ij/). Images shown in the same panel have been scaled identically. Quantification of kinetochore intensities was done as previously described by Hoffman et al. (*1*) implemented in an ImageJ macro. For each measurement, at least 25 kinetochores were measured from at least 5 different cells. Cyclin-B levels were measured as average cytoplasmic intensity.

Immunoprecipitation experiments

Antibodies raised against pApc1 (phosphorylated S355), Apc2, Cdc27, Apc4, Apc5, Apc7, Cdh1 and Cdc20 were described previously (*2*-*6*). Antibodies against BubR1, Mad2 and Bub3 were raised by immunizing rabbits with human BubR1$^{1\text{-}715}$, Mad2 and Bub3 protein. BubR1$^{1\text{-}715}$ and Mad2 were recombinantly expressed in *E. coli* and Bub3 in Baculovirus infected Sf9 insect cells. Preparation of cell extracts and immunoprecipitation (IP) using antibodies crosslinked to beads (Affi-prep protein A beads, BioRad) were described elsewhere (*7*).

Re-immunoprecipitation (reIP) experiments

APC/C was affinity-purified from HeLa cells arrested with an active checkpoint using Cdc27 antibody-crosslinked beads. The native complex was eluted with 2 bead volumes of 1 mg/ml antigenic peptide dissolved in IP buffer (20 mM Tris-HCl pH7.5, 150 mM KCl, 10% glycerol, 0.1% Tween and 0.5 mM DTT). Two subpopulations of APC/C were separated by consecutive reIP. 3 volumes of APC/C peptide eluate were incubated first with 1 volume of BubR1, Cdc20 or Mad2 antibody coupled beads and second with anti-Apc4 beads. Beads were washed 3 times by resuspending them in 20 bead volumes of IP buffer for 5 min at 4°C and APC/C was recovered by elution with the antigenic peptides or 100 mM glycine-HCl at pH 2.2.

Cdc20 and Cdh1 were bound to the mix of both APC/C species immobilized on Cdc27 beads by incubating them with 3.6, 1.8 or 0.9 μM of either of the coactivators in IP buffer. 2 bead volumes of coactivator dilution were mixed with 1 volume APC/C beads on a rotary shaker for 30 min at room temperature. The excess of coactivator was removed by washing the beads 4 times with 50 volumes IP buffer prior to peptide elution and separation of the two APC/C populations by reIP. His_6-tagged Cdc20 and Cdh1 were expressed in Baculovirus-infected Sf9 insect cells (*8*).

Mass spectrometry

Tryptic peptides were loaded onto the trap column at a flow rate of 20 µL/min with mobile phase A (5% acetonitrile, 0.1% formic acid) and were washed for 10 min. The sample was eluted from the trap column and separated on the separation column with a gradient from 0% to 50% mobile phase B (80% acetonitrile, 0.08% formic acid) in 30 min at a flow rate of 300 nL/min. Eluting peptides were ionized with a spray voltage set to 1.5 kV. CAD fragmentation and spectra acquisition were carried out in the linear ion trap using a data dependent neutral loss MS^3 method. Acquired data (Xcalibur RAW-file) was converted into Sequest DTA-files using the program extract_msn, part of Sequest Bioworks Browser (version 3.2 - Thermo Electron), and further merged into Mascot generic files using Mascot Daemon (Matrix Science). For peptide identification a database search against a custom database containing all relevant proteins was performed using Mascot (Matrix Science; version 2.2.0).

All nano-HPLC separations were performed using UltiMate 3000 Nano-LC system (Dionex Benelux) equipped with a trap column (PepMap C18, 300 µm). Mass spectrometric analyses were conducted on a hybrid linear ion trap / Fourier transform ion cyclotron resonance (FTICR) mass spectrometer (LTQ-FT Ultra, ThermoElectron). The mass spectrometer was equipped with a nano-electrospray ionization source (Proxeon Biosystems). Metal coated nano ESI needles were used (New Objective).

***In vitro* ubiquitylation assay**

To measure the ubiquitylation activity of immunopurified APC/C, 1-3 µl APC/C bound antibody beads were used in XB buffer (10 mM Hepes-KOH, pH 7.7, 100 mM KCl, 2 mM $MgCl_2$, 0.1 mM $CaCl_2$ and 1 mM DTT) containing purified E1 (0.5 µM), UbcH10 (8.2 µM), ubiquitin (0.3 mM), ATP regenerating system (7.5 mM creatine phosphate, 1 mM ATP, 1 mM $MgCl_2$, 0.1 mM EGTA, 30 U/ml rabbit creatine phosphokinase type I (Sigma)). Human His-E1 and His-UbcH10 were expressed in *E.coli* and purified on a Ni-NTA resin (*8*). To charge UbcH10 with ubiquitin before addition of APC/C and substrate, E1, UbcH10, ubiquitin and ATP were preincubated at 36°C for 5 min. The substrate, an iodinated human cyclin-B1 fragment (amino acid residues 1-87, 3.5 µM) and APC/C bound beads were incubated with the reaction mix in a total volume of 10 µl at 36°C and 1200 rpm in a thermomixer (Eppendorf). The reaction was stopped by the addition of 4 x SDS sample buffer. The radiolabel of the substrate protein allowed detection by SDS-PAGE and autoradiography and the quantification of substrate-ubiquitin conjugates over time was performed with ImageJ (http://rsb.info.nih.gov/ij/).

Full length human cyclin-A2, cyclin-B1, securin and Nek2A were generated by coupled transcription/translation in rabbit reticulocyte lysates (TNT, Invitrogen). APC/C bound antibody beads were incubated with 10 µl reaction mix containing 2-3.5 µl of IVT-substrate, 5 µM MG132 and 2.3 µM ubiquitin aldehyde (Sigma).

Preparation of APC/C for electron microscopy

APC/C was isolated on Cdc27 antibody beads from lysates of HeLa cells (*7*). Bound protein was washed four times with 50 bead volumes of TBS (20 mM Tris-HCl, pH 7.6, 150 mM NaCl and 0.5 mM DTT). APC/C was eluted with TBS containing 1 mg/ml Cdc27 peptide for 15 minutes at 4°C. The excess of peptide was removed and APC/C particles were stabilized by applying the APC/C peptide eluate onto a glycerol density gradient containing glutaraldehyde. This procedure is called *GraFix* and was described by Kastner et al. (*9*).

Negative staining electron microscopy at low temperatures

Purified APC/C or APC/C-antibody complexes were adsorbed to a thin film of carbon and then transferred to an electron microscopic grid covered with a perforated carbon film. The bound APC/C particles were stained with 2% uranyl formate, blotted and air dried for ~1 min at room temperature. For negative staining at low temperatures (*10*) the grids were subsequently plunged into liquid nitrogen. Under these conditions samples are not fully dehydrated because glycerol in the sample prevents complete evaporation of water from the grid. Evidence for the presence of water can directly be obtained by exposing the specimen to the electron beam immediately after cryo-transfer in the electron micorscope (fig. S6). Images were recorded at a magnification of 155.000 x on a 4k x 4k CCD camera (TVIPS GmbH) using two-fold pixel binning (1.8 Å/pixel) in a Philips CM200 FEG electron microscope (Philips/FEI) operated at 160kV acceleration voltage. APC/C-antibody complexes were imaged at room temperature using the same magnification. The number of particles used for each project varies between ~8700 and ~73.000 and the obtained resolutions are in the range of 19-35 Å. The highest resolution was obtained for the negative stain 3D reconstruction of apo-APC/C (19 Å). Details about image statistics and resolution are provided in table S2.

Unstained cryo-electron microscopy

GraFix peak fractions were subjected to desalting spin columns (Zeba spin columns, Pierce) to remove glycerol. APC/C was bound to a thin layer of carbon and flash frozen into liquid ethane (*11*). Images were recorded using the same procedure and the same microscope as

described for negative staining at low temperatures. We have used unstained cryo-EM and negative staining EM for 3D structure determination of apo-APC/C (fig. S5) as well as APC/C^{MCC} (Fig. 2C).

Processing of electron microscopy images

Particle images (200 x 200 pixel) were selected using the semi-automated software boxer as part of the Eman package. Images were coarsened by a factor of two resulting in 100 x 100 pixels per image with a sampling of ~3.8 Å/pixel. After CTF correction (*12*), images were aligned using an exhaustive multi-reference alignment based on resampling to polar coordinates (*13*). Characteristic views were obtained by averaging after multivariate statistical analysis and classification (*14*). Angular reconstitution (*15*) was used to determine the relative orientations of the projection images prior to computing the 3D reconstruction.

We have performed supervised classification based on projection matching to separate apo-APC/C from APC/C^{MCC} or APC/C^{Cdc20} complexes. Projection matching was also used to separate the three different conformations that we found for the apo-APC/C complex. Initially, these three different conformations were obtained by the random conical tilt reconstruction technique (*16*). 3D structures were visualized with the software AmiraDev 2.3 (TGS Europe, Merignac Cedex).

Localization of APC/C subunits and the coactivators Cdc20 and Cdh1 by negative staining EM

Loading of recombinant Cdc20 and Cdh1 in vitro

N-terminally His_6-tagged human Cdc20 and Cdh1 were expressed in Baculovirus-infected Sf9 cells and purified via the His-tag (*8*). Apo-APC/C was purified from HeLa cells arrested with an active checkpoint by Cdc27-IP followed by consecutive reIP as described. Apo-APC/C bound to beads was incubated with ~0.5-1.0 µM recombinant Cdc20 or Cdh1 for 30 min at 4°C. Beads were washed three times with 50 volumes of TBS and eluted with the antigenic peptide. In case of Cdh1, experiments were also performed in parallel with APC/C isolated from Xenopus interphase egg extracts (7).

Antibody labeling

Peptide eluted human APC/C preparations were incubated with decreasing concentrations of pApc1, Cdc27, Apc4, Apc5, Cdc16, Apc7 and BubR1 antibodies starting at a molar APC/C to IgG ratio of 2:1. At the antibody concentration yielding a high percentage of APC/C dimers, samples were processed using the *GraFix* protocol and analyzed by negative staining EM.

The concentration of particles on the EM grid was chosen to be very low to ensure that APC/C dimers were not formed accidentally by the presence of large amounts of APC/Cs. 200-300 APC/C dimers were selected for each antibody labeling experiment to determine the antibody binding sites. First the projection direction of each APC/C monomer was determined and a rectangular plane was drawn in 3D, perpendicular to the imaging plane at the antibody binding site. The x,y dimensions of the rectangular planes reflect the uncertainties of detecting the binding site of the antibody (fig S8). However, in case of Apc1, Cdc27, Apc4, Apc5 and BubR1 labeling experiments the rectangular planes did precisely intersect in 3D describing a single spot on the surface of APC/C. We were thus able to determine the location of APC/C subunits at an accuracy that is reflected by the size of the spheres shown in Fig. 3A. In case of Apc7 and Cdc16 the labeling was considerably less accurate, possibly due to the presence of multiple copies of these subunits. Single labeling spots were not obtained in those cases. However, both proteins were found to be located in the "arc lamp" domain of APC/C.

Random conical tilt 3D reconstruction

The recently published 3D structure of the fission yeast APC/C (*17*) has mirrored handedness with respect to the *Xenopus* APC/C 3D structure determined by Dube et al. (*18*). We have therefore repeated the random conical tilt experiment of negatively stained human apo-APC/C to solve the handedness problem. 8859 tilted image pairs were collected in negative stain and 350 random conical tilt 3D reconstructions were computed. Individual RCT 3D models were aligned by an automated exhaustive 3D alignment via polar coordinates combined with a weighted averaging procedure (*19*). The entire procedure was first tested with a 70S *E. coli* ribosome data set to make sure that the obtained handedness is correct. We have obtained a well defined consensus 3D structure of human APC/C (fig. S5) which unambiguously confirms the handedness that we have determined for *Xenopus* APC/C (*18*). In addition to providing the APC/C structure with correct handedness, the set of aligned RCT 3D reconstructions was subjected to three-dimensional multivariate statistical analysis and classification to analyse the structural variation within one single data set. Using this unsupervised classification procedure, three distinct structures of the apo-APC/C were obtained that differ in their relative orientation of the two major APC/C domains. The obtained structures were subsequently refined using standard projection matching techniques (Fig. 2A, apo-APC/C).

Crosslinking of UbcH10

UbcH10 was covalently linked to the heterobifunctional crosslinker Sulfo-GMBS (N-[g-Maleimidobutyryloxy]sulfosuccinimide ester, Pierce) via its free –SH groups as described by Vodermaier et al. (*5*). APC/C was purified on Cdc27 antibody beads from lysates of HeLa cells arrested in mitosis with an active or inhibited checkpoint. Beads were equilibrated in 20 mM HEPES pH 7.5, 100 mM NaCl. For crosslinking, 12 µl APC/C bound beads were mixed with UbcH10-GMBS or unmodified UbcH10 at a final concentration of 1 or 2 µM in a total volume of 30 µl. After 2 to 15 min incubation at 25°C, samples were washed twice with 20 mM HEPES pH 8.0, 100 mM NaCl and were incubated for 10 min at pH 8.0 and 25°C. APC/C was eluted with 1.5 volumes of 1 mg/ml of the antigenic peptide and analyzed by SDS-PAGE and immunoblotting. To quantify crosslinking of UbcH10 to APC/C a fluorescently labeled (Alexa 630) secondary antibody was used and the signal intensities were measured by a Odyssey scanner (LI-COR Biosciences).

***In vitro* substrate binding assay**

A tandem fragment of the N-terminal 70 residues of fission yeast cyclin-B Cdc13 (*20*), full length human securin and the fragment of Hsl1$^{667\text{-}872}$ were expressed in *E.coli* and purified. APC/C was isolated by Cdc27-IP and peptide elution from lysates of HeLa cells arrested with checkpoint on or off.

Glutathione-sepharose beads (Amersham) were first equilibrated in buffer A (50 mM Tris-HCl pH7.5, 10% glycerol, 1 mM DTT) containing 2 mg/ml of BSA on a rotary shaker at room temperature for 1 hr. 20 µl of glutathione-sepharose were incubated with different dilutions of wild type or D-box mutant cyclin-B protein in 30 µl of buffer A containing 4 mg/ml BSA for 1 hr (Fig. 4A). The beads were washed 3 times with buffer A and mixed with 80 µl of APC/C eluate for 1 hr at RT. Subsequently, the excess of soluble APC/C was removed, beads were washed 3 times with buffer B (50 mM Tris-HCl, pH7.5, 150 mM NaCl, 0.5% Tween, 5 mM EDTA) and bound proteins were eluted with 30 µl 2 x SDS sample buffer containing 5 mg/ml BSA.

Conversely, 15 µl samples of APC/C bound beads were incubated with various dilutions of wild type or D-box mutant cyclin-B (Fig.4B), wild type securin (Fig. 4C) or wild type Hsl1$^{667\text{-}872}$ (fig. S11) protein in 45 µl of buffer A containing 4 mg/ml BSA for 1hr at room temperature. Beads were washed with buffer B and bound proteins were eluted off the beads with 25 µl of 100 mM glycine-HCl, pH 2.2.

Supplementary Figures

Figure S1

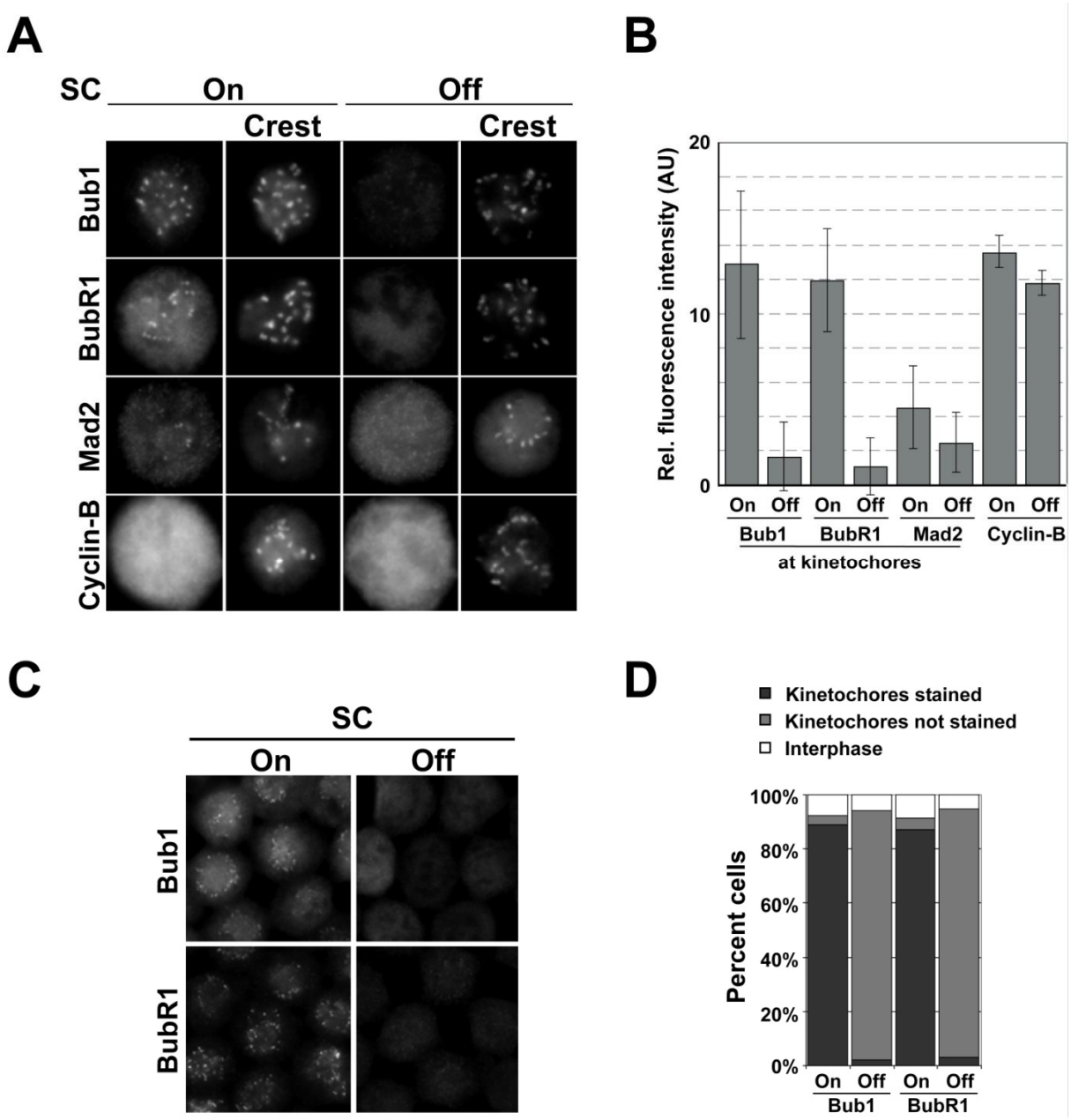

Figure S1. **Immunofluorescence microscopy of HeLa cells arrested in mitosis with an active or inhibited checkpoint using the Taxol/Hesperadin protocol.**

(A) HeLa cells were arrested either in prometaphase by activating the spindle checkpoint (SC on) with Taxol or in a metaphase-like state (SC off) by overriding the Taxol-arrest with the Aurora B inhibitor Hesperadin, and by blocking anaphase onset by the addition of the proteasome inhibitor MG132 (see Materials and Methods). Cells were fixed and analyzed by immunofluorescence microscopy (IFM) using the indicated antibodies.

(B) Quantification of the IFM staining intensities shown in (A) (AU, arbitrary units).

(C) HeLa cells were synchronized in a checkpoint on or off state using the Taxol/Hesperadin protocol with an initial 16 hr Taxol treatment (see Materials and Methods). Cells were harvested by mitotic shake off and fixed after Cyctospin. Bub1 and BubR1 localization was analyzed by IFM and DNA was visualized by DAPI.

(D) Cells were classified according to their Bub1, BubR1 and DNA staining.

Figure S2

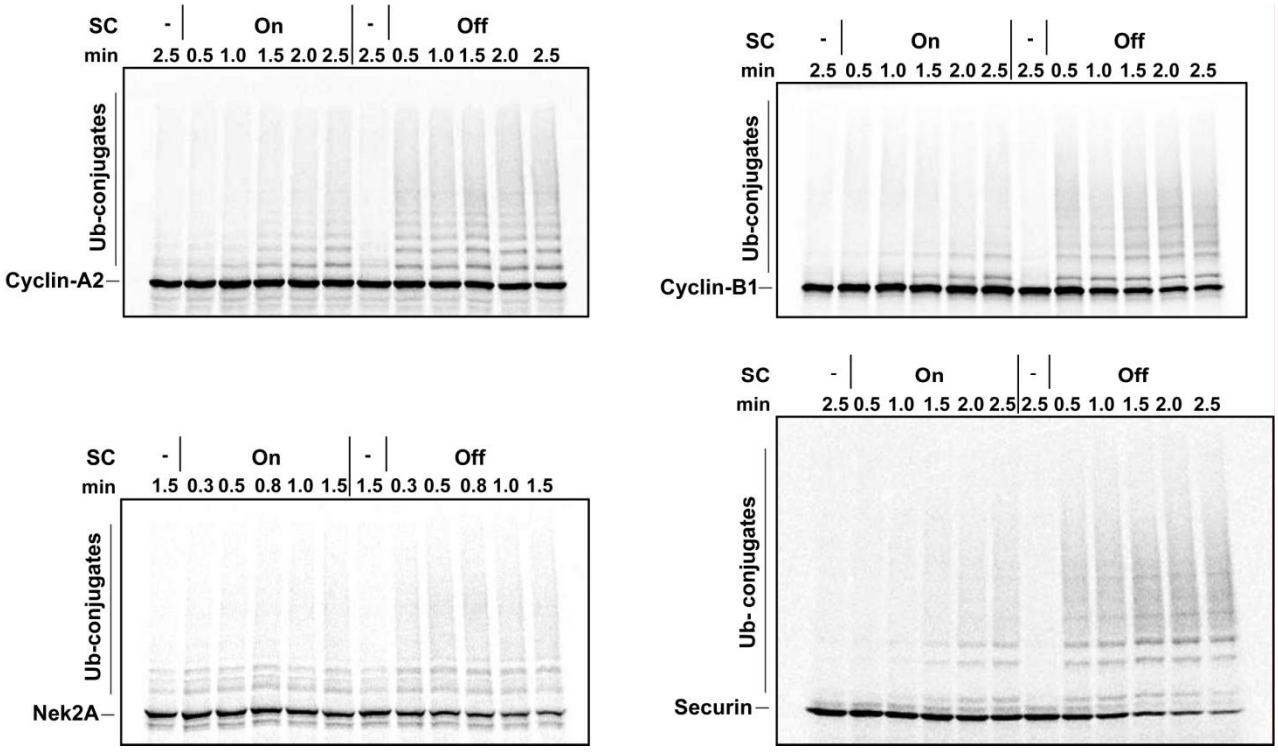

Figure S2. *In vitro* ubiquitylation of securin, cyclin-B1, cyclin-A2 and Nek2A reveals similarly reduced APC/C activity towards all substrates upon MCC binding.

^{35}S-labeled human full-length securin, cyclin-B1, cyclin-A2 and Nek2A were generated by in vitro translation. APC/C purified from checkpoint on or off cells and the ^{35}S-labeled substrate proteins were incubated with E1, UbcH10, ubiquitin and ATP for the indicated times. Substrate ubiquitylation was analyzed by SDS-PAGE and quantified by autoradiography.

Figure S3

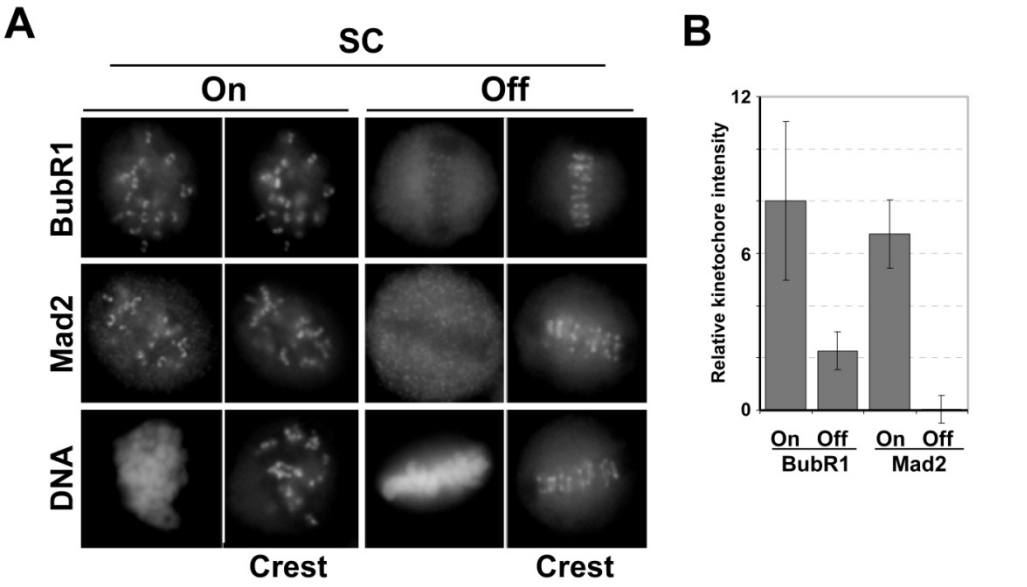
A
SC
On
Off
BubR1
Mad2
DNA
Crest
Crest
B
Relative kinetochore intensity
12
6
0
On Off
BubR1
On Off
Mad2

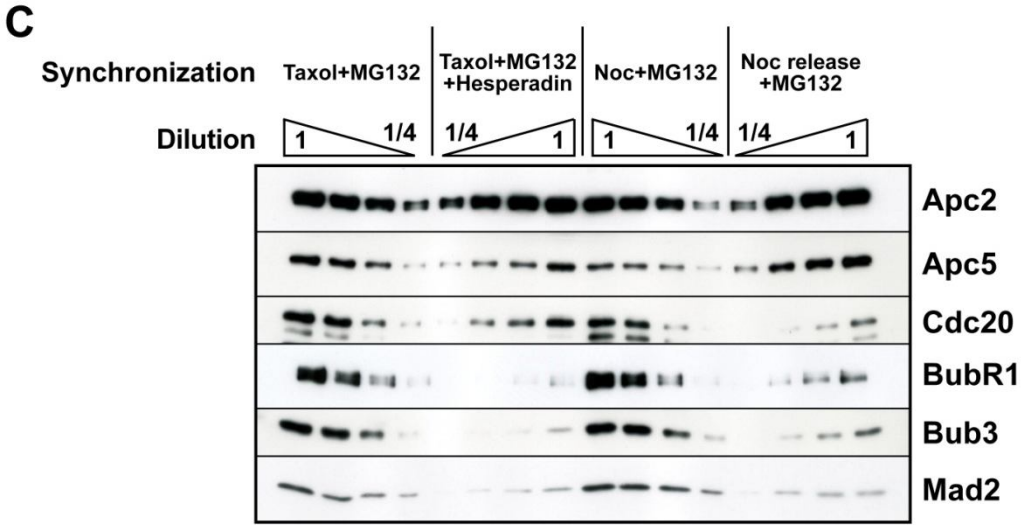
C
Synchronization
Taxol+MG132
Taxol+MG132
+Hesperadin
Noc+MG132
Noc release
+MG132
Dilution
1
1/4
1/4
1
1
1/4
1/4
1
Apc2
Apc5
Cdc20
BubR1
Bub3
Mad2

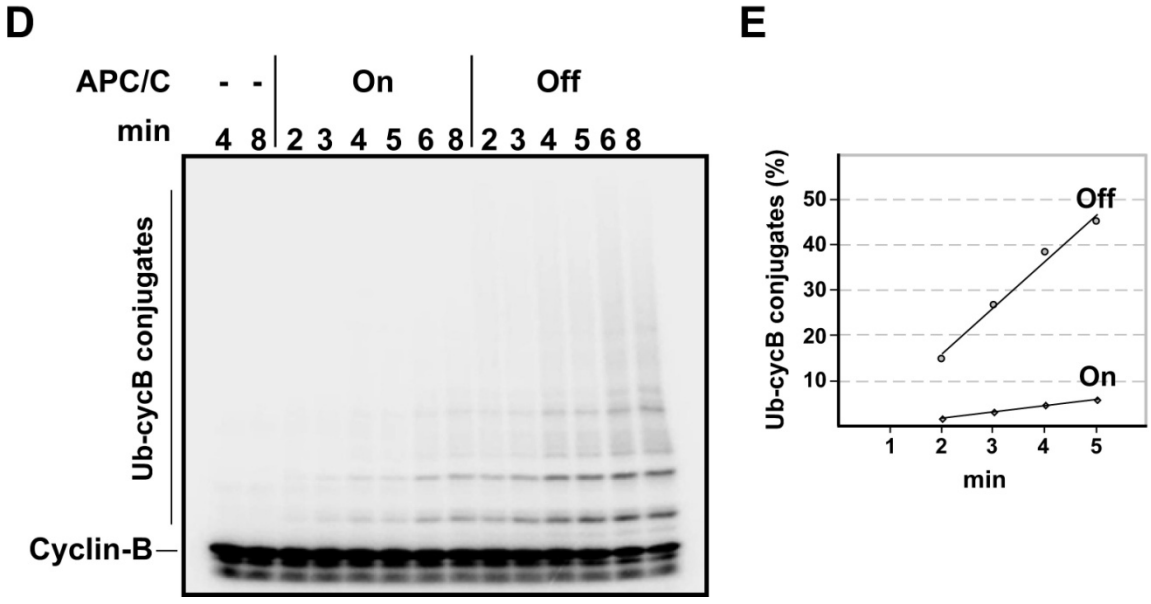
D
APC/C
-
-
On
Off
min
4 8 2 3 4 5 6 8 2 3 4 5 6 8
Ub-cycB conjugates
Cyclin-B
E
Ub-cycB conjugates (%)
50
40
30
20
10
Off
On
1 2 3 4 5
min

Figure S3. An alternative protocol using Nocodazole to arrest HeLa cells in mitosis with an active or inhibited spindle checkpoint.

(A) HeLa cells were arrested either in prometaphase by activating the spindle checkpoint with Nocodazole (SC on) or in a metaphase-like state (SC off) by washing out Nocodazole and blocking progression of the released cells to anaphase by adding the proteasome inhibitor MG132. Cells were fixed and analyzed by immunofluorescence microscopy (IFM) using the indicated antibodies and DAPI to visualize DNA.

(B) Quantification of the IFM staining intensities of BubR1 and Mad2 at kinetochores.

(C) HeLa cells were arrested in a checkpoint on or off state using the Taxol/Hesperadin or the Nocodazole release protocol (see Materials and Methods). APC/C complexes were immunoprecipitated from lysates of the differentially synchronized cells by Cdc27 antibodies. A dilution series of the purified proteins were analyzed by SDS-PAGE and immunoblotting using the indicated antibodies. From 1 to 1/4, 1, 0.75, 0.5, and 0.25 volumes were loaded.

(D) APC/C was immunopurified from checkpoint on or off arrested HeLa cells obtained by the Nocodazole release protocol. The *in vitro* ubiquitylation activities of these two APC/C preparations were assessed using an iodinated fragment of human cyclin-B as a substrate. Reactions were stopped at the indicated time points and analyzed by SDS-PAGE and autoradiography.

(E) Quantification of the *in vitro* ubiquitylation assays shown in (D) revealed an eight-fold reduction of cyclin–ubiquitin conjugation upon association of MCC with APC/C.

Figure S4

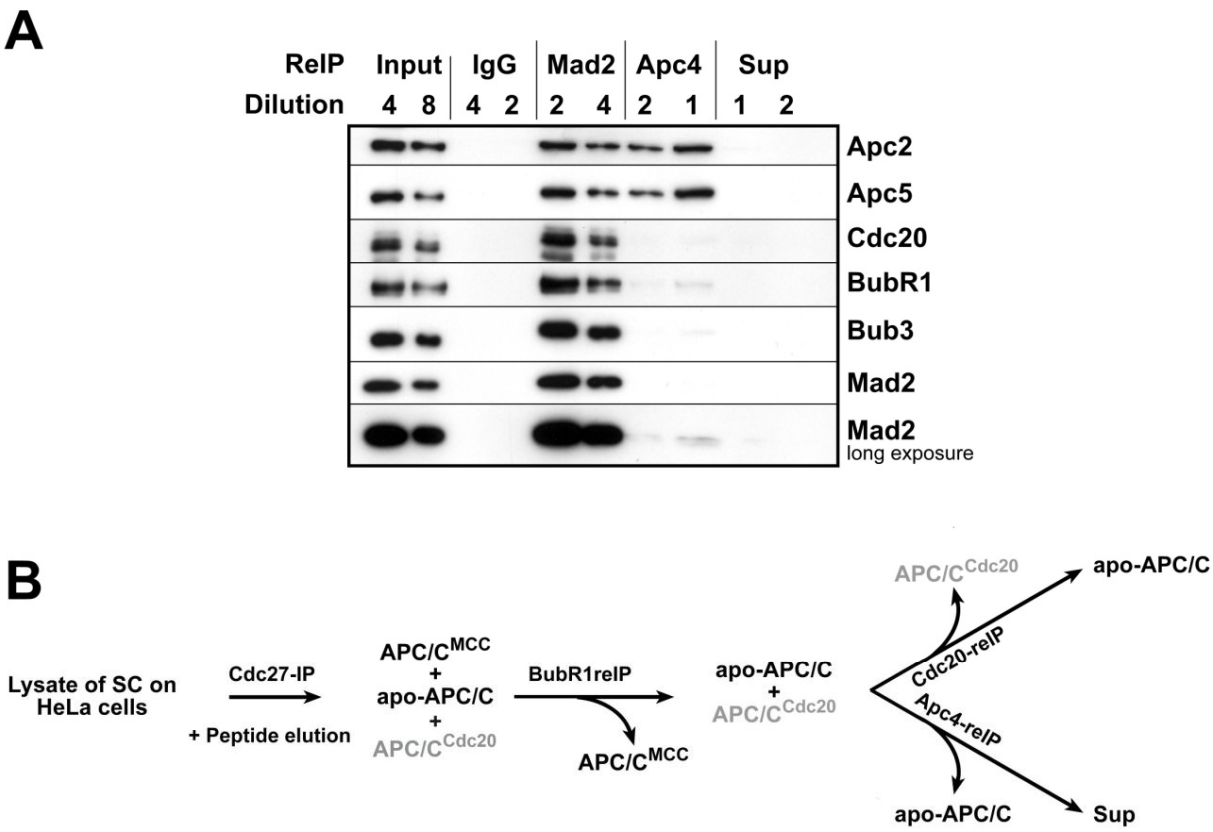
A
RelP Input IgG Mad2 Apc4 Sup
Dilution 4 8 4 2 2 4 2 1 1 2
Apc2
Apc5
Cdc20
BubR1
Bub3
Mad2
Mad2 long exposure
B
Lysate of SC on HeLa cells
Cdc27-IP
+ Peptide elution
APC/C^MCC + apo-APC/C + APC/C^Cdc20
BubR1relP
APC/C^MCC
apo-APC/C + APC/C^Cdc20
APC/C^Cdc20
apo-APC/C
Cdc20-relP
Apc4-relP
apo-APC/C
Sup
C
RelP Input IgG BubR1 Cdc20 Sup Cdc20 Apc4 Sup Apc4
Dilution 4 8 4 2 2 4 2 1 1 2 2 1 1 2
Apc2
Apc5
Cdc20
BubR1
Bub3
Mad2

Figure S4. Re-immunoprecipitation experiments to separate APC/C species isolated from Hela cells arrested with an active checkpoint.

(A) APC/C was purified from HeLa cells arrested with an active checkpoint by immunoprecipiation (IP) with Cdc27 antibody and peptide elution (Fig. 1F). APC/C^{MCC} was isolated by Mad2-IP from the Cdc27 peptide eluate. Remaining APC/C particles were recovered by Apc4-IP from the supernatant of the Mad2-IP. Bound proteins were eluted with 100 mM glycine-HCl (pH 2.2) and analyzed by SDS-PAGE/immunoblotting. Note that the majority of BubR1, Bub3 and Cdc20 co-IP with Mad2, indicating that Mad2 is a stoichiometric component of APC/C^{MCC}.

(B) Schematic representation of an experiment designed to test if APC/C^{Cdc20} is present in HeLa cells arrested with an active checkpoint.

(C) Immunoblot analysis of protein complexes obtained in (B). Note that no APC/C^{Cdc20} could be detected by Cdc20 reIP, suggesting that cells with an active checkpoint contain very little if any APC/C^{Cdc20}.

Figure S5

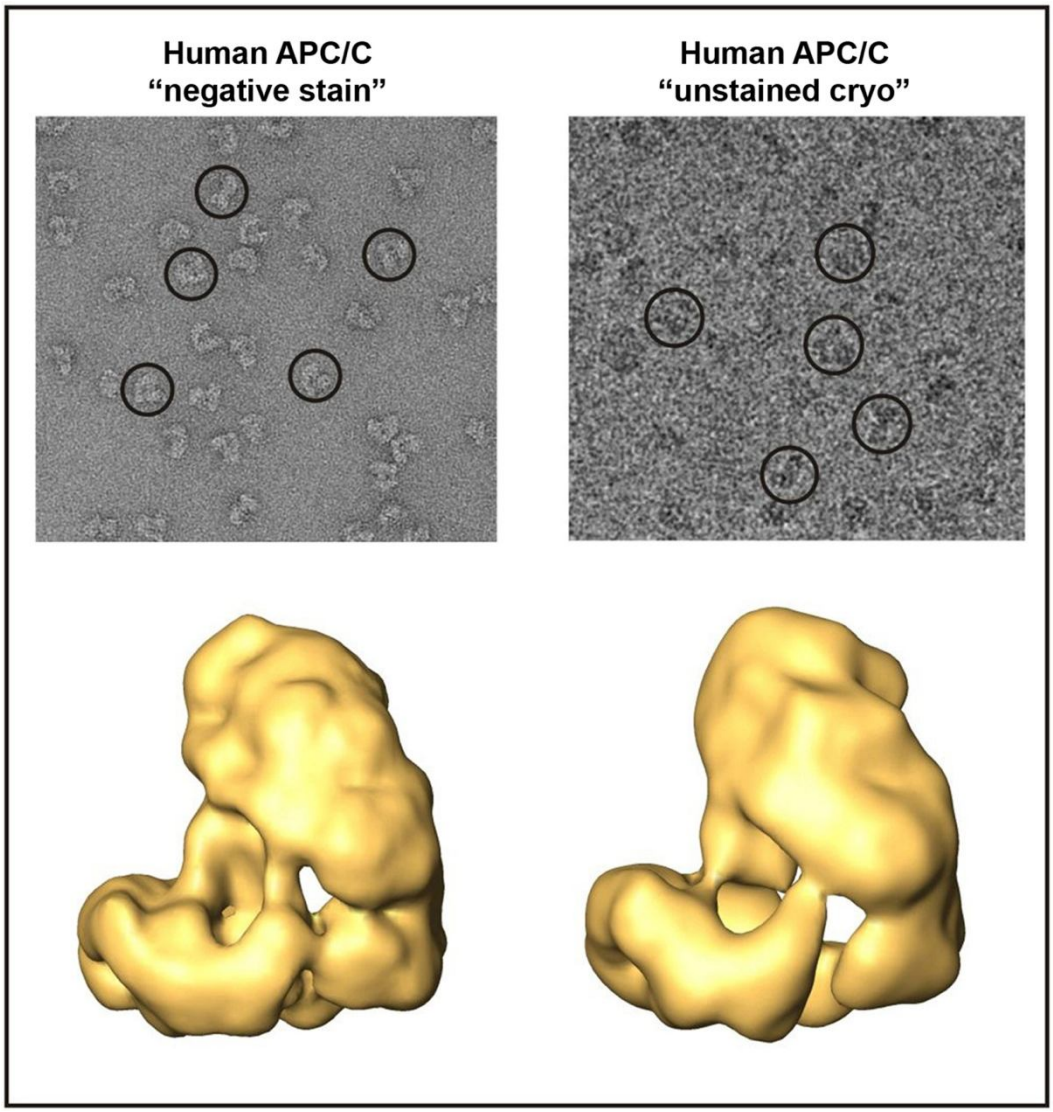

Figure S5. Comparison of unstained cryo- and negative stain electron microscopy.
Unless indicated otherwise, APC/C structures presented in this paper were obtained using negative staining EM at low temperatures. Stabilization of APC/C during *GraFix* allowed us to remove glycerol from the gradient fractions and to perform also unstained cryo-imaging of APC/C embedded in vitrified buffer. The 3D reconstructions obtained by both techniques for apo-APC/C (shown here) and for APC/C^{MCC} (Fig. 2C) are very similar. The resolution obtained for the unstained cryo-EM reconstructions is considerably lower than the resolution obtained by negative staining at low temperatures (table S2). This can be attributed to the final buffer exchange step which is important to remove glycerol for unstained cryo-EM but which has significantly affected the integrity of APC/C particles.

Figure S6

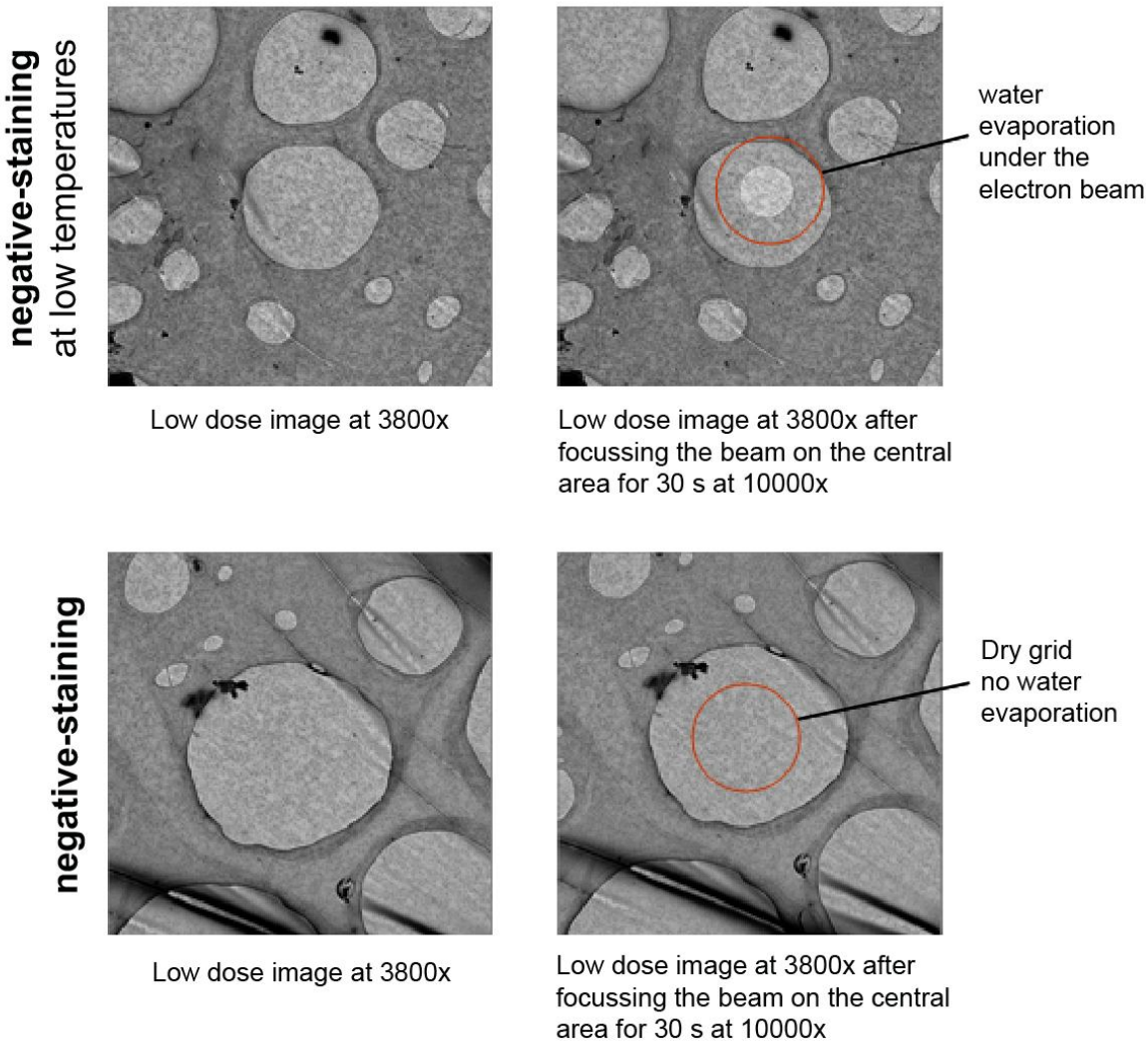

Figure S6. Water evaporation upon illumination under the electron beam is observed in samples negatively stained at low temperatures. The test was carried out shortly after cryo-transfer of the grid to avoid any artefacts by ice contamination inside the microscope column. Focusing the electron beam on a small area reveals a bright spot in the center due to water evaporation. As a control, the grid was allowed to warm up to RT inside the microscope and then the test was repeated on an adjacent area. In this case (representing normal negative stain conditions at room temperature) no water was evaporated after focusing the beam at an increased magnification for 30 seconds. These observations indicate that APC/C molecules are still hydrated when using negative staining at low temperatures in contrast to conventional negative staining.

Figure S7

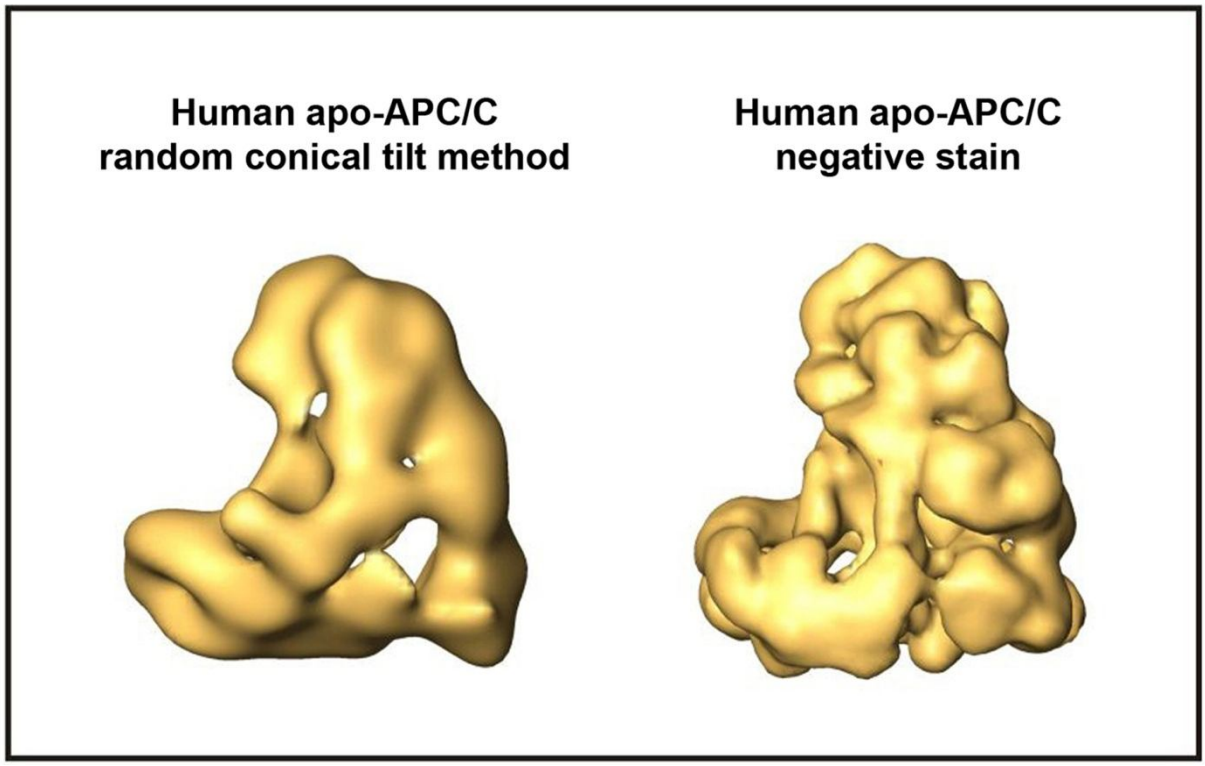

Figure S7. Random conical tilt 3D reconstruction of apo-APC/C.

The random conical tilt (RCT) technique (*16*) in combination with a maximum-likelihood based alignment and weighted averaging approach (*19*) was used to corroborate the handedness of the APC/C reconstruction (*18*). The RCT 3D reconstruction of human apo-APC/C is depicted on the left showing the correct handedness of the APC/C reconstruction. Recently, a 3D model of fission yeast APC/C has been published which shows overall similarity to the structure of vertebrate APC/C (*17*), but the handedness of the yeast 3D reconstruction appears to be the mirrored version of the one we determined previously for *Xenopus* APC/C (*18*). Ohi et al. (*17*) did not determine the handedness of their 3D reconstruction. We therefore performed additional RCT analyses and confirmed the handedness of human APC/C as it is shown here. The entire RCT procedure was first calibrated with a 70S ribosome and subsequently applied in exactly the same way for the APC/C to ensure the correct handedness of the APC/C reconstruction. The correct handedness of APC/C now allows reliable docking experiments using known X-ray structures or homology models (Fig. 3B).

Figure S8

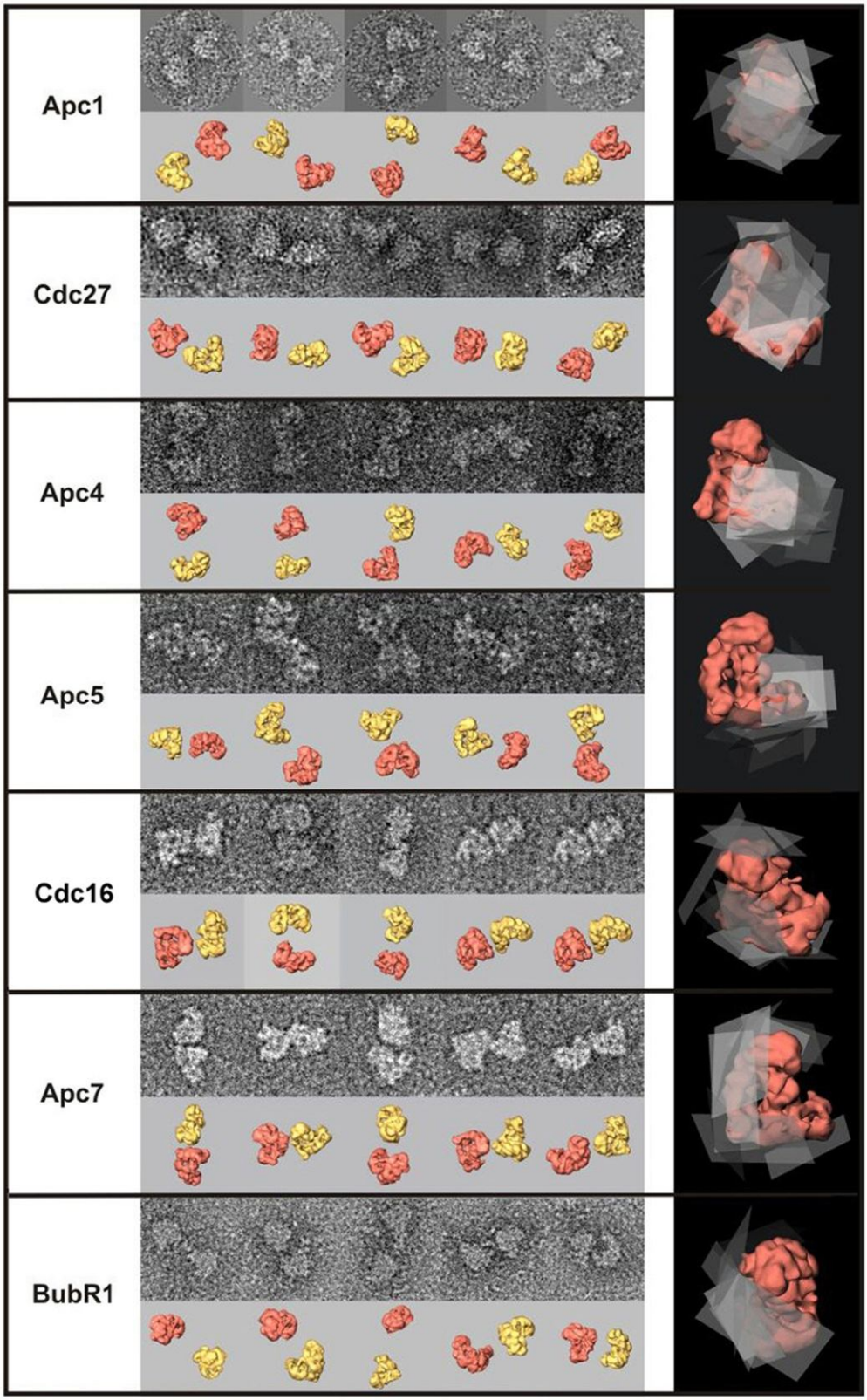

Figure S8. Antibody labeling of APC/C subunits and of BubR1.

Antibody labeling experiments were performed for the APC/C subunits Apc1, Cdc27, Apc4, Apc5, Apc6, Apc7, and for the MCC subunit BubR1,. The complexes were purified according to the *GraFix* protocol (*9*). The concentration of APC/C on the EM grid was intentionally kept low to make sure that trimeric complexes (two APC/C particles bound to one antibody) were analyzed, and not two APC/C particles which were coincidentally positioned next to each other. The orientation of the APC/Cs within the APC/C-antibody complex was evaluated based on the known structure of APC/C. The exact binding sites of the antibody at the interface between two APC/Cs cannot be exactly determined in a single image. Rectangles were thus modeled to the APC/C 3D structure at the respective binding sites of the antibody and the binding site was determined as the main crossing 3D area of all rectangles. This method provides unique labeling positions for most of the proteins studied. Only for Cdc16 and Apc7 a larger area was covered by the rectangles preventing a detailed interpretation. Cdc16 and Apc7 antibodies revealed a more disperse localization pattern at the arc lamp domain which may reflect the presence of at least two copies of Cdc16 and Apc7 per APC/C while there is only a single copy of all other subunits studied.

Figure S9

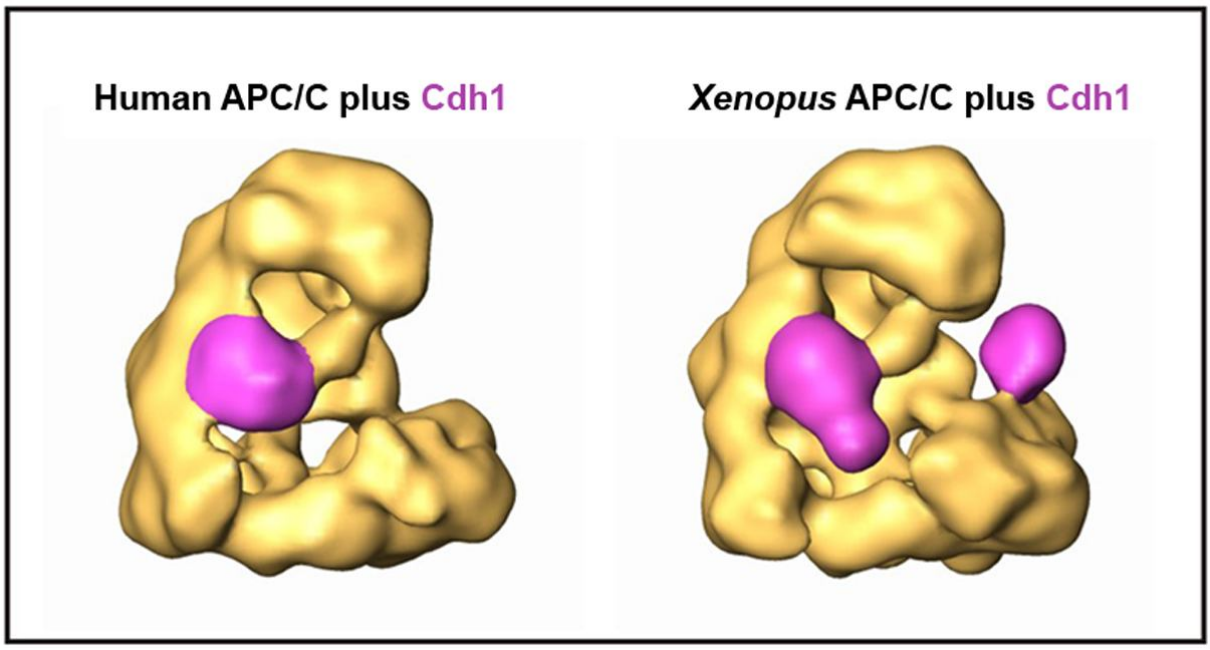

Figure S9. Cdh1 labeling of human and *Xenopus* APC/C.

In parallel to the Cdc20 labeling experiments, recombinant Cdh1 was bound to human apo-APC/C and analyzed by negative staining EM (left panel). We identified a single protein mass bound in a position that is similar to the position of Cdc20 in human APC/C^{Cdc20} (Fig. 2B). In contrast to this situation, we had previously observed two extra densities in the *Xenopus* APC/C structure following binding of recombinant Cdh1 (*18*). However, only the position on the right side was previously interpreted as a Cdh1 binding site because only this site could be confirmed by Cdh1 antibody labeling experiments *(18)*. We therefore re-analyzed the *Xenopus* APC/C^{Cdh1} complex using the new *GraFix* sample preparation protocol (*9*) which led to a 3D reconstruction of significantly higher quality (right panel). The new *Xenopus* APC/C^{Cdh1} 3D reconstruction shows again two extra densities, one on the right hand side, and one in a central position where Cdh1 can also be seen in human APC/C. It is therefore possible that APC/C contains more than one Cdh1 binding site. Which of these sites is functionally more important, and why two sites can only be detected in *Xenopous* APC/C will require further investigation.

Figure S10

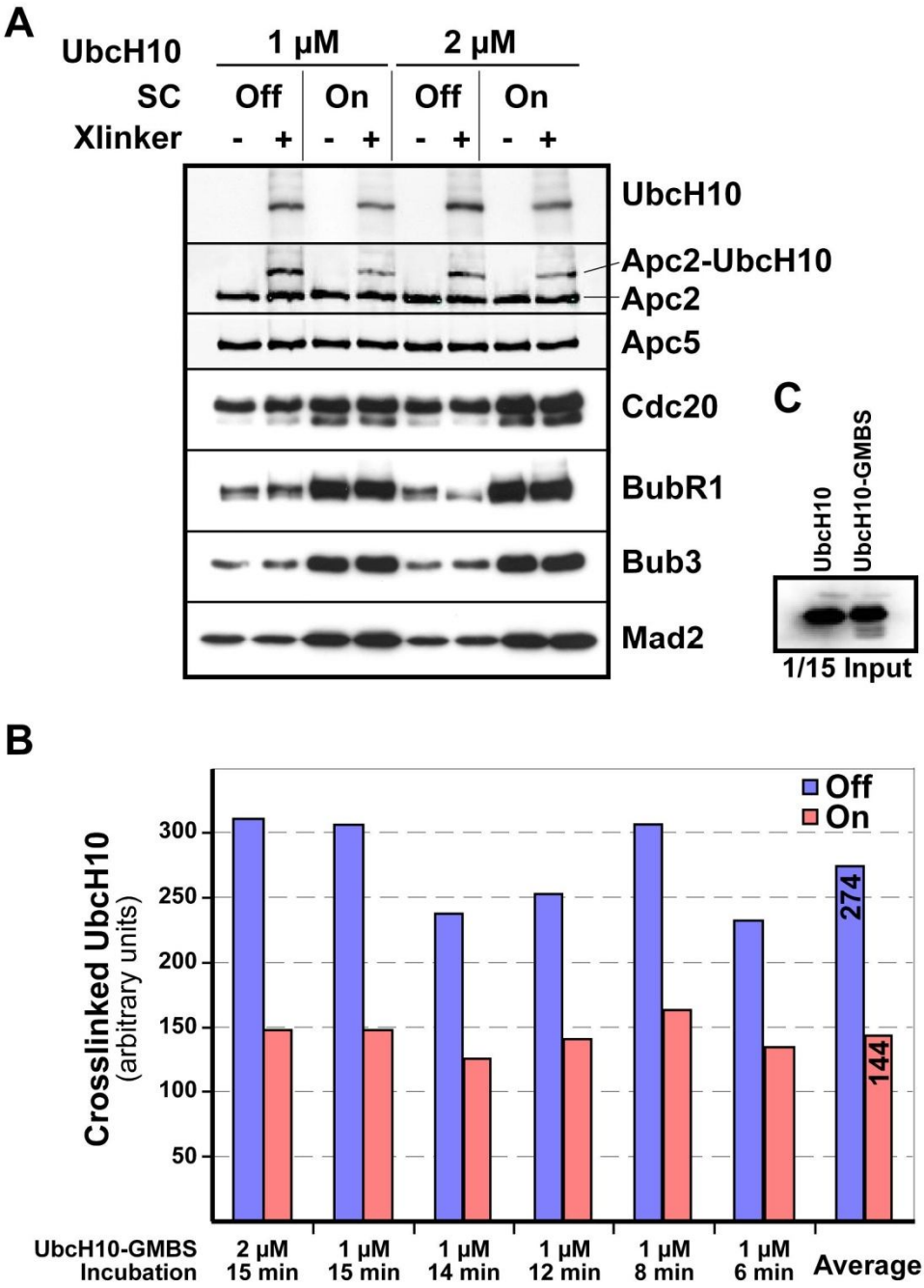
A
UbcH10
1 μM
2 μM
SC
Off
On
Off
On
Xlinker
- + - + - + - +
UbcH10
Apc2-UbcH10
Apc2
Apc5
Cdc20
BubR1
Bub3
Mad2
C
UbcH10
UbcH10-GMBS
1/15 Input
B
Crosslinked UbcH10
(arbitrary units)
Off
On
300
250
200
150
100
50
274
144
UbcH10-GMBS Incubation
2 μM 15 min
1 μM 15 min
1 μM 14 min
1 μM 12 min
1 μM 8 min
1 μM 6 min
Average

Figure S10. MCC association correlates with a twofold reduction in binding of APC/C to UbcH10 *in vitro*.

(A) APC/C was isolated on Cdc27 antibody beads from Hela cells arrested in a checkpoint on or off state. UbcH10 was covalently linked to the bifunctional crosslinker Sulfo-GMBS. 2 or 1 μM of UbcH10-GMBS or UbcH10 were incubated with APC/C for 6 to 15 min. Bound proteins were analyzed by SDS-PAGE and immunoblotting. Binding of UbcH10 was quantified using a fluorescently labeled secondary antibody. The UbcH10 signal intensity was measured by a Odyssey scanner and normalized to the levels of Apc2 present in the sample. **(B)** Quantification of UbcH10 crosslinking to APC/C from checkpoint off or on cells under 6 different conditions.

(C) Input levels of UbcH10 and UbcH10-GMBS were visualized by immunoblotting with a fluorescently labeled secondary antibody.

Figure S11

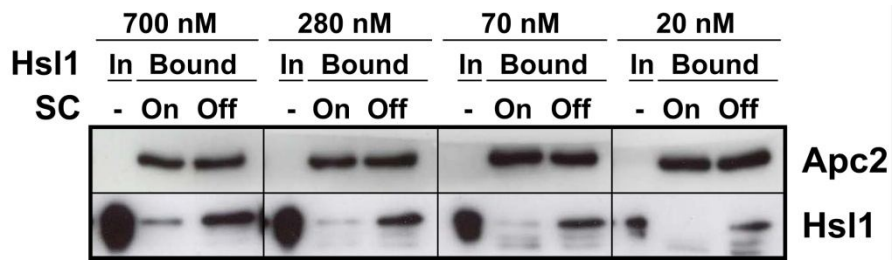

Figure S11. MCC binding reduces interaction of APC/C with substrate proteins *in vitro.* APC/C was immunoprecipitated by Cdc27 antibody coupled beads from lysates of checkpoint on or off arrested HeLa cells. A wild type Hsl1 fragment was applied to APC/C carrying beads at the indicated concentrations. The excess of Hsl1 was washed off and levels of bound Hsl1 were analyzed by SDS-PAGE/immunoblotting.

Table S1. Mass spectrometric analysis.

Protein complexes immunoprecipitated with Cdc27, Cdc20 und BubR1 antibodies from cells arrested in a checkpoint on or off state were identified by LC-MS. The numbers listed represent the ratio of Mascot score and the molecular mass (M) of the identified proteins and are a qualitative index for identification. (nd, not detected)

	M (Da)	Score/MW					
IP		**Cdc27**		**Cdc20**		**BubR1**	
SC		**On**	**Off**	**On**	**Off**	**On**	**Off**
APC/C subunits							
Apc1	218528	12.2	12.2	10.7	10.5	10.3	8.8
Apc2	94624	13.0	12.3	10.5	9.7	10.4	5.4
Cdc27	92893	13.8	10.6	10.6	10.3	10.8	9.4
Apc4	92856	14.2	15.2	12.8	10.3	13.8	8.9
Apc5	85707	21.5	21.7	22.4	21.5	19.4	10.9
Cdc16	72408	14.3	16.6	14.7	12.9	14.7	11.1
Apc7	67440	17.6	17.6	19.2	16.7	16.5	17.1
Cdc23	69588	21.4	22.6	18.2	17.6	17	13.3
Doc1	25352	8.9	12.2	9.6	9.8	11.5	6.6
Cdc26	9771	22.1	25.9	18.7	18.1	21.6	15.9
Apc11	10518	8.8	11.9	nd	nd	nd	nd
Apc13 (Swm1)	8516	10.1	19.7	nd	nd	nd	nd
APC/C activator							
Cdc20	55078	10.9	9.6	12	14.1	12.1	12.5
Cdh1	55544	7.1	7.4	nd	nd	nd	nd
SC							
BubR1	120753	14.3	12.4	16.8	15.3	20.3	20.7
Bub3	37330	11.5	10.8	12.5	13.2	15.5	17.9
Mad2	23666	8.3	7.6	14.4	6.9	16.5	10.3
Bub1	123451	nd	nd	3.6	12.0	14.7	15.8
Mad1	83274	nd	nd	nd	nd	nd	nd
APC/C regulators							
Cdk1 (Cdc2)	34117	5.5	26.3	7.8	15	nd	nd
Cdk2	34089	nd	9.2	6.6	13.8	nd	nd
Cks2	9854	nd	7.8	nd	nd	nd	nd
Emi1	51427	nd	8.3	nd	nd	nd	nd

Table S1. continued

IP	MW (Da)	Score/MW					
		Cdc27		Cdc20		BubR1	
SC		On	Off	On	Off	On	Off
APC/C substrates							
Nek2A	52130	10.7	10.4	nd	2.1	nd	nd
cyclin-A2	48696	2.4	6.7	5.9	14.2	nd	nd
cyclin-B1	48591	nd	5.3	nd	nd	nd	nd
Kinetochore							
Hec1 (Ndc80)	74380	nd	nd	nd	2.7	12.9	15.4
Nuf2	54637	nd	nd	nd	nd	8.8	7.9
Spc24	22486	nd	nd	nd	8.1	19.5	nd
Spc25	26194	nd	nd	nd	6.9	10.3	12.8
Mis12	24466	nd	nd	nd	nd	9.3	9.8
Zwint-1	35747	nd	nd	nd	5.3	11.6	12.5
DC8	32569	nd	nd	nd	4.7	7.5	14.8

Table S2. Statistics of EM image analysis.

Summary of several APC/C complexes studied by EM. Human apo-APC/C and APC/C^{MCC} were studied by unstained cryo-EM as well as negative staining at low temperatures. All other complexes were studied only by negative staining at low temperatures. A higher number of disintegrated APC/C particles is observed in unstained cryo-EM images. The occupancy of MCC binding in the APC/C^{MCC} is also significantly reduced (43% compared to 56%) in the sample used for unstained cryo-EM.

Sample	EM Method	Number of Particles	Percentage of binding	Resolution
Human apo-APC/C	unstained cryo	8731	-	~35 Å
Human apo-APC/C	negative stain	46996	-	19-25 Å
Human APC/C-MCC	unstained cryo	73389	43%	~32 Å
Human APC/C-MCC	negative stain	41760	56%	20-25 Å
Human APC/C-Cdc20	negative stain	15760	30%	~27 Å

Movie S1. The movie shows an animated morphing scene between different populations of apo-APC/C that were found to be present in one single sample. It is important to note that the transition between the different populations is just an animation to illustrate the major structural differences, namely a different relative orientation of the "platform" and "arc lamp" domain.

3D-pdf S1 and 3D-pdf S2. The 3D-pdf files S1 and S2 display 3D models of human apo-APC/C and APC/C^{MCC}, respectively. The MCC protein mass of APC/C^{MCC} is coloured in red visualizing the contacts formed between MCC and APC/C (Adobe Reader 9).

Supplementary References

1. D. B. Hoffman, C. G. Pearson, T. J. Yen, B. J. Howell, E. D. Salmon, *Mol Biol Cell* **12**, 1995 (2001).
2. E. R. Kramer, C. Gieffers, G. Holzl, M. Hengstschlager, J. M. Peters, *Curr Biol* **8**, 1207 (1998).
3. C. Gieffers, B. H. Peters, E. R. Kramer, C. G. Dotti, J. M. Peters, *Proc Natl Acad Sci U S A* **96**, 11317 (1999).
4. R. Grossberger *et al.*, *J Biol Chem* **274**, 14500 (1999).
5. H. C. Vodermaier, C. Gieffers, S. Maurer-Stroh, F. Eisenhaber, J. M. Peters, *Curr Biol* **13**, 1459 (2003).
6. C. Kraft *et al.*, *Embo J* **22**, 6598 (2003).
7. F. Herzog, J. M. Peters, *Methods Enzymol* **398**, 175 (2005).
8. C. Kraft, M. Gmachl, J. M. Peters, *Methods* **38**, 39 (2006).
9. B. Kastner *et al.*, *Nat Methods* **5**, 53 (2008).
10. M. M. Golas, B. Sander, C. L. Will, R. Luhrmann, H. Stark, *Science* **300**, 980 (2003).
11. M. Adrian, J. Dubochet, J. Lepault, A. W. McDowall, *Nature* **308**, 32 (1984).
12. B. Sander, M. M. Golas, H. Stark, *J Struct Biol* **142**, 392 (2003).
13. B. Sander, M. M. Golas, H. Stark, *J Struct Biol* **143**, 219 (2003).
14. M. van Heel, *Ultramicroscopy* **13**, 165 (1984).
15. M. Van Heel, *Ultramicroscopy* **21**, 111 (1987).
16. M. Radermacher, T. Wagenknecht, A. Verschoor, J. Frank, *J Microsc* **146**, 113 (1987).
17. M. D. Ohi *et al.*, *Mol Cell* **28**, 871 (2007).
18. P. Dube *et al.*, *Mol Cell* **20**, 867 (2005).
19. (H.S. and B.S, unpublished data).
20. H. Yamano, J. Gannon, H. Mahbubani, T. Hunt, *Mol Cell* **13**, 137 (2004).

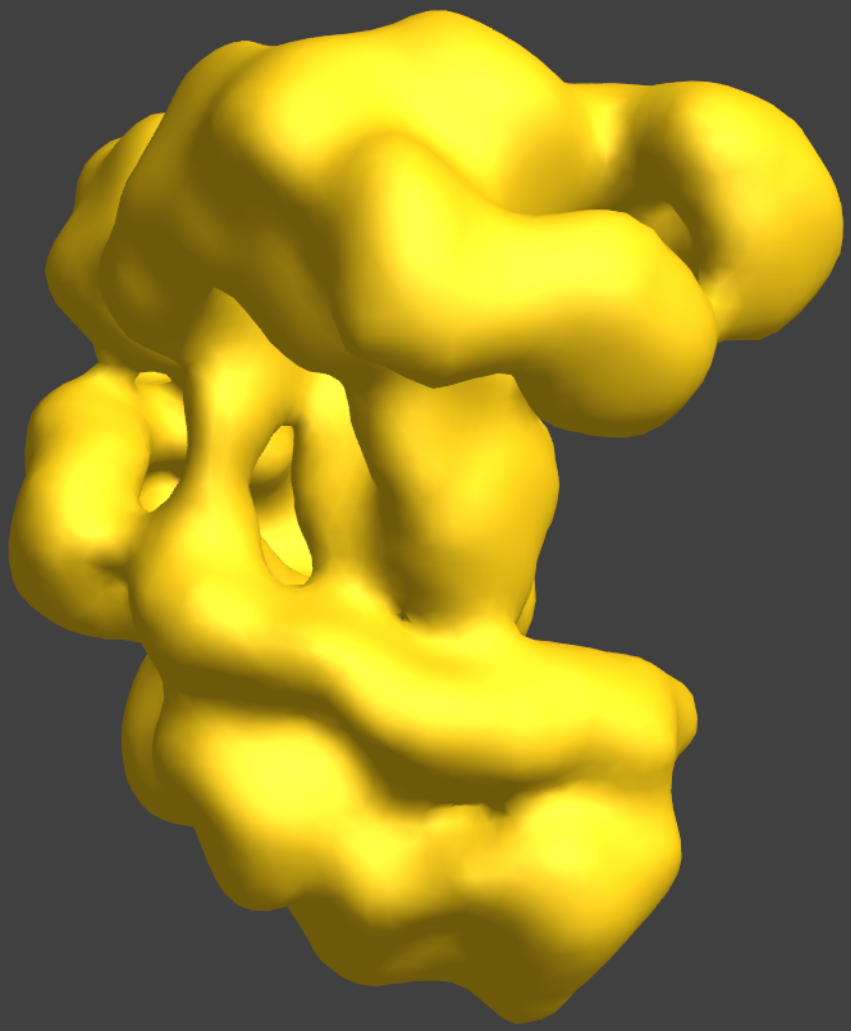

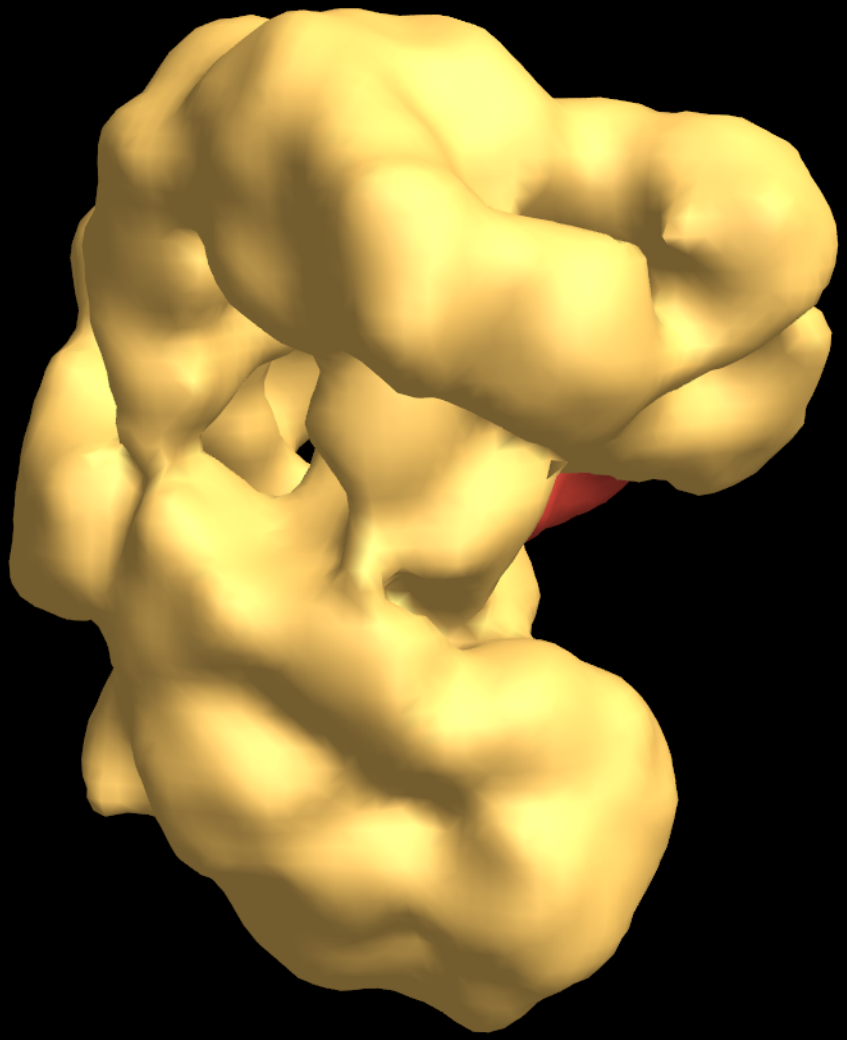

6. Abbreviations

Å	Angström
ab	antibody
amp	ampicillin
APC/C	anaphase-promoting complex/cyclosome
ATP	adenosine triphosphate
a.u.	arbitrary unit
bp	base pairs
BSA	bovine serum albumin
cDNA	complementary DNA
cdc	cell devision cycle
Cdk	cyclin dependent kinase
Cm	C box mutant
3 D	three-dimensional
DMP	dimethylpimelimidate
DNA	deoxyribonucleic acid
dm	D-box mutant
dkm	D-box and KEN box double mutant
DMEM	Dulbecco's Modified Eagle Medium
DMSO	dimethylsulfoxyde
DTT	dithiothreithol
DUB	deubiquitinating enzyme
E1	ubiquitin-activating enzyme
E2	ubiquitin conjugating enzyme

E3	ubiquitin ligase
E. coli	Escherichia coli
EDTA	ethylenediamine tetraacetic acid
EM	electron microscopy
FL	full length
GAL	galactose
GST	glutathione-S-transferase
h	hour
HA	epitope on influenza virus hemagglutinin (sequence:YPYDVPDYA)
H6	His-tag comprising 6 histidines
HECT	homology to E6-AP C-terminus
H.s.	Homo sapiens
IR	isoleucine-arginine
IgG	immunoglobulin G
IPTG	isopropyl β-D-1-thiogalactopyranoside
IVT	in vitro translation
kDa	kilo Dalton
km	KEN box mutant
LB	Luria-Bertani
leu	leucine
log	logarithmic
MCC	mitotic checkpoint complex
MDa	mega Dalton
min	minute
MR	methionine-arginine

myc	human c-myc epitope (sequence: EQKLISEEDL)
Ni-NTA	nickel-nitrilotriacetic acid
noc	nocodazole
OD600	optical density at 600 nm
PAGE	polyacrylamide gel electrophoresis
PBS	phosphate buffered saline
PCR	polymerase chain reaction
PEG	polyethylenglycole
PGK	phosphoglycerate kinase
PMSF	phenylmethylsulphonyl fluoride
PVDF	polyvinylidene fluoride transfer membrane
RING	really interesting new gene
RNA	ribonucleic acid
rpm	revolutions per minute
S	Svedberg
SAC	spindle assembly checkpoint
S. c.	Saccharomyces cerevisiae
SCF	Skp1/Cul1/F box
SDS	sodium dodecyl sulphate
Sf	Spodoptera frugiperda
S. p.	Schizosaccharomyces pombe
TBS	tris-buffered saline
TBT-T	tris-buffered saline with Tween20 detergent
TEV	tobacco etch virus
TPR	tetratrico peptide repeat

trp	tryptophane
ura	uracil
v/v	volume per volume
WB	Western blot
WD	tryptophane aspartate
wt	wild type
YPD	yeast extract peptone dextrose

7. References

Amerik, A. Y., and Hochstrasser, M. (2004). Mechanism and function of deubiquitinating enzymes. Biochim Biophys Acta 1695, 189-207.

Amon, A., Irniger, S. and Nasmyth, K. (1994). Closing the cell cycle circle in yeast: G2 cyclin proteolysis initiated at mitosis persists until the activation of G1 cyclins in the next cycle. Cell 7, 1037-50.

Au, S. W., Leng, X., Harper, J. W. and Barford, D. (2002). Implications for the ubiquitination reaction of the anaphase-promoting complex from the crystal structure of the Doc1/Apc10 subunit. J Mol Biol 4, 955-68.

Benmaamar, R. and Pagano, M. (2005). Involvement of the SCF complex in the control of Cdh1 degradation in S-phase. Cell Cycle 9, 1230-2.

Blatch, G. L., and Lassle, M. (1999). The tetratricopeptide repeat: a structural motif mediating protein-protein interactions. Bioessays 21, 932-939.

Braunstein I, Miniowitz S, Moshe Y, Hershko A. (2007) Inhibitory factors associated with anaphase-promoting complex/cylosome in mitotic checkpoint. Proc Natl Acad Sci U S A. 12:4870-5.

Burton, J. L. and Solomon, M. J. (2001). D box and KEN box motifs in budding yeast Hsl1p are required for APC-mediated degradation and direct binding to Cdc20p and Cdh1p. Genes Dev 18, 2381-95.

Burton, J. L., Tsakraklides, V. and Solomon, M. J. (2005). Assembly of an APCdh1- substrate complex is stimulated by engagement of a destruction box. Mol Cell 5, 533-42.

Burton JL, Solomon MJ. (2007) Mad3p, a pseudosubstrate inhibitor of APCCdc20 in the spindle assembly checkpoint. Genes Dev. 6:655-67.

Camasses, A., Bogdanova, A., Shevchenko, A. and Zachariae, W. (2003) The CCT chaperonin promotes activation of the anaphase-promoting complex through the generation of functional Cdc20. Mol Cell, 12, 87-100.

Carroll, C. W. and Morgan, D. O. (2002). The Doc1 subunit is a processivity factor for the anaphase-promoting complex. Nat Cell Biol 11, 880-7.

Carroll, C. W., Enquist-Newman, M. and Morgan, D. O. (2005). The APC subunit Doc1 promotes recognition of the substrate destruction box. Curr Biol 1, 11-8.

Castro A, Vigneron S, Bernis C, Labbé JC, Lorca T. (2003). Xkid is degraded in a D-box, KEN-box, and A-box-independent pathway. Mol Cell Biol. 12:4126-38.

Cheeseman IM, Anderson S, Jwa M, Green EM, Kang J, Yates JR 3rd, Chan CS, Drubin DG, Barnes G. (2002). Phospho-regulation of kinetochore-microtubule attachments by the Aurora kinase Ipl1p. Cell 2:163-72.

Cheeseman IM, Chappie JS, Wilson-Kubalek EM, Desai A. (2006). The conserved KMN network constitutes the core microtubule-binding site of the kinetochore. Cell. 5:983-97.

Chen, R. H., Waters, J. C., Salmon, E. D. and Murray, A. W. (1996). Association of spindle assembly checkpoint component XMAD2 with unattached kinetochores. Science 5285, 242-6.

Chung E, Chen RH. (2003) Phosphorylation of Cdc20 is required for its inhibition by the spindle checkpoint. Nat Cell Biol. 8:748-53.

Clute, P. and Pines, J. (1999). Temporal and spatial control of cyclin B1 destruction in metaphase. Nat Cell Biol 2, 82-7.

Cooper, K. F., Mallory, M. J., Egeland, D. B., Jarnik, M. and Strich, R. (2000). Ama1p is a meiosis-specific regulator of the anaphase promoting complex/cyclosome in yeast. Proc Natl Acad Sci U S A 26, 14548-53.

Davenport J, Harris LD, Goorha R. (2006) Spindle checkpoint function requires Mad2-dependent Cdc20 binding to the Mad3 homology domain of BubR1. Exp Cell Res. 10:1831-42.

Dawson IA, Roth S, Akam M, Artavanis-Tsakonas S. (1993) Mutations of the fizzy locus cause metaphase arrest in Drosophila melanogaster embryos. 1:359–376.

Dawson, I. A., Roth, S. and Artavanis-Tsakonas, S. (1995). The Drosophila cell cycle gene fizzy is required for normal degradation of cyclins A and B during mitosis and has homology to the CDC20 gene of Saccharomyces cerevisiae. J Cell Biol 3, 725-37.

D'Andrea LD, Regan L. (2003). TPR proteins: the versatile helix. Trends Biochem Sci. 12:655-62.

DeAntoni, A., Sala, V. and Musacchio, A. (2005). Explaining the oligomerization properties of the spindle assembly checkpoint protein Mad2. Philos Trans R Soc Lond B Biol Sci 1455, 637-47, discussion 447-8.

DeLuca JG, Gall WE, Ciferri C, Cimini D, Musacchio A, Salmon ED. (2006). Kinetochore microtubule dynamics and attachment stability are regulated by Hec1. Cell. 5:969-82.

den Elzen, N. and Pines, J. (2001). Cyclin A is destroyed in prometaphase and can delay chromosome alignment and anaphase. J Cell Biol 1, 121-36.

Deshaies RJ, Joazeiro CA.(2009) RING domain E3 ubiquitin ligases. Annu Rev Biochem. 78:399-434.

Diffley, J. F. (2004). Regulation of early events in chromosome replication. Curr Biol 18, R778-86.

Ditchfield C, Johnson VL, Tighe A, Ellston R, Haworth C, Johnson T, Mortlock A, Keen N, Taylor SS. (2003) Aurora B couples chromosome alignment with anaphase by targeting BubR1, Mad2, and Cenp-E to kinetochores. J Cell Biol. 161(2):267-80.

Dong, X., Zavitz, K. H., Thomas, B. J., Lin, M., Campbell, S. and Zipursky, S. L. (1997). Control of G1 in the developing Drosophila eye: rca1 regulates Cyclin A. Genes Dev 1, 94-105.

Dunn AY, Melville MW, Frydman J. (2001) Review: cellular substrates of the eukaryotic chaperonin TRiC/CCT. J Struct Biol. 2:176-84.

Enquist-Newman M, Sullivan M, Morgan DO. (2008) Modulation of the mitotic regulatory network by APC-dependent destruction of the Cdh1 inhibitor Acm1. Mol Cell. 4:437-46.

Evans, T., Rosenthal, E. T., Youngblom, J., Distel, D. and Hunt, T. (1983). Cyclin: a protein specified by maternal mRNA in sea urchin eggs that is destroyed at each cleavage division. Cell 2, 389-96.

Eytan, E., Moshe, Y., Braunstein, I. and Hershko, A. (2006). Roles of the anaphase promoting complex/cyclosome and of its activator Cdc20 in functional substrate binding. Proc Natl Acad Sci U S A 7, 2081-6.

Fang G, Yu H, Kirschner MW. (1998) Direct binding of CDC20 protein family members activates the anaphase-promoting complex in mitosis and G1. Mol Cell. 2:163-71.

Fang, G. (2002). Checkpoint protein BubR1 acts synergistically with Mad2 to inhibit anaphase-promoting complex. Mol Biol Cell 3, 755-66.

Feine O, Zur A, Mahbubani H, Brandeis M.(2007) Human Kid is degraded by the APC/C(Cdh1) but not by the APC/C(Cdc20). Cell Cycle. 20:2516-23

Fraschini, R., Beretta, A., Sironi, L., Musacchio, A., Lucchini, G. and Piatti, S. (2001). Bub3 interaction with Mad2, Mad3 and Cdc20 is mediated by WD40 repeats and does not require intact kinetochores. Embo J 23, 6648-59.

García-Higuera I, Manchado E, Dubus P, Cañamero M, Méndez J, Moreno S, Malumbres M. (2008) Genomic stability and tumour suppression by the APC/C cofactor Cdh1. Nat Cell Biol. 7:802-11.

Geley, S., Kramer, E., Gieffers, C., Gannon, J., Peters, J. M. and Hunt, T. (2001). Anaphase-promoting complex/cyclosome-dependent proteolysis of human cyclin A starts at the beginning of mitosis and is not subject to the spindle assembly checkpoint. J Cell Biol 1, 137-48.

Gieffers, C., Dube, P., Harris, J. R., Stark, H. and Peters, J. M. (2001). Threedimensional structure of the anaphase-promoting complex. Mol Cell 4, 907-13.

Glotzer, M., Murray, A. W. and Kirschner, M. W. (1991). Cyclin is degraded by the ubiquitin pathway. Nature 6305, 132-8.

Gmachl, M., Gieffers, C., Podtelejnikov, A. V., Mann, M. and Peters, J. M. (2000). The RING-H2 finger protein APC11 and the E2 enzyme UBC4 are sufficient to ubiquitinate substrates of the anaphase-promoting complex. Proc Natl Acad Sci U S A 16, 8973-8.

Grossberger, R., Gieffers, C., Zachariae, W., Podtelejnikov, A. V., Schleiffer, A., Nasmyth, K., Mann, M. and Peters, J. M. (1999). Characterization of the DOC1/APC10 subunit of the yeast and the human anaphase-promoting complex. J Biol Chem 20, 14500-7.

Grosskortenhaus, R. and Sprenger, F. (2002). Rca1 inhibits APC-Cdh1(Fzr) and is required to prevent cyclin degradation in G2. Dev Cell 1, 29-40.

Guardavaccaro D, Pagano M. (2006). Stabilizers and destabilizers controlling cell cycle oscillators. Mol Cell. 22(1):1-4

Habu, T., Kim, S. H., Weinstein, J. and Matsumoto, T. (2002). Identification of a MAD2-binding protein, CMT2, and its role in mitosis. Embo J 23, 6419-28.

Hagting, A., Den Elzen, N., Vodermaier, H. C., Waizenegger, I. C., Peters, J. M. and Pines, J. (2002). Human securin proteolysis is controlled by the spindle checkpoint and reveals when the APC/C switches from activation by Cdc20 to Cdh1. J Cell Biol 7, 1125-37.

Hames, R. S., Wattam, S. L., Yamano, H., Bacchieri, R. and Fry, A. M. (2001). APC/C-mediated destruction of the centrosomal kinase Nek2A occurs in early mitosis and depends upon a cyclin A-type D-box. Embo J 24, 7117-27.

Hansen, D. V., Loktev, A. V., Ban, K. H. and Jackson, P. K. (2004). Plk1 regulates activation of the anaphase promoting complex by phosphorylating and triggering SCFbetaTrCP-dependent destruction of the APC Inhibitor Emi1. Mol Biol Cell 12, 5623-34.

Hardwick KG, Johnston RC, Smith DL, Murray AW. (2000) MAD3 encodes a novel component of the spindle checkpoint which interacts with Bub3p, Cdc20p, and Mad2p. J Cell Biol. 5:871-82.

Harper, J. W., Burton, J. L. and Solomon, M. J. (2002). The anaphase-promoting complex: it's not just for mitosis any more. Genes Dev 17, 2179-206.

Hartwell LH, Mortimer RK, Culotti J, Culotti M. (1973) Genetic Control of the Cell Division Cycle in Yeast: V. Genetic Analysis of cdc Mutants. Genetics. 2:267-286.

Hartwell LH, Smith D. (1985) Altered fidelity of mitotic chromosome transmission in cell cycle mutants of S. cerevisiae. Genetics. 3:381-95.

Hauf S, Cole RW, LaTerra S, Zimmer C, Schnapp G, Walter R, Heckel A, van Meel J, Rieder CL, Peters JM. (2003). The small molecule Hesperadin reveals a role for Aurora B in correcting kinetochore-microtubule attachment and in maintaining the spindle assembly checkpoint. J Cell Biol. 2:281-94.

Hayes, M. J., Kimata, Y., Wattam, S. L., Lindon, C., Mao, G., Yamano, H. and Fry, A. M. (2006). Early mitotic degradation of Nek2A depends on Cdc20-independent interaction with the APC/C. Nat Cell Biol 6, 607-14.

Hershko A, Ganoth D, Sudakin V, Dahan A, Cohen LH, Luca FC, Ruderman JV, Eytan E. (1994). Components of a system that ligates cyclin to ubiquitin and their regulation by the protein kinase cdc2. J Biol Chem. 7:4940-6.

Herzog, F. and Peters, J. M. (2005). Large-scale purification of the vertebrate anaphase-promoting complex/cyclosome. Methods Enzymol 175-95.

Herzog F, Primorac I, Dube P, Lenart P, Sander B, Mechtler K, Stark H, Peters JM. (2009) Structure of the anaphase-promoting complex/cyclosome interacting with a mitotic checkpoint complex. Science. 5920:1477-81.

Hochegger H, Takeda S, Hunt T. (2008) Cyclin-dependent kinases and cell-cycle transitions: does one fit all? Nat Rev Mol Cell Biol. (11):910-6.

Hochstrasser, M. (1996). Ubiquitin-dependent protein degradation. Annu Rev Genet 405-39.

Howell BJ, McEwen BF, Canman JC, Hoffman DB, Farrar EM, Rieder CL, Salmon ED. (2001) Cytoplasmic dynein/dynactin drives kinetochore protein transport to the spindle poles and has a role in mitotic spindle checkpoint inactivation. J Cell Biol. 7:1159-72.

Hoyt, M. A., Totis, L. and Roberts, B. T. (1991). S. cerevisiae genes required for cell cycle arrest in response to loss of microtubule function. Cell 3, 507-17.

Huang, J. N., Park, I., Ellingson, E., Littlepage, L. E. and Pellman, D. (2001). Activity of the APC(Cdh1) form of the anaphase-promoting complex persists until S phase and prevents the premature expression of Cdc20p. J Cell Biol 1, 85-94.

Hsu JY, Reimann JD, Sørensen CS, Lukas J, Jackson PK. (2002). E2F-dependent accumulation of hEmi1 regulates S phase entry by inhibiting APC(Cdh1). Nat Cell Biol. 4(5):358-66.

Hwang, L. H. and Murray, A. W. (1997). A novel yeast screen for mitotic arrest mutants identifies DOC1, a new gene involved in cyclin proteolysis. Mol Biol Cell 10, 1877-87.

Hwang, L. H., Lau, L. F., Smith, D. L., Mistrot, C. A., Hardwick, K. G., Hwang, E. S.,

Amon, A. and Murray, A. W. (1998). Budding yeast Cdc20: a target of the spindle checkpoint. Science 5353, 1041-4.

Irniger, S., Piatti, S., Michaelis, C. and Nasmyth, K. (1995). Genes involved in sister chromatid separation are needed for B-type cyclin proteolysis in budding yeast. Cell 2, 269-78.

Izawa D, Goto M, Yamashita A, Yamano H, Yamamoto M. (2005) Fission yeast Mes1p ensures the onset of meiosis II by blocking degradation of cyclin Cdc13p. Nature. 7032:529-33.

Jallepalli, P. V., Waizenegger, I. C., Bunz, F., Langer, S., Speicher, M. R., Peters, J. M., Kinzler, K. W., Vogelstein, B. and Lengauer, C. (2001). Securin is required for chromosomal stability in human cells. Cell 4, 445-57.

Jaspersen, S. L., Charles, J. F. and Morgan, D. O. (1999). Inhibitory phosphorylation of the APC regulator Hct1 is controlled by the kinase Cdc28 and the phosphatase Cdc14. Curr Biol 5, 227-36.

Jaquenoud M, van Drogen F, Peter M. (2002). Cell cycle-dependent nuclear export of Cdh1p may contribute to the inactivation of APC/C(Cdh1). EMBO J. 21(23):6515-26.

Jeganathan KB, Malureanu L, van Deursen JM. (2005) The Rae1-Nup98 complex prevents aneuploidy by inhibiting securin degradation. Nature. 7070:1036-9.

Juang YL, Huang J, Peters JM, McLaughlin ME, Tai CY, Pellman D. (1997) APC-mediated proteolysis of Ase1 and the morphogenesis of the mitotic spindle. Science. 5304:1311-4.

Kim, S. H., Lin, D. P., Matsumoto, S., Kitazono, A. and Matsumoto, T. (1998). Fission yeast Slp1: an effector of the Mad2-dependent spindle checkpoint. Science 5353, 1045-7.

Kimata Y, Baxter JE, Fry AM, Yamano H. (2008) A role for the Fizzy/Cdc20 family of proteins in activation of the APC/C distinct from substrate recruitment. Mol Cell. 4:576-83.

King, R. W., Peters, J. M., Tugendreich, S., Rolfe, M., Hieter, P. and Kirschner, M. W. (1995). A 20S complex containing CDC27 and CDC16 catalyzes the mitosis specific conjugation of ubiquitin to cyclin B. Cell 2, 279-88.

King RW, Glotzer M, Kirschner MW. (1996). Mutagenic analysis of the destruction signal of mitotic cyclins and structural characterization of ubiquitinated intermediates. Mol Biol Cell. 9:1343-57.

Klotzbücher A, Stewart E, Harrison D, Hunt T. (1996) The 'destruction box' of cyclin A allows B-type cyclins to be ubiquitinated, but not efficiently destroyed. EMBO J. 12:3053-64.

Kobayashi H, Stewart E, Poon R, Adamczewski JP, Gannon J, Hunt T. (1992) Identification of the domains in cyclin A required for binding to, and activation of, p34cdc2 and p32cdk2 protein kinase subunits. Mol Biol Cell. 11:1279-94.

Kominami, K., Seth-Smith, H. and Toda, T. (1998). Apc10 and Ste9/Srw1, two regulators of the APC-cyclosome, as well as the CDK inhibitor Rum1 are required for G1 cell-cycle arrest in fission yeast. Embo J 18, 5388-99.

Kops GJ, Foltz DR, Cleveland DW. (2004). Lethality to human cancer cells through massive chromosome loss by inhibition of the mitotic checkpoint. Proc Natl Acad Sci U S A. 101(23):8699-704.

Kraft, C., Herzog, F., Gieffers, C., Mechtler, K., Hagting, A., Pines, J. and Peters, J. M. (2003). Mitotic regulation of the human anaphase-promoting complex by phosphorylation. Embo J 24, 6598-609.

Kraft, C., Vodermaier, H. C., Maurer-Stroh, S., Eisenhaber, F. and Peters, J. M. (2005). The WD40 propeller domain of Cdh1 functions as a destruction box receptor for APC/C substrates. Mol Cell 5, 543-53.

Kramer, E. R., Gieffers, C., Holzl, G., Hengstschlager, M. and Peters, J. M. (1998).
Activation of the human anaphase-promoting complex by proteins of the CDC20/Fizzy family. Curr Biol 22, 1207-10.

Kramer, E. R., Scheuringer, N., Podtelejnikov, A. V., Mann, M. and Peters, J. M. (2000). Mitotic regulation of the APC activator proteins CDC20 and CDH1. Mol Biol Cell 5, 1555-69.

Kulukian A, Han JS, Cleveland DW. (2009) Unattached kinetochores catalyze production of an anaphase inhibitor that requires a Mad2 template to prime Cdc20 for BubR1 binding. Dev Cell. 1:105-17.

Lamb, J. R., Michaud, W. A., Sikorski, R. S. and Hieter, P. A. (1994). Cdc16p, Cdc23p and Cdc27p form a complex essential for mitosis. Embo J 18, 4321-8.

Lampson MA, Renduchitala K, Khodjakov A, Kapoor TM. (2004) Correcting improper chromosome-spindle attachments during cell division. Nat Cell Biol. 3:232-7.

Leverson, J. D., Joazeiro, C. A., Page, A. M., Huang, H., Hieter, P. and Hunter, T. (2000). The APC11 RING-H2 finger mediates E2-dependent ubiquitination. Mol Biol Cell 7, 2315-25.

Li, R. and Murray, A. W. (1991). Feedback control of mitosis in budding yeast. Cell 3, 519-31.

Li, Y. and Benezra, R. (1996). Identification of a human mitotic checkpoint gene: hsMAD2. Science 5285, 246-8.

Lindon, C. and Pines, J. (2004). Ordered proteolysis in anaphase inactivates Plk1 to contribute to proper mitotic exit in human cells. J Cell Biol 2, 233-41.

Littlepage LE, Ruderman JV. (2002). Identification of a new APC/C recognition domain, the A box, which is required for the Cdh1-dependent destruction of the kinase Aurora-A during mitotic exit. Genes Dev. 17:2274-85.

Liu D, Vader G, Vromans MJ, Lampson MA, Lens SM. (2009) Sensing chromosome bi-orientation by spatial separation of aurora B kinase from kinetochore substrates. Science. 323(5919):1350-3.

Lohka, M. J., Hayes, M. K. and Maller, J. L. (1988). Purification of maturationpromoting factor, an intracellular regulator of early mitotic events. Proc Natl Acad Sci U S A 9, 3009-13.

Lukas C, Sørensen CS, Kramer E, Santoni-Rugiu E, Lindeneg C, Peters JM, Bartek J, Lukas J. (1999) Accumulation of cyclin B1 requires E2F and cyclin-A-dependent rearrangement of the anaphase-promoting complex. Nature. 6755:815-8.

Luo, X., Tang, Z., Rizo, J. and Yu, H. (2002). The Mad2 spindle checkpoint protein undergoes similar major conformational changes upon binding to either Mad1 or Cdc20. Mol Cell 1, 59-71.

Mao Y, Abrieu A, Cleveland DW. (2003) Activating and silencing the mitotic checkpoint through CENP-E-dependent activation/inactivation of BubR1. Cell. 1:87-98.

Mao Y, Desai A, Cleveland DW. (2005) Microtubule capture by CENP-E silences BubR1-dependent mitotic checkpoint signaling. J Cell Biol. 6:873-80.

Mapelli M, Musacchio A. (2007) MAD contortions: conformational dimerization boosts spindle checkpoint signaling. Curr Opin Struct Biol. 6:716-25.

Margottin-Goguet, F., Hsu, J. Y., Loktev, A., Hsieh, H. M., Reimann, J. D. and Jackson, P. K. (2003). Prophase destruction of Emi1 by the SCF(betaTrCP/Slimb) ubiquitin ligase activates the anaphase promoting complex to allow progression beyond prometaphase. Dev Cell 6, 813-26.

Maresca TJ, Salmon ED. (2009). Intrakinetochore stretch is associated with changes in kinetochore phosphorylation and spindle assembly checkpoint activity. J Cell Biol.184(3):373-81.

Martinez JS, Jeong DE, Choi E, Billings BM, Hall MC. (2006). Acm1 is a negative regulator of the CDH1-dependent anaphase-promoting complex/cyclosome in budding yeast. Mol Cell Biol. (24):9162-76.

Masui, Y. and Markert, C. L. (1971). Cytoplasmic control of nuclear behavior during meiotic maturation of frog oocytes. J Exp Zool 2, 129-45.

Matyskiela ME, Morgan DO. (2009) Analysis of activator-binding sites on the APC/C supports a cooperative substrate-binding mechanism. Mol Cell. 1:68-80.

McGarry TJ, Kirschner MW. (1998). Geminin, an inhibitor of DNA replication, is degraded during mitosis. Cell. 6:1043-53.

Miller JJ, Summers MK, Hansen DV, Nachury MV, Lehman NL, Loktev A, Jackson PK. (2006). Emi1 stably binds and inhibits the anaphase-promoting complex/cyclosome as a pseudosubstrate inhibitor. Genes Dev. 20(17):2410-20.

Morgan, D.O. (2007) The cell cycle - Principles of control. Oxford University Press.

Morrow, C. J., Tighe, A., Johnson, V. L., Scott, M. I., Ditchfield, C. and Taylor, S. S. (2005). Bub1 and aurora B cooperate to maintain BubR1-mediated inhibition of APC/CCdc20. J Cell Sci Pt 16, 3639-52.

Moshe, Y., Boulaire, J., Pagano, M. and Hershko, A. (2004). Role of Polo-like kinase in the degradation of early mitotic inhibitor 1, a regulator of the anaphase promoting complex/cyclosome. Proc Natl Acad Sci U S A 21, 7937-42.

Murray AW, Solomon MJ, Kirschner MW.(1989). The role of cyclin synthesis and degradation in the control of maturation promoting factor activity. Nature. 6222:280-6.

Murray AW, Kirschner MW. (1989). Cyclin synthesis drives the early embryonic cell cycle. Nature. 1989 May 25;339(6222):275-80.

Murray, A. W. (2004). Recycling the cell cycle: cyclins revisited. Cell 2, 221-34.

Musacchio, A. and Hardwick, K. G. (2002). The spindle checkpoint: structural insights into dynamic signalling. Nat Rev Mol Cell Biol 10, 731-41.

Nakayama KI, Nakayama K. (2006) Ubiquitin ligases: cell-cycle control and cancer. Nat Rev Cancer. 6(5):369-81.

Nasmyth K. (2001) Disseminating the genome: joining, resolving, and separating sister chromatids during mitosis and meiosis. Annu Rev Genet. 35:673-745.

Nasmyth, K. (2002). Segregating sister genomes: the molecular biology of chromosome separation. Science 5581, 559-65.

Nasmyth K. (2005) How do so few control so many? Cell. 6:739-46.

Ohi, M. D., Feoktistova, A., Ren, L., Yip, C., Cheng, Y., Chen, J. S., Yoon, H. J., Wall, J. S., Huang, Z., Penczek, P. A., et al. (2007). Structural organization of the anaphase-promoting complex bound to the mitotic activator Slp1. Mol Cell 28, 871-885.

Orlicky, S., Tang, X., Willems, A., Tyers, M., and Sicheri, F. (2003). Structural basis for phosphodependent substrate selection and orientation by the SCFCdc4 ubiquitin ligase. Cell 112, 243-256.

Pagano, M., and Jackson, P. K. (2004). Wagging the dogma; tissue-specific cell cycle control in the mouse embryo. Cell 118, 535-538.

Pal, M., Varga, K., Nagy, O., and Deak, P. (2007b). Characterization of the Apc10/Doc1 subunit of the anaphase promoting complex in Drosophila melanogaster. Acta Biol Hung *58 Suppl*, 51-64.

Pan, J. and Chen, R. H. (2004). Spindle checkpoint regulates Cdc20p stability in Saccharomyces cerevisiae. Genes Dev 12, 1439-51.

Parker, C. W. (1990). Radiolabeling of proteins. Methods Enzymol 721-37.

Passmore, L. A., McCormack, E. A., Au, S. W., Paul, A., Willison, K. R., Harper, J. W. and Barford, D. (2003). Doc1 mediates the activity of the anaphase-promoting complex by contributing to substrate recognition. Embo J 4, 786-96.

Passmore, L. A. and Barford, D. (2005). Coactivator functions in a stoichiometric complex with anaphase-promoting complex/cyclosome to mediate substrate recognition. EMBO Rep 9, 873-8.

Peters JM, King RW, Höög C, Kirschner MW. (1996) Identification of BIME as a subunit of the anaphase-promoting complex. Science. 5290:1199-201.

Peters, J. M. (2002). The anaphase-promoting complex: proteolysis in mitosis and beyond. Mol Cell 5, 931-43.

Peters, J. M. (2006). The anaphase promoting complex/cyclosome: a machine designed to destroy. Nat Rev Mol Cell Biol 9, 644-56.

Petroski, M. D., and Deshaies, R. J. (2005). Function and regulation of cullin-RING ubiquitin ligases. Nat Rev Mol Cell Biol 6, 9-20.

Pfleger, C. M. and Kirschner, M. W. (2000). The KEN box: an APC recognition signal distinct from the D box targeted by Cdh1. Genes Dev 6, 655-65.

Pfleger, C. M., Lee, E. and Kirschner, M. W. (2001a). Substrate recognition by the Cdc20 and Cdh1 components of the anaphase-promoting complex. Genes Dev 18, 2396-407.

Pfleger, C. M., Salic, A., Lee, E. and Kirschner, M. W. (2001b). Inhibition of Cdh1-APC by the MAD2-related protein MAD2L2: a novel mechanism for regulating Cdh1. Genes Dev 14, 1759-64.

Pickart, C. M. (2001). Mechanisms underlying ubiquitination. Annu Rev Biochem 503-33.

Pines J, Hunter T. (1991) Human cyclins A and B1 are differentially located in the cell and undergo cell cycle-dependent nuclear transport. J Cell Biol. 1:1-17.

Prinz, S., Hwang, E. S., Visintin, R. and Amon, A. (1998). The regulation of Cdc20 proteolysis reveals a role for APC components Cdc23 and Cdc27 during S phase and early mitosis. Curr Biol 13, 750-60.

Poddar A, Stukenberg PT, Burke DJ. (2005) Two complexes of spindle checkpoint proteins containing Cdc20 and Mad2 assemble during mitosis independently of the kinetochore in Saccharomyces cerevisiae. Eukaryot Cell. 5:867-78.

Rape, M. and Kirschner, M. W. (2004). Autonomous regulation of the anaphase promoting complex couples mitosis to S-phase entry. Nature 7017, 588-95.

Rape M, Reddy SK, Kirschner MW. (2006). The processivity of multiubiquitination by the APC determines the order of substrate degradation. Cell. 2006 1:89-103.

Reddy SK, Rape M, Margansky WA, Kirschner MW. (2007) Ubiquitination by the anaphase-promoting complex drives spindle checkpoint inactivation. Nature. 7138:921-5.

Reimann, J. D., Freed, E., Hsu, J. Y., Kramer, E. R., Peters, J. M. and Jackson, P. K. (2001a). Emi1 is a mitotic regulator that interacts with Cdc20 and inhibits the anaphase promoting complex. Cell 5, 645-55.

Reimann, J. D., Gardner, B. E., Margottin-Goguet, F. and Jackson, P. K. (2001b). Emi1 regulates the anaphase-promoting complex by a different mechanism than Mad2 proteins. Genes Dev 24, 3278-85.

Rudner, A. D. and Murray, A. W. (2000). Phosphorylation by Cdc28 activates the Cdc20-dependent activity of the anaphase-promoting complex. J Cell Biol 7, 1377-90.

Schwab, M., Lutum, A. S. and Seufert, W. (1997). Yeast Hct1 is a regulator of Clb2 cyclin proteolysis. Cell 4, 683-93.

Schwab, M., Neutzner, M., Mocker, D. and Seufert, W. (2001). Yeast Hct1 recognizes the mitotic cyclin Clb2 and other substrates of the ubiquitin ligase APC. Embo J 18, 5165-75.

Shah JV, Botvinick E, Bonday Z, Furnari F, Berns M, Cleveland DW. (2004) Dynamics of centromere and kinetochore proteins; implications for checkpoint signaling and silencing. Curr Biol. 11:942-52.

Sharp-Baker, H. and Chen, R. H. (2001). Spindle checkpoint protein Bub1 is required for kinetochore localization of Mad1, Mad2, Bub3, and CENP-E, independently of its kinase activity. J Cell Biol 6, 1239-50.

Shirayama M, Zachariae W, Ciosk R, Nasmyth K. (1998). The Polo-like kinase Cdc5p and the WD-repeat protein Cdc20p/fizzy are regulators and substrates of the anaphase promoting complex in Saccharomyces cerevisiae. EMBO J. 17(5):1336-49.

Shteinberg, M., Protopopov, Y., Listovsky, T., Brandeis, M. and Hershko, A. (1999). Phosphorylation of the cyclosome is required for its stimulation by Fizzy/cdc20. Biochem Biophys Res Commun 1, 193-8.

Sigrist S, Jacobs H, Stratmann R, Lehner CF. (1995) Exit from mitosis is regulated by Drosophila fizzy and the sequential destruction of cyclins A, B and B3. EMBO J. 19:4827-38.

Sironi, L., Melixetian, M., Faretta, M., Prosperini, E., Helin, K. and Musacchio, A. (2001). Mad2 binding to Mad1 and Cdc20, rather than oligomerization, is required for the spindle checkpoint. Embo J 22, 6371-82.

Skoufias, D. A., Andreassen, P. R., Lacroix, F. B., Wilson, L. and Margolis, R. L. (2001). Mammalian mad2 and bub1/bubR1 recognize distinct spindleattachment and kinetochore-tension checkpoints. Proc Natl Acad Sci U S A 8, 4492-7.

Smith TF, Gaitatzes C, Saxena K, Neer EJ. (1999) The WD repeat: a common architecture for diverse functions. Trends Biochem Sci. 5:181-5.

Sørensen CS, Lukas C, Kramer ER, Peters JM, Bartek J, Lukas J. (2001) A conserved cyclin-binding domain determines functional interplay between anaphase-promoting complex-Cdh1 and cyclin A-Cdk2 during cell cycle progression. Mol Cell Biol.11:3692-703.

Stegmeier, F., Rape, M., Draviam, V. M., Nalepa, G., Sowa, M. E., Ang, X. L., McDonald, E. R., 3rd, Li, M. Z., Hannon, G. J., Sorger, P. K., et al. (2007). Anaphase initiation is regulated by antagonistic ubiquitination and deubiquitination activities. Nature 446, 876-881.

Stemmann, O., Zou, H., Gerber, S. A., Gygi, S. P. and Kirschner, M. W. (2001). Dual inhibition of sister chromatid separation at metaphase. Cell 6, 715-26.

Stern, B. M. and Murray, A. W. (2001). Lack of tension at kinetochores activates the spindle checkpoint in budding yeast. Curr Biol 18, 1462-7.

Stewart E, Kobayashi H, Harrison D, Hunt T. (1994) Destruction of Xenopus cyclins A and B2, but not B1, requires binding to p34cdc2. EMBO J. 3:584-94.

Sudakin, V., Ganoth, D., Dahan, A., Heller, H., Hershko, J., Luca, F. C., Ruderman, J. V. and Hershko, A. (1995). The cyclosome, a large complex containing cyclin-selective ubiquitin ligase activity, targets cyclins for destruction at the end of mitosis. Mol Biol Cell 2, 185-97.

Sudakin, V., Chan, G. K. and Yen, T. J. (2001). Checkpoint inhibition of the APC/C in HeLa cells is mediated by a complex of BUBR1, BUB3, CDC20, and MAD2. J Cell Biol 5, 925-36.

Sullivan, M., and Morgan, D. O. (2007). Finishing mitosis, one step at a time. Nat Rev Mol Cell Biol 8, 894-903.

Swan A, Schüpbach T. (2007) The Cdc20 (Fzy)/Cdh1-related protein, Cort, cooperates with Fzy in cyclin destruction and anaphase progression in meiosis I and II in Drosophila. Development. 5:891-9.

Tanaka TU, Rachidi N, Janke C, Pereira G, Galova M, Schiebel E, Stark MJ, Nasmyth K. (2002). Evidence that the Ipl1-Sli15 (Aurora kinase-INCENP) complex promotes chromosome bi-orientation by altering kinetochore-spindle pole connections. Cell.108(3):317-29.

Tang, Z., Bharadwaj, R., Li, B. and Yu, H. (2001a). Mad2-Independent inhibition of APCCdc20 by the mitotic checkpoint protein BubR1. Dev Cell 2, 227-37.

Tang, Z., Li, B., Bharadwaj, R., Zhu, H., Ozkan, E., Hakala, K., Deisenhofer, J. and Yu, H. (2001b). APC2 Cullin protein and APC11 RING protein comprise the minimal ubiquitin ligase module of the anaphase-promoting complex. Mol Biol Cell 12, 3839-51.

Tang Z, Shu H, Oncel D, Chen S, Yu H. (2004) Phosphorylation of Cdc20 by Bub1 provides a catalytic mechanism for APC/C inhibition by the spindle checkpoint. Mol Cell. 3:387-97.

Taylor, S. S. and McKeon, F. (1997). Kinetochore localization of murine Bub1 is required for normal mitotic timing and checkpoint response to spindle damage. Cell 5, 727-35.

Taylor, S. S., Ha, E. and McKeon, F. (1998). The human homologue of Bub3 is required for kinetochore localization of Bub1 and a Mad3/Bub1-related protein kinase. J Cell Biol 1, 1- 11.

Thornton, B. R. and Toczyski, D. P. (2003). Securin and B-cyclin/CDK are the only essential targets of the APC. Nat Cell Biol 12, 1090-4.

Thornton, B. R., Ng, T. M., Matyskiela, M. E., Carroll, C. W., Morgan, D. O. and Toczyski, D. P. (2006). An architectural map of the anaphase-promoting complex. Genes Dev 4, 449-60.

Thornton BR, Toczyski DP. (2006) Precise destruction: an emerging picture of the APC. Genes Dev. 22:3069-78.

Thrower JS, Hoffman L, Rechsteiner M, Pickart CM. (2000). Recognition of the polyubiquitin proteolytic signal. EMBO J. 19(1):94-102.

Tunquist BJ, Maller JL. (2003). Under arrest: cytostatic factor (CSF)-mediated metaphase arrest in vertebrate eggs. Genes Dev. 6:683-710.

Uchida KS, Takagaki K, Kumada K, Hirayama Y, Noda T, Hirota T. (2009) Kinetochore stretching inactivates the spindle assembly checkpoint. J Cell Biol. 184(3):383-90. Epub 2009 Feb 2.

Vink M, Simonetta M, Transidico P, Ferrari K, Mapelli M, De Antoni A, Massimiliano L, Ciliberto A, Faretta M, Salmon ED, Musacchio A. (2006) In vitro FRAP identifies the minimal requirements for Mad2 kinetochore dynamics. Curr Biol. 8:755-66.

Visintin, R., Prinz, S. and Amon, A. (1997). CDC20 and CDH1: a family of substrate specific activators of APC-dependent proteolysis. Science 5337, 460-3.

Visintin, R., Craig, K., Hwang, E. S., Prinz, S., Tyers, M. and Amon, A. (1998). The phosphatase Cdc14 triggers mitotic exit by reversal of Cdk-dependent phosphorylation. Mol Cell 6, 709-18.

Vodermaier HC (2001) Cell cycle: Waiters serving the Destruction machinery. Curr Biol. 20:R834-7.

Vodermaier, H. C., Gieffers, C., Maurer-Stroh, S., Eisenhaber, F. and Peters, J. M. (2003). TPR subunits of the anaphase-promoting complex mediate binding to the activator protein CDH1. Curr Biol 17, 1459-68.

Vodermaier, H. C. (2004). APC/C and SCF: controlling each other and the cell cycle. Curr Biol 18, R787-96.

Wan, Y. and Kirschner, M. W. (2001). Identification of multiple CDH1 homologues in vertebrates conferring different substrate specificities. Proc Natl Acad Sci U S A 23, 13066-71.

Wang X, Babu JR, Harden JM, Jablonski SA, Gazi MH, Lingle WL, de Groen PC, Yen TJ, van Deursen JM. (2001) The mitotic checkpoint protein hBUB3 and the mRNA export factor hRAE1 interact with GLE2p-binding sequence (GLEBS)-containing proteins. J Biol Chem. 28:26559-67.

Wang J, Dye BT, Rajashankar KR, Kurinov I, Schulman BA. (2009) Insights into anaphase promoting complex TPR subdomain assembly from a CDC26-APC6 structure. Nat Struct Mol Biol.

Wassmann K, Benezra R. (1998) Mad2 transiently associates with an APC/p55Cdc complex during mitosis. Proc Natl Acad Sci U S A. 19:11193-8.

Waters JC, Chen RH, Murray AW, Salmon ED. (1998) Localization of Mad2 to kinetochores depends on microtubule attachment, not tension. J Cell Biol. 5:1181-91.

Wendt, K. S., Vodermaier, H. C., Jacob, U., Gieffers, C., Gmachl, M., Peters, J. M., Huber, R. and Sondermann, P. (2001). Crystal structure of the APC10/DOC1 subunit of the human anaphase-promoting complex. Nat Struct Biol 9, 784-8.

Wickliffe K, Williamson A, Jin L, Rape M. (2009). The multiple layers of ubiquitin-dependent cell cycle control. Chem Rev. 109(4):1537-48.

Wirth KG, Ricci R, Giménez-Abián JF, Taghybeeglu S, Kudo NR, Jochum W, Vasseur-Cognet M, Nasmyth K. (2004) Loss of the anaphase-promoting complex in quiescent cells causes unscheduled hepatocyte proliferation. Genes Dev. 1:88-98.

Wolthuis R, Clay-Farrace L, van Zon W, Yekezare M, Koop L, Ogink J, Medema R, Pines J. (2008) Cdc20 and Cks direct the spindle checkpoint-independent destruction of cyclin A. Mol Cell. 3:290-302.

Wu, G., Xu, G., Schulman, B.A., Jeffrey, P.D., Harper, J.W. and Pavletich, N.P. (2003) Structure of a beta-TrCP1-Skp1-beta-catenin complex: destruction motif binding and lysine specificity of the SCF(beta-TrCP1) ubiquitin ligase. Mol Cell, 11, 1445-1456.

Xia, G., Luo, X., Habu, T., Rizo, J., Matsumoto, T. and Yu, H. (2004). Conformation specific binding of p31(comet) antagonizes the function of Mad2 in the spindle checkpoint. Embo J 15, 3133-43.

Yamano H, Tsurumi C, Gannon J, Hunt T. (1998). The role of the destruction box and its neighbouring lysine residues in cyclin B for anaphase ubiquitin-dependent proteolysis in fission yeast: defining the D-box receptor. EMBO J. 19:5670-8.

Yamano, H., Gannon, J., Mahbubani, H. and Hunt, T. (2004). Cell cycle-regulated recognition of the destruction box of cyclin B by the APC/C in Xenopus egg extracts. Mol Cell 1, 137-47.

Yamashita YM, Nakaseko Y, Samejima I, Kumada K, Yamada H, Michaelson D, Yanagida M. (1996) 20S cyclosome complex formation and proteolytic activity inhibited by the cAMP/PKA pathway. Nature. 6606:276-9.

Yu, H., King, R. W., Peters, J. M. and Kirschner, M. W. (1996). Identification of a novel ubiquitin-conjugating enzyme involved in mitotic cyclin degradation. Curr Biol 4, 455-66.

Yu, H., Peters, J. M., King, R. W., Page, A. M., Hieter, P. and Kirschner, M. W. (1998). Identification of a cullin homology region in a subunit of the anaphase promoting complex. Science 5354, 1219-22.

Yu H. (2007) Cdc20: a WD40 activator for a cell cycle degradation machine. Mol Cell. 1:3-16.

Zachariae, W., Shin, T. H., Galova, M., Obermaier, B. and Nasmyth, K. (1996). Identification of subunits of the anaphase-promoting complex of Saccharomyces cerevisiae. Science 5290, 1201-4.

Zachariae, W., Schwab, M., Nasmyth, K. and Seufert, W. (1998). Control of cyclin ubiquitination by CDK-regulated binding of Hct1 to the anaphase promoting complex. Science 5394, 1721-4.

Zachariae, W., Shevchenko, A., Andrews, P. D., Ciosk, R., Galova, M., Stark, M. J., Mann, M. and Nasmyth, K. (1998). Mass spectrometric analysis of the anaphase-promoting complex from yeast: identification of a subunit related to cullins. Science 5354, 1216-9.

Zheng, N., Schulman, B. A., Song, L., Miller, J. J., Jeffrey, P. D., Wang, P., Chu, C., Koepp, D. M., Elledge, S. J., Pagano, M., Conaway, R. C., Conaway, J. W., Harper, J. W. and Pavletich, N.

P. (2002). Structure of the Cul1-Rbx1-Skp1-F boxSkp2 SCF ubiquitin ligase complex. Nature 6882, 703-9.

Zur, A. and Brandeis, M. (2002). Timing of APC/C substrate degradation is determined by fzy/fzr specificity of destruction boxes. Embo J 17, 4500-10.

Acknowledgements

I would like to thank Jan for his scientific guidance during my PhD thesis. Jan thought me, among many other things, how to design a biochemical experiment, how important it is to control it and to critically analyze its outcome. I had the freedom to perform experiments addressing questions I was curious about, and got help and support when I needed it.

I am grateful to Franz Herzog for introducing me to experimental biochemistry. I have learned many biochemical tricks from him during our collaboration on the spindle assembly checkpoint project.

I would like to thank all the members of the Peters lab, past and present, with who I had the joy of sharing days over all these years. I felt the lab was a playground I liked coming to, and the people I spent time there with were like a family to me. I would also like to thank everyone at the IMP for making it such a friendly place and an excellent home for science.

Finally, I would like to thank my parents, my sister, Zevi, Lindes and Miroslav for their constant support and encouragement during my studies. Especially I would like to thank my mom for always being there for me when the times were hard.

Personal Information

Name: Ivana Primorac
Nationality:
Date of Birth: 5. July 1979.
Place of Birth: Sarajevo, Bosnia and Herzegowina
Email: primorac@imp.ac.at
Language skills: Serbian, Croatian, Hungarian, English, German

Education

1986-1992 Primary school, Sarajevo, Bosnia and Herzegowina

1992-1994 Primary school, Subotica, Serbia and Montenegro.

1994-1998 Gymnasium "Svetozar Markovic", Subotica, Serbia and Montenegro.

1998-2005. University of Belgrade, Serbia and Montenegro
Department of Molecular Biology and Physiology, Faculty of Biology.

July 2003-October 2003 Internship in the laboratory of Prof. Dr. Meinrad Busslinger
Research Institute of Molecular Pathology, Vienna, Austria.

March 2004- March 2005 Laboratory of Prof. Dr. Meinrad Busslinger
Research Institute of Molecular Pathology, Vienna, Austria
Diploma thesis:
"Conditional knock-out of the mouse eed gene"

August 2005-present PhD thesis in the laboratory of Dr. Jan-Michael Peters
Research Institute of Molecular Pathology, Vienna, Austria

Publications

Herzog F, Primorac I, Dube P, Lenart P, Sander B, Mechtler K, Stark H, Peters JM. Structure of the anaphase promoting complex/cyclosome interacting with the mitotic checkpoint complex. Science, 2009 Mar 13;323(5920):1477-81.